

DEVELOPMENT OF CHEMICAL TOOLS FOR STUDYING REACTIVE SULFUR
SPECIES

by

MATTHEW MICHAEL CERDA

A DISSERTATION

Presented to the Department of Chemistry and Biochemistry
and the Graduate School of the University of Oregon
in partial fulfillment of the requirements
for the degree of
Doctor of Philosophy

June 2020

DISSERTATION APPROVAL PAGE

Student: Matthew Michael Cerda

Title: Development of Chemical Tools for Studying Reactive Sulfur Species

This dissertation has been accepted and approved in partial fulfillment of the requirements for the Doctor of Philosophy degree in the Department of Chemistry and Biochemistry by:

Michael M. Haley	Chairperson
Michael D. Pluth	Advisor
Darren W. Johnson	Core Member
Raghuveer Parthasarathy	Institutional Representative

and

Kate Mondloch	Interim Vice Provost and Dean of the Graduate School
---------------	--

Original approval signatures are on file with the University of Oregon Graduate School.

Degree awarded June 2020

© 2020 Matthew Michael Cerda
This work is licensed under a Creative Commons
Attribution-NonCommerical-NoDerivs (United States) License.



DISSERTATION ABSTRACT

Matthew Michael Cerda

Doctor of Philosophy

Department of Chemistry and Biochemistry

June 2020

Title: Development of Chemical Tools for Studying Reactive Sulfur Species

Hydrogen sulfide (H_2S) has recently emerged as an important biological signaling molecule involved in a number of key physiological processes. These observations have generated interest in harnessing H_2S as a potential therapeutic agent to treat disease states and chronic conditions associated with H_2S -based signaling. A mechanistic analysis of these physiological processes reveals the prevalence of H_2S and other reactive sulfur species including sulfane sulfur and persulfides. To better understand the biological properties of these reactive sulfur species, chemical tools which provide methods of generating these fleeting species under controlled reaction conditions are needed.

Chapter I is a comprehensive review discussing the large library of small molecule H_2S donors reported to date and their respective mechanisms of activation. Chapter II describes the discovery of a highly efficient, chemoselective reaction between free cysteine and thionoesters to generate H_2S at physiological pH. Chapter III builds upon the findings of Chapter II to provide a tunable method of H_2S generation upon treatment of functionalized dithioesters with free cysteine. Chapter IV demonstrates the validity of using synthetic organic polysulfides in the presence of biological thiols to generate H_2S through the intermediate formation of persulfides. Chapter V reports the effect of varying sulfane sulfur content in benzyl polysulfides on thiol-mediated H_2S release and the

biological activity of these compounds. Chapter VI highlights the use of dithiasuccinoyl protecting groups to improve current methods of H₂S generation which function through the intermediate generation of carbonyl sulfide (COS) in the presence of carbonic anhydrase. Building upon growing interest in the potential biological activity of COS, Chapter VII demonstrates the use of a benzobisimidazolium salt for selective detection of COS by UV-Vis and fluorescent spectroscopy.

This dissertation includes previously published and unpublished co-authored material.

CURRICULUM VITAE

NAME OF AUTHOR: Matthew Michael Cerda

GRADUATE AND UNDERGRADUATE SCHOOLS ATTENDED:

University of Oregon, Eugene
State University of New York College (SUNY) at Potsdam

DEGREES AWARDED:

Doctor of Philosophy, Chemistry, 2020, University of Oregon
Master of Science, Chemistry, 2017, University of Oregon
Bachelor of Science, Chemistry 2015, SUNY Potsdam

AREAS OF SPECIAL INTEREST:

Organic Chemistry
Physical Organic Chemistry
Chemical Biology

PROFESSIONAL EXPERIENCE:

Graduate Teaching Fellow, University of Oregon, 2015-2020

GRANTS, AWARDS, AND HONORS:

John Keana Graduate Fellowship, University of Oregon, 2019

Promising Scholar Award, University of Oregon, 2015

Departmental Scholar, SUNY Potsdam, 2015

Alexander G. Major Award, SUNY Potsdam, 2014

Jesse J. McNall Award, SUNY Potsdam, 2014

PUBLICATIONS:

Cerda, M.M.; Mancuso, J.L.; Mullen, E.J.; Hendon, C.H.; Pluth, M.D. Use of Dithiasuccinoyl-Caged Amines Enables COS/H₂S Release Lacking Electrophilic Byproducts. *Chem. Eur. J.* **2020**, DOI: 10.1002/chem.201905577

Levinn, C.M.; Cerda, M.M.; Pluth, M.D. Activatable Small Molecule H₂S Donors. *Antioxid. Redox Signal.* **2020**, 32 (2), 96-109.

Levinn, C.M.; Cerda, M.M.; Pluth, M.D. Development and Application of Carbonyl Sulfide-based Donors for H₂S Delivery. *Acc. Chem. Res.* **2019**, 52 (9), 2723-2731.

Zhao, Y.; Cerda, M.M.; Pluth, M.D. Fluorogenic Hydrogen Sulfide (H₂S) Donors Based on Sulfenyl Thiocarbonates Enable H₂S Tracking and Quantification. *Chem. Sci.* **2019**, 10 (6), 1873-1878.

Bolton, S.G.; Cerda, M.M.; Gilbert, A.K.; Pluth, M.D. Effects of Sulfane Sulfur in Benzyl Polysulfides on Thiol-Triggered H₂S Release and Cell Proliferation. *Free Radic. Biol. Med.* **2019**, 131, 393-398.

Cerda, M.M.; Newton, T.D.; Zhao, Y.; Collins, B.K.; Hendon, C.H.; Pluth, M.D. Dithioesters: Simple, Tunable, Cysteine-Selective H₂S Donors. *Chem. Sci.* **2019**, 10 (6), 1773-1779.

Cerda, M.M.; Zhao, Y.; Pluth, M.D. Thionoesters: A Native Chemical Ligation-Inspired Approach to Cysteine-Triggered H₂S Donors. *J. Am. Chem. Soc.* **2018**, 140 (39), 12574-12579.

Cerda, M.M.; Pluth, M.D. S Marks the Spot: Linking the Antioxidant Activity of N-Acetyl Cysteine to H₂S and Sulfane Sulfur Species. *Cell Chem. Biol.* **2018**, 25 (4), 353-355.

Guo, W.; Wawrzyniakowski, Z.D.; Cerda, M.M.; Bhargav, A.; Pluth, M.D.; Ma, Y.; Fu, Y. Bis(aryl) Tetrasulfides as Cathode Materials for Rechargeable Lithium Batteries. *Chem. Eur. J.* **2017**, 23 (67), 16941-16947.

Cerda, M.M.; Hammers, M.D.; Earp, M.S.; Zakharov, L.N.; Pluth, M.D. Applications of Synthetic Organic Tetrasulfides as H₂S Donors. *Org. Lett.* **2017**, 19 (9), 2314-2317.

Hammers, M.D.; Taormina, M.J.; Cerda, M.M.; Montoya, L.A.; Seidenkranz, D.T.; Parthasarathy, R.; Pluth, M.D. A Bright Fluorescent Probe for H₂S Enables Analyte-Responsive, 3D Imaging in Live Zebrafish Using Light Sheet Fluorescence Microscopy. *J. Am. Chem. Soc.* **2015**, 137 (32), 10216-10223.

ACKNOWLEDGMENTS

First and foremost, I would like to thank my parents Eileen Enmanuel and Luis E. Cerda for their unwavering support in my upbringing and education. I also wish to thank my grandparents Altagracia Soto, Angela Cerda, and Luis A. Cerda for their sacrifices and the hardships they endured as immigrants from the Dominican Republic in the US.

I wish to express my deepest appreciation to the educators who have guided my path in chemistry beginning with my high school chemistry teacher, Br. Robert Chiulli, O. Carm, for introducing me to chemistry and encouraging me to pursue higher education. My undergraduate research advisor, Dr. Anthony A. Molinero, for his patience and unparalleled mentorship as I tackled the total synthesis of (+)-carotol under his supervision. My chemistry professors, Dr. Maria Hepel, Dr. Martin A. Walker, and Dr. Fadi Bou-Abdallah, for teaching me how to appreciate the interdisciplinary nature of chemistry. My graduate advisor, Dr. Michael D. Pluth, for his exceptional guidance throughout my graduate career. My rotation mentors, Dr. Brittany M. White, Dr. Alan D. Moghaddam, and Dr. Matthew D. Hammers, for their encouragement during my turbulent first year of graduate school. My committee chair, Dr. Michael D. Haley, and members, Dr. Darren W. Johnson and Dr. Raghuvveer Parthasarathy, for their curiosity and key insights.

I would not have survived graduate school without the friends I have made during my time at UO and I would like to acknowledge their contributions to my graduate career. To my former lab mates, Hillary A. Henthorn and Dr. Daniel T. Seidenkranz for teaching me how to successfully navigate through graduate school and Dr. Yu Zhao for insightful scientific discussions. To Dr. Nathanael Lau, for his outstanding graphic design skills and our sports related banter. To my graduate and undergraduate student mentees, Annie K.

Gilbert, Turner D. Newton, Emma J. Mullen, and Julia M. Fehr, for their persistence in lab and respective contributions to research. To current members of the Pluth lab, Carolyn M. Levinn, Sarah G. Bolton, and Dr. Tobias J. Sherbow, for fostering a supportive and collaborative research environment. To Dr. Justin T. Barry and Dr. Jeff M. Van Raden, for their critical feedback in preparation for my advancement to candidacy exam. To my collaborators aboard the H.M.S Oregon, Brylee K. Collins, Jenna L. Mancuso, and Dr. Christopher H. Hendon, for providing vital computational insights. To my cohort, Danielle M. Hamann, Justin J. Dressler, Erik J. Leonhardt, for their constant support during our journey through graduate school. To Joshua E. Barker and Jeremy P. Bard for supporting our contributions to Max's Tavern. To members of the chemistry recreational softball team "Alkynes of Trouble" for good times on and off the field. To my trusty feline companion, Maximus (Max) Mojo Cerda, for keeping me sane and contributing unwanted edits as he walked across my keyboard. To my partner, Kiana E. Kawamura, for her companionship, love, and countless baked goods.

Lastly, I would like to thank the National Institute of Health (R01GM113030), National Science Foundation (CHE-1454747), Camille and Henry Dreyfus Foundation, and the University of Oregon (John Keana Graduate Student Fellowship) for the funding support that made this dissertation possible.

Dedicated to Altagracia Soto, Angela Cerda, Luis A. Cerda, and the American Dream.

TABLE OF CONTENTS

Chapter	Page
I. ACTIVATABLE SMALL-MOLECULE HYDROGEN SULFIDE DONORS	1
1.1 Introduction.....	1
1.2 Enzyme Activated Donors	5
1.3 Reactive Oxygen Species-Activated Donors	9
1.4 Hydrolysis-Based and pH-Sensitive Donors	11
1.5 Thiol-Activated Donors	14
1.6 Photoactivated Donors	20
1.7 Miscellaneous Activatable Donors	24
1.8 Conclusions and Outlook.....	26
II. THIONOESTERS: A NATIVE-CHEMICAL LIGATION INSPIRED APPROACH TO CYSTEINE-TRIGGERED H ₂ S DONORS.....	28
2.1 Introduction.....	28
2.2 Results and Discussion	32
2.3 Conclusions.....	42
2.4 Experimental Details.....	43
III. DITHIOESTERS: SIMPLE, TUNABLE CYSTEINE-SELECTIVE H ₂ S DONORS	48
3.1 Introduction.....	48
3.2 Results and Discussion	52
3.3 Conclusions.....	64
3.4 Experimental Details.....	65
Chapter	Page

IV. APPLICATIONS OF SYNTHETIC ORGANIC TETRASULFIDES AS H ₂ S DONORS	74
4.1 Introduction.....	74
4.2 Results and Discussion	76
4.3 Conclusions.....	83
4.4 Experimental Details.....	84
V. EFFECTS OF SULFANE SULFUR CONTENT IN BENZYL POLYSULFIDES ON THIOL-TRIGGERED H ₂ S RELEASE AND CELL PROLIFERATION	90
5.1 Introduction.....	90
5.2 Results and Discussion	93
5.3 Conclusions.....	99
5.4 Experimental Details.....	100
VI. USE OF DITHIASUCCINOYL-CAGED AMINES ENABLES COS/H ₂ S RELEASE LACKING ELECTROPHILIC BYPRODUCTS	106
6.1 Introduction.....	106
6.2 Results and Discussion	109
6.3 Conclusions.....	116
6.4 Experimental Details.....	117
VII. COLORIMETRIC AND FLUORESCENT DETECTION OF CARBONYL SULFIDE	131
7.1 Introduction.....	131
7.2 Results and Discussion	133
7.3 Conclusions.....	137
7.4 Concluding Remarks.....	138
Chapter	Page

7.5 Experimental Details.....	138
APPENDICES	141
A. CHAPTER I SUPPLEMENTARY INFORMATION	141
B. CHAPTER II SUPPLEMENTARY INFORMATION	155
C. CHAPTER III SUPPLEMENTARY INFORMATION.....	160
D. CHAPTER IV SUPPLEMENTARY INFORMATION	175
E. CHAPTER V SUPPLEMENTARY INFORMATION	186
F. CHAPTER VI SUPPLEMENTARY INFORMATION.....	195
G. CHAPTER VII SUPPLEMENTARY INFORMATION.....	222
REFERENCES CITED.....	225

LIST OF FIGURES

Figure	Page
1. Figure 1.1 Selected roles of H ₂ S in major organ systems	2
2. Figure 1.2 General classes of H ₂ S release from small-molecule donors	5
3. Figure 1.3 Enzyme-activated donors and associated enzymes. (a) Structures of enzymatically-activated COS and H ₂ S donors. (b) Structure of PLE and <i>Escherichia coli</i> NTR.....	6
4. Figure 1.4 H ₂ O ₂ -activated COS donors scaffolds	9
5. Figure 1.5 Hydrolysis-activated H ₂ S donors. The pH windows shown represent specific pH values or pH windows in which H ₂ S release was reported or in which H ₂ S release was reported to be optimal.....	12
6. Figure 1.6 Structures of donor compounds activated in the presence of biological thiols. (a) H ₂ S donors activated in the presence of cysteine. (b) H ₂ S donors activated in the presence of cysteine and GSH	15
7. Figure 1.7 Structures and excitation wavelengths of selected photoactivatable H ₂ S donors	21
8. Figure 1.8 Structures of COS-based donor compounds activated by miscellaneous activators. (a) H ₂ S-activated analyte replacement probe. (b) “Click and release” biorthogonal COS-based H ₂ S donors. (c) Activation of <i>N</i> -thiocarboxyanhydride by glycine to generate H ₂ S.....	25
9. Figure 2.1 (a) Representative examples of common synthetic, small molecule H ₂ S donors; (b) Selected small molecule, thiol-triggered H ₂ S donors	29
10. Figure 2.2 Generalized reaction scheme for native chemical ligation and release of H ₂ S upon addition of cysteine to a <i>bis</i> (phenyl) thionoester	31
11. Figure 2.3 (a) Release of H ₂ S from DPTE in the presence of increasing cysteine concentrations (25, 125, 250, and 500 μM) in 10 mM PBS (pH 7.4) at 25 °C. (b) Lack of H ₂ S release from structurally related compounds (25 mM) in the presence of cysteine (500 mM, 20 equiv.)	33

12. **Figure 2.4** Selectivity of H₂S release from DPTE in the presence of different analytes. Data were acquired at 1, 5, 10, 15, 30, 45, and 60 min. Methylene blue absorbance values are relative to the maximum absorbance value obtained from H₂S release in the presence of cysteine (1). Analytes: H₂O/PBS buffer (2), serine (3), lysine (4), L-homocysteine (5), DL-penicillamine (6), L-cysteine methyl ester hydrochloride (7), *N*-acetyl-L-cysteine (8), *N*-acetyl-L-cysteine methyl ester (9), *S*-methyl-L-cysteine (10), GSH (11), cysteine + GSH (12), cysteine + lysine (13), PLE (1.0 U/mL) (14)34
13. **Figure 2.5** (a) H₂S release by DPTE in the presence of increasing cysteine concentrations (250, 500, 1000, and 1250 μM). (b) Plot of log(*k*_{obs}) vs log([Cys]) for DPTE. (c) Plot of *k*_{obs} vs [Cys]38
14. **Figure 2.6** (a) Effect of temperature on rate of H₂S release from DPTE (25 μM) in the presence of cysteine (500 μM, 20 equiv). (b) Eyring analysis of H₂S release from DPTE39
15. **Figure 2.7** (a) Reaction conditions; (b) 100 μM DPTE in 10 mM PBS (pH 7.4) with 10% THF; (c) 100 μM PhOH in 10 mM PBS (pH 7.4) with 10% THF; (d) 100 μM CysDHT in 10 mM PBS (pH 7.4) with 10% THF; (e) reaction aliquot after 1 h41
16. **Figure 3.1** Selected examples of synthetic H₂S donors.....50
17. **Figure 3.2** (a) Cysteine-triggered H₂S release from thionoesters. (b) Cysteine-triggered H₂S release from dithioesters51
18. **Figure 3.3** (a) Release of H₂S from PDTE (25 μM) in the presence of increasing cysteine concentrations (250, 500, 1000, and 1250 μM). (b) Plot of log(*k*_{obs}) vs. log([Cys]). (c) Plot of *k*_{obs} vs. [Cys]54
19. **Figure 3.4** Selectivity of H₂S release from PDTE in the presence of different analytes. Data were acquired at 1, 5, 10, 15, 30, 45, and 60 min. Methylene blue absorbance values are relative to the maximum absorbance value obtained from H₂S release in the presence of cysteine (1). Analytes: H₂O (2), *N*-acetyl-L-cysteine (3), *S*-methyl-L-cysteine (4), L-cysteine methyl ester hydrochloride (5), *N*-acetyl-L-cysteine methyl ester (6), DL-homocysteine (7), DL-penicillamine (8), GSH (9), cysteine + 1 mM GSH (10).....56
20. **Figure 3.5** (a) Effect of temperature on rate of H₂S release from PDTE (25 μM) in the presence of cysteine (500 μM, 20 equiv.). (b) Eyring analysis of cysteine-triggered H₂S release from PDTE58

Figure	Page
21. Figure 3.6 Potential energy surface for the attack of cysteine thiolate on PDTE . Calculations were performed in Gaussian 09 at the B3LYP/6-311++G(d,p) level of theory applying the IEF-PCM water solvation model.....	60
22. Figure 3.7 Effect of alkyl functionalization on the rate of H ₂ S release from dithioesters	61
23. Figure 3.8 (a) Effect of pendant groups on thiocarbonyl electrophilicity and carbocation stability. (b) Scale of increasing H ₂ S releasing rates for reported dithioesters	62
24. Figure 4.1 (a) Mechanism of H ₂ S release from DATS in the presence of GSH . (b) Representative examples of natural products containing polysulfides.....	76
25. Figure 4.2 (a) Mass spectrum (EI-MS) of 3 . (b) ORTEP representation (50% ellipsoids) of the molecular structure of 4	79
26. Figure 4.3 Proposed mechanisms of H ₂ S release from tetrasulfides, including initial nucleophilic attack by GSH at the (a) β -sulfur or (b) α -sulfur	80
27. Figure 4.4 (a) GSH -dependent H ₂ S release from 3 . (b) $\log(k)$ vs $\log[\text{GSH}]$ plot demonstrating a 1st-order dependence in $[\text{GSH}]$ on H ₂ S release from 3	81
28. Figure 4.5 GSH -triggered (250 equiv) H ₂ S release from 5 μM tetrasulfides 1–8 and 5 μM DATS (pH 7.4, room temperature).....	82
29. Figure 5.1 Common S ⁰ -containing small molecule species release H ₂ S upon reaction with biological thiols.....	91
30. Figure 5.2 (a) Synthesis of Bn₂S₄ . (b) Synthesis of Bn₂S₃ . (c) Comparison of benzylic ¹ H NMR (500 MHz) signals between Bn₂S₂ , Bn₂S₃ , and Bn₂S₄ in CDCl ₃	94
31. Figure 5.3 (a) Reaction conditions for thiol-triggered release of H ₂ S from Bn₂S_n (n = 1, 2, 3, or 4). (b) Release of H ₂ S in the presence of cysteine. (c) Release of H ₂ S in the presence of GSH	96
32. Figure 5.4 bEnd.3 cell viability after 24-h treatment of a series of organic polysulfides: (a) Bn₂S , (b) Bn₂S₂ , (c) Bn₂S₃ , (d) Bn₂S₄ , and (e) DATS . * $p < 0.05$, ** $p < 0.01$, *** $p < 0.001$	98

Figure	Page
33. Figure 6.1 (a) Generalized reaction mechanism for COS release from self-immolative thiocarbamates and subsequent hydrolysis of COS to H ₂ S by carbonic anhydrase. (b) Overall reaction scheme of COS release from dithiasuccinoyl groups in the presence of thiols	108
34. Figure 6.2 Activation profiles of H ₂ S release from PhDTS (25 μM) in the presence of different nucleophiles (500 μM, 20 equiv) and carbonic anhydrase (25 μg mL ⁻¹). Data were acquired at 1, 5, 10, 15, 30, 45, and 60 min. Methylene blue absorbance values are relative to the maximum absorbance value obtained from H ₂ S release in the presence of cysteine (3). Analytes: H ₂ O with no carbonic anhydrase (1), cysteine with no carbonic anhydrase (2), <i>N</i> -acetyl-L-cysteine (4), L-cysteine methyl ester (5), <i>N</i> -acetyl-L-cysteine methyl ester (6), homocysteine (7), reduced glutathione (8), serine (9), lysine (10), only carbonic anhydrase (11), <i>S</i> -methyl cysteine (12).....	110
35. Figure 6.3 (a) H ₂ S release from aryl-based DTS compounds. (b) H ₂ S release from alkyl-based DTS compounds	113
36. Figure 6.4 Potential energy surface for COS release from PhDTS and AlkylDTS compounds. Calculations were performed using Gaussian 09 at the B3LYP/6-311++G(d,p) level of theory applying the IEF-PCM water solvation model. MeSH was used as the thiol nucleophile to simplify accessible protonation states of non-participating functional groups on the thiol nucleophile.....	115
37. Figure 7.1 (a) Reaction of CO ₂ and TBBI in the presence of fluoride. (b) Reaction between CS ₂ and TBBI in the presence of fluoride. (c) Proposed reaction between COS and TBBI in the presence of fluoride	133
38. Figure 7.2 (a) Acid-mediated hydrolysis of KSCN to generate COS. (b) Schematic of laboratory-scale COS synthesis and purification	134
39. Figure 7.3 (a) Reaction of TBBI with COS. (b) UV-Vis spectra and (c) Fluorescence spectra for TBBI (15 mM), TBAF (90 mM), and COS (5.0 mL).....	136
40. Figure 7.4 Naked-eye detection and differentiation of CO ₂ , CS ₂ , and COS using TBBI (10 mM) in the presence of TBAF (60 mM).....	137

LIST OF TABLES

Table	Page
1. Table 4.1 Synthesis of <i>bis</i> (aryl) and <i>bis</i> (alkyl) tetrasulfides	77

LIST OF SCHEMES

Scheme	Page
1. Scheme 2.1 Proposed mechanism of H ₂ S release from DPTE in the presence of cysteine	37
2. Scheme 2.2 Preparative scale synthesis of CysDHT from DPTE	45
3. Scheme 2.3 Synthesis of CysDHT from DPTE for reaction product analysis by HPLC	46
4. Scheme 2.4 Synthesis of <i>O</i> -phenyl benzothioate (DPTE)	47
5. Scheme 3.1 General synthesis of dithioesters	52
6. Scheme 3.2 Proposed mechanism for release of H ₂ S from PDTE in the presence of cysteine	57
7. Scheme 3.3 Preparative scale synthesis of CysDHT from PDTE	67
8. Scheme 3.4 Synthesis of thioesters.....	68
9. Scheme 3.5 Synthesis of dithioesters	71
10. Scheme 6.1 Synthesis of DTS-based COS/H ₂ S donors.....	110
11. Scheme 6.2 Reaction analysis products of PhDTS in the presence of cysteine	128
12. Scheme 7.1 Synthesis of TBBI	140

CHAPTER I

ACTIVATABLE SMALL-MOLECULE HYDROGEN SULFIDE DONORS

This chapter includes previously published and co-authored material from Levinn, C.M.; Cerda, M.M.; Pluth, M.D. Activatable Small-Molecule Hydrogen Sulfide Donors. *Antioxid. Redox Signal.* **2020**, *32* (2), 96-109. This review was co-written by Carolyn M. Levinn and Matthew M. Cerda with editorial assistance from Professor Michael D. Pluth.

1.1 Introduction

Hydrogen sulfide (H₂S), historically dismissed as a toxic and malodorous gas, has emerged in the scientific community as an important biological signaling molecule.¹ The physicochemical properties of H₂S have been studied extensively, and we refer the interested reader to recent reviews that cover this area in depth.² Since its initial recognition as a relevant biomolecule, diverse scientific communities ranging from chemists to physiologists have focused on investigating the role of H₂S in various biological systems. H₂S is produced endogenously in mammals predominantly from cysteine through the action of three main enzymes. Cystathionine-β-synthase is primarily localized in the nervous system, brain, and liver; cystathionine-γ-lyase produces H₂S primarily in the cardiovascular system; and 3-mercaptopyruvate sulfurtransferase is localized in the mitochondria.^{1a, 3} Investigations into the biological roles of H₂S have established its critical roles in different disease states and pathologies in almost every human organ system (Figure 1.1).⁴

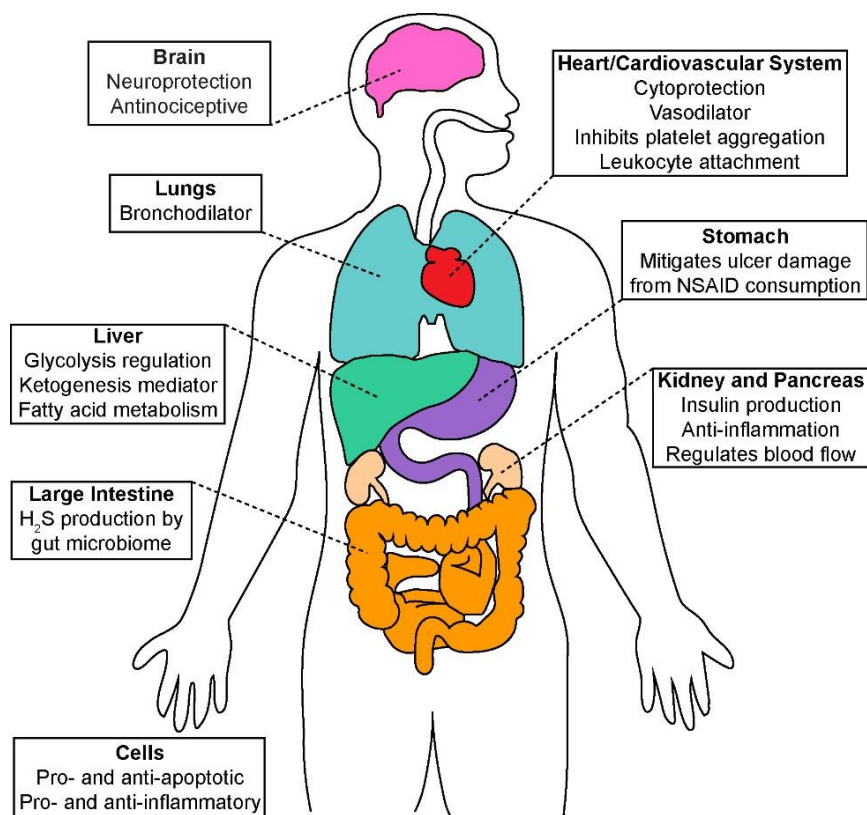


Figure 1.1 Selected roles of H₂S in major organ systems.

As brief examples, H₂S plays important roles in the central nervous system, participates in neurotransmission, and has been shown to have neuroprotective effects, specifically in mouse models of Parkinson’s disease.⁵ In addition, H₂S upregulates glutathione (GSH) production in the brain during periods of high oxidative stress and contributes to regulating key sodium channels in neuronal cells.^{5c} In the respiratory system, H₂S plays roles in different conditions, including chronic obstructive pulmonary disease, pulmonary fibrosis, and hypoxia-induced pulmonary hypertension.⁶ In the cardiovascular system, H₂S mitigates oxidative stress and reduces myocardial injury related to ischemia–reperfusion events.⁷ Moreover, lower circulating H₂S levels are found in experimental models of heart

failure, and CSE-deficient mice exhibit greater cardiac dysfunction after transverse aortic constriction, both of which suggest additional roles of H₂S in heart failure.⁸

More broadly, H₂S interacts through several signaling pathways, such as the K_{ATP} channels, and promotes angiogenesis by the protein kinase B and phosphatidylinositol 3-kinase pathways. Low levels of H₂S have been demonstrated to promote cell proliferation and migration.⁹ Importantly, the activity of administered H₂S often shows a stark concentration dependence, with low versus high concentrations frequently producing contrasting effects. More recently, a study of psoriasis patients demonstrated lower serum H₂S levels than healthy patients, underscoring the potential role that H₂S plays in skin protection and repair.¹⁰ As a whole, the established pathophysiological targets of H₂S are

incredibly diverse, and they include activities as an established antiapoptotic,¹¹ anti-inflammatory,¹² and antioxidative agent,¹³ as well as contributing to many other processes.

With such a broad range of biological targets and activities, significant effort has focused on investigating and understanding the direct effects of H₂S on specific systems with a long-term goal of leveraging these insights to deliver H₂S-related therapeutic interventions. Much of the preliminary work in this area relied on direct inhalation of H₂S or administration of inorganic sulfide salts, such as sodium hydrosulfide and sodium sulfide (Na₂S). Although highly efficient, these systems often release an instantaneous bolus of H₂S and fail to mimic the more gradual rates or distributions of endogenous H₂S production.¹⁴ This discrepancy, as well as other significant limitations, has driven the development of small-molecule “donors” that are capable of releasing H₂S under physiologically-relevant conditions and in response to specific stimuli.

Many reported H₂S donor systems respond to specific exogenous or biocompatible stimuli to release H₂S.^{2b, 2f, 15} Such activation profiles allow for donor activities to be tuned to respond to specific activators and stimuli present in a given system. Although there is no single universal “ideal donor,” certain donor classes provide distinct advantages and useful properties. For example, donors should have readily accessible control compounds that can be used to clearly delineate observed biological activities and outcomes associated with H₂S from those of donor byproducts. Similarly, donors that respond to specific stimuli enable experiments in which H₂S delivery can be controlled or triggered by specific activators. Coincident with these primary needs, significant advances in the development of activatable H₂S donors have occurred in the past 5 years, with key examples including donors activated by light, various pH regimes, enzymes, biological thiols, and hydrogen peroxide (H₂O₂).

In developing activatable H₂S-releasing donors, a number of primary strategies have emerged, which are summarized briefly in this section but are expanded on in various sections of this review (Figure 1.2). The first commonly used strategy is to replace an oxygen atom in a molecule with a sulfur, such that hydrolysis releases H₂S. A second common strategy is to develop systems that generate an intermediate persulfide, which can be subsequently cleaved by thiols, such as reduced glutathione (GSH) or cysteine, to generate H₂S and a disulfide. A third strategy is to develop systems that release carbonyl sulfide (COS) as an intermediate, which can be quickly converted to H₂S, the ubiquitous mammalian enzyme carbonic anhydrase (CA).¹⁶ These three general approaches are summarized in Figure 1.2 and will be discussed briefly throughout the review. Rather than focus on the mechanistic details of each structure in this review, we refer interested readers

to the Supplementary Appendix, which includes the activation mechanism of different donor platforms (Appendix A).

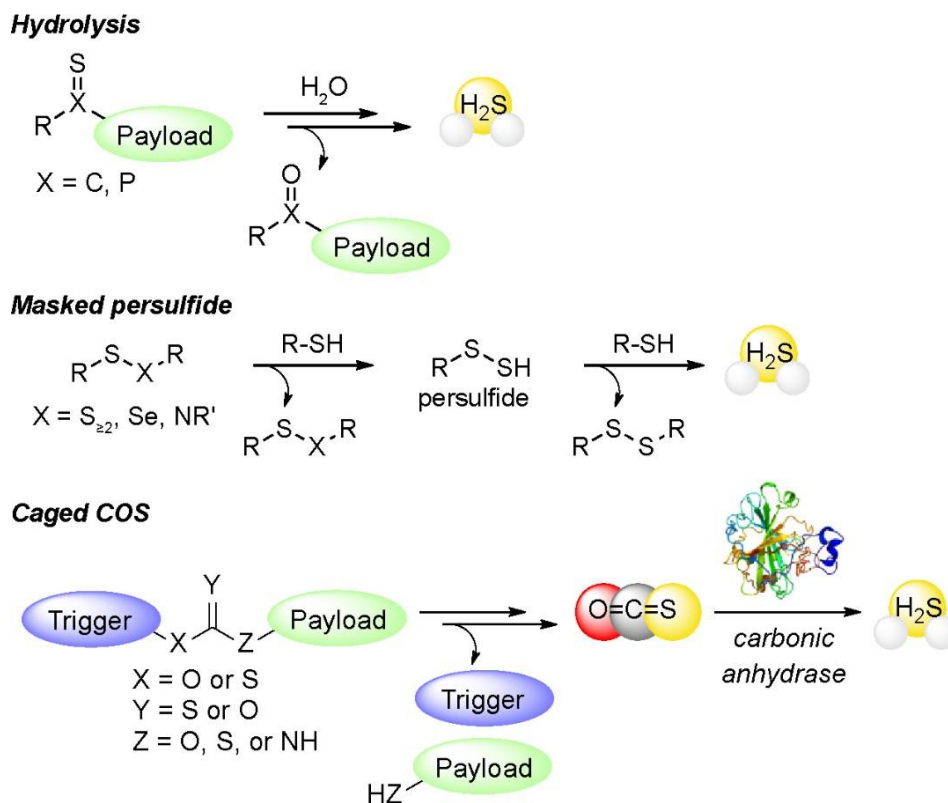


Figure 1.2 General classes of H₂S release from small-molecule donors

1.2 Enzyme-Activated Donors

Because H₂S has myriad biological targets, disentangling the effects of sulfide delivery in specific environments can be challenging. One approach to overcome this difficulty is to incorporate an enzymatically cleaved trigger on a sulfide donor. This approach allows for donors to be developed that are stable until the activating group is cleaved or modified by the target enzyme to release H₂S or an H₂S equivalent, such as COS. This strategy has the benefit of being readily tuned to specific triggering groups and enzyme pairs. In

addition, utilizing an enzyme to carry out the donor activation event does not consume cellular nucleophiles or thiols, which could otherwise perturb the redox balance of related reactive sulfur species – an inherent challenge with many thiol-triggered H₂S donors

The first enzyme-triggered H₂S donor, HP-101, was reported by Zheng *et al.* (Figure 1.3a).¹⁷

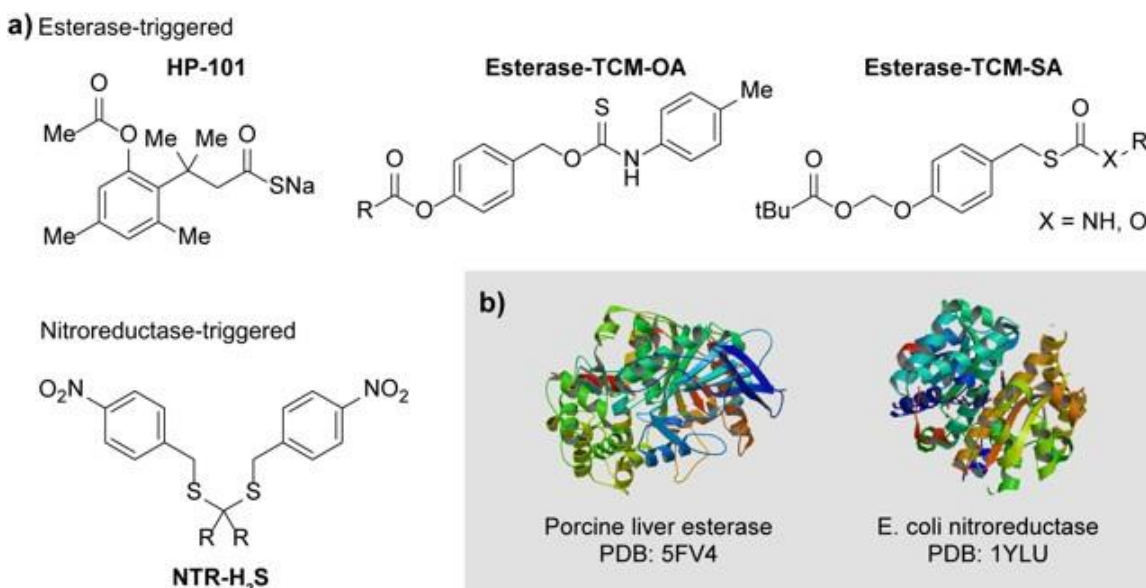


Figure 1.3 Enzyme-activated donors and associated enzymes. (a) Structures of enzymatically-activated COS and H₂S donors. (b) Structure of PLE and *Escherichia coli* NTR.

In this system, esterase-mediated cleavage of an acyl-protecting group on the donor motif was used to generate an unstable phenolic intermediate that subsequently underwent an intramolecular lactonization with a pendant thioacid to release H₂S.¹⁷ Esterases are expressed in most tissue types and are involved in the activation or metabolism of ~10% of drugs (Figure 1.3b).¹⁸ One benefit of this design is that the rate of H₂S release could be tuned by varying the identity of the ester triggering group or by modifying the geminal-dimethyl substitution in the “trimethyl lock” backbone to facilitate lactonization. Notably,

the authors were able to conjugate this sulfide-donating scaffold to the nonsteroidal anti-inflammatory drug naproxen, forming an activatable H₂S-drug hybrid.

In 2017, both Chauhan *et al.*¹⁹ and our group²⁰ independently reported esterase-activated donors that functioned through the intermediacy of COS release. In these approaches, self-immolative thiocarbamates or thiocarbonates functionalized with ester motifs were enzymatically activated to release COS, which is rapidly metabolized to H₂S by CA, rather than H₂S directly. In this context, “self-immolation” refers to the spontaneous cascade reaction of a molecular linker after a chemical triggering event that results in release of a desired payload.

Chauhan *et al.*¹⁹ utilized a *tert*-butyl ester trigger with an extended methylenedioxy linker to connect the donor motif to the core amine scaffold. These donors, such as Esterase-TCM-SA, encompassed both aryl and benzyl amine terminating *S*-alkyl thiocarbamates, as well as *S*-alkyl thiocarbonates (Figure 1.3a). The different scaffolds exhibited different release rates based on the identity of the parent amine, and different toxicity profiles toward MCF-7 (human breast cancer) cells. Our group also reported *tert*-butyl ester triggered motifs, including the donor compound Esterase-TCM-OA, as well as the analogous triggerless and sulfide-depleted carbamate control compounds (Figure 1.3a).²⁰ The COS/H₂S donors showed significant cytotoxicity in BEAS 2B human lung epithelial cells when compared with the carbamate and triggerless control compounds or with equivalent concentrations of the H₂S sources/donors Na₂S, AP39, or GYY4137.

Further investigations using bioenergetics assays revealed that the esterase-activated thiocarbamate donors inhibited mitochondrial respiration, whereas exogenous H₂S or the triggerless and sulfur-depleted control compounds did not. Building from the

hypothesis that the observed cytotoxicity could be due to a buildup of COS in the mitochondria, due to faster rates of ester cleavage and self-immolation than COS hydrolysis by CA, we prepared a suite of esterase-triggered self-immolative thiocarbamates with esters of varying steric bulk. These esters displayed different rates of COS release, which correlated inversely with cytotoxicity in HeLa (human cervical cancer) cells. Again, the triggerless control and sulfur-depleted control compounds failed to show significant cytotoxicity, showing the utility of having readily accessible control compounds. These results support the hypothesis that COS may function as more than a simple H₂S shuttle in certain circumstances; however, these observations do not account for differences in subcellular localization of different donors or differential activities of various CA isoforms toward COS.²¹ We do note that as a whole, most developed COS-releasing compounds appear to function as H₂S donors, with activities directly attributable to the release of H₂S.

Shukla *et al.*²² further expanded work on enzyme-triggered donor platforms to develop donors activated by bacterial nitroreductase (NTR) (Figure 1.3b). NTRs are frequently found in bacteria and are also upregulated under hypoxic conditions in different cell types.²³ The NTR-mediated reduction of the electron-withdrawing nitro groups on NTR-H₂S to the corresponding aniline, with the nitrogen lone pair now free to resonate through to release the (imino)quinone methide, was used to reveal a geminal-dithiol intermediate that hydrolyzes in buffer to generate H₂S (Figure 1.3a). H₂S release was confirmed and measured in these systems by using monobromobimane and fluorescence assays. These donors have been used to study the role of H₂S in the intracellular redox

balance and the development of antibiotic resistance in bacteria, specifically *Escherichia coli*.²²

1.3 Reactive Oxygen Species-Activated Donors

H₂S exhibits anti-inflammatory activities and protective effects against reactive oxygen species (ROS), which has motivated a number of groups to develop H₂S donors that are activated in the presence of ROS, such as H₂O₂. The cellular localization and levels of these ROS can vary in response to different stress states. In 2016, our group reported a caged thiocarbamate equipped with a pinacol boronate ester, Peroxy-TCM-OA, that self-immolates on exposure to H₂O₂ to release COS (Figure 1.4).²⁴

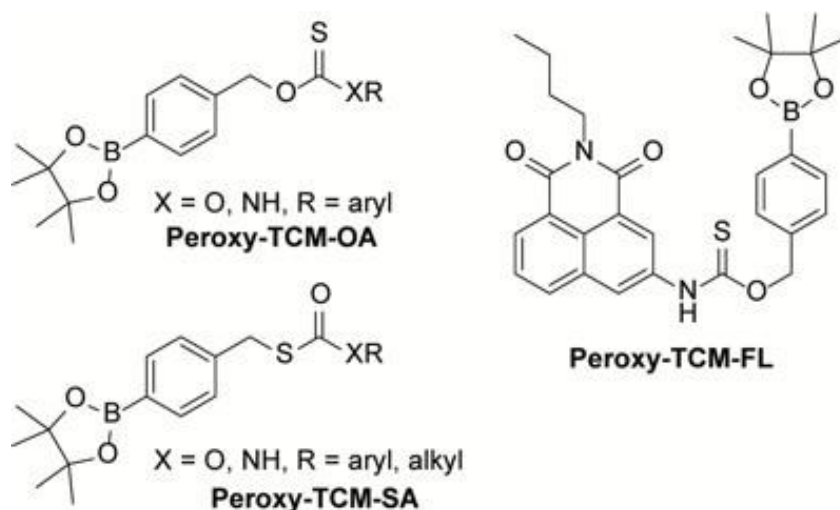


Figure 1.4 H₂O₂-activated COS donor scaffolds.

These thiocarbamate donors are stable toward aqueous hydrolysis, but respond to H₂O₂, and to a lesser extent to superoxide and peroxynitrite, to release H₂S. In these studies, H₂S release was measured by using an H₂S-responsive electrode, and fluorescence imaging in HeLa cells confirmed that the thiocarbamate donor could be activated in a biological

environment with either exogenous H₂O₂ or endogenous ROS. Cytotoxicity experiments showed that the donor provided cytoprotection against exogenous H₂O₂ treatment. The sulfur-depleted control compounds showed modest cytoprotection, due to H₂O₂ consumption by the boronate moiety, whereas the triggerless control compounds failed to provide protection against H₂O₂ as expected. These experiments underscore the importance of having high fidelity control compounds to fully understand the mechanism of action of donor molecules.

Expanding from this initial report, we reported experimental and computational investigations of all the COS-releasing isomers of boronate-functionalized thiocarbamates and thiocarbonates.²⁵ We found that *S*-alkyl thiocarbamates, Peroxy-TCM-SA, released H₂S slower than the analogous *S*-alkyl thiocarbonates, and that *S*-alkyl dithiocarbonate released H₂S faster and more efficiently than the other *S*-alkyl derivatives. Further contributing to the understanding of COS/H₂S release profiles, Chauhan *et al.*²⁶ employed related *S*-alkyl boronate-functionalized thiocarbamates to demonstrate that the rate of H₂O₂-triggered COS release can additionally be tuned by the basicity of the amine payload. These investigations also demonstrated that alkyl amine payload, such as a propylamine, significantly reduced the rate of H₂S release when compared with aryl amine payloads.

More recently, Hu *et al.*²⁷ further leveraged the boronate-functionalized self-immolative thiocarbamates to access the turn-on fluorescent H₂S donor Peroxy-FL (Figure 1.4). Exchanging the amine payload with the 3-amino-*N*-butyl-1,8-naphthalimide fluorophore allowed for the fluorescence of this system that is modulated by cleavage of the thiocarbamate motif to generate the parent aryl amine on the naphthalimide fluorophore. H₂S generation was confirmed by using the methylene blue assay, and the

fluorescence response was demonstrated in both HeLa and RAW 264.7 (murine macrophage) cells. These donors released H₂S in response to both exogenous and endogenous H₂O₂, as demonstrated in cell culture experiments.

1.4 Hydrolysis-Based and pH-Sensitive Donors

Numerous H₂S donors are activated by hydrolysis mechanisms, and most of these respond through acid-mediated pathways. Figure 1.5 shows the structures of these donors and the pH value or ranges at which the compounds have been reported to release H₂S. This class of H₂S donors provides the unique opportunity to target specific diseases, cells, and/or organelles in which acidic microenvironments are present. As a simple example, thioacetamide can function as a pH-activated H₂S donor in extremely acidic environments (pH 1.0) and was initially used for the precipitation of dissolved metals as metal sulfides from acidic solutions for qualitative analysis.²⁸ We note that the inherent toxicity of thioacetamide has severely limited the use of this H₂S donor in biological studies.

As interest in the chemical biology of H₂S has grown, the use of related thioamides as H₂S donors has expanded to include various aryl thioamides, which are highlighted in a separate review.²⁹ Other simple small molecules have also been reported as pH-activated H₂S donors. For example, both thioglycine and thiovaline release H₂S in the presence of bicarbonate (HCO₃⁻) at physiological pH.³⁰ Both of these thioamino acids were demonstrated to increase intracellular cyclic guanosine monophosphate levels and promote vasorelaxation in mouse aortic rings, with both being more efficacious and potent than GYY4137.

One of the most commonly used, GYY4137, is a water-soluble H₂S donor that draws inspiration from Lawesson's Reagent,³¹ which is traditionally used in organic synthesis to prepare various organosulfur compounds.³² The release of H₂S from GYY4137 occurs slowly at physiological pH, but it can be accelerated under acidic conditions (pH <3.0).³³ Relative to other pH-sensitive H₂S donors, the biological activities of GYY4137

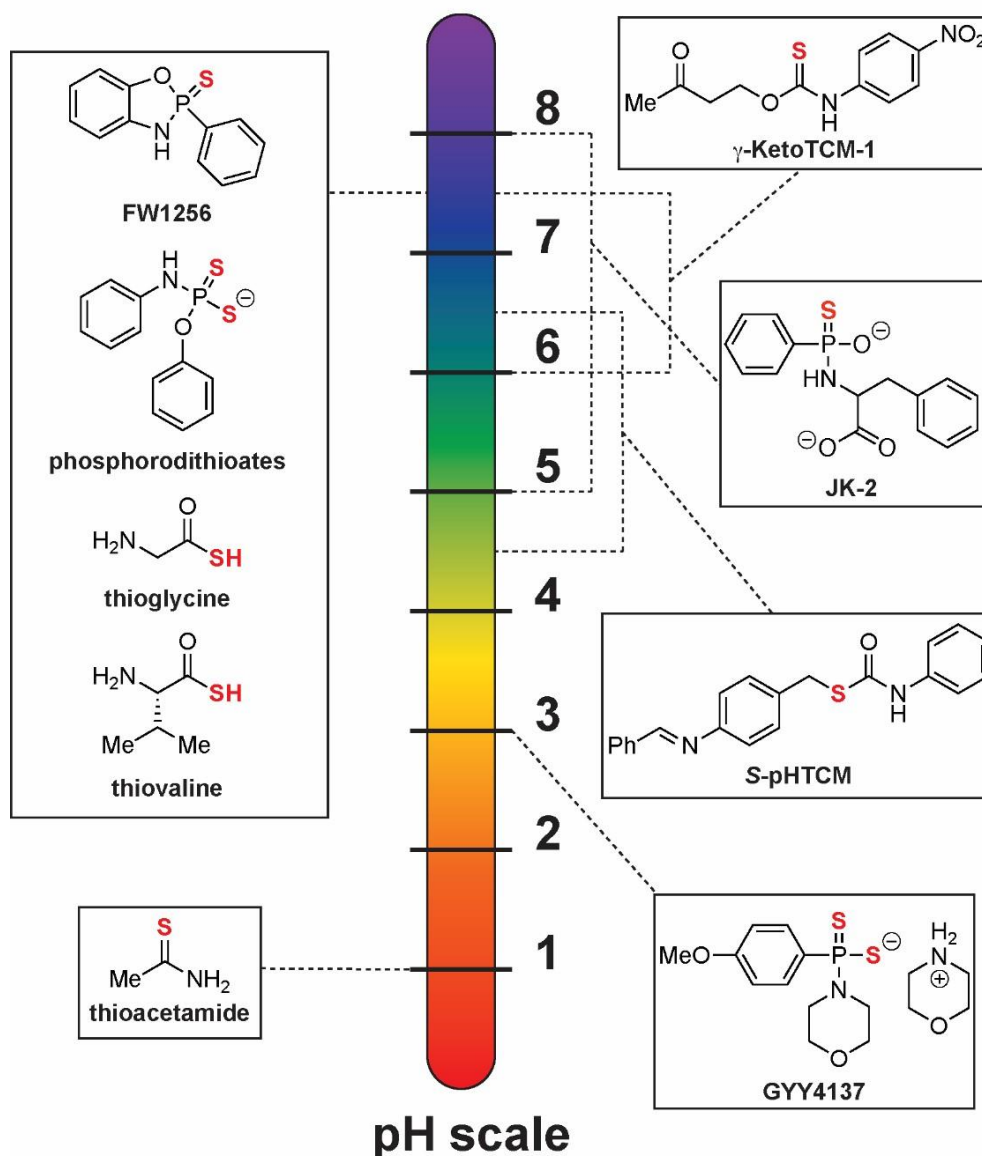


Figure 1.5 Hydrolysis-activated H₂S donors. The pH windows shown represent specific pH values or pH windows in which H₂S release was reported or in which H₂S release was reported to be optimal.

have been studied extensively and are highlighted in a separate review.³⁴ To tune the rate of pH-dependent H₂S release from P=S motifs related to GYY4137, Park *et al.*³⁵ investigated the use of analogous phosphorodithioates as H₂S donors. The inclusion of phenolic groups was found to enhance the rates of H₂S release at physiological pH, whereas alkyl alcohols decreased the efficiency of H₂S production consistent with the enhanced leaving group ability of phenols relative to alkyl alcohols. Moreover, pretreatment of H9c2 mouse cardiomyocytes with these H₂S donors provided significant cytoprotection against H₂O₂-induced oxidative damage. Interestingly, analogous experiments with GYY4137 failed to provide similar results due to the inherent cytotoxicity of this donor at higher concentrations.

In a follow-up study of phosphorodithioate-based H₂S donors by Feng *et al.*,³⁶ they prepared a library of derivative compounds and examined the H₂S-releasing properties of these compounds. The cyclized derivative FW1256 displayed relatively high levels of H₂S release and potent cytotoxicity against MCF7 breast cancer cells. In 2016, this concept was revisited by Kang *et al.*,³⁷ leading to the design of GYY4137 derivatives, including JK-2, that bear a pendant nucleophile that can participate in an intramolecular cyclization to generate H₂S.³⁷ H₂S release was demonstrated within a range of pH 5.0 to 8.0, with significant enhancements in releasing efficiency more than GYY4137. Moreover, treatment with JK-2 resulted in significant reductions in infarction size in a myocardial ischemia–reperfusion injury mouse model.

In an alternative approach, our group recently reported pH-sensitive γ -ketothiocarbamate donors, including γ -KetoTCM-1, that function through intermediate COS release. This system was inspired by the use of 4-hydroxy-2-butanone esters to

prepare self-immolative carbamate polymers that undergo β -elimination to generate carbon dioxide as a function of pH.³⁸ The release of H₂S from γ -KetoTCM-1 was measured over a range of pH values (6.0–8.0), with increasing rates in more basic solution. The H₂S release half-life could be modified by structural tuning, and the donors provided anti-inflammatory activity in RAW 264.7 cells.³⁹ More recently, we reported a self-immolative thiocarbamate (*S*-pHTCM) with a pendant aryl imine trigger as a pH-sensitive donor that releases COS/H₂S.⁴⁰ Notably, this triggering motif was designed to be activated within a specific acidic pH window and showed optimal cleavage rates between pH 4.3 and 7.3.

1.5 Thiol-Activated Donors

Compounds activated by biological thiols, including cysteine and reduced GSH, represent the largest class of small-molecule H₂S donors (Figure 1.6). The activation of many of these compounds proceed through persulfide intermediates, although others function through poorly understood mechanisms. The fundamental role and abundance of biological thiols, especially GSH, allows researchers to use these nucleophiles to probe the effects of H₂S donor administration.

Expanding from thioacetamide, many aryl thioamides have been reported as H₂S donors. These compounds are stable at physiological pH and exhibit a cysteine-dependent H₂S release, yet the mechanism of H₂S release is unclear.²⁹ The use of structurally related iminothioethers as cysteine-activated H₂S donors was reported by Barresi *et al.*⁴¹ H₂S release from these donors was evaluated in buffer containing 4 mM cysteine, and releasing efficiencies were dependent on donor derivatization. In isolated rat hearts, two donors were demonstrated to reverse the effects of angiotensin II induced reduction in basal coronary

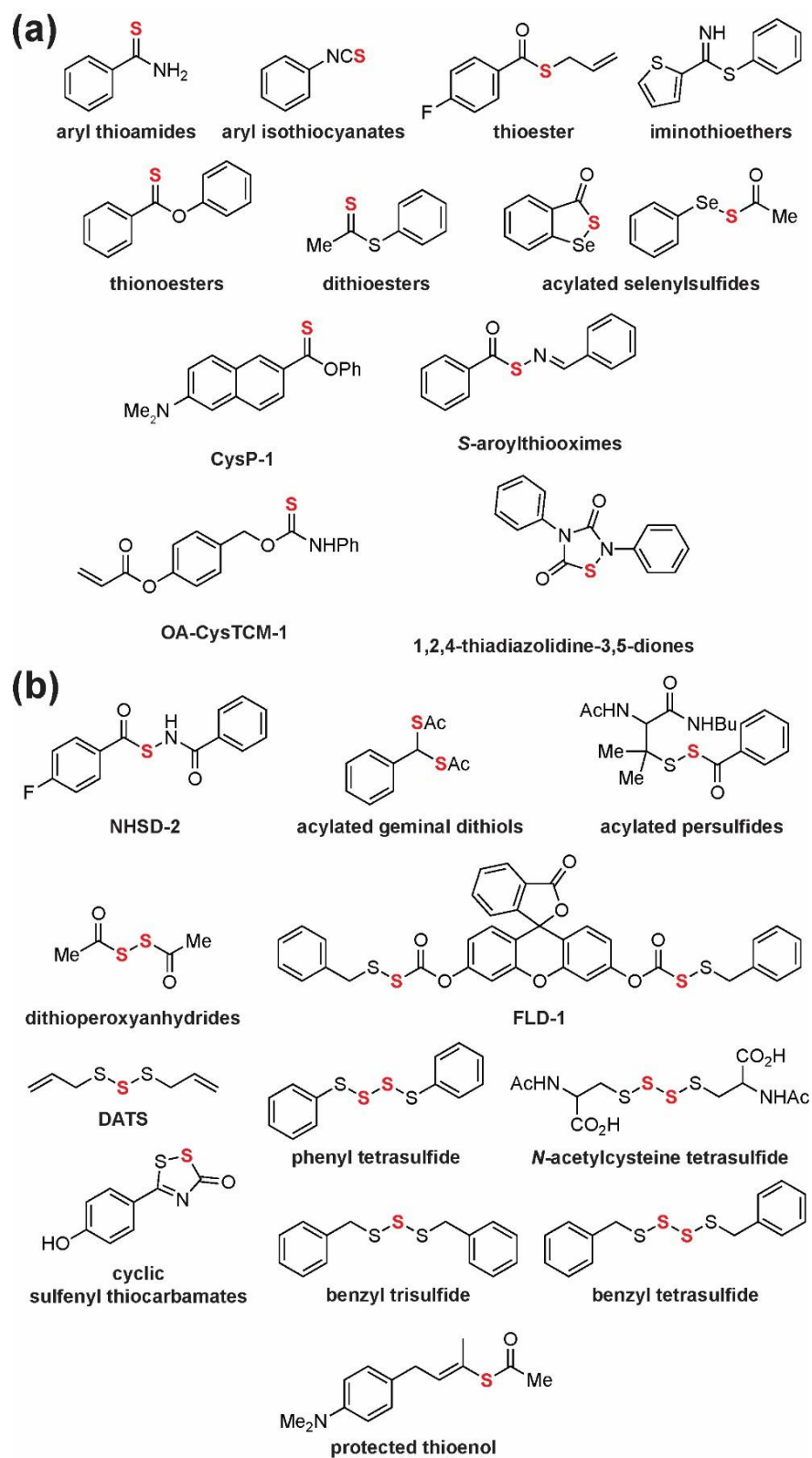


Figure 1.6 Structures of donor compounds activated in the presence of biological thiols. (a) H₂S donors activated in the presence of cysteine. (b) H₂S donors activated in the presence of cysteine and GSH.

flow, and studies on human aortic smooth muscle cells showed that these donors exhibited membrane hyperpolarizing effects. The mechanism of cysteine-mediated H₂S release from iminothioethers remains unclear.

Aryl isothiocyanates were first reported as cysteine-activated H₂S donors in 2014 by Martelli *et al.*⁴² Although release efficiency from these compounds was relatively low and required millimolar levels of cysteine for release, the isothiocyanates were found to cause membrane hyperpolarization of vascular smooth muscle cells and vasorelaxation in coronary arteries, both of which are consistent with H₂S release. In 2019, Lin *et al.*⁴³ investigated the mechanism of H₂S release from aryl isothiocyanates, and their data suggest that H₂S release proceeds through a native chemical ligation-type mechanism after initial attack on the isothiocyanate by the cysteine sulfhydryl group.

Also building from a native chemical ligation mechanistic approach,⁴⁴ our group reported in 2018 that thionoesters, which are structural isomers of thioesters commonly used in native chemical ligation, respond selectively to cysteine over other thiols to release H₂S with >80% efficiency.⁴⁵ Mechanistic investigations demonstrated that the *N*-to-*S* acyl transfer step was the rate-limiting step of this reaction. We later expanded this approach to demonstrate that dithioesters, which are more synthetically diversifiable than thionoesters, release H₂S selectively in the presence of cysteine.⁴⁶ This approach has also been extended to provide fluorescent H₂S donors activated in the presence of cysteine (CysP-1).⁴⁷ Proceeding through a key *N*-to-*S* acyl transfer step, Zhao *et al.*⁴⁸ showed that acyl-protected geminal dithiols react selectively to release H₂S in the presence of cysteine, through generation of an unstable geminal dithiol intermediate. Expanding to bioactive thioketone derivatives, Zhu *et al.*⁴⁹ demonstrated during an investigation into the metabolism of

clopidogrel (Plavix) that an intermediate metabolite containing a thioenol motif releases H₂S efficiently at physiological pH, suggesting possible future application of these and related compounds as H₂S donor motifs.

Also building from a native chemical ligation mechanistic approach,⁴⁴ our group reported in 2018 that thionoesters, which are structural isomers of thioesters commonly used in native chemical ligation, respond selectively to cysteine over other thiols to release H₂S with >80% efficiency.⁴⁵ Mechanistic investigations demonstrated that the *N*-to-*S* acyl transfer step was the rate-limiting step of this reaction. We later expanded this approach to demonstrate that dithioesters, which are more synthetically diversifiable than thionoesters, release H₂S selectively in the presence of cysteine.⁴⁶ This approach has also been extended to provide fluorescent H₂S donors activated in the presence of cysteine (CysP-1).⁴⁷ Proceeding through a key *N*-to-*S* acyl transfer step, Zhao *et al.*⁴⁸ showed that acyl-protected geminal dithiols react selectively to release H₂S in the presence of cysteine, through generation of an unstable geminal dithiol intermediate. Expanding to bioactive thioketone derivatives, Zhu *et al.*⁴⁹ demonstrated during an investigation into the metabolism of clopidogrel (Plavix) that an intermediate metabolite containing a thioenol motif releases H₂S efficiently at physiological pH, suggesting possible future application of these and related compounds as H₂S donor motifs.

Inspired by the unique reactivity of S–N motifs present in *S*-nitrosothiols, Zhao *et al.*⁵⁰ developed a series of compounds termed “*N*-mercapto donors” and demonstrated H₂S release in the presence of cysteine. The mechanism of H₂S release from these donors proceeds through the *N*-acylation of cysteine and generation of cysteine persulfide as the key H₂S-releasing intermediate. This class of donors was later expanded on in the

development of NHSD-2, which exhibited significant cardioprotective effects in a murine model of myocardial–ischemia reperfusion injury.⁵¹ Also leveraging the generation of intermediate persulfide motifs, Zhao *et al.*⁵² investigated the use of protected cysteine and penicillamine persulfide derivatives as H₂S donors in the presence of cysteine and GSH. These compounds function by initial attack on the donor by cysteine to generate a cysteine persulfide, which undergoes subsequent reaction with thiols to generate H₂S. These donors also provided H₂S-related protection against *in vivo* murine models of myocardial ischemia–reperfusion injury.

In a related approach, Foster *et al.*⁵³ reported the related *S*-aroylthiooxime class of compounds, which release H₂S in the presence of cysteine and can be tuned predictably by simple electronic modulation. H₂S release from these compounds likely proceeds by initial attack by cysteine on the donor to release an iminothiol intermediate, which further reacts with cysteine to generate a cysteine persulfide intermediate en route to H₂S release. More recently, the intermediate persulfide generation from S–X hybrid systems was further leveraged by Kang *et al.*⁵⁴ to develop a series of cyclic sulfur–selenium compounds and by Hamsath *et al.*⁵⁵ to develop acyclic sulfur–selenium compounds, which generate H₂S-releasing persulfides and analogous selenylsulfides in the presence of cysteine. In an alternative approach, Roger *et al.*⁵⁶ reported that dithioperoxyanhydrides also function as H₂S donors through the intermediate generation of persulfides in the presence of GSH and cysteine. These compounds were demonstrated to induce vasorelaxation in isolated rat aortic rings. In general, the use of persulfides as H₂S-releasing species has been of particular interest because a number of H₂S signaling mechanisms involve persulfidation of cysteine residues. In parallel to these developments, different methods of direct

persulfide generation in water are of significant interest and advances in this area will be highlighted elsewhere.⁵⁷

An often overlooked yet uncontrolled method of generating H₂S from persulfide intermediates is by treatment of organic polysulfides with thiols.⁵⁸ The most widely used organic polysulfide, diallyl trisulfide (DATS), is a simple organosulfur compound readily isolated from alliums, including garlic.⁵⁹ In the presence of thiols, DATS is reduced to generate allyl persulfide, which is further reduced by thiols to generate H₂S. We note that although diallyl disulfide (DADS) is often used in the literature as an H₂S donor, its apparent H₂S-releasing activity has been demonstrated to be a result of a DATS impurities.⁶⁰ Both experimental and computational results support the lack of direct H₂S release from DADS in the presence of thiols, except for a minor, slow pathway involving attack at the α -carbon by a thiol to generate an allyl persulfide intermediate.⁶¹ Consistent with this slow release, the generation of H₂S from thioester donors reported by Yao *et al.*⁶² is likely due to the intermediate release of allyl thiol and subsequent oxidation to form DADS, which results in slow H₂S donation.

Expanding investigations into H₂S from organic polysulfides, our group recently reported *bis*(aryl) and *bis*(alkyl)tetrasulfides as H₂S donors and demonstrated that tetrasulfides release more H₂S than trisulfides, as expected.⁶³ In comparing a series of benzyl di-, tri-, and tetra-sulfides,⁶⁴ we confirmed cysteine and GSH-mediated H₂S release occurs exclusively from dibenzyl trisulfide and dibenzyl tetrasulfide, which is consistent with the presence of sulfane sulfur.⁶⁵ A related study by Ercole *et al.*⁶⁶ highlighted the efficient release of H₂S from polysulfide-based donors built around polyethylene glycol/trisulfide/cholesterol conjugates that assemble into supramolecular macrostructures.

COS-based H₂S donors that are activated by thiols have also been reported. In 2018, we reported a small library of sulfenyl thiocarbonate motifs, including FLD-1 that undergoes thiol-mediated decomposition to generate COS.⁶⁷ By using a fluorophore as a payload that is released upon COS/H₂S donation, these donors provide a fluorescent response that correlates linearly with COS/H₂S release and allows for spatiotemporal resolution of cellular COS/H₂S release in live cell imaging. We also reported cysteine-selective COS-based H₂S donors, such as OA-CysTCM-1, which utilized a cysteine-mediated cyclization to activate a self-immolative donor motif.⁶⁸ A large library of 1,2,4-thiadiazolidine-3,5-diones was reported by Severino *et al.*⁶⁹ that was demonstrated to release H₂S in the presence of cysteine. We note that the proposed mechanism of donor activation in this system proceeds through an anionic thiocarbamate intermediate, which likely results in the direct release of COS with concomitant hydrolysis to H₂S.

1.6 Photoactivated Donors

The ability to control H₂S donation using external bio-orthogonal stimuli that selectively activate the desired compound in the presence of diverse biological functional groups is a powerful method that has garnered significant interest. Of such strategies, photoactivatable donors offer the potential for high spatiotemporal control of H₂S release (Figure 1.7). Photocaged species react on exposure to specific wavelengths of light to cleave a protecting group and reveal, in these cases, an H₂S-releasing moiety. This approach allows for noninvasive triggering of H₂S release in cells *in vitro* and the potential for photo-triggering on skin or at shallow sub-cutaneous levels.⁷⁰

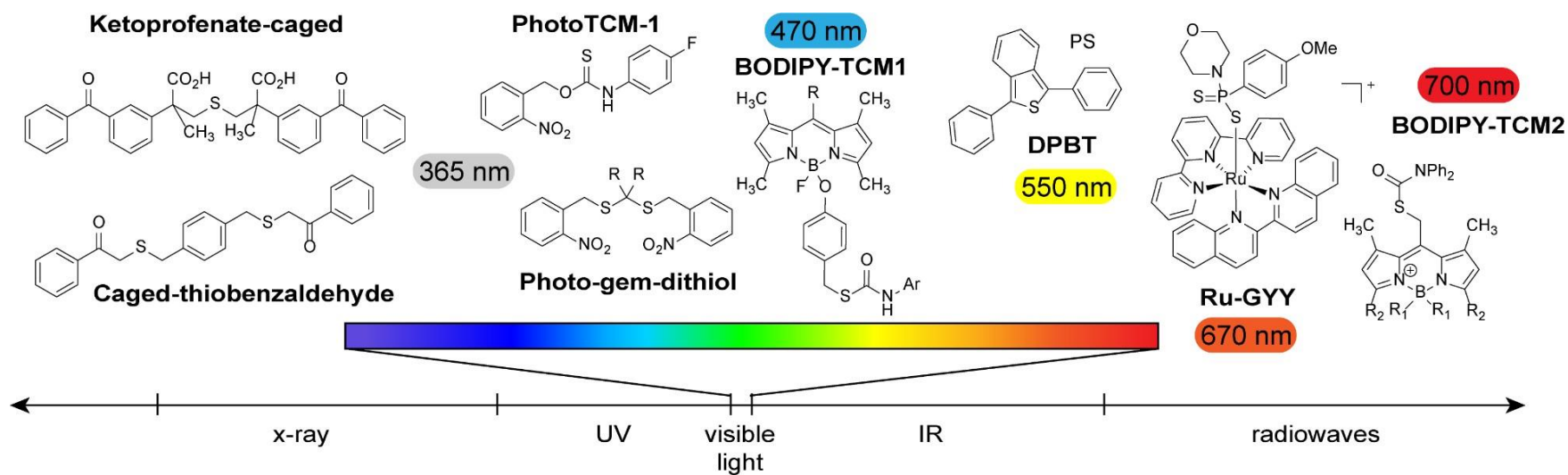


Figure 1.7 Structures and excitation wavelengths of selected photoactivable H₂S donors.

The first photoactivated H₂S donor Photo-gem-dithiol was reported by Devarie-Baez *et al.*,⁷¹ in which a *bis*-orthonitrobenzyl protected geminal-dithiol undergoes a Norrish type II rearrangement on irradiation ($\lambda_{\text{irr}} = 365 \text{ nm}$) to unmask an unstable gem-dithiol intermediate that is subsequently hydrolyzed to release H₂S. Sulfide release was confirmed by using the methylene blue assay, as well as through fluorescence imaging with HeLa cells. Moreover, these donors displayed pH-dependent H₂S release, consistent with other donors involving hydrolysis of gem-dithiols, an acid-mediated process. Similar photocleavable gem-dithiol scaffolds ($\lambda_{\text{irr}} = 365 \text{ nm}$) have since been incorporated into water-soluble polymers and block copolymer nanoparticles,⁷² as well as upconverting nanoparticles, which absorb low-energy near- infrared light ($\lambda_{\text{irr}} = 980 \text{ nm}$) and emit ultraviolet to visible light, that can trigger H₂S release.⁷³

An alternative photocontrollable H₂S donor was reported by Fukushima *et al.*,⁷⁴ which centers around a functionalized thioether that releases H₂S directly after photocleavage of the protecting groups, rather than relying on a subsequent hydrolysis step. Initially employing 2-nitrobenzyl photoactivatable groups, this approach was expanded to incorporate ketoprofenate photocages to avoid the production of the potentially deleterious 2-nitrosobenzaldehyde byproduct. These donors were further adapted to function by photoexcitation ($\lambda_{\text{irr}} = 325\text{--}385 \text{ nm}$) of xanthone chromophores.⁷⁵ Photocaged thiobenzaldehydes have also been used as light-activated H₂S donors. In these systems, irradiation ($\lambda_{\text{irr}} = 355 \text{ nm}$) reveals a thiobenzaldehyde intermediate that requires a subsequent nucleophilic attack by an amine to liberate the H₂S.⁷⁶ Such donors have been incorporated into both water-soluble H₂S releasing polymers and hydrogels. One benefit

of this approach is that the byproduct of photolysis is simply acetophenone, which is a benign and Food and Drug Administration-approved excipient.

Expanding to visible light photoexcitation, Yi *et al.*⁷⁷ harnessed the photogeneration of singlet oxygen to trigger H₂S release. Irradiation ($\lambda_{\text{irr}} = 500\text{--}550\text{ nm}$) of a photosensitizer in the presence of ambient oxygen and 1,3-diphenylisobenzothiophene generated an unstable endoperoxide intermediate, which undergoes rapid fragmentation to generate 2-benzoylbenzophenone and H₂S.⁷⁷ This system was incorporated into artificial vesicles or polymersomes, which enabled H₂S generation in water. An interesting advantage of this system is that the photoirradiation wavelengths are dictated by the choice of photosensitizer rather than the donor itself, which allows for a broad range of wavelengths to be used ($\lambda_{\text{ex}} = 380\text{--}550\text{ nm}$ demonstrated).

A number of photoactivatable COS-based H₂S donors have also been reported. In 2017, our group reported the first light-activated COS-based H₂S donor, PhotoTCM-1, in which an *o*-nitrobenzyl protecting group masked a caged thiocarbamate, which was cleaved on irradiation ($\lambda_{\text{irr}} = 365\text{ nm}$) to release COS.⁷⁸ PhotoTCM-1 was also shown through a series of selectivity studies to be stable to relevant biological thiols and nucleophiles, releasing COS only on photoirradiation. This strategy was later expanded by Sharma *et al.*⁷⁹ with a BODIPY-based photolabile group protecting an *S*-alkyl thiocarbamate that releases COS under irradiation at a more biocompatible wavelength ($\lambda_{\text{irr}} = 470\text{ nm}$) (BODIPY-TCM-1). More recently, efforts in this area have been focused on developing light-activated donors that function within a “tissue-transparent” window, the bounds of which are set by the absorbance of hemoglobin below 600 nm and of water above 900 nm.⁸⁰ This goal was accomplished by Stacko *et al.*⁸¹ using a COS-based delivery

approach coupled to a modified BODIPY core protecting an *S*-alkyl thiocarbamate. COS release from BODIPY-TCM-2 was accomplished with longer wavelength irradiation ($\lambda_{\text{irr}} = 700 \text{ nm}$), which is a significant improvement over prior COS donors.

In a hybrid system, Woods *et al.*⁸² reported a red-light activated complex of GYY-4137 and a common ruthenium photocage (Ru-GYY) that releases H₂S on irradiation ($\lambda_{\text{irr}} = 626 \text{ nm}$). Interestingly, although GYY-4137 is known to spontaneously hydrolyze in aqueous systems, complexation to the ruthenium metal center suppresses this H₂S release. The authors were thus able to demonstrate controlled H₂S release from this donor, as well as its activity against a model of ischemia–reperfusion injury in H9c2 heart myoblast cells. The Singh lab recently reported a novel optical-readout-based phototriggered H₂S donor. Harnessing excited-state intramolecular proton transfer, which had been previously applied to monitoring nitric oxide donation⁸³ among other analytes, they developed a *p*-hydroxyphenacyl triggered donor that releases H₂S under irradiation ($\lambda_{\text{irr}} = 410 \text{ nm}$), while simultaneously shifting the fluorescence of the donor.⁸⁴ This change in fluorescence allowed for H₂S release to be monitored, and it was demonstrated to function in HeLa cells.

1.7 Miscellaneous Activatable Donors

In addition to the compounds described earlier in this review, a number of H₂S donors that are triggered by specific stimuli have been reported and do not correspond to the categories outlined earlier (Figure 1.8). For example, our group reported the initial demonstration of leveraging intermediate COS release to access H₂S donors by developing self-immolative thiocarbamates, which we incorporated into analyte replacement

fluorescent probes (Figure 1.8a).¹⁶ This donor serves as an analyte-replacement probe, as it regenerates the consumed H₂S during the mechanism of release.

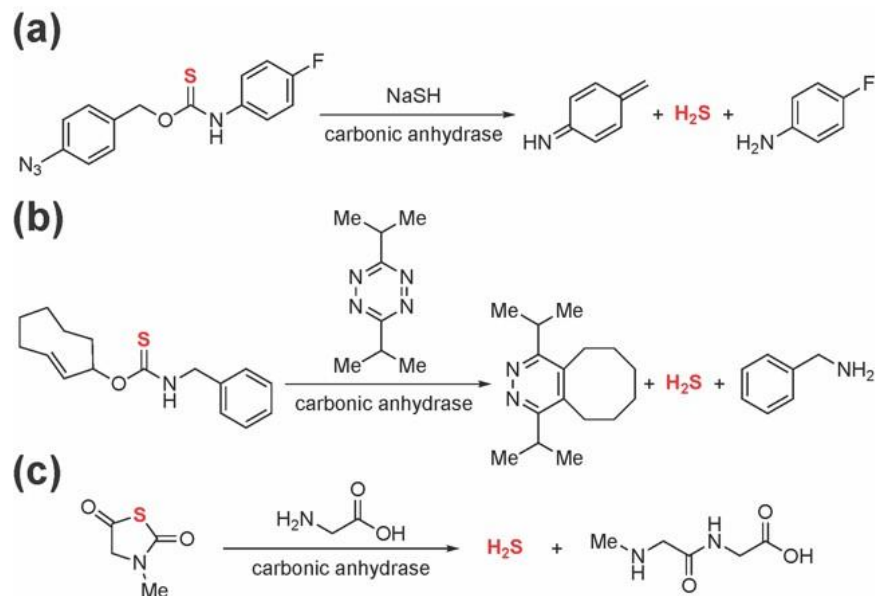


Figure 1.8 Structures of COS-based donor compounds activated by miscellaneous activators. (a) H₂S-activated analyte replacement probe. (b) “Click and release” bioorthogonal COS-based H₂S donor. (c) Activation of *N*-thiocarboxyanhydride by glycine to generate H₂S.

In a bioorthogonal delivery approach, we also demonstrated that self-immolative thiocarbamates bearing a *trans*-cyclooctene moiety can be utilized as “click and release” COS-based H₂S donors in the presence of tetrazines undergoing an inverse-electron demand Diels–Alder reaction (Figure 1.8b).⁸⁵ Such bioorthogonal approaches leverage the bimolecular reaction between two specific components to form a chemical bond while remaining inert to common reactive functional groups present in the surrounding biological milieu.⁸⁶ The development of *N*-thiocarboxyanhydrides (NTA) by Powell *et al.*⁸⁷ provides an alternative to self-immolative thiocarbamates (Figure 1.8c). This donor scaffold was demonstrated to release COS and generate a peptide byproduct in the presence of glycine

and has recently been leveraged to develop a number of macromolecular H₂S donors,⁸⁸ which is the topic of another review.⁸⁹ One benefit of the NTA-based approach is that donor activation does not release electrophilic byproducts such as a *p*-quinone methide, which are often found in other self-immolative COS-based donors.

1.8 Conclusions and Outlook

The development of activatable small-molecule H₂S donors has been one of the most significant advances in the field of H₂S chemical biology over the past 5 to 10 years. This palette of activatable H₂S donors provides researchers with a toolbox to better probe the biological activities of H₂S. The range of activators for controlled H₂S release has grown significantly in the past 5 years, and it is poised to enable new types of biological investigations that are not feasible with simple sulfide salts. Key needs include broader comparisons of different classes of donors in specific biological contexts to better delineate the bioavailability and localized release of H₂S from different donor constructs. Moreover, H₂S-releasing dynamics measured *in vitro* are likely to be perturbed in a biological system and may significantly alter the biological viability of these donors. As the chemistry that enables triggered release of H₂S and related reactive sulfur species from synthetic donors continues to evolve, the development of donors that respond to molecular stimuli up-regulated during specific disease states is likely to provide new tools to harness the therapeutic potential of H₂S, alongside more finely tuned organelle or cell-type specific targeted donors. Overall, the rapid expansion of chemistry that enables small-molecule H₂S donors is poised to advance the field and help elucidate the inherent complexities of reactive sulfur species in biology.

In parallel to the growing number of physiological processes involving H₂S-based signaling, the development of small molecule H₂S donors as chemical tools to better understand the biological effects H₂S and related reactive sulfur species has rapidly expanded. The research discussed in this dissertation highlights contributions to thiol-activated, small molecules capable of generating H₂S directly and through the intermediate generation of COS or persulfides (Chapters II through VI). In the interest of investigating the potential signaling role of COS independent of H₂S, Chapter VII discusses the development of a fluorescent probe selective for COS detection. Chapters I through VI include previously published, co-authored material. Chapter VII includes unpublished, co-authored material.

CHAPTER II

THIONOESTERS: A NATIVE-CHEMICAL LIGATION INSPIRED APPROACH TO CYSTEINE-TRIGGERED H₂S DONORS

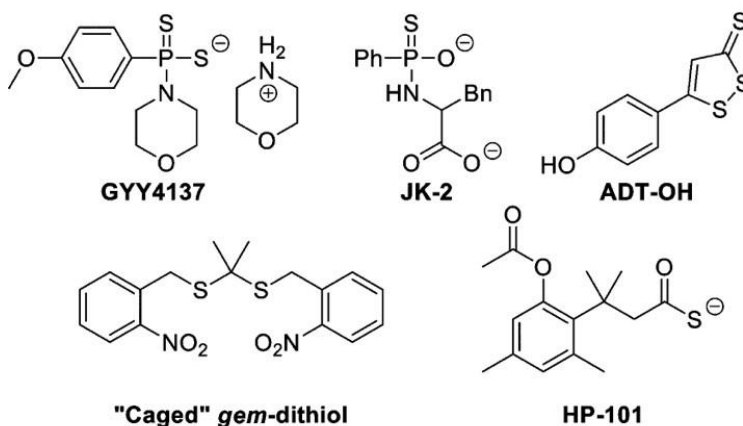
This chapter includes previously published and coauthored material from Cerda, M.M.; Zhao, Y.; Pluth, M.D. Thionoesters: A Native Chemical Ligation Inspired Approach to Cysteine-Triggered H₂S Donors. *J. Am. Chem. Soc.* **2018**, *140* (39), 12574-12579. This manuscript was written by Matthew M. Cerda with editorial assistance from Professor Michael D. Pluth. The project in this chapter was conceived by Matthew M. Cerda with insight from Dr. Yu Zhao. The experimental work in this chapter was performed by Matthew M. Cerda.

2.1 Introduction

Hydrogen sulfide (H₂S) is now recognized as an important biological signaling molecule⁹⁰ that is produced endogenously, cell membrane permeable, and reactive toward cellular and/or molecular targets.^{1c} The endogenous production of H₂S stems primarily from catabolism of cysteine and homocysteine by cystathionine β-synthase (CBS), cystathionine γ-lyase (CSE), and 3-mercaptopyruvate sulfurtransferase (3-MST).⁹¹ Recently, increasing interest has focused on harnessing H₂S as a potential therapeutic agent⁹² based on its role in vasodilation,⁹³ neurotransmission,⁹⁴ and angiogenesis.⁹⁵ Although the majority of prior reports have used sodium hydrosulfide (NaSH) or sodium sulfide (Na₂S) as sources of H₂S, the addition of these salts to a buffer leads to an almost

instantaneous increase in H₂S concentration, which is in stark contrast to the slow, gradual endogenous production of H₂S.⁹⁶ In efforts to provide more physiologically relevant rates of H₂S release, researchers have developed different types of H₂S-releasing molecules (Figure 2.1a).^{2f, 15d, 15f}

(a) Representative H₂S Donors



(b) Thiol-Triggered H₂S Donors

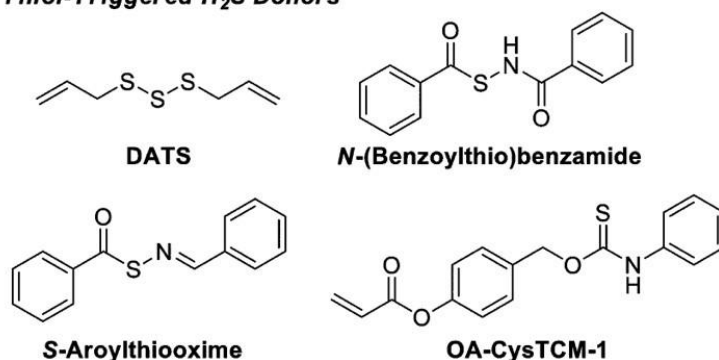


Figure 2.1 (a) Representative examples of common synthetic, small molecule H₂S donors; (b) selected small molecule, thiol-triggered H₂S donors.

For example, Lawesson's Reagent and related derivatives^{33, 37} have been used as hydrolysis-activated H₂S donors that function at physiological pH, and dithiolethiones, such as ADT-OH, have been conjugated to nonsteroidal anti-inflammatory drugs (NSAIDs) to access H₂S prodrug conjugates.^{12b} More recently, "triggered-release" scaffolds have also been reported, including those activated by light⁷¹ and enzymatic

activation.¹⁷ In addition, recent work has demonstrated that carbonyl sulfide (COS)-releasing scaffolds can also function as H₂S donors via the rapid conversion of the released COS to H₂S by carbonic anhydrase.¹⁶

Drawing parallels to the enzymatic conversion of cysteine or homocysteine to H₂S, a number of H₂S donor motifs have been developed that are activated by thiols, such as cysteine and reduced glutathione (GSH) (Figure 2.1b). Polysulfides, such as the commonly used diallyl trisulfide (DATS)⁵⁹ or more recently reported synthetic trisulfides⁶⁶ and tetrasulfides⁶³ release H₂S in the presence of thiols via an intermediate persulfide. Building in complexity, Xian and co-workers have reported thiol-triggered H₂S donors based on protected *N*-mercaptan⁵¹ or persulfide⁵² platforms. Similarly, Matson and co-workers reported *S*-arylothiooxime compounds,⁵³ which generate a thiol-reactive intermediate thiooxime. Thiol-mediated H₂S release from arylthioamides²⁹ and aryl isothiocyanates⁴² has also been reported, although the mechanisms of H₂S release remains uninvestigated and low releasing efficiencies (~2% and 3%, respectively) are observed. To the best of our knowledge, the only reported cysteine-selective H₂S donor utilizes the established reactivity of acrylate Michael acceptors toward cysteine,⁹⁷ to subsequently trigger the generation of COS, which is quickly converted to H₂S by carbonic anhydrase.⁶⁸

To further the development of thiol-triggered H₂S donors, we were inspired by the well-established chemistry of native chemical ligation due to the high biological compatibility and presence of a sulfur atom. Native chemical ligation is the chemoselective reaction between a thioester and an N-terminal cysteine residue to generate a new amide bond.⁴⁴ This reaction has been applied extensively in the field of protein synthesis, including in the semisynthesis of a potassium channel protein.⁹⁸ The mechanism of this

important ligation reaction begins by the nucleophilic addition of a cysteine sulfhydryl group to form an intermediate thioester, which then undergoes a rapid S to N acyl transfer to generate the more thermodynamically stable amide product (Figure 2.2).⁹⁹

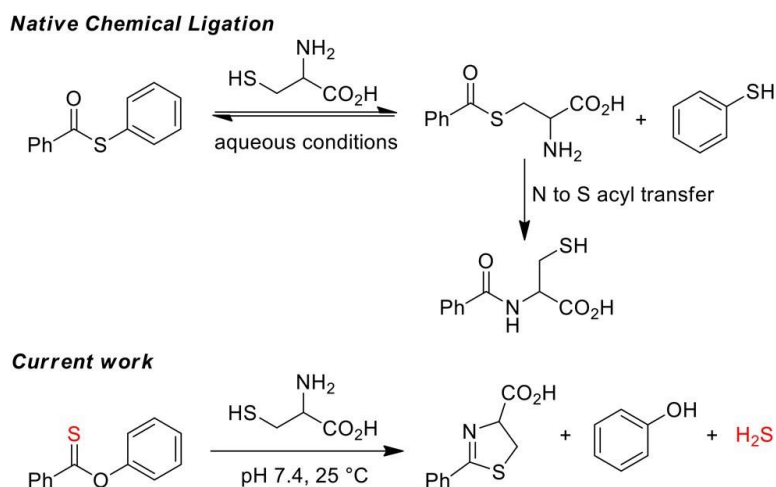


Figure 2.2 Generalized reaction scheme for native chemical ligation and release of H₂S upon addition of cysteine to a *bis*(phenyl) thionoester.

Despite the broad use of thioesters as activated coupling partners for native chemical ligation, to the best of our knowledge there have not been investigations into similar reactions with thionoesters, which are a constitutional isomer of thioesters. Building from our interest in the chemistry of reactive sulfur species,^{2b, 58, 100} we hypothesized that thionoesters would undergo a similar reaction pathway in the presence of cysteine, but would also generate H₂S during the S to N acyl transfer step of the reaction. Such reactivity would not only provide access to new H₂S-releasing motifs but also provide insights into new mechanisms of chemical ligation that could be accessed by simple interchange of oxygen and sulfur atoms in a reactive electrophile. Additionally, such platforms are also attractive because they mimic the enzymatic conversion of cysteine to H₂S. Herein, we present a mechanistic and kinetic investigation of thionoesters with cysteine and related

species and also demonstrate that thionoesters function as cysteine-selective H₂S donors that proceed through a native chemical ligation-type mechanism.

2.2 Results and Discussion

To prepare a model thionoester system, we treated phenyl chlorothionoformate with phenylmagnesium bromide at $-78\text{ }^{\circ}\text{C}$ in anhydrous THF to yield *O*-phenyl benzothioate (**DPTE**).¹⁰¹ Despite previous reports,¹⁰² we found that treatment of phenyl benzoate with Lawesson's reagent required extended reaction times and afforded undesirable yields, which is consistent with the predicted decrease in reactivity of esters toward Lawesson's reagent.¹⁰³ The structure and purity of **DPTE** were confirmed by NMR spectroscopy and HPLC (Appendix B). To determine whether thionoesters are a viable platform for H₂S release, we added 25 μM **DPTE** to buffered aqueous solutions (10 mM PBS, pH 7.4) containing varying concentrations of cysteine (25–500 μM) and monitored H₂S generation using the spectrophotometric methylene blue assay (Figure 2.3a).¹⁰⁴ Consistent with our design hypothesis, we observed an increase in H₂S release from **DPTE** at higher cysteine concentrations, suggesting that thionoesters are a viable platform for cysteine-triggered H₂S donation.

To assess the H₂S-releasing efficiency from thionoesters, we used a methylene blue calibration curve to quantify the H₂S release (Figure B.8). We measured that 20 μM of H₂S was released from a 25 μM solution of **DPTE** in the presence of 500 μM cysteine (20 equiv.), which corresponds to a releasing efficiency of 80%. In addition to the thionoester system, we also investigated H₂S release from structurally related diphenyl ester (**2**) and diphenyl thioester (**3**) compounds under our conditions (Figure 2.3b). As expected, neither

of these compounds released H₂S when treated with excess cysteine. Similarly, a representative secondary thioamide (**4**) failed to release H₂S in the presence of cysteine, suggesting the release of H₂S occurs exclusively from the thionoester moiety in the presence of cysteine.

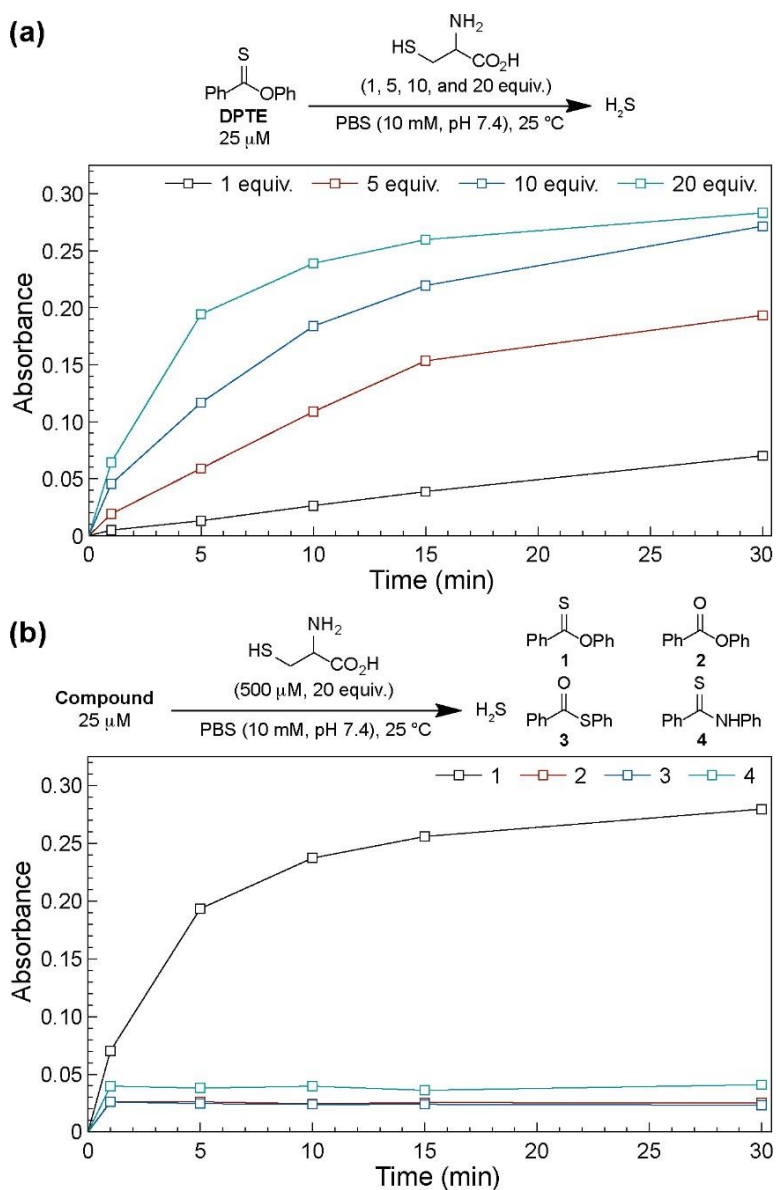


Figure 2.3 (a) Release of H₂S from **DPTE** in the presence of increasing cysteine concentrations (25, 125, 250, and 500 μM) in 10 mM PBS (pH 7.4) at 25 °C. (b) Lack of H₂S release from structurally related compounds (25 μM) in the presence of cysteine (500 mM, 20 equiv.).

To further investigate the selectivity of H₂S release from thionoesters, we treated **DPTE** with other biologically relevant nucleophiles (Figure 2.4).¹⁰⁵

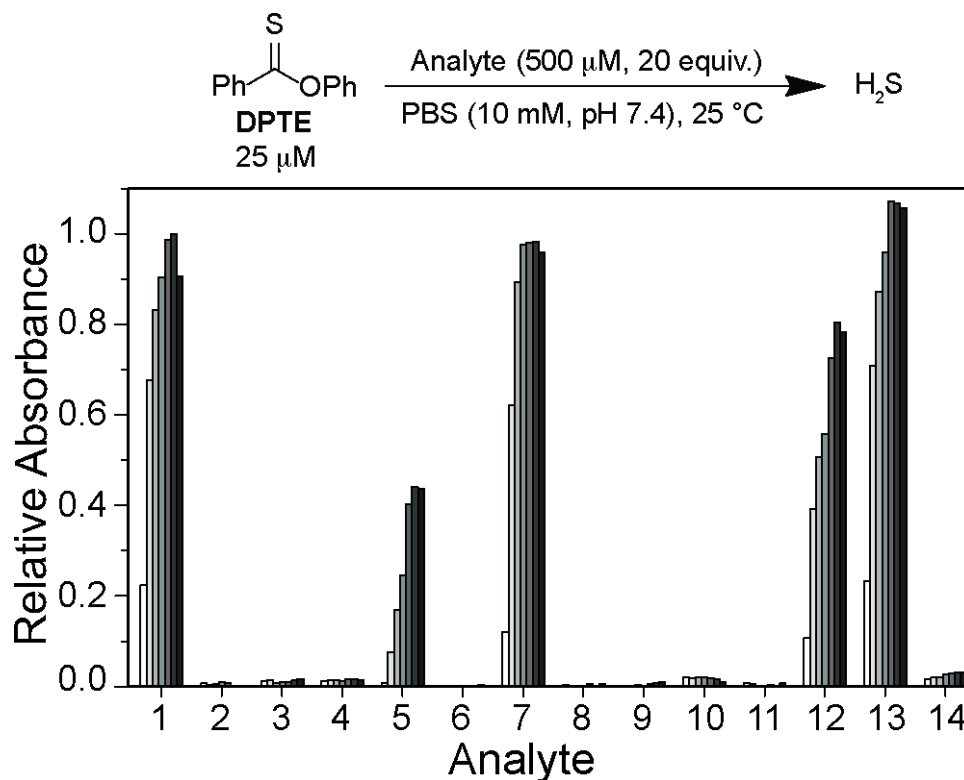


Figure 2.4 Selectivity of H₂S release from DPTE in the presence of different analytes. Data were acquired at 1, 5, 10, 15, 30, 45, and 60 min. Methylene blue absorbance values are relative to the maximum absorbance value obtained from H₂S release in the presence of cysteine (1). Analytes: H₂O/PBS buffer (2), serine (3), lysine (4), L-homocysteine (5), DL-penicillamine (6), L-cysteine methyl ester hydrochloride (7), *N*-acetyl-L-cysteine (8), *N*-acetyl-L-cysteine methyl ester (9), *S*-methyl-L-cysteine (10), GSH (11), cysteine + GSH (12), cysteine + lysine (13), PLE (1.0 U/mL) (14).

In the absence of any added nucleophiles, no hydrolysis-mediated H₂S release was observed from **DPTE** at physiological pH, although we note prior reports show that thionoesters are hydrolyzed under basic conditions to afford the corresponding thioacid and alcohol.¹⁰⁶ Treatment of **DPTE** with serine or lysine, chosen as representative alcohol- and amine-based nucleophiles respectively, did not result in H₂S release, although prior

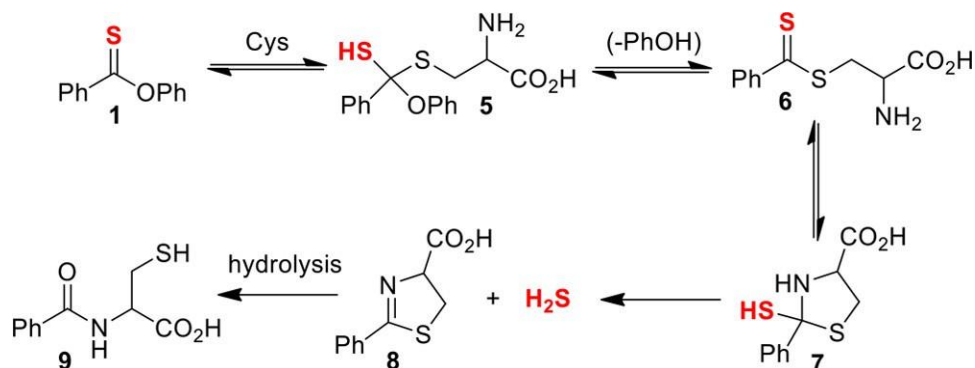
reports suggest that amines can react with thionoesters to yield thioamides via displacement of the corresponding alcohols.¹⁰⁷ To investigate this potential side reactivity, cysteine-triggered (500 μM) H_2S release from **DPTE** (25 μM) was measured in the presence of lysine (500 μM) and we observed no change in H_2S -releasing efficiency. We also investigated the reactivity of **DPTE** with thiol-based nucleophiles. Treatment of **DPTE** with homocysteine also resulted in H_2S release, although at a slower rate than from treatment with cysteine. This observation is consistent with a larger, less favorable transition state required for an intramolecular S to N acyl transfer in the homocysteine system in comparison with the cysteine system. Alternatively, the reduced rate may be reflective of the significant pKa difference between cysteine (pKa \approx 8.5) and homocysteine (pKa \approx 10),¹⁰⁸ meaning that, under physiological conditions, the effective concentration of cysteine thiolate is much greater than homocysteine thiolate (\sim 10% vs \sim 0.03%). Surprisingly, treatment of **DPTE** with penicillamine did not result in H_2S release. We anticipated that geminal methyl groups would help to preorganize the intermediate dithioester generated after nucleophilic attack and would result in faster H_2S release.¹⁰⁹ However, the geminal methyl groups also likely significantly reduce the nucleophilicity of the thiol moiety due to steric congestion, which would subsequently disfavor the initial nucleophilic attack on the thionoester.

We also investigated whether different cysteine derivatives could generate H_2S release from **DPTE** to further understand the requirements for H_2S release from thionoesters. Treatment of **DPTE** with cysteine methyl ester did not affect H_2S production, suggesting that the carboxylic acid is not required for H_2S generation. By contrast, treatment of **DPTE** with *N*-acetylcysteine, *N*-acetylcysteine methyl ester, or *S*-

methylcysteine completely abolished H₂S release, highlighting the requirement of a 2-aminoethanethiol moiety for productive H₂S release. Consistent with these results, treatment of **DPTE** with GSH, the most abundant biological thiol, did not generate H₂S, which is consistent with the requirement of a pendant amine to generate H₂S release. Despite the lack of H₂S release, we anticipated that GSH would still attack **DPTE** to form an intermediate dithioester, which should still be sufficiently electrophilic to react with cysteine to generate H₂S. To test this hypothesis, we treated **DPTE** (25 μM) with GSH (1 mM) and cysteine (500 μM) and observed a reduced rate of H₂S release. These results suggest that the competitive, nonproductive, addition of GSH to the thionoester is reversible, and that the thionoester moiety can still react with Cys in the presence of GSH to release H₂S. Adding to the selectivity investigations, treatment of **DPTE** with porcine liver esterase (PLE) failed to generate H₂S; however, we cannot rule out consumption of the thionoester moiety by PLE or other native enzymes. Taken together, these results demonstrate the high selectivity of the thionoester moiety toward cysteine and homocysteine for H₂S release.

Building from the selectivity studies, as well as from the established mechanism of native chemical ligation, we proposed a mechanism for cysteine-mediated H₂S release from thionoesters (Scheme 2.1). Initial nucleophilic addition by cysteine on **1** generates tetrahedral intermediate **5**, which collapses to form dithioester intermediate **6** and extrude 1 equiv. of phenol. Similar to native chemical ligation, subsequent nucleophilic attack by the pendant amine on the thiocarbonyl leads to the formation of substituted thiazolidine **7**. Loss of H₂S, by either direct extrusion of HS⁻ or solvent-assisted extrusion of H₂S, results

in formation of dihydrothiazole **8**, which could be further hydrolyzed to form N-benzoyl-cysteine (**9**).



Scheme 2.1 Proposed mechanism of H₂S release from **DPTE** in the presence of cysteine

As a first step toward investigating our proposed mechanism, we determined the reaction order in cysteine by treating **DPTE** (25 μM) with varying concentrations of cysteine under pseudo-first-order conditions at 25 $^{\circ}\text{C}$ and measuring H₂S release using the methylene blue assay (Figure 2.5). As expected, we observed that increased cysteine concentrations led to increased rates of H₂S production. The resultant releasing curves were fit to obtain pseudo-first-order rate constants (k_{obs}), and plotting $\log[\text{Cys}]$ versus $\log[k_{\text{obs}}]$ confirmed a first-order dependence in cysteine, which is consistent with our proposed mechanism. Additionally, the obtained k_{obs} values were plotted against Cys concentrations to obtain a second-order rate constant of $9.1 \pm 0.3 \text{ M}^{-1} \text{ s}^{-1}$ for the reaction. In comparison to other known reactivities, the rate of cysteine-triggered H₂S release from **DPTE** is comparable to the rate (10–100 $\text{M}^{-1} \text{ s}^{-1}$) of copper(I)-catalyzed azide–alkyne cycloadditions (CuAAC), a classic example of a “click reaction”.¹¹⁰

To further evaluate our proposed mechanism, we sought to identify the rate-determining step in cysteine-triggered release of H₂S from thionoesters. In native chemical

ligation, the initial nucleophilic attack by thiols to form intermediate thioesters is reversible and has been utilized to enhance the reactivity of alkyl thioesters for native chemical ligation. However, in the presence of cysteine, the transthioesterification resulting from

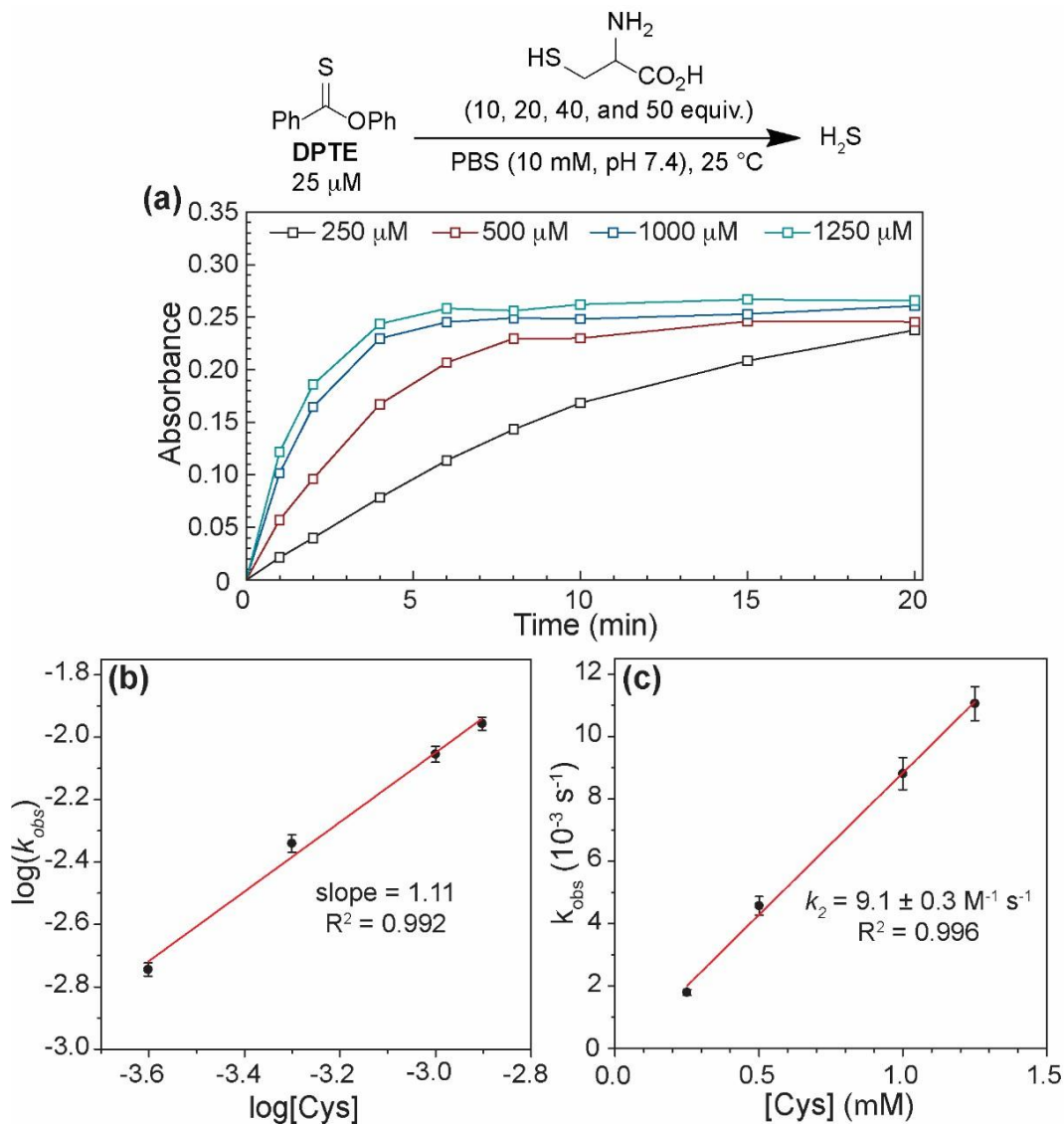


Figure 2.5 (a) H₂S release by **DPTE** in the presence of increasing cysteine concentrations (250, 500, 1000, and 1250 μM). (b) Plot of log(*k*_{obs}) vs log([Cys]) for **DPTE**. (c) Plot of *k*_{obs} vs [Cys].

nucleophilic attack of the sulfhydryl group on the thioester is thought to be rate-limiting due to the rapid and irreversible subsequent S to N acyl transfer to form the more

thermodynamically stable amide bond.⁹⁹ In the thionoester system, the initial attack by a thiol on **DPTE** results in extrusion of phenol, which is a much weaker nucleophile than a thiol and should not attack the generated dithioester intermediate. If other thiols are present in solution, then it is likely that they could attack the dithioester intermediate in a transdithioesterification reaction. This thiol exchange is supported by the observed reduced rate of H₂S generation from **DPTE** in the presence of competing thiols, suggesting that the initial nucleophilic attack on dithioesters is reversible.

Using similar pseudo-first-order conditions as those used for the cysteine order dependence investigations (25 μM **DPTE**, 500 μM cysteine), we performed an Eyring analysis to determine the activation parameters for the reaction in an effort to further understand the amount of disorder in the rate-limiting transition state for the reaction (Figure 2.6). Our expectation was that if initial thiol addition is the rate-limiting step, then

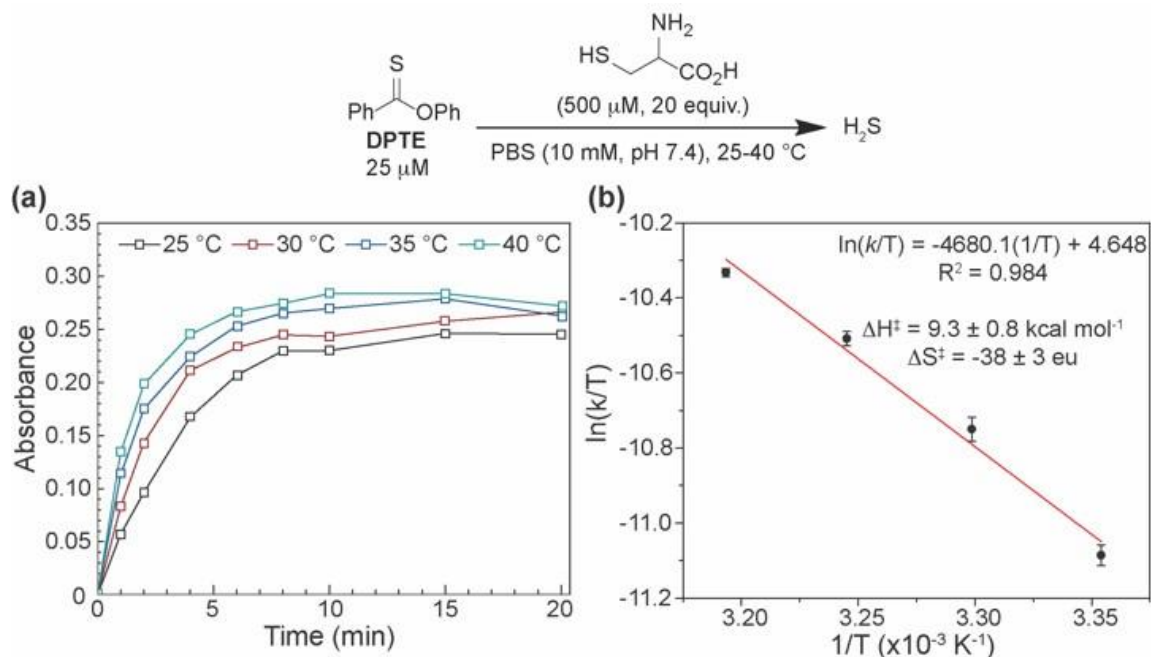


Figure 2.6 (a) Effect of temperature on rate of H₂S release from **DPTE** (25 μM) in the presence of cysteine (500 μM, 20 equiv). (b) Eyring analysis of H₂S release from **DPTE**.

we would observe a negative entropy of activation (ΔS^\ddagger) of approximately -20 eu, which is typical for a bimolecular reaction. In contrast, if the intramolecular S to N thioacyl transfer to form the substituted thiazolidine is the rate-limiting step, then we would expect a larger, more negative ΔS^\ddagger due to the highly ordered structure required for the intramolecular cyclization. Under our experimental conditions, we observed $\Delta S^\ddagger = -38 \pm 3$ eu, which is most consistent with intramolecular cyclization being the rate-determining step of the reaction.

As a final step of characterizing the proposed mechanism, we performed a preparative scale reaction and isolated the reaction products. In addition to recovered starting material, we isolated a cysteine-derived dihydrothiazole (**CysDHT**) rather than *N*-benzoyl-L-cysteine as the major product of the reaction (Figure 2.7). These results suggest that the dihydrothiazole is stable under aqueous conditions and is not further hydrolyzed to *N*-benzoyl-L-cysteine. To further confirm the formation of **CysDHT** from **DPTE**, we synthesized an authentic sample of **CysDHT** and used HPLC to monitor the reaction progress. We treated a $100 \mu\text{M}$ solution of **DPTE** with 20 equiv. of L-cysteine methyl ester and observed nearly complete conversion to phenol and **CysDHT** within 1 h. Using known concentrations of phenol and **CysDHT** to construct an HPLC calibration curve, we measured that the concentrations of phenol and **CysDHT** after 1 h were approximately $76 \mu\text{M}$ and $64 \mu\text{M}$, respectively, which supports the high H_2S -releasing efficiency of thionoesters. Although we were initially surprised by the inherent stability of the dihydrothiazole product, we note that biological formation of the dihydrothiazole moiety is a known post-translation modification of cysteine residues in bacteria.¹¹¹ For example, the cyclodehydration of internal cysteine residues results in formation of Fe(III)-

coordinating dihydrothiazole, which is commonly found in sideophores,¹¹² such as yersiniabactin¹¹³ and pyochelin.¹¹⁴ Additionally, adjacent dihydrothiazole moieties can be oxidized to a *bis*(thiazole), and the planarity of this motif allows for intercalation of DNA as seen in bleomycin.¹¹⁵ Taken together, these observations highlight the biological significance of the dihydrothiazole motif and provides new areas of investigation using this established reactivity.

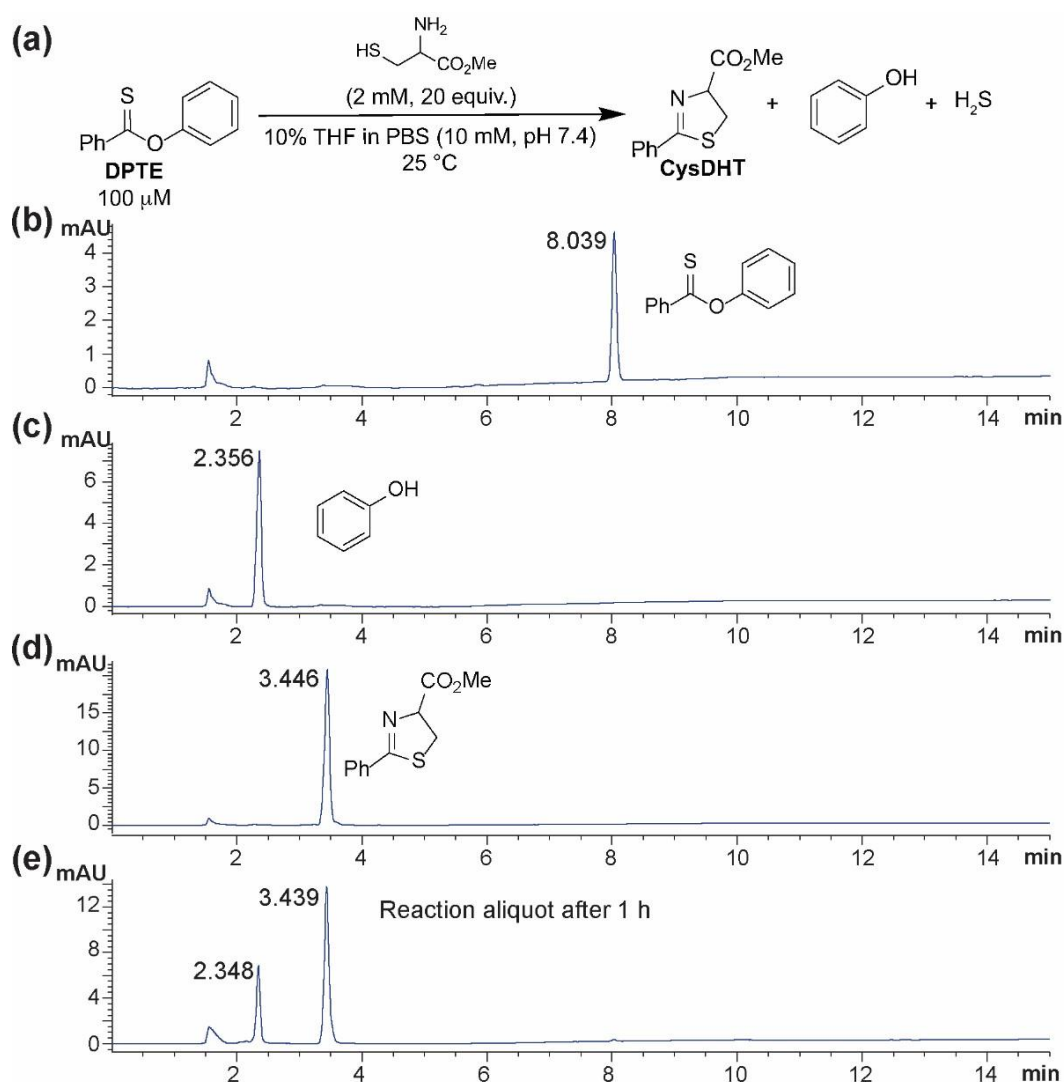


Figure 2.7 (a) Reaction conditions; (b) 100 μ M DPTE in 10 mM PBS (pH 7.4) with 10% THF; (c) 100 μ M PhOH in 10 mM PBS (pH 7.4) with 10% THF; (d) 100 μ M CysDHT in 10 mM PBS (pH 7.4) with 10% THF; (e) reaction aliquot after 1 h.

2.3 Conclusions

By investigating the reactivity of **DPTE** with cysteine, we not only demonstrated the inherent reactivity of thionoesters toward cysteine in a native chemical ligation-type mechanism but also demonstrated that this functional group provides a novel platform for highly efficient H₂S donation. We demonstrated that this reaction occurs at rates similar to those for the commonly used Cu(II)-mediated azide/alkyne click reaction, with a second-order rate constant of $9.1 \pm 0.3 \text{ M}^{-1} \text{ s}^{-1}$. Our mechanistic investigations suggest that, in comparison to native chemical ligation, the rate-determining step has been shunted from the addition of cysteine to the intramolecular S to N thioacyl transfer. Taken together, these investigations demonstrate that thionoesters are a novel, cysteine-triggered H₂S releasing scaffold. Additionally, the high selectivity of **DPTE** toward cysteine warrants future exploration into the thionoester functional group for cysteine-selective reactive probes.

The chemistry and established reactivity of **DPTE** in the presence of cysteine provided a platform for efficient, thiol-activated H₂S release from a simple donor scaffold. However, the ability to tune the rate of H₂S release from thionoesters is limited by the lack of synthetic accessibility to structurally diverse thionoesters. A critical analysis of the proposed H₂S-releasing mechanism from **DPTE** revealed the intermediate formation of a dithioester, a well-established structural motif in the field of polymer chemistry. Given the structural similarity between thionoesters and dithioesters, we hypothesized dithioesters would provide similar reactivity to generate H₂S in the presence of cysteine and could readily be tuned by structural modifications. Chapter III discusses the use of dithioesters as cysteine-activated H₂S donors and ability to tune H₂S release by simple alkyl functionalization.

2.4 Experimental Details

2.4.1 Materials and Methods

Reagents were purchased from Sigma-Aldrich, Tokyo Chemical Industry (TCI) or VWR and used directly as received. *S*-Phenyl benzothioate was synthesized according to a previous report.¹¹⁶ *N*-phenylthiobenzamide was synthesized according to a previous report.¹¹⁷ Methyl 2-phenyl-4,5-dihydrothiazole-4-carboxylate (**CysDHT**) was synthesized according to a previous report.¹¹⁸ Deuterated solvents were purchased from Cambridge Isotope Laboratories and used as received. ¹H and ¹³C{¹H} NMR spectra were recorded on a Bruker 500 MHz instrument. Chemical shifts are reported relative to residual protic solvent resonances. Silica gel (SiliaFlash F60, Silicycle, 230-400 mesh) was used for column chromatography. All air-free manipulations were performed under an inert atmosphere using standard Schlenk technique or an Innovative Atmospheres N₂- filled glove box. UV-Vis spectra were acquired on an Agilent Cary 60 UV-Vis spectrophotometer equipped with a Quantum Northwest TC-1 temperature controller at 25 °C ± 0.05 °C.

H₂S Detection Materials and Methods

Phosphate buffered saline (PBS) tablets (1X, CalBioChem) were used to prepare buffered solutions (140 mM NaCl, 3 mM KCl, 10 mM phosphate, pH 7.4) in deionized water. Buffer solutions were sparged with N₂ to remove dissolved oxygen and stored in an N₂-filled glovebox. Donor stock solutions (in DMSO) were prepared inside an N₂-filled glovebox and stored at -25 °C until immediately before use. Trigger stock solutions (in PBS) were freshly prepared in an N₂-filled glovebox immediately before use.

High Performance Liquid Chromatography (HPLC) Analysis

HPLC analysis was performed on an Agilent 1260 HPLC instrument with a Poroshell 120 EC-C18 4.6x100 mm column and monitored at 280 nm. Solvent A: 95% H₂O, 5% MeOH, Solvent B: 100% MeCN. Gradient: 35% Solvent A/65% Solvent B for 2 min. Change to 100% Solvent B over 4 min and hold for 6.5 min. Change to 35% Solvent A/65% Solvent B over 0.5 min and hold for 4.5 min. Flow Rate: 0.5 mL/min, 2 μ L injection.

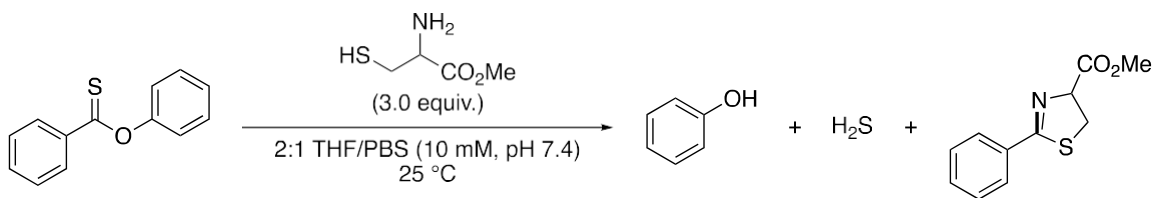
General Procedure for Measuring H₂S Release via Methylene Blue Assay (MBA)

Scintillation vials containing 20 mL of PBS were prepared in an N₂-filled glovebox. To these solutions, 20 μ L of 500 mM analyte stock solution (in PBS) was added for a final concentration of 500 μ M. While stirring, the solutions were allowed to thermally equilibrate in heating block at the desired temperature for approximately 20-30 min. Immediately prior to donor addition, 0.5 mL solution of the methylene blue cocktail were prepared in disposable 1.5 mL cuvettes. The methylene blue cocktail solution contained: 200 μ L of 30 mM FeCl₃ in 1.2 M HCl, 200 μ L of 20 mM *N,N*-dimethyl-*p*-phenylene diamine in 7.2 M HCl, and 100 μ L of 1% (w/v) Zn(OAc)₂. To begin an experiment, 20 μ L of 25 mM donor stock solution (in DMSO) was added for a final concentration of 25 μ M. At set time points after the addition of donor, 500 μ L reaction aliquots were added to the methylene blue cocktail solutions and incubated for 1 h at room temperature shielded from light. Absorbance values at 670 nm were measured 1 h after addition of reaction aliquot. Each experiment was performed in quadruplicate unless stated otherwise.

MBA Calibration Curve

Solutions containing 0.5 mL of the methylene blue cocktail and 0.5 mL PBS containing 500 μM cysteine were freshly prepared in disposable cuvettes (1.5 mL). Under inert conditions, a 10 mM stock solution of NaSH (Strem Chemicals) in PBS was prepared and diluted to 1 mM. Immediately after dilution, 1 mM NaSH was added to 1.0 mL solutions for final concentrations of 10, 20, 30, 40, and 50 μM . Solutions were mixed thoroughly, incubated at room temperature for 1 h, and shielded from light. Absorbance values at 670 nm were measured after 1 h. (Figure B.7)

Reaction Product Analysis

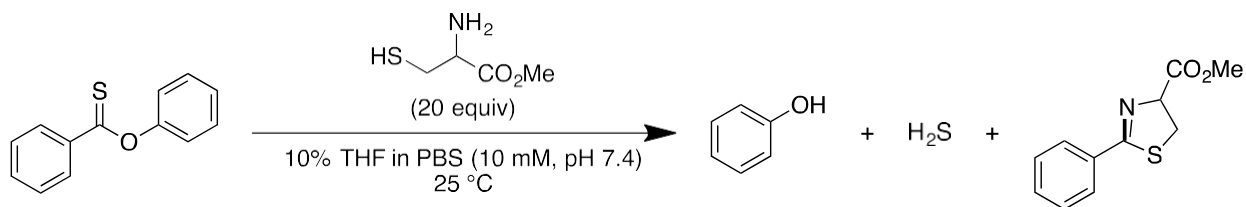


Scheme 2.2 Preparative scale synthesis of **CysDHT** from **DPTE**

DPTE (0.39 mmol, 1.0 equiv.) was dissolved in 15 mL of 2:1 THF/PBS (10 mM, pH 7.4). L-cysteine methyl ester hydrochloride (1.17 mmol, 3.0 equiv.) was added in a single portion and stirred at room temperature for 2 h. The reaction mixture was diluted with deionized H₂O (~20 mL) and extracted with CH₂Cl₂ (3 x 20 mL). The combined organic extracts were washed with brine and dried over MgSO₄. After filtration, the solvent was removed under reduced pressure, and the purified by preparative thin layer chromatography (1:1 CH₂Cl₂ in hexanes). **DPTE** $R_f = 0.75$ (63.6 mg, 76%) and **CysDHT** $R_f = 0.03$ (11.0 mg, 13%) were isolated and characterized by ¹H and ¹³C{¹H} NMR

spectroscopy. The significant recovery of **DPTE** is likely due to the lack of buffering capacity in the preparative-scale reaction.

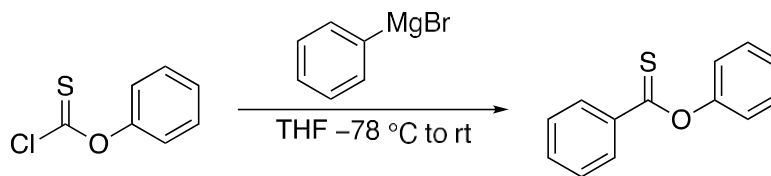
Reaction Product Analysis by HPLC



Scheme 2.3 Synthesis of **CysDHT** from **DPTE** for reaction product analysis by HPLC

To a 20 mL solution of 10% THF in PBS (10 mM, pH 7.4) containing 2 mM L-cysteine methyl ester (20 equiv.), 20 μ L of 100 mM **DPTE** in THF was added and stirred at room temperature. After 1 h, a 1 mL reaction aliquot was analyzed by HPLC. HPLC analysis was performed on an Agilent 1260 HPLC instrument with a Poroshell 120 EC-C18 4.6x100 mm column and monitored at 280 nm. Solvent A: 95% H₂O, 5% MeOH, Solvent B: 100% MeCN. Gradient: 35% Solvent A/65% Solvent B for 2 min. Change to 100% Solvent B over 4 min and hold for 6.5 min. Change to 35% Solvent A/65% Solvent B over 0.5 min and hold for 4.5 min. Flow Rate: 0.5 mL/min, 4 μ L injection. The concentration of **CysDHT** and phenol present at the end of the reaction were determined by measurement against calibration curves for each compound (Figure B.5, B.6)

2.4.2 Synthesis



Scheme 2.4 Synthesis of *O*-phenyl benzothioate (**DPTE**)

O-Phenyl benzothioate (**DPTE**) was synthesized using a slightly-modified procedure.¹¹⁶ Phenyl chlorothionoformate (14.8 mmol, 1.1 equiv.) was added to anhydrous THF (20 mL) at -78 °C under N₂. While stirring, phenylmagnesium bromide (12.8 mmol, 1.0 M in THF, 1.0 equiv.) was added dropwise, and the reaction solution was stirred for 1 h at -78 °C. After 1 h, the reaction solution was allowed to warm to room temperature and stirred for an additional 2 h. The reaction was then quenched by addition of deionized H₂O (30 mL) and extracted with CH₂Cl₂ (3 x 30 mL). The combined organic extractions were washed with brine (30 mL) and dried over MgSO₄. After filtration, the solvent was removed under reduced pressure, and the desired product purified by column chromatography (10% CH₂Cl₂ in hexanes, *R_f* = 0.33). The resultant product was isolated as a bright orange-yellow liquid. 938 mg (34%). H NMR (500 MHz, CDCl₃) δ: 8.37 (d, *J* = 7.3 Hz, 2 H), 7.63 (t, *J* = 7.5 Hz, 1 H), 7.48 (q, *J* = 7.2 Hz, 4 H), 7.33 (t, *J* = 7.4 Hz, 1 H), 7.14 (d, *J* = 7.5 Hz, 2 H). ¹³C{¹H} NMR (126 MHz, CDCl₃) δ: 211.22, 155.03, 138.11, 133.46, 129.76, 129.44, 128.42, 126.53, 122.31. HRMS-EI+ (*m/z*): [M + H]⁺ calcd for C₁₃H₁₀OS, 214.04524; found, 214.04478.

CHAPTER III

DITHIOESTERS: SIMPLE, TUNABLE, CYSTEINE-SELECTIVE H₂S DONORS

This chapter includes previously published and coauthored material from Cerda, M.M.; Newton, T.D.; Zhao, Y.; Collins, B.K.; Hendon, C.H.; Pluth, M.D. Dithioesters: Simple, Tunable, Cysteine-Selective H₂S Donors. *Chem. Sci.* **2019**, *10* (6), 1773-1779. This manuscript was written by Matthew M. Cerda with editorial assistance from Professor Michael D. Pluth. The project in this chapter was conceived by Matthew M. Cerda with insight from Dr. Yu Zhao. The experimental work in this chapter was performed by Matthew M. Cerda and Turner D. Newton. The computational work in this chapter was performed by Brylee K. Collins with assistance from Professor Christopher H. Hendon.

3.1 Introduction

Prevalent in the field of polymer chemistry, dithioesters are utilized as chain transfer agents in reversible addition-fragmentation chain transfer (RAFT) polymerizations.¹¹⁹ Arising from the ability to readily react with propagating radical monomers, the design of thiocarbonyl-containing motifs such as dithioesters, trithiocarbonates, and dithiocarbamates has been well studied to enhance the RAFT polymerization of various monomers.¹²⁰ In Chapter II, we demonstrated that related thionoesters, which are structural isomers of thioesters bearing a thiocarbonyl motif, undergo a chemoselective reaction with cysteine to generate a dihydrothiazole and hydrogen sulfide (H₂S).¹²¹ Despite recent advancements in the synthesis of thionoesters,¹²²

the ability to prepare a diverse library of thionoester-based H₂S donors is limited by the availability of stable, readily-accessible starting materials. However, based on structural similarities between thionoesters and dithioesters, we hypothesized that dithioesters could provide similar reactivity in the presence of cysteine and allow for the development of tunable H₂S donors with precise control over H₂S release rates and efficiencies.

Complementing carbon monoxide and nitric oxide, H₂S is now classified as an important biological signaling molecule.¹²³ Commonly referred to as gasotransmitters, these small, gaseous molecules are produced endogenously, readily permeate cell membranes, and exert physiological responses upon binding to or reacting with cellular and/or molecular targets.¹²⁴ The involvement of H₂S-mediated signaling has been observed in a variety of physiological processes such as vasodilation,⁹³ angiogenesis,¹²⁵ and scavenging of reactive oxygen species.¹²⁶ In recent years, researchers have become increasingly interested in utilizing H₂S donors for the development of both important research tools and novel therapeutics.¹²⁷ Towards this goal, researchers have relied heavily on the use of sodium hydrosulfide (NaSH), which is a water-soluble source of H₂S, for preliminary studies. However, a comparison between H₂S production from native enzymes including cystathionine- β -synthase and cystathionine- γ -lyase against exogenous administration of H₂S (via NaSH) has revealed stark differences which should be taken into consideration.¹²⁸ The dissolution of NaSH in buffered solutions leads to a rapid, almost spontaneous increase in local H₂S concentration,¹²⁹ whereas endogenous H₂S production occurs at a slower, at a slower rate. To address this issue, researchers have developed synthetic H₂S donors, which release H₂S either passively via hydrolysis or in the presence of a specific analyte at rates comparable to enzymatic H₂S production (Figure 3.1).^{15a, 130}

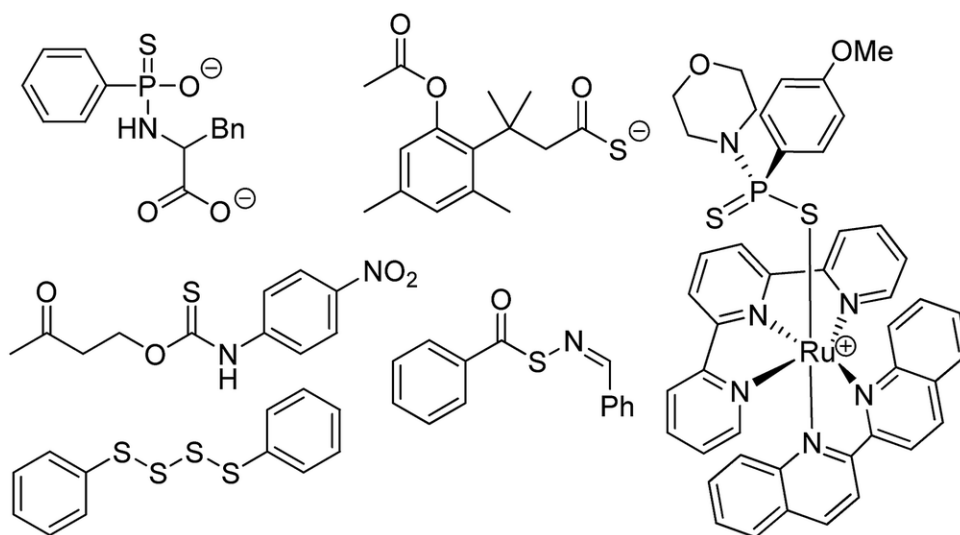


Figure 3.1 Selected examples of synthetic H₂S donors

Drawing parallels to the dissolution of NaSH, small molecules derived from dithiole-3-thione¹³¹ and phosphorodithioate^{33,35} motifs respectively have been synthesized as hydrolysis-activated H₂S donors, although we note the overall low H₂S-releasing efficiencies from these donors. Towards improving releasing yields and tuning rates of H₂S release, analyte-responsive small molecules have been prepared to release H₂S as a function of pH,³⁷ in the presence of native enzymes,¹³² and upon irradiation with light.^{71,}

133

Initially reported by our group,¹³⁴ the conversion of carbonyl sulfide (COS) to H₂S by carbonic anhydrase has been used to access a library of COS/H₂S donors.¹³⁵ Inspired by the endogenous production of H₂S *via* enzymatic conversion of cysteine, a number of thiol-triggered H₂S donors have been reported. Abundant in nature, organic polysulfides⁵⁸ have been shown to release H₂S in the presence of biological thiols including cysteine¹³⁶ and reduced glutathione (GSH).¹³⁷ The generation of persulfides, an important class of biologically-relevant reactive sulfur species,¹³⁸ *via* thiol-mediated reduction has been used to prepare a series of synthetic H₂S donors with potent protective effects against

myocardial-ischemia reperfusion injury.⁵² Similarly, the generation of *N*-mercaptan species in the presence of thiols has been demonstrated as a viable platform for H₂S delivery with tunable releasing kinetics.¹³⁹ Under physiological conditions, thionoesters react rapidly with cysteine *via* a native chemical ligation-like mechanism to afford an equivalent of phenol, H₂S, and a cysteine-derived dihydrothiazole (Figure 3.2a).

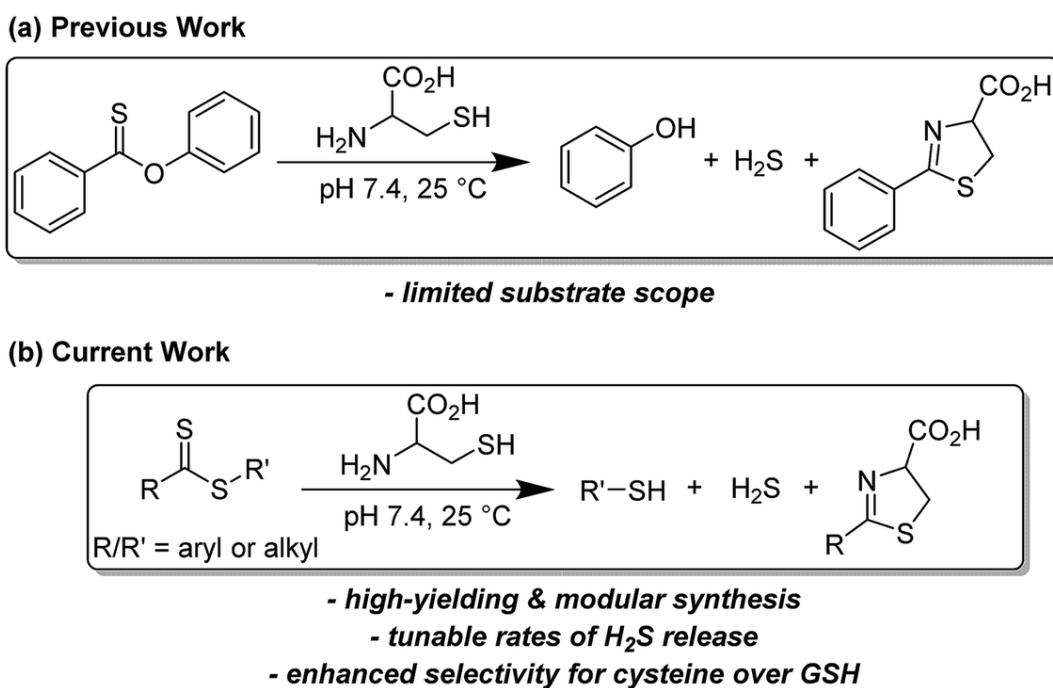


Figure 3.2 (a) Cysteine-triggered H₂S release from thionoesters. (b) Cysteine-triggered H₂S release from dithioesters.

Although dithioesters have been used to prepare polymeric H₂S donors,¹⁴⁰ direct use of this motif as an H₂S donor scaffold has not been reported. Herein, we present our findings on the development of dithioesters as novel, cysteine-triggered H₂S donors (Figure 3.2b) In this chapter, we demonstrate the release of H₂S in the presence of cysteine from a representative (*bis*)phenyl dithioester with a comprehensive kinetic analysis. Additionally, we demonstrate the ability to tune the rate of H₂S release from dithioesters *via* simple alkyl functionalization.

fluorophores and known therapeutics for the development of H₂S-releasing prodrugs. In the interest of accessing tunable H₂S donors, we hypothesized modulation of thiocarbonyl electrophilicity and thiolate leaving group ability would directly alter the rates of cysteine-triggered H₂S release from dithioesters.

With synthesized dithioesters in hand, we began our studies by examining the reactivity of **PDTE** (25 μM) as a representative dithioester towards various concentrations of cysteine (250, 500, 1000, and 1250 μM) and monitoring the release of H₂S *via* the spectrophotometric methylene blue assay, which allows for H₂S quantification (Figure 3.3a).¹⁴² Consistent with our hypothesis, we observed increasing amounts of H₂S released with increasing cysteine concentrations from **PDTE**. To quantify the H₂S-releasing efficiency, we used a methylene blue calibration curve generated with NaSH (Figure C.25) and we found 25 μM **PDTE** released approximately 17 μM H₂S after 1 h, which corresponds to a releasing efficiency of ~68%. Under identical conditions, we note a slight decrease in H₂S-releasing efficiency between dithioesters and thionoesters (80%), although both of these constructs are efficient H₂S-releasing motifs. To quantify the rate of H₂S release, we were able to fit these releasing curves and obtain pseudo-first order rate constants (k_{obs}). A plot of $\log[\text{Cys}]$ *versus* $\log(k_{\text{obs}})$ provided a linear plot with slope near one, which suggests the overall reaction is first order in cysteine and proceeds *via* a mechanism similar to the reaction of thionoesters with cysteine (Figure 3.3b). A plot of $[\text{Cys}]$ *versus* k_{obs} yielded a second-order rate constant (k_2) of $1.8 \pm 0.1 \text{ M}^{-1} \text{ s}^{-1}$ (Figure 3.3c), which is approximately five times slower relative to cysteine-triggered H₂S from thionoesters ($9.1 \pm 0.3 \text{ M}^{-1} \text{ s}^{-1}$).

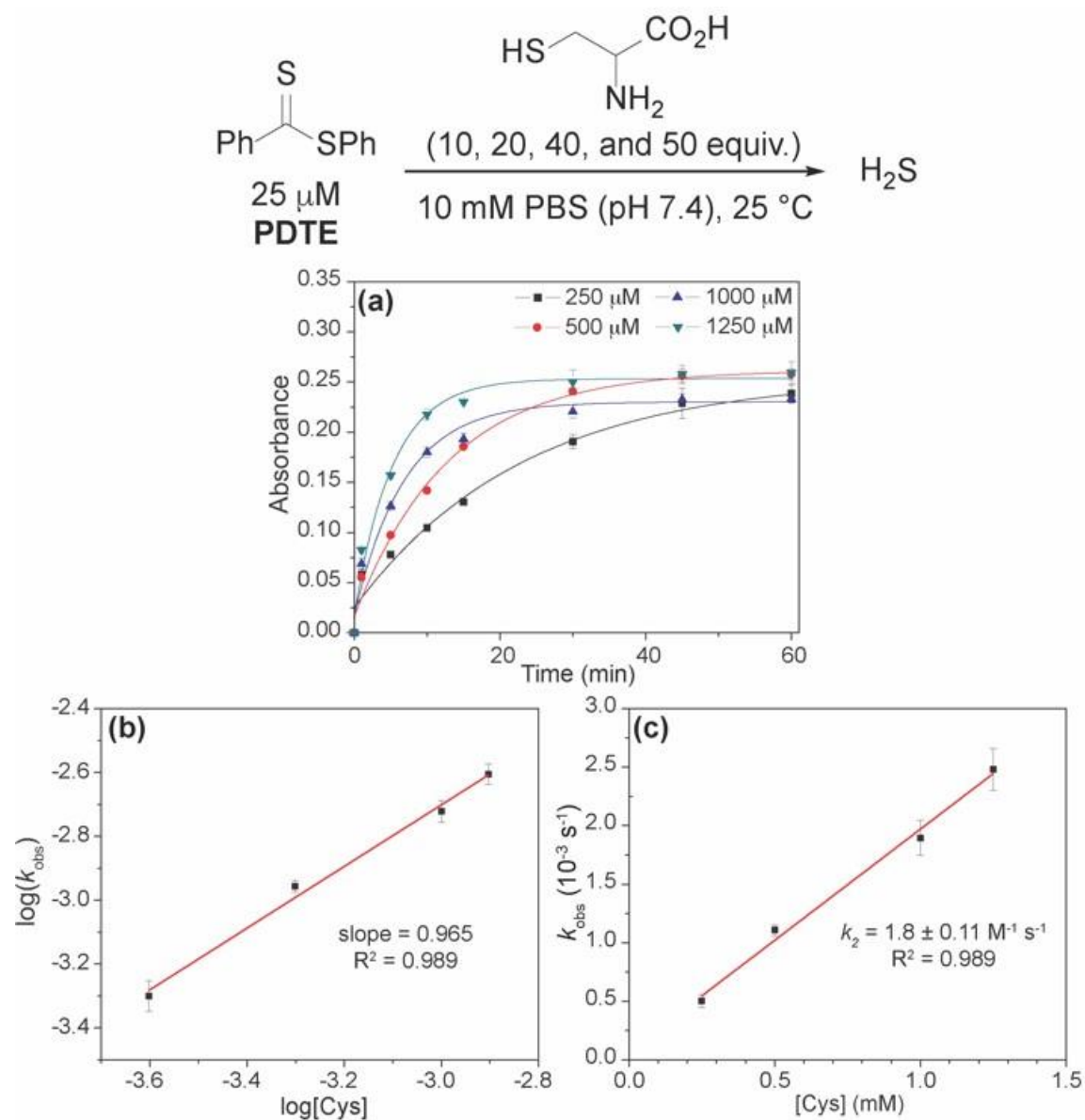


Figure 3.3 (a) Release of H_2S from PDTE (25 μM) in the presence of increasing cysteine concentrations (250, 500, 1000, and 1250 μM). (b) Plot of $\log(k_{\text{obs}})$ vs. $\log([\text{Cys}])$. (c) Plot of k_{obs} vs. $[\text{Cys}]$.

This difference in H_2S -releasing kinetics prompted us to further investigate the kinetics of cysteine-triggered H_2S release from dithioesters and elucidate potential mechanistic differences between both classes of H_2S donors. To further probe the reactivity of dithioesters with respect to H_2S release, we next investigated the effect of cysteine

derivatives and related thiol-based nucleophiles on H₂S release from **PDTE** (Figure 3.4). In the absence of nucleophiles, we did not observe H₂S release under hydrolytic conditions. Although the conversion of a thiocarbonyl to the corresponding carbonyl is thermodynamically favorable with an enthalpic gain of ~ 43 kcal mol⁻¹ when comparing C=S *versus* C=O bond strengths, the hydrolysis of dithioesters is a slow process and can be considered negligible when considering the rate of cysteine-triggered H₂S release.¹⁴³ Further supporting a similar mechanism of cysteine-triggered H₂S release between thionoesters and dithioesters, masking of either the thiol or amine moieties in cysteine completely abolished H₂S release from **PDTE**. Additionally, the use of cysteine methyl ester did not affect H₂S release when compared to H₂S release in the presence of cysteine. To assess the effect of cysteine analogues on H₂S release, we measured H₂S release in the presence of homocysteine and penicillamine. Interestingly, we observed a significant reduction in the H₂S release rate in the presence of homocysteine relative to cysteine-triggered H₂S release. In the presence of penicillamine, we failed to observe significant H₂S release, which we attribute to a reduction in nucleophilicity due to the presence of geminal methyl groups.

We next examined the release of H₂S from **PDTE** in the presence of reduced glutathione (GSH), which is the most abundant biological thiol to determine the effect of competitive thiols on H₂S release. In the presence of 500 μ M GSH, we did not observe significant H₂S release, but also could not rule out that transthioesterification by GSH, which would result in consumption of the dithioester moiety with a lack of H₂S release. Considering the nucleophilicity of the departing thiophenol, we hypothesized that the reversibility of transthioesterification is likely to be more efficient for dithioesters than for

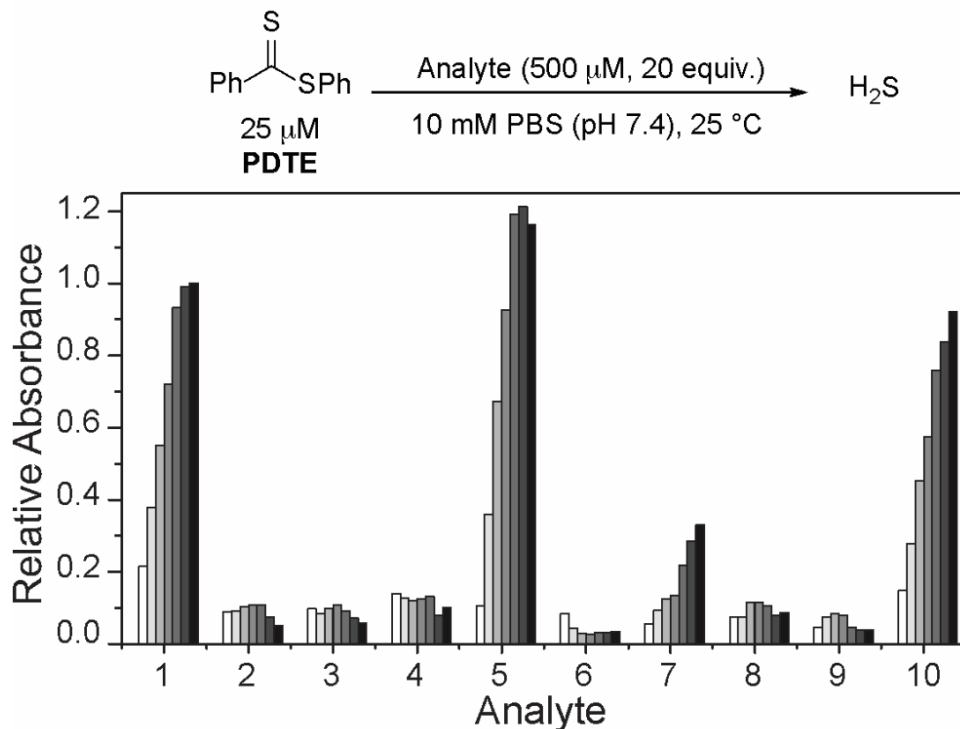
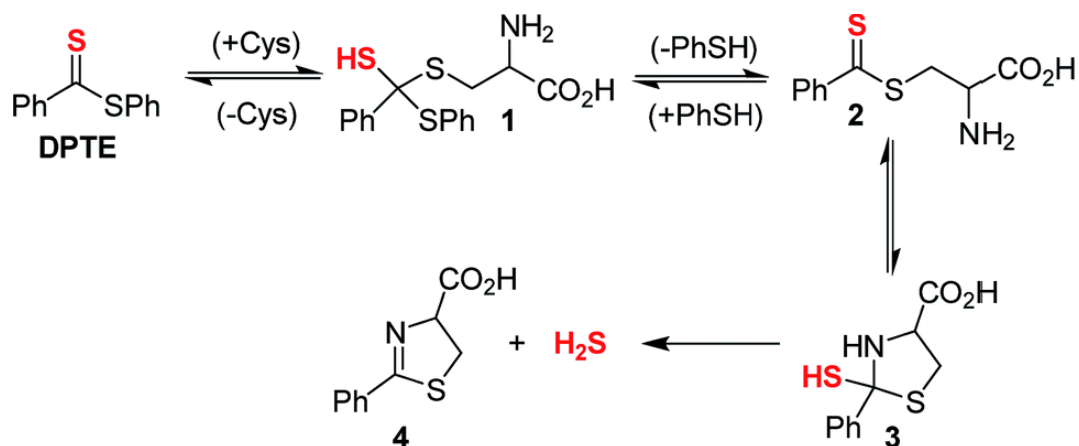


Figure 3.4 Selectivity of H₂S release from **PDTE** in the presence of different analytes. Data were acquired at 1, 5, 10, 15, 30, 45, and 60 min. Methylene blue absorbance values are relative to the maximum absorbance value obtained from H₂S release in the presence of cysteine (1). Analytes: H₂O (2), *N*-acetyl-L-cysteine (3), *S*-methyl-L-cysteine (4), L-cysteine methyl ester hydrochloride (5), *N*-acetyl-L-cysteine methyl ester (6), DL-homocysteine (7), DL-penicillamine (8), GSH (9), cysteine + 1 mM GSH (10).

thionoesters, which should result in enhanced selectivity for cysteine over GSH. To test this hypothesis, we measured H₂S release from **PDTE** in the presence of 500 μM cysteine and 1 mM GSH. In support of the expected enhanced reversibility, we observed minimal change on the cysteine-triggered H₂S release from **PDTE** even in the presence of excess GSH. This presents a considerable advancement over the thionoester scaffold, which yielded a decreased H₂S-releasing efficiency in the presence of GSH and cysteine. Taken together, these results demonstrate the selectivity of the dithioester scaffold for cysteine over other thiol-based nucleophiles including GSH and we proposed the following mechanism of H₂S release (Scheme 3.2).



Scheme 3.2 Proposed mechanism for release of H₂S from **PDTE** in the presence of cysteine.

Initial nucleophilic attack by cysteine on **PDTE** generates tetrahedral intermediate **1**, which collapses upon thiocarbonyl formation and extrusion of thiophenol to yield intermediate **2**. Nucleophilic attack by the pendant amine generates intermediate **3**, which extrudes H₂S upon formation of dihydrothiazole **4**. Based on the negligible loss in H₂S-releasing efficiency in the presence of excess GSH, the generation of **1** and **2** is likely highly reversible and could provide enhanced selectivity of the dithioester moiety for cysteine. In the mechanism of cysteine-triggered release of H₂S from thionoesters, the poor nucleophilicity of the departing alcohol likely impedes formation of the initial thionoester. In our proposed mechanism of H₂S release from dithioesters, the departing thiolate bears enhanced nucleophilicity and likely reacts with the intermediate dithioester to regenerate the initial dithioester effectively reversing cysteine addition. Additionally, the enhanced reversibility of transthioesterification supports the considerably slower kinetics between dithioesters and thionoesters. Taken together, we hypothesized this enhanced reversibility would result in the initial nucleophilic attack by cysteine being the rate-determining step of cysteine-triggered H₂S release from dithioesters.

To confirm the formation of a cysteine-based dihydrothiazole, **PDTE** (100 μM) was treated with l-cysteine methyl ester (2 mM, 20 equiv.) and a reaction aliquot after 1 h was subjected to HPLC analysis (Figure C.26). In agreement with our proposed mechanism, the HPLC analysis revealed the formation of the expected dihydrothiazole in $\sim 61\%$ yield, which is consistent with the H_2S -releasing efficiency of **PDTE** as measured *via* the methylene blue assay. To gain insights on the rate-determining step, we measured the effect of temperature on the rate of H_2S release from **PDTE** (25 μM) in the presence of cysteine (500 μM , 20 equiv.) (Figure 3.5).

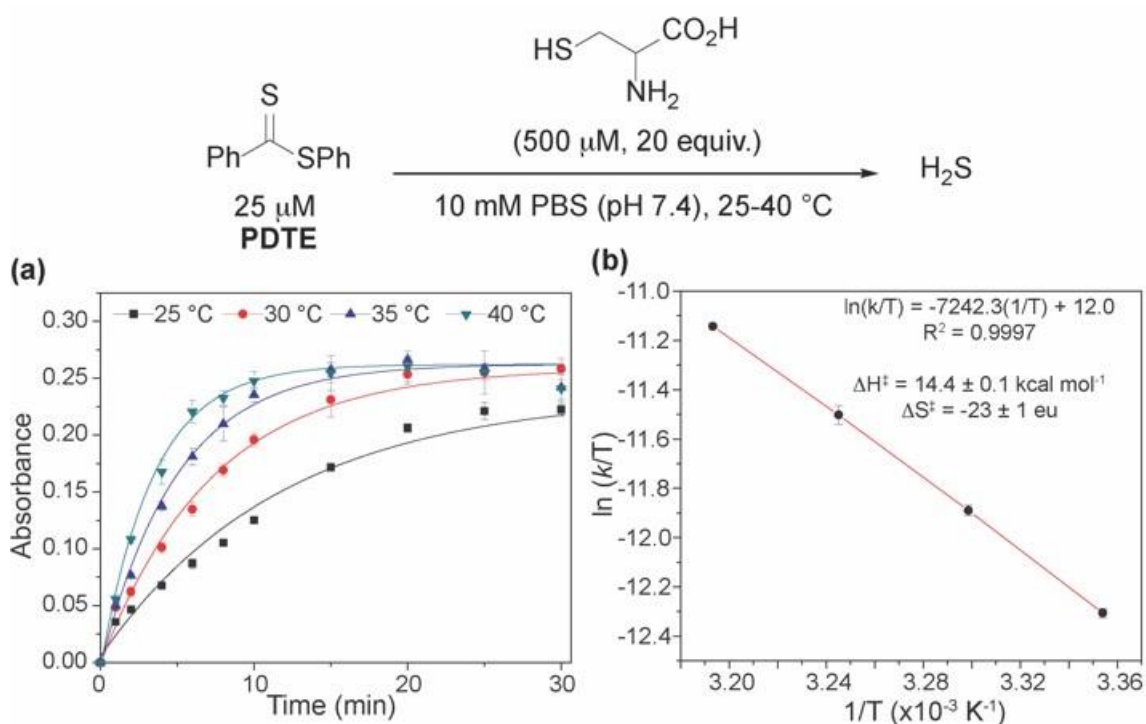


Figure 3.5 (a) Effect of temperature on rate of H_2S release from **PDTE** (25 μM) in the presence of cysteine (500 μM , 20 equiv.). (b) Eyring analysis of cysteine-triggered H_2S release from **PDTE**.

If nucleophilic attack by cysteine on **PDTE** is the rate-determining step of the reaction, we would expect to observe an entropy of activation (ΔS^\ddagger) of approximately -20 eu , which would be characteristic of a bimolecular reaction.

Upon measuring the rates of H₂S release at different temperatures, we constructed an Eyring plot using the obtained k_{obs} values, which afforded $\Delta S^\ddagger = -23 \pm 1$ eu. The observed ΔS^\ddagger supports our mechanistic hypothesis and is consistent with the initial addition of cysteine to the dithioester to generate **1** being the rate-determining step of cysteine-triggered H₂S release from dithioesters. In the reaction of thionoesters with cysteine, we interpreted an experimentally determined $\Delta S^\ddagger = -38 \pm 3$ eu to suggest the intramolecular cyclization as the rate determining step. In comparison between both mechanisms, by simply altering the nucleophilicity of the leaving group (*i.e.* alcohol *vs.* thiol) we have shunted the rate-determining step of the reaction. Additionally, our results suggest that cysteine-triggered H₂S release from dithioesters and native chemical ligation share a similar rate-determining step.

To complement our experimental results, we used density functional theory (DFT) to examine the potential energy surface for H₂S release from dithioesters. Because **PDTE** was used for our experimental mechanistic investigations, we chose to investigate the reaction of **PDTE** with cysteine thiolate using Gaussian 09 at the B3LYP/6-311++G(d,p) level of theory applying the IEF-PCM water solvation model. We found that the initial nucleophilic attack by cysteine thiolate on **PDTE** resulted in an activation barrier of 19.1 kcal mol⁻¹, which was the highest barrier on the reaction coordinate and qualitatively agrees with the experimentally observed ΔH^\ddagger of 14.4 kcal mol⁻¹. The resultant transthioesterified cysteine adduct is 3.7 kcal mol⁻¹ more stable than the **PDTE** starting material, and subsequently undergoes an intramolecular S to N thioacyl transfer reaction with an associated barrier of 8.9 kcal mol⁻¹, resulting in the final and more thermodynamically favorable dihydrothiazole product (Figure 3.6).

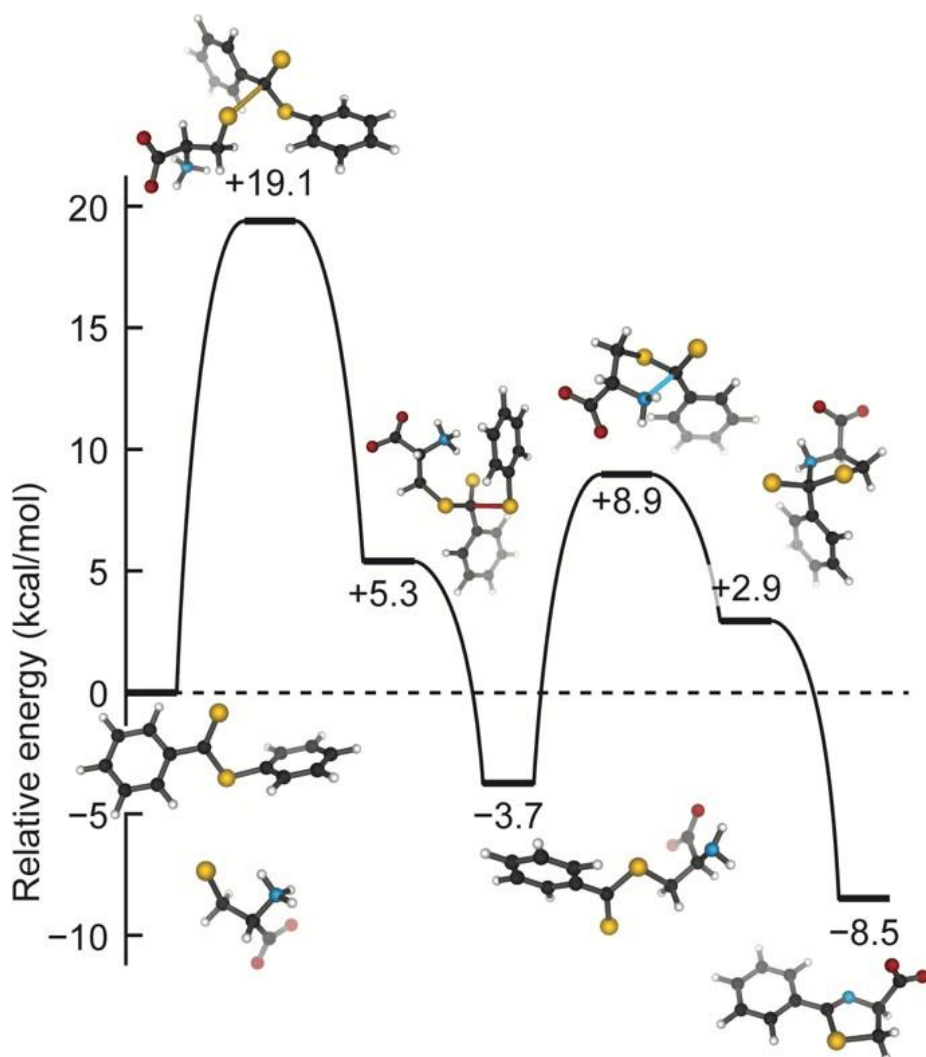


Figure 3.6 Potential energy surface for the attack of cysteine thiolate on **PDTE**. Calculations were performed in Gaussian 09 at the B3LYP/6-311++G(d,p) level of theory applying the IEF-PCM water solvation model.

The ease of synthesis of dithioester compounds also enabled further investigation into the effect of alkyl functionalization on H₂S release. We hypothesized that the electrophilicity at the thiocarbonyl position could be modified directly by introducing various alkyl, and thus alter the rate of H₂S release. Additionally, we hypothesized that modification of the departing thiolate nucleophilicity would also alter the rate of H₂S

release from dithioesters. We anticipated the introduction of inductively donating alkyl groups, such as methyl and isopropyl, would decrease the thiocarbonyl electrophilicity and resulting in decreased rates of H₂S release. Additionally, we anticipated that replacement of thiophenol with benzyl mercaptan would result in decreased rates of H₂S release due to the enhanced nucleophilicity of benzyl mercaptan over thiophenol. To test our hypotheses, we measured H₂S release from our library of alkyl functionalized dithioesters (25 μM) in the presence of cysteine (500 μM, 20 equiv.) (Figure 3.7).

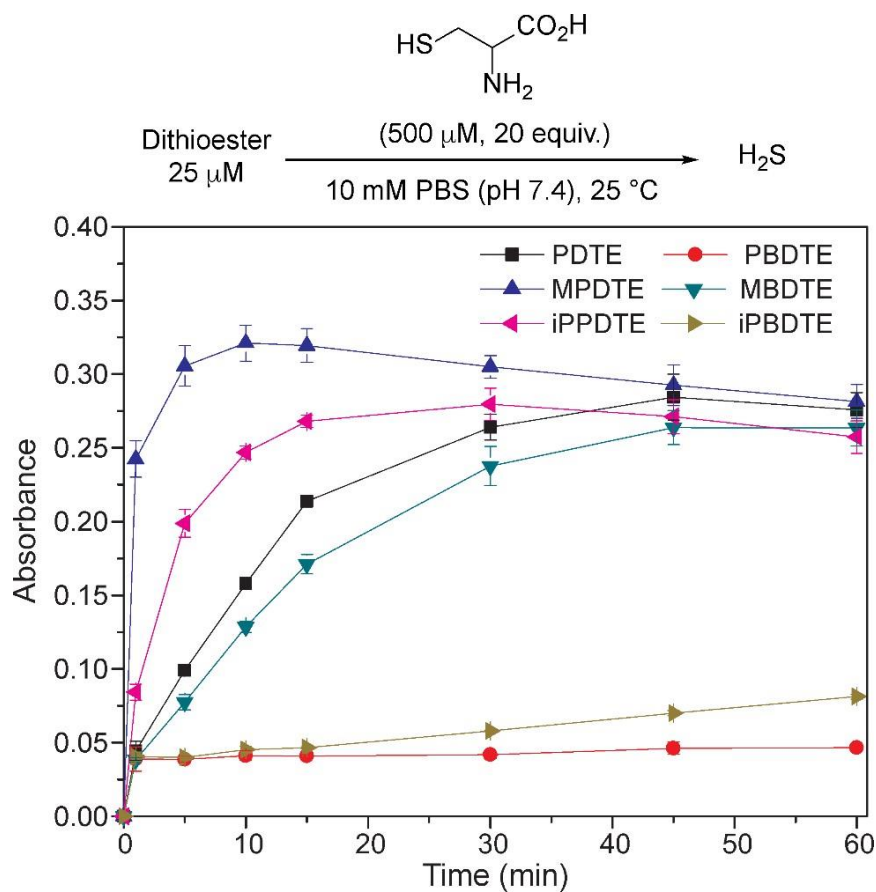


Figure 3.7 Effect of alkyl functionalization on the rate of H₂S release from dithioesters.

Contrary to our initial hypothesis, the incorporation of inductively-donating alkyl groups led to enhanced rates of H₂S release relative to **PDTE**. To better understand the

apparent releasing trends, we considered the stability of the charge-separated thiocarbonyl motif and the effect of different alkyl groups (Figure 3.8).

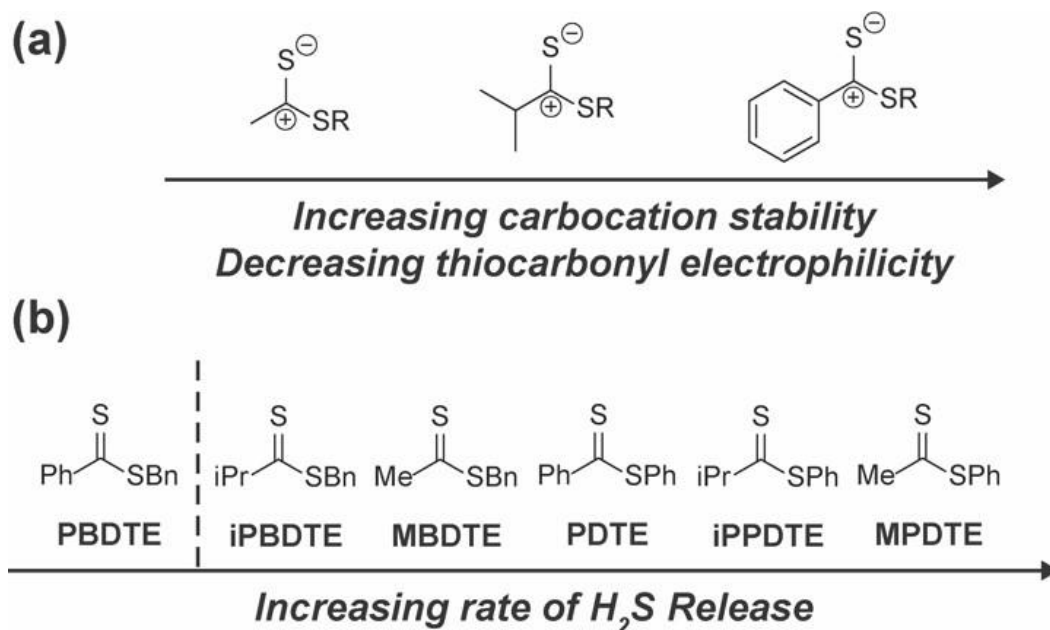


Figure 3.8 (a) Effect of pendant groups on thiocarbonyl electrophilicity and carbocation stability. (b) Scale of increasing H₂S releasing rates for reported dithioesters.

In the case of **PDTE**, a charge-separated thiocarbonyl yields a benzylic carbocation which can readily delocalize *via* resonance effectively altering the electrophilicity of the thiocarbonyl *via* delocalization of the carbocation. In the presence of inductively donating groups such as methyl and isopropyl in **MPDTE** and **iPPDTE** respectively, the resulting carbocation is localized to the thiocarbonyl position, which would result in enhanced rates of H₂S release in comparison to **PDTE**. Incorporation of an isopropyl group in **iPPDTE**, however, also introduces the potential for an intermediate 1,2-methyl shift which would partially delocalize the carbocation and hinder H₂S release relative to **MPDTE**. Considering these contributions, we interpret the enhanced release of H₂S from alkyl-functionalized dithioesters as a reflection of altered thiocarbonyl

electrophilicity *via* carbocation delocalization. Although this outcome was contrary to our initial hypothesis, these findings demonstrate the ability to tune the rate of H₂S release from dithioesters by simple alkyl substitutions.

Furthering our studies, we also examined the effect of benzyl mercaptan as a leaving group on H₂S release from **MBDTE**, **PBDTE**, and **iPBDTE** respectively. In comparison to thiophenol, benzyl mercaptan is a considerably better nucleophile and likely perturbs the equilibrium of transthioesterification to disfavor the addition of cysteine. In concert with the effect of alkyl groups on thiocarbonyl electrophilicity, we anticipated H₂S release from dithioesters bearing benzyl mercaptan to be dramatically altered relatively to their thiophenol analogue. In agreement with our hypothesis, H₂S release was observed exclusively from **MBDTE**. Considering the lack of carbocation delocalization by the pendant methyl group, this result suggests the thiocarbonyl moiety in **MBDTE** is sufficiently electrophilic to promote H₂S release in the presence of cysteine. Alternatively, we observed effectively no H₂S release from **PBDTE** and relatively slow H₂S release from **iPBDTE**. Considering the effect of alkyl groups on thiocarbonyl electrophilicity *via* carbocation delocalization in concert with the enhanced nucleophilicity of benzyl mercaptan, a significantly hindered rate of release from **iPBDTE** and complete shutdown of H₂S release from **PBDTE** is also in agreement with our hypothesis. Overall, we found the use of benzyl mercaptan decreased overall H₂S-releasing efficiency and yielded hindered rates of release in comparison to thiophenol-based dithioesters. Taken together, these findings demonstrate the rate of H₂S release from dithioesters can be enhanced or decreased as a function of alkyl substitution.

3.3 Conclusions

Advancing our previous work on synthetic H₂S donors *via* the chemoselective condensation of thionoesters and cysteine, we have identified that dithioesters are a viable and tunable platform for developing cysteine-triggered H₂S donors. Using **PDTE** as a representative dithioester, we have demonstrated H₂S release in the presence of cysteine proceeds with good efficiency, and that dithioesters provide significant advancements over thionoesters, including ease of functionalization and enhanced selectivity for cysteine over other thiol-based nucleophiles including GSH. Mechanistic investigations, including rate-order analysis and activation parameters support a mechanism in which the initial nucleophilic attack by cysteine on the dithioesters is the rate-determining step of the reaction, which is also supported by computation. Furthermore, we demonstrated that the rate of H₂S release from a small library of dithioesters can be controlled by alkyl substitution. The findings presented herein provide several advancements over thionoesters as cysteine-triggered H₂S donors and provides a foundation for further development of dithioesters for expanding upon the chemical biology of H₂S.

The ability to tune H₂S release from dithioesters provides a H₂S donor which can be altered to meet the demands of specific diseases states or local cysteine concentrations. The enzymatic production of H₂S is primarily based upon cysteine catabolism and the formation of H₂S-releasing persulfide intermediates. Chapter IV discusses our work on organic tetrasulfides which release H₂S through intermediate persulfide generation.

3.4 Experimental Details

3.4.1 Materials and Methods

Reagents were purchased from Tokyo Chemical Industry and/or Oakwood Chemicals and used directly as received. Deuterated solvents were purchased from Cambridge Isotope Laboratories and used as received. ^1H and $^{13}\text{C}\{^1\text{H}\}$ NMR were recorded on Bruker 500 and 600 MHz instruments. Chemical shifts are reported relative to residual protic solvent resonances. MS data was collected on a Xevo Waters ESI LC/MS instrument. Silica gel (SiliaFlash F60, Silicycle, 230- 400 mesh) was used for column chromatography. All air-free manipulations were performed under an inert atmosphere using standard Schlenk technique or an Innovative Atmospheres N_2 -filled glove box. UV-Vis spectra were acquired on an Agilent Cary 60 UV-Vis spectrophotometer equipped with a Quantum Northwest TC-1 temperature controller at $25\text{ }^\circ\text{C} \pm 0.05\text{ }^\circ\text{C}$.

H₂S Detection Materials and Methods

Phosphate buffered saline (PBS) tablets (1X, CalBioChem) were used to prepare buffered solutions (140 mM NaCl, 3 mM KCl, 10 mM phosphate, pH 7.4) in deionized water. Buffer solutions were sparged with N_2 to remove dissolved oxygen and stored in an N_2 -filled glovebox. Donor stock solutions (in DMSO) were prepared inside an N_2 -filled glovebox and stored at $-25\text{ }^\circ\text{C}$ until immediately before use. Trigger stock solutions (in PBS) were freshly prepared in an N_2 -filled glovebox immediately before use.

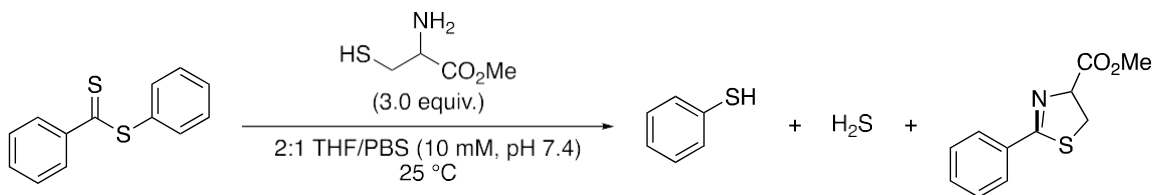
General Procedure for Measuring H₂S Release via Methylene Blue Assay (MBA)

Scintillation vials containing 20 mL of PBS were prepared in an N₂-filled glovebox. To these solutions, 20 μ L of 500 mM analyte stock solution (in PBS) was added for a final concentration of 500 μ M. While stirring, the solutions were allowed to thermally equilibrate in heating block at the desired temperature for approximately 20-30 min. Immediately prior to donor addition, 0.5 mL solutions of methylene blue cocktail were prepared in disposable 1.5 mL cuvettes. The methylene blue cocktail solution contains: 200 μ L of 30 mM FeCl₃ in 1.2 M HCl, 200 μ L of 20 mM *N,N*-dimethyl-*p*-phenylene diamine in 7.2 M HCl, and 100 μ L of 1% (w/v) Zn(OAc)₂. To begin an experiment, 20 μ L of 25 mM donor stock solution (in DMSO) was added for a final concentration of 25 μ M. At set time points after the addition of donor, 500 μ L reaction aliquots were added to the methylene blue cocktail solutions and incubated for 1 h at room temperature shielded from light. Absorbance values at 670 nm were measured 1 h after addition of reaction aliquot. Each experiment was performed in quadruplicate unless stated otherwise.

MBA Calibration Curve

Solutions containing 0.5 mL of the methylene blue cocktail and 0.5 mL PBS containing 500 μ M cysteine were freshly prepared in disposable cuvettes (1.5 mL). Under inert conditions, a 10 mM stock solution of NaSH (Strem Chemicals) in PBS was prepared and diluted to 1 mM. Immediately after dilution, 1 mM NaSH was added to 1.0 mL solutions for final concentrations of 10, 20, 30, 40, and 50 μ M. Solutions were mixed thoroughly, incubated at room temperature for 1 h, and shielded from light. Absorbance values at 670 nm were measured after 1 h (Figure C.27)

Reaction Product Analysis by High Performance Liquid Chromatography (HPLC)



Scheme 3.3 Preparative scale synthesis of **CysDHT** from **PDTE**

To a 20 mL solution of 10% THF in PBS (10 mM, pH 7.4) containing 2 mM L-cysteine methyl ester (20 equiv.), 20 mL of 100 mM **PDTE** in THF was added for 100 mM **PDTE** and stirred at room temperature. After 1 h, a 1 mL reaction aliquot was analyzed by HPLC. HPLC analysis was performed on an Agilent 1260 HPLC instrument with a Poroshell 120 EC-C18 4.6x100 mm column and monitored at 280 nm. Solvent A: 95% H₂O, 5% MeOH, Solvent B: 100% MeCN. Gradient: 35% Solvent A/65% Solvent B for 2 min. Change to 100% Solvent B over 4 min and hold for 6.5 min. Change to 35% Solvent A/65% Solvent B over 0.5 min and hold for 4.5 min. Flow Rate: 0.5 mL/min, 2 μ L injection. The concentration of **CysDHT** present at the end of the reaction was determined by measurement against calibration curves for each compound.

Computational Details and Geometries

Structures were initially constructed in Avogadro and optimized using the UFF force field. These resultant structures were then further geometrically optimized using a hybrid GGA functional, B3LYP, with a large triple zeta basis, 6-311++G**, that includes diffuse and polarization functions for all atoms. A pseudosolvent polarizable continuum model was used (water), to partially account for solvent stabilization. VeryTight convergence criteria

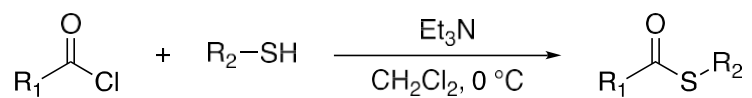
for forces and displacements, as implemented in Gaussian 09. Energetics were compared to a double zeta basis, 6-31+G*, which showed similar trends and energies.

Transition states were located using i) a potential energy surface scan with the modredundant feature to locate a good starting point for ii) a transition state search. The transition states were confirmed using vibrational analysis as evidenced by a single imaginary frequency corresponding to the direction of bond making / breaking.

3.4.2 Synthesis

General procedure for the synthesis of thioesters

This procedure was modified from a previous report.¹¹⁶



Scheme 3.4 Synthesis of thioesters

The desired thiol (1.1 equiv.) and triethylamine (1.1 equiv.) were added to anhydrous CH₂Cl₂ (20 mL) and cooled to 0 °C. Once cooled, the desired acid chloride (1.0 equiv.) was added dropwise, and the reaction was stirred at 0 °C for 1 h. The reaction was quenched with deionized H₂O (30 mL), and the organic layer was separated. The aqueous layer was extracted with CH₂Cl₂ (2 x 20 mL) and the combined organic extractions were washed with brine (1 x 20 mL), dried over MgSO₄, and concentrated under reduced pressure. The desired product was purified by column chromatography.

S-phenyl benzothioate

White powder, 852 mg (96%) $R_f = 0.23$ (25% CH_2Cl_2 in hexanes)

^1H NMR (600 MHz, CDCl_3) δ : 8.04 (d, 2 H), 7.61 (t, 1 H), 7.55 – 7.44 (m, 7 H). $^{13}\text{C}\{^1\text{H}\}$ NMR (151 MHz, CDCl_3) δ : 190.14, 136.63, 135.09, 133.65, 129.52, 129.24, 128.74, 127.48, 127.34. TOF MS (ASAP⁺) (m/z): $[\text{M} + \text{H}]^+$ calc'd for $\text{C}_{13}\text{H}_{10}\text{OS}$ 215.0531; found 215.0548

S-phenyl ethanethioate.

Clear oil, 538 mg (86%) $R_f = 0.42$ (50% CH_2Cl_2 in hexanes)

^1H NMR (500 MHz, CDCl_3) δ : 7.42 (s, 5 H), 2.43 (s, 3 H). $^{13}\text{C}\{^1\text{H}\}$ NMR (151 MHz, CDCl_3) δ : 194.06, 134.44, 129.43, 129.19, 127.91, 30.19. TOF MS (ASAP⁺) (m/z): $[\text{M} + \text{H}]^+$ calc'd for $\text{C}_8\text{H}_8\text{OS}$ 153.0374; found 153.0374

S-phenyl 2-methylpropanethioate.

Clear oil, 492 mg (66%) $R_f = 0.56$ (50% CH_2Cl_2 in hexanes)

^1H NMR (500 MHz, CDCl_3) δ : 7.41 (s, 5 H), 2.87 (hept, $J = 6.9, 1.9$ Hz, 1 H), 1.27 (d, $J = 7.0, 1.8$ Hz, 6 H). ^{13}C NMR (126 MHz, CDCl_3) δ : 201.85, 134.56, 129.17, 129.09, 127.87, 42.99, 19.37. TOF MS (ASAP⁺) (m/z): $[\text{M} + \text{H}]^+$ calc'd for $\text{C}_{10}\text{H}_{12}\text{OS}$ 181.0687; found 181.0705

S-benzyl benzothioate.

Clear oil, 779 mg (93%) $R_f = 0.40$ (33% CH_2Cl_2 in hexanes)

^1H NMR (500 MHz, CDCl_3) δ : 7.98 (d, $J = 7.6$ Hz, 2 H), 7.57 (t, $J = 7.4$ Hz, 1H), 7.45 (t, $J = 8.0$ Hz, 2 H), 7.39 (d, $J = 8.1$ Hz, 2 H), 7.33 (t, $J = 7.5$ Hz, 2 H), 7.29 – 7.24 (m, 1 H), 4.33 (s, 2 H). ^{13}C NMR (126 MHz, CDCl_3) δ : 191.27, 137.45, 136.78, 133.42, 128.96, 128.61, 127.31, 127.28, 33.32. TOF MS (ASAP⁺) (m/z): $[\text{M} + \text{H}]^+$ calc'd for $\text{C}_{14}\text{H}_{12}\text{OS}$ 229.0687; found 229.0655

S-benzyl ethanethioate.

Clear oil, 405 mg (67%) $R_f = 0.24$ (25% CH_2Cl_2 in hexanes)

^1H NMR (600 MHz, CDCl_3) δ : 7.31 – 7.27 (m, 4 H), 7.27 – 7.23 (m, 1 H), 4.13 (s, 2 H), 2.35 (s, 3 H). ^{13}C NMR (151 MHz, CDCl_3) δ : 195.09, 137.56, 128.77, 128.60, 127.24, 33.42, 30.29. TOF MS (ASAP⁺) (m/z): $[\text{M} + \text{Na}]^+$ calc'd for $\text{C}_9\text{H}_{10}\text{OS}$ 189.0350; found 189.0485

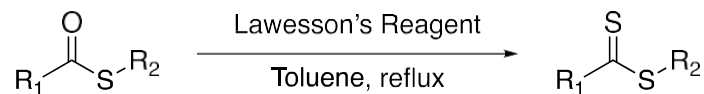
S-benzyl 2-methylpropanethioate.

Clear oil, 577 mg (66%) $R_f = 0.48$ (33% CH_2Cl_2 in hexanes)

^1H NMR (600 MHz, CDCl_3) δ : 7.31 – 7.28 (m, 4 H), 7.25 – 7.22 (m, 1 H), 4.11 (s, 2 H), 2.76 (hept, $J = 6.9$ Hz, 1 H), 1.21 (d, $J = 6.9$ Hz, 6 H). ^{13}C NMR (151 MHz, CDCl_3) δ : 203.44, 137.73, 128.79, 128.59, 127.17, 42.88, 32.89, 19.35. TOF MS (ASAP⁺) (m/z): $[\text{M} + \text{H}]^+$ calc'd for $\text{C}_{11}\text{H}_{14}\text{OS}$ 195.0844; found 195.0835

General procedure for the synthesis of dithioesters

This procedure has been modified from a previous report.¹¹⁶



Scheme 3.5 Synthesis of dithioesters

The desired thioester (1.0 equiv.) and Lawesson's Reagent (0.75 equiv.) were added to anhydrous toluene (20 mL) and heated to 120 °C under reflux. After 5.5 h, the reaction mixture was cooled to room temperature and filtered. The filtrate was concentrated under reduced pressure, and the desired product purified by column chromatography.

Phenyl benzodithioate (**PDTE**).

Red-violet solid, 217 mg (81%) R_f = 0.42 (20% CH₂Cl₂ in hexanes)

¹H NMR (600 MHz, CDCl₃) δ : 8.10 (d, J = 7.1 Hz, 1 H), 7.57 (t, 1H), 7.54 – 7.47 (m, 6 H), 7.45 – 7.40 (m, 2 H). ¹³C NMR (151 MHz, CDCl₃) δ : 228.49, 144.59, 135.38, 132.60, 131.38, 130.36, 129.66, 128.40, 126.99. TOF MS (ASAP⁺) (m/z): [M + H]⁺ calc'd for C₁₃H₁₀S₂ 231.0302; found 231.0302

Phenyl ethanedithioate (**MPDTE**).

Burnt orange oil, 185 mg (67%) R_f = 0.40 (20% CH₂Cl₂ in hexanes)

¹H NMR (500 MHz, CDCl₃) δ : 7.52 – 7.46 (m, 3 H), 7.45 – 7.40 (m, 2 H), 2.87 (s, 3 H). ¹³C NMR (151 MHz, CDCl₃) δ : 234.30, 134.74, 131.77, 130.36, 129.60, 38.95. TOF MS (ASAP⁺) (m/z): [M + H]⁺ calc'd for C₈H₈S₂ 169.0146; found 169.0132

Phenyl 2-methylpropanedithioate (**iPPDTE**).

Yellow oil, 129 mg (59%) $R_f = 0.58$ (25% CH_2Cl_2 in hexanes)

^1H NMR (600 MHz, CDCl_3) δ : 7.50 – 7.47 (m, 3 H), 7.42 – 7.39 (m, 2 H), 3.54 (hept, $J = 6.7$ Hz, 1 H), 1.38 (d, $J = 6.6$ Hz, 6 H). ^{13}C NMR (151 MHz, CDCl_3) δ : 246.77, 134.97, 130.83, 130.18, 129.51, 48.70, 24.24. TOF MS (ASAP⁺) (m/z): $[\text{M} + \text{H}]^+$ calc'd for $\text{C}_{10}\text{H}_{12}\text{S}_2$ 197.0459; found 197.0463

Benzyl benzodithioate (**PBDTE**).

Red oil, 243 mg (91%) $R_f = 0.41$ (20% CH_2Cl_2 in hexanes)

^1H NMR (500 MHz, CDCl_3) δ : 8.00 (d, $J = 7.7$ Hz, 2 H), 7.53 (t, $J = 7.5$ Hz, 1 H), 7.42 – 7.27 (m, 8 H), 4.61 (s, 2 H). $^{13}\text{C}\{^1\text{H}\}$ NMR (126 MHz, CDCl_3) δ : 227.69, 144.75, 134.97, 132.40, 129.29, 128.72, 128.34, 127.75, 126.90, 42.28. TOF MS (ASAP⁺) (m/z): $[\text{M} + \text{H}]^+$ calc'd for $\text{C}_{14}\text{H}_{12}\text{S}_2$ 245.0459; found 245.0471

Benzyl ethanedithioate (**MBDTE**).

Yellow-brown oil, 181 mg, (82%) $R_f = 0.54$ (25% CH_2Cl_2 in hexanes)

^1H NMR (600 MHz, CDCl_3) δ : 7.34 – 7.26 (m, 5 H), 4.46 (s, 2 H), 2.85 (s, 3 H). $^{13}\text{C}\{^1\text{H}\}$ NMR (151 MHz, CDCl_3) δ : 232.29, 135.13, 129.09, 128.67, 127.66, 41.98, 38.85. TOF MS (ASAP⁺) (m/z): $[\text{M} + \text{Na}]^+$ calc'd for $\text{C}_9\text{H}_{10}\text{S}_2$ 183.0302; found 183.028

Benzyl 2-methylpropanedithioate (**iPBDTE**).

Orange-brown oil, 164 mg (76%) $R_f = 0.58$ (25% CH_2Cl_2 in hexanes)

^1H NMR (600 MHz, CDCl_3) δ : 7.34 – 7.26 (m, 5 H), 4.45 (s, 2H), 3.42 (hept, $J = 6.7$ Hz, 1 H), 1.34 (d, $J = 6.7$ Hz, 7 H). $^{13}\text{C}\{^1\text{H}\}$ NMR (151 MHz, CDCl_3) δ : 245.91, 135.22, 129.13, 128.67, 127.58, 49.35, 40.52, 24.19. TOF MS (ASAP⁺) (m/z): $[\text{M} + \text{H}]^+$ calc'd for $\text{C}_{11}\text{H}_{14}\text{S}_2$ 211.0615; found 211.0612

CHAPTER IV

APPLICATIONS OF SYNTHETIC ORGANIC TETRASULFIDES AS H₂S DONORS

This chapter includes previously published and coauthored material from Cerda, M.M.; Hammers, M.D.; Earp, M.S.; Zakharov, L.N.; Pluth, M.D. Applications of Synthetic Organic Tetrasulfides as H₂S Donors. *Org. Lett.* **2017**, *19* (9), 2314-2317. This manuscript was written by Matthew M. Cerda with editorial assistance from Professor Michael D. Pluth. The project in this chapter was conceived by Dr. Matthew D. Hammers and Mary S. Earp. The experimental work in this chapter was performed by Matthew M. Cerda. The crystallographic data in this chapter was collected by Dr. Lev N. Zakharov.

4.1 Introduction

Nitric oxide (NO), carbon monoxide (CO), and hydrogen sulfide (H₂S) are small gaseous molecules, often called gasotransmitters, which are produced endogenously, freely permeate cell membranes, and act on molecular or cellular targets to exert physiological effects.¹²⁴ Over the past decade, the accepted roles of H₂S in biology have expanded and now include important roles in neurotransmission,¹⁴⁴ vasodilation,¹⁴⁵ apoptosis,¹⁴⁶ and other physiological processes.^{127a} Aligned with these physiological roles, new chemical tools that enable H₂S delivery are needed for both research and potential therapeutic applications.^{15e, 147} Because direct administration of H₂S gas is not practical in most biological contexts, many researchers employ inorganic sulfide salts, such as sodium

hydrosulfide (NaSH) or sodium sulfide (Na₂S), as a primary sulfide source. By comparison to enzymatic H₂S production profiles, these sulfide salts release H₂S instantaneously upon dissolution, often resulting in unwanted volatilization, oxidation, and/or reduced effective residence times.¹²⁹ To address this issue, small molecule H₂S donors that release H₂S at controlled rates comparable to enzymatic H₂S production have been prepared and investigated.^{130c} Current common motifs found in H₂S donation include aryl isothiocyanates,¹⁴⁸ phosphinodithioates,¹⁴⁹ thioacids¹³²/amides,¹⁵⁰ dithiolethiones,¹⁵¹ thiolysis of trisulfides,¹⁵² and protected persulfides¹⁵³ and stimulated release of carbonyl sulfide (COS) from thiocarbamates, which is subsequently converted to H₂S by carbonic anhydrase.¹³⁴ Of these methods, one of the simplest and most commonly used for H₂S donation is the allium-derived diallyl trisulfide (DATS), which releases H₂S upon reaction with thiols (Figure 4.1a). The mechanism of this reaction has been investigated in detail,¹⁵⁴ and the sulfide from DATS has been attributed to the beneficial cardiovascular effects of garlic.¹⁵⁵ Despite this widespread utility, DATS is the only polysulfide that has been used broadly as an H₂S donor despite other accessible polysulfides, many of which have higher sulfane sulfur content and therefore higher H₂S releasing capacity.

Polysulfides are a class of naturally occurring molecules and are in part responsible for the beneficial cardiovascular effects associated with consumption of alliums such as garlic.^{152, 156} More exotic polysulfides, including varacin and chaetocin C (Figure 4.1b), have also been isolated from natural sources indicative of their abundance and biological importance. Independent of H₂S releasing capacities, polysulfides are also involved

directly in a variety of physiological processes, including inhibition of cholesterol synthesis, anti-inflammation, and antioxidant activity.¹⁵⁷ Inspired by the prevalence of

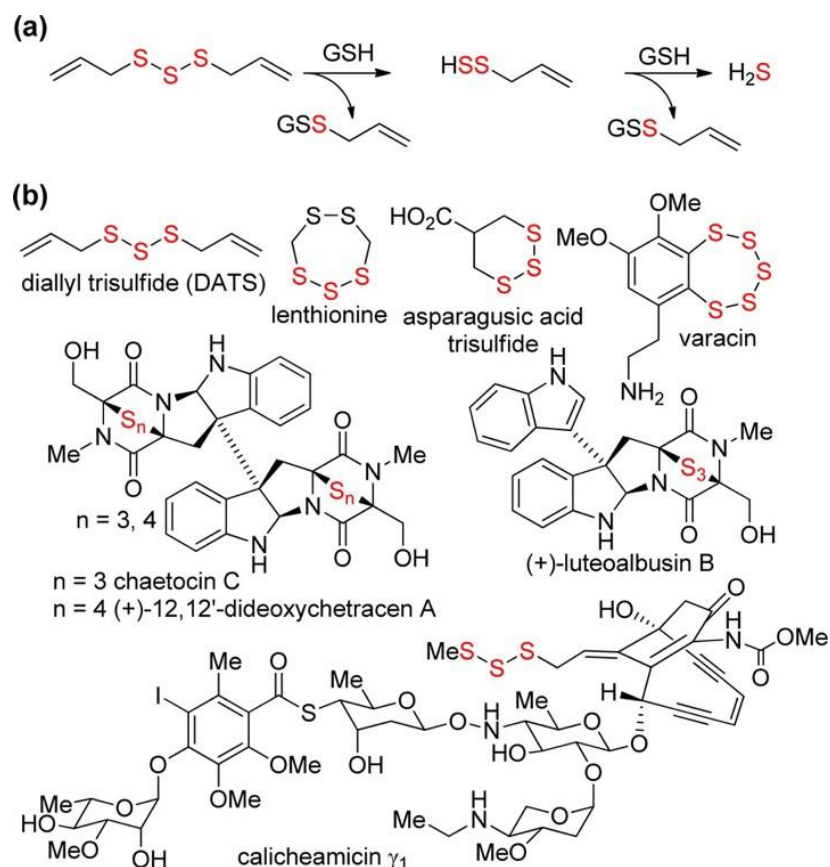


Figure 4.1 (a) Mechanism of H₂S release from DATS in the presence of GSH. (b) Representative examples of natural products containing polysulfides.

naturally occurring polysulfides and the widespread utility of DATS, we envisioned accessing synthetic polysulfides for GSH-triggered H₂S donation and expanding the toolbox of polysulfide-based H₂S donors. Herein, we report the synthesis and evaluation of *bis*(aryl)- and *bis*(alkyl) tetrasulfides which release H₂S in the presence of excess GSH.

4.2 Results and Discussion

With the goal of expanding the toolbox of polysulfide based H₂S donors, we evaluated previous methods for simple polysulfide synthesis. Both trisulfides and

tetrasulfides are synthetically accessible by treating a desired thiol with sulfur dichloride (SCl_2) or sulfur monochloride (S_2Cl_2), respectively.¹⁵⁸ We chose to focus on tetrasulfides due to their higher sulfane sulfur content, thus higher H_2S releasing potential with respect to trisulfides. Treatment of the parent thiol with S_2Cl_2 and pyridine in anhydrous solvent at $-78\text{ }^\circ\text{C}$ afforded the desired tetrasulfide in good to excellent yield with no required purification (Table 4.1).¹⁵⁹

$$\text{R-SH} \xrightarrow[\text{solvent, } -78\text{ }^\circ\text{C}]{\text{S}_2\text{Cl}_2, \text{ pyridine}} \text{R-S-S-S-S-R}$$

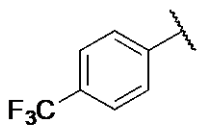
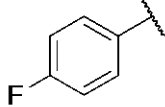
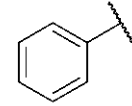
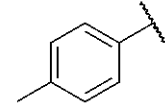
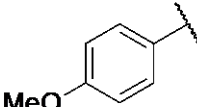
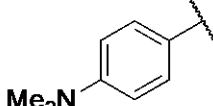
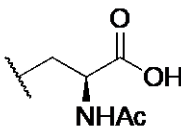
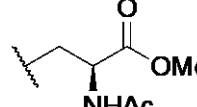
entry	R	solvent	yield (%)
1		Et_2O	87
2		Et_2O	84
3		Et_2O	70
4		Et_2O	73
5		Et_2O	95
6		Et_2O	68
7		THF	80
8		CH_2Cl_2	85

Table 4.1 Synthesis of *bis*(aryl) and *bis*(alkyl) tetrasulfides

In addition to facile tuning of the electron-donating or -withdrawing ability of the *bis*(aryl) tetrasulfides (**1–6**), this route also enabled access to *bis*(alkyl) tetrasulfides, including *N*-acetylcysteine-derived tetrasulfides (**7** and **8**). These two compounds provide a promising scaffold for combining the physiological effects of H₂S with those of *N*-acetylcysteine (NAC), which is used as an antidote for acetaminophen overdose,¹⁶⁰ CO poisoning,¹⁶¹ and other conditions. Notably, the use of S₂Cl₂ to access tetrasulfides is tolerant of varying thiol nucleophilicity and could prove useful in the synthesis of other organic tetrasulfides.

The prepared tetrasulfides were characterized by ¹H and ¹³C{¹H} NMR spectroscopy to assess the purity of each product and EI-MS to confirm selective tetrasulfide formation. A representative mass spectrum of **3** is shown in Figure 4.2a, which clearly shows the parent ion peak corresponding to Ph₂S₄ (282.0), as well as daughter fragmentation peaks corresponding to extrusion of one and two sulfane sulfur atoms to generate Ph₂S₃ (250.0) and Ph₂S₂ (218.0), respectively. In addition, the most intense ion peak corresponds to homolysis of the weak¹⁶² internal S–S bond to generate PhSS[•] (141.0). Additionally, HPLC analysis of **3** further supports the high purity of the synthesized tetrasulfide (Figure D.19). Taken together, the spectroscopic and spectrometric data support clean formation of the desired tetrasulfide product. In addition, single crystals of **4** suitable for X-ray diffraction were obtained by slow evaporation from *n*-pentane, further confirming the molecular structure (Figure 4.2b). Tetrasulfide **4** crystallized in *P2*₁/*c* with a central S–S dihedral angle of 82.8° and nearly perpendicular 89.9° angle between the two phenyl rings, which were oriented in a slip stacked orientation with a 3.50 Å interplanar spacing. Additional stabilizing forces in the lattice include C–H hydrogen bonds from the methyl (3.7 Å) and *meta* aryl (3.9 Å) hydrogens, consistent with recent work demonstrating that sulfur is

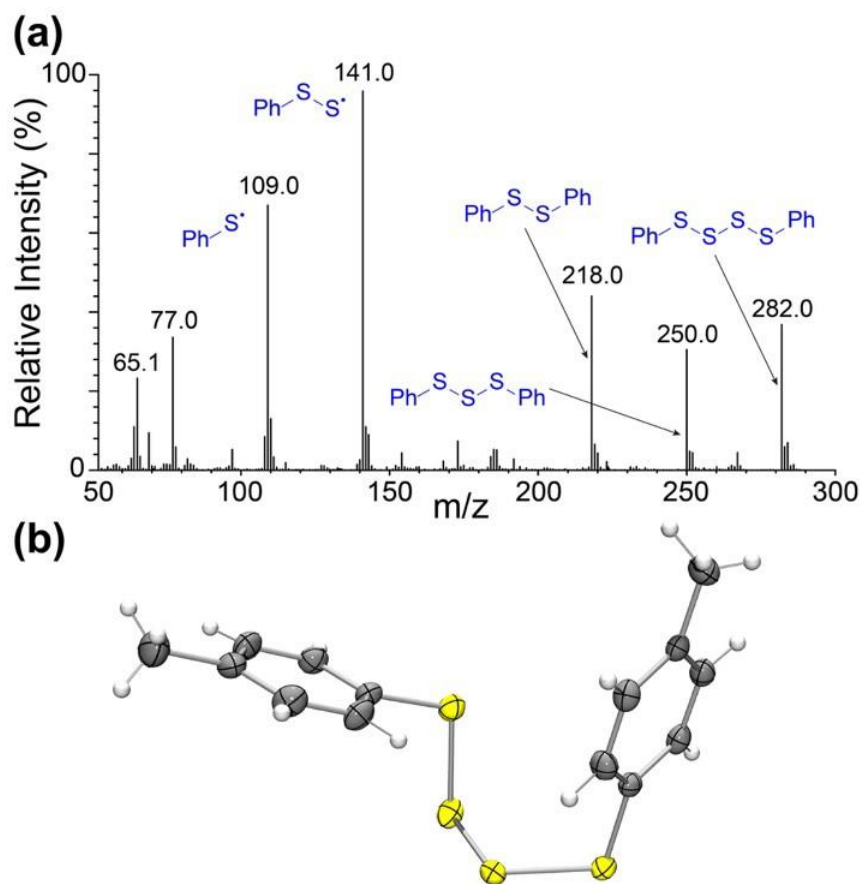


Figure 4.2 (a) Mass spectrum (EI-MS) of **3**. (b) ORTEP representation (50% ellipsoids) of the molecular structure of **4**.

a C–H hydrogen bond acceptor.¹⁶³ With tetrasulfides in hand, we next investigated the release of H₂S upon addition of GSH. We chose to use GSH as the trigger for H₂S release due to higher intracellular levels (~1–10 mM) relative to other biological thiols, although other biological reductants, such as NADH, can also trigger H₂S release from polysulfides.¹⁶⁴ We hypothesized that H₂S release from tetrasulfides is likely to proceed through an analogous mechanism to that of trisulfides (Figure 4.1 a), although the addition of a second sulfane sulfur in tetrasulfides increases the mechanistic complexity because GSH can attack at either the α - or β -sulfur (Figure 4.3). For example, nucleophilic attack by GSH at the β -sulfur can either lead to a nonproductive pathway by formation of the

parent thiol and a mixed glutathione tetrasulfide or to a productive pathway via formation of a persulfide and mixed glutathione trisulfide (Figure 4.3a).

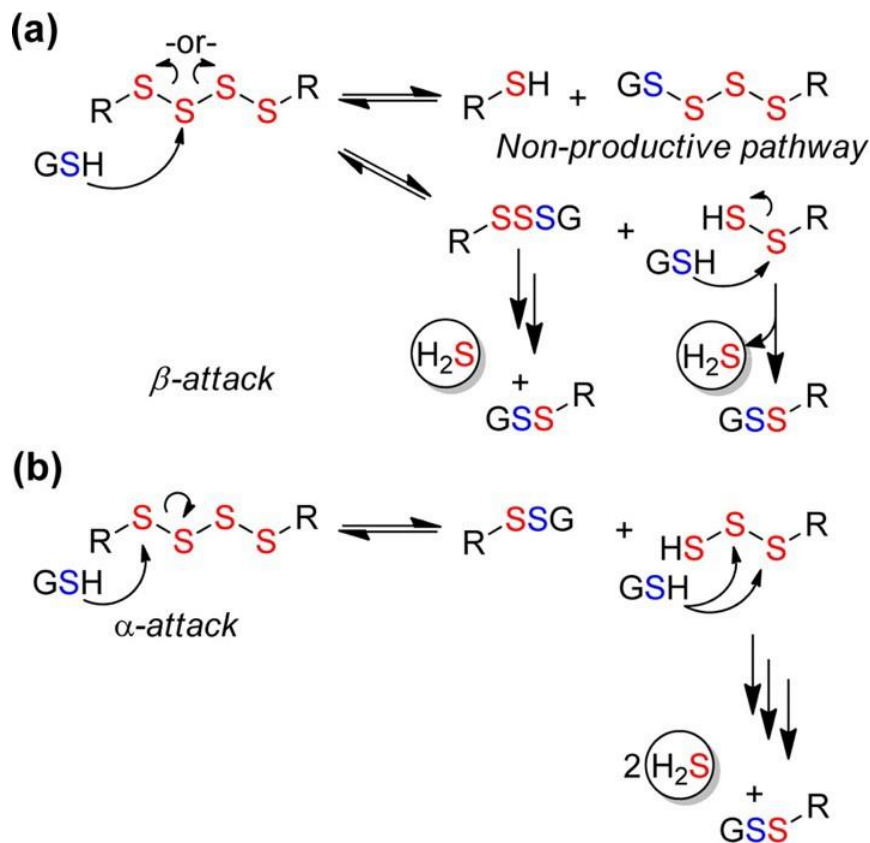


Figure 4.3 Proposed mechanisms of H₂S release from tetrasulfides, including initial nucleophilic attack by GSH at the (a) β -sulfur or (b) α -sulfur.

These reactive intermediates would further react with GSH leading to the generation of 2 equiv of H₂S and terminating in the formation of a mixed glutathione disulfide. Alternatively, nucleophilic attack by GSH at the α -sulfur results in the formation of a hydropolysulfide and a mixed glutathione disulfide (Figure 4.3b). This hydropolysulfide would further react with another equivalent of GSH to generate H₂S and a mixed glutathione trisulfide. Repetition of this process generates oxidized GSH (GSSG) and a persulfide, which should rapidly react with GSH to generate another equivalent of H₂S and terminate in a mixed glutathione disulfide. Overall, a single tetrasulfide molecule should

release 2 equivalents of H₂S following reduction by GSH and terminate in a mixed glutathione disulfide.

To gain preliminary mechanistic insights into H₂S release from the prepared tetrasulfides, we measured the GSH dependence of H₂S release from 5 μM **3** (10 mM PBS, pH 7.4) using a sulfide-selective electrode. As expected, no H₂S release was observed in the absence of GSH, demonstrating that the tetrasulfides are stable in solution in the absence of thiols. Increasing the GSH concentration resulted in an increased rate of H₂S production (Figure 4.4a). The acquired H₂S release data did not fit cleanly to pseudo-first-order kinetics, suggesting that the complexity of the H₂S-releasing pathway and possibility for competing reactions may complicate the observed rate profiles. To circumvent this problem, we used initial rate analysis and construction of a log–log plot of rate as a function of [GSH], which demonstrated a first-order rate dependence (Figure 4.4b)

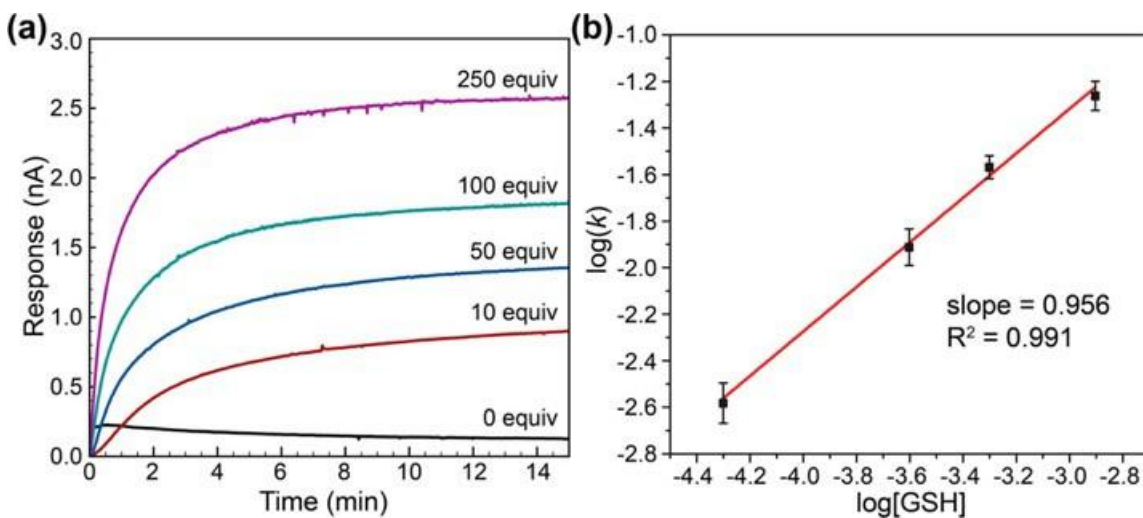


Figure 4.4 (a) GSH-dependent H₂S release from **3**. (b) log(*k*) vs log[GSH] plot demonstrating a 1st-order dependence in [GSH] on H₂S release from **3**.

Given the ease of functionalization for the *bis*(aryl) tetrasulfides, we also investigated the effects of electronic substitution on H₂S release. We anticipated that

electronic modulation of the *bis*(aryl) tetrasulfides would favor a specific pathway due to change in electrophilicity at the α - or β -sulfur. Alternatively, it is possible that although the balance of the competing pathways could shift, it would not do so sufficiently to result in different H₂S release profiles. Similar to our observation for **3**, GSH-triggered H₂S release from the remaining *bis*(aryl) tetrasulfides was observed with initial rates ranging from 0.0032 to 0.054 nA·s⁻¹ (Table D.2). The Hammett plot constructed from the initial rate data did not provide a linear relationship, suggesting that factors other than electronic effects may influence H₂S release rates from the *bis*(aryl) tetrasulfides (Figure D.20). We next compared the rates of release of alkyl tetrasulfides **7** and **8**, both of which released H₂S more slowly than the aryl tetrasulfides (Figure 4.5).

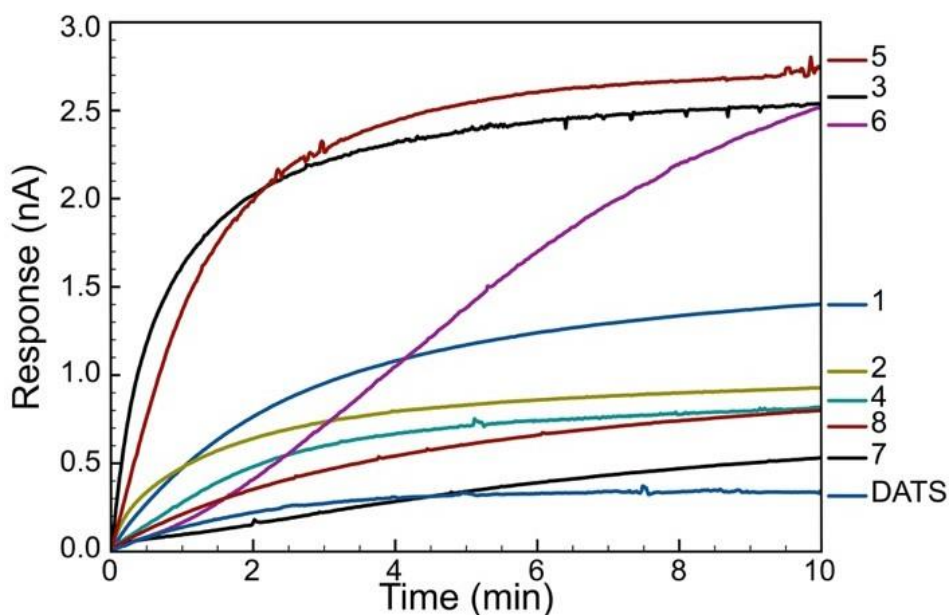


Figure 4.5 GSH-triggered (250 equiv) H₂S release from 5 μ M tetrasulfides **1–8** and 5 μ M DATS (pH 7.4, room temperature).

Notably, all of the prepared aryl and alkyl tetrasulfides resulted in greater H₂S donation than the well-established trisulfide donor DATS under the reported conditions, thus

highlighting the efficacy of tetrasulfides as viable H₂S donors. The differences in H₂S releasing profiles of the reported donors are likely due to varying electronic contributions between the different compounds. Clearly further mechanistic investigations are required to fully elucidate the mechanism of GSH-mediated release of H₂S from tetrasulfides.

4.3 Conclusions

In summary, a diverse array of *bis*(alkyl) and *bis*(aryl) tetrasulfides are readily accessible from simple synthetic procedures. The prepared tetrasulfides readily release H₂S upon treatment with GSH and release more H₂S per molecule than commonly used DATS. Overall, we expect that these and other simple polysulfides will provide researchers interested in H₂S donating molecules with a broader palette of available polysulfide donor motifs with different release profiles and biological activities.

The accessibility of thiol-mediated H₂S release from these compounds demonstrates the ability to expand the chemical toolbox of synthetic, organic polysulfides for H₂S generation. To gain a better, fundamental understanding of H₂S release from this class of donor compounds, we sought to investigate the effect of varying sulfane sulfur content within a single series of organic polysulfides on H₂S release. Chapter V discusses our findings on thiol-mediated H₂S release from benzyl polysulfides and highlights the potential significance of intermediate persulfide generation on the biological activity of polysulfides.

4.4 Experimental Details

4.4.1 Materials and Methods

4-(trifluoromethyl)benzene thiol, and *p*-Toluenethiol were purchased from Toyko Chemical Industry (TCI). 4-fluorothiophenol, and thiophenol were purchased from Alfa Aesar. Sulfur monochloride, 4-Methoxythiophenol, and L-Glutathione reduced were purchased from Sigma-Aldrich. 4-(Dimethylamino)thiophenol was purchased from Oakwood Chemicals. All reagents were used as received. Deuterated solvents were purchased from Cambridge Isotope Laboratories and used as received. ^1H , $^{13}\text{C}\{^1\text{H}\}$, and ^{19}F NMR spectra were recorded on a Bruker 500 MHz or 600 MHz instrument. Chemical shifts are reported in ppm relative to residual protic solvent resonances. Sulfide selective electrode data was acquired with a World Precision Instruments (WPI) ISO-H2S100 sensor connected to a TBR4100 Free Radical Analyzer. All air-free manipulations were performed under an inert atmosphere using standard Schlenk techniques or an Innovative Atmospheres N_2 -filled glove box.

H₂S Electrode Materials and Methods

Phosphate buffered saline (PBS) tablets (1X, CalBioChem) were used to make buffered solutions (PBS, 140 mM NaCl, 3 mM KCl, 10 mM phosphate, pH 7.4) in deionized water. Buffer solutions were sparged with N_2 to remove dissolved oxygen and stored in an N_2 -filled glovebox. Tetrasulfide stock solutions (in DMSO) were prepared in an N_2 -filled glovebox and stored at $-25\text{ }^\circ\text{C}$ until immediately before use. GSH stock solutions (in PBS, 1X, pH 7.4) were freshly prepared in an N_2 -filled glovebox immediately before use.

General Procedure for H₂S Electrode Experiments

Scintillation vials containing 20 mL of PBS (1X, 140 mM NaCl, 3 mM KCl, 10 mM phosphate, pH 7.4) were prepared in an N₂-filled glovebox. A split-top septum cap was placed on the vial after probe insertion and the headspace was sparged with Ar via balloon to avoid unwanted oxidation. The electrode was then inserted into the solution and the measured current was allowed to equilibrate over 5 min. With moderate stirring, tetrasulfide (20 μ L of 5 mM in DMSO) was injected and allowed to equilibrate for 1 min followed by injection of GSH (100 μ L of 250 mM GSH in PBS). H₂S release was monitored for 1 h. H₂S release from each tetrasulfide donor was repeated a minimum of three times.

X-ray Crystallography

Diffraction intensities for **4** were collected at 173 K on a Bruker Apex2 CCD diffractometer using CuK α radiation (1.54178 Å). The space group was determined based on systematic absences. Absorption corrections were applied by SADABS. The structure was solved by direct methods and Fourier techniques refining on F^2 using full matrix least-squares procedures. All non-H atoms were refined with anisotropic thermal parameters. All H atoms were found on the residual density map and refined with isotropic thermal parameters. All calculations were performed by the Bruker SHELXL-2014 package.

4.4.2 Synthesis

General Procedure for the Preparation of Aryl and Alkyl Tetrasulfides

The desired thiol (1.0 equiv.) and pyridine (1.0 equiv.) were added to anhydrous solvent (30 mL) in an oven-dried round bottom flask under nitrogen. The solution was cooled to -78 °C for 1 hour, after which sulfur monochloride (0.6 equiv.) was added dropwise. A white precipitate formed within seconds, and the reaction was stirred for 2 hours and then allowed to warm to room temperature. The reaction was quenched with deionized water (30 mL), and the aqueous layer was discarded. The organic layer was washed with deionized water (30 mL) and brine (30 mL). The organic layer was dried over sodium sulfate, filtered, and evaporated under reduced pressure to afford the pure product.

1,4-*bis*-(4-(trifluoromethyl)phenyl)tetrasulfane (**1**, Et₂O)

Yellow liquid. 256 mg (87%)

¹H NMR (500 MHz, CDCl₃) δ 7.58 (d, *J* = 8.3 Hz, 4 H), 7.51 (d, *J* = 8.2 Hz, 4 H). ¹⁹F NMR (471 MHz, CDCl₃) δ -62.77. ¹³C{¹H} NMR (126 MHz, CDCl₃) δ 123.89 (q, *J* = 272.1 Hz), 126.13 (q, 3.7 Hz), 128.54, 130.08 (q, 32.8 Hz), 140.73. HRMS-EI+ (*m/z*): [M + H]⁺ calcd for C₁₄H₈S₄F₆, 417.94130; found, 417.94100.

1,4-*bis*-(4-fluorophenyl)tetrasulfane (**2**, Et₂O)

Yellow liquid. 261 mg (84%)

¹H NMR (600 MHz, CDCl₃) δ 7.53 (m, 4 H), 7.03 (t, *J* = 8.6 Hz, 4 H). ¹⁹F NMR (565 MHz, CDCl₃) δ -111.82 (tt, *J* = 9.0, 5.1 Hz). ¹³C{¹H} NMR (151 MHz, CDCl₃) δ 116.54 (d, *J* =

22.1 Hz), 131.59 (d, $J = 3.3$ Hz), 133.53 (d, $J = 8.4$ Hz), 162.54, 164.19. HRMS-EI+ (m/z): [M + H]⁺ calcd for C₁₂H₈S₄F₂, 317.94771; found, 317.94790.

1,4-phenyltetrasulfane (**3**, Et₂O)

Yellow liquid (may solidify upon standing). 225 mg (70%)

¹H NMR (500 MHz, CDCl₃) δ 7.32 (q, $J = 6.6$ Hz, 6 H), 7.56 (m, 4 H). ¹³C{¹H} NMR (126 MHz, CDCl₃) δ 128.49, 129.29, 130.32, 136.35. HRMS-EI+ (m/z): [M + H]⁺ calcd for C₁₂H₁₀S₄, 281.96655; found, 281.96618.

1,4-di-*p*-tolyltetrasulfane (**4**, Et₂O)

Yellow powder. 303 mg (73%)

¹H NMR (500 MHz, CDCl₃) δ 7.46 (d, $J = 7.9$ Hz, 4 H), 7.14 (d, $J = 7.9$ Hz, 4 H), 2.35 (s, 6 H). ¹³C{¹H} NMR (126 MHz, CDCl₃) δ 139.02, 133.00, 131.21, 130.05, 21.36. HRMS-EI+ (m/z): [M + H]⁺ calcd for C₁₄H₁₄S₄, 309.99785; found, 309.99746.

1,4-*bis*-(4-methoxyphenyl)tetrasulfane (**5**, Et₂O)

Yellow powder. 290 mg (95%)

¹H NMR (500 MHz, CDCl₃) δ 3.82 (s, 6 H), 6.86 (d, $J = 8.8$ Hz, 4 H), 7.51 (d, $J = 8.8$ Hz, 4 H). ¹³C{¹H} NMR (126 MHz, CDCl₃) 55.56, 114.91, 127.21, 134.33, 160.81. HRMS-EI+ (m/z): [M + H]⁺ calcd for C₁₄H₁₄O₂S₄, 341.98768; found, 341.98780.

4,4'-tetrasulfaneylbis(*N,N*-dimethylaniline) (**6**, Et₂O)

Yellow powder. 204 mg (68%)

¹H NMR (500 MHz, CDCl₃) δ 7.48 (d, *J* = 8.9 Hz, 2 H), 6.65 (d, *J* = 8.5 Hz, 2 H), 2.98 (s, 6H). ¹³C {¹H} NMR (126 MHz, CDCl₃) δ 151.11, 135.04, 112.87, 40.58. TOF HRMS ES+ (*m/z*): [M + H]⁺ calcd for C₁₆H₂₁N₂S₄, 369.0588; found, 369.0582.

3,3'-tetrasulfaneylbis(2-acetamidopropanoic acid) (**7**, THF)

Modification from general procedure: S₂Cl₂ (0.6 equiv.) was added to parent thiol (1.0 equiv.) dissolved in anhydrous THF at room temperature under N₂. The solution was stirred for 2 h and subjected to an aqueous workup.

White powder. 704 mg (80%)

¹H NMR (500 MHz, *d*⁶-DMSO) δ 12.95 (s, 1 H), 8.36 (d, *J* = 7.9 Hz, 2 H), 4.55 (td, *J* = 8.4, 4.6 Hz, 2 H), 3.39 (dd, *J* = 13.8, 4.7 Hz, 2 H), 3.23 (dd, *J* = 13.8, 8.9 Hz, 2 H), 1.86 (s, 6 H). ¹³C {¹H} NMR (126 MHz, *d*⁶-DMSO) δ 171.63, 169.38, 54.90, 51.31, 22.37. TOF HRMS-ES+ (*m/z*): [M + H]⁺ calcd for C₁₀H₁₇N₂O₆S₄, 388.9969; found, 388.9966.

Dimethyl 3,3'-tetrasulfaneylbis(2-acetamidopropanoate) (**8**, DCM)

White powder. 300 mg (85%)

¹H NMR (500 MHz, *d*⁶-DMSO) δ 8.49 (s, 2 H), 4.65 (dtd, *J* = 13.1, 8.3, 4.9 Hz, 2 H) 3.66 (s, 6 H), 3.41 (ddd, *J* = 23.5, 14.0, 4.9 Hz, 2 H), 3.26 (m, 2 H) 1.86 (s, 6 H). ¹³C {¹H} NMR (126 MHz, CDCl₃) δ 170.68, 169.46, 52.28, 52.26, 52.23, 51.28, 51.12, 22.29, 22.27. TOF HRMS-ES+ (*m/z*): [M + H]⁺ calcd for C₁₂H₂₁N₂O₆S₄, 417.0282; found, 417.0275.

4.4.3 Crystallographic Data for 4

$C_{14}H_{14}S_4$, $M = 310.49$, $0.10 \times 0.09 \times 0.04$ mm, $T = 173(2)$ K, Monoclinic, space group $P2_1/c$, $a = 14.0418(4)$ Å, $b = 6.1192(2)$ Å, $c = 17.3990(5)$ Å, $\beta = 101.306(2)^\circ$, $V = 1465.99(8)$ Å³, $Z = 4$, $D_c = 1.407$ Mg/m³, $\mu(\text{Cu}) = 5.770$ mm⁻¹, $F(000) = 648$, $2\theta_{\text{max}} = 133.24^\circ$, 8807 reflections, 2535 independent reflections [$R_{\text{int}} = 0.0406$], $R1 = 0.0356$, $wR2 = 0.0928$ and $\text{GOF} = 1.036$ for 2535 reflections (219 parameters) with $I > 2\sigma(I)$, $R1 = 0.0412$, $wR2 = 0.0969$ and $\text{GOF} = 1.036$ for all reflections, max/min residual electron density $+0.846/-0.288$ e·Å⁻³.

CHAPTER V

EFFECTS OF SULFANE SULFUR CONTENT IN BENZYL POLYSULFIDES ON THIOL-TRIGGERED H₂S RELEASE AND CELL PROLIFERATION

This chapter includes previously published and coauthored material from Bolton, S.G.; Cerda, M.M.; Gilbert, A.K.; Pluth, M.D. Effects of Sulfane Sulfur Content in Benzyl Polysulfides on Thiol-Triggered H₂S and Cell Proliferation. *Free Radic. Biol. Med.* **2019**, *131*, 393-398. This manuscript was written by Matthew M. Cerda and Sarah G. Bolton with editorial assistance from Professor Michael D. Pluth. The project in this chapter was conceived by Matthew M. Cerda. The synthetic procedures and methylene blue experiments in this chapter were performed by Matthew M. Cerda and Annie K. Gilbert. The cell proliferation assays were performed by Sarah G. Bolton.

5.1 Introduction

Sulfane sulfur (S⁰) is formally defined as a sulfur atom that bears six valence electrons, has no formal charge, can exist in a thiosulfoxide tautomer, and is bonded to two or more sulfur atoms or to a sulfur atom and an ionizable hydrogen.¹⁶⁵ This sulfur oxidation state is found in various sulfur-containing species including elemental sulfur, persulfides, and polysulfides.¹⁶⁶ Under physiological conditions, S⁰ can be reduced in the presence of biological thiols, such as reduced glutathione (GSH) or cysteine (Cys), to generate the important signaling molecule hydrogen sulfide (H₂S) (Figure 5.1).¹⁶⁷

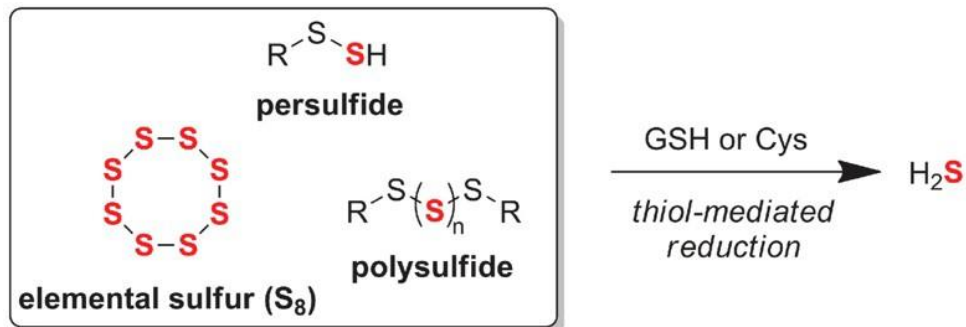


Figure 5.1 Common S^0 -containing small molecule species release H_2S upon reaction with biological thiols.

H_2S is now commonly associated with the gasotransmitter family, which includes nitric oxide and carbon monoxide, because it is produced endogenously, can freely permeate cell membranes, and can act on specific cellular and/or molecular targets to exert physiological effects.¹²⁴ Recent work has demonstrated H_2S -mediated signaling in processes including neurotransmission,¹⁶⁸ vasodilation,¹⁶⁹ and anti-inflammation.¹⁷⁰

Towards efforts to provide exogenous H_2S as either a pharmacological tool or as a potential therapeutic,^{127a} a number of groups have prepared small molecules capable of releasing H_2S under different conditions.^{15a, 130} Notably, a number of these developed donor motifs generate persulfides en route to H_2S release, which complicates whether the observed biological effects from such donors is due to H_2S release or S^0 . Recently, evaluation of H_2S -signaling mechanisms has revealed the formation of persulfides as a common intermediate leading to questions of whether persulfides and related S^0 -containing species are key signaling intermediates.¹⁷¹

When considering sulfur oxidation states, persulfides possess reduced sulfur and S^0 , implying potential significance of S^0 in sulfur biology.¹⁷² Under physiological conditions, S^0 readily oxidizes free thiol residues to generate persulfides via a reaction mechanism known as persulfidation,¹⁷³ and this process has been shown to upregulate the

activity of key enzymes such as xanthine oxidase.¹⁷⁴ Additionally, the formation of persulfides under physiological conditions has been proposed to occur via the reaction of oxidized reactive sulfur species including disulfides, sulfenic acids, and *S*-nitrosothiols with H₂S.¹⁷⁵ Interestingly, persulfidation of thiol-based antioxidants such as GSH leads to enhanced antioxidant activity when compared to corresponding thiols.¹⁷⁶ Within the active sites of specific enzymes, persulfides can be stabilized and the H₂S release from an enzyme-bound persulfide has been shown in 3-mercaptopyruvate sulfurtransferase via thioredoxin-mediated reduction.¹⁷⁷ Toward directly studying small molecule persulfide reactivity, recent work has demonstrated the ability to generate persulfides under physiological conditions¹⁷⁸ for applications in protein persulfidation,¹⁷⁹ reactive oxygen species scavenging,¹⁸⁰ and H-atom transfer agents.¹⁸¹ Previous work by our group demonstrated the ability to access discrete persulfides¹⁸² and study their reactivity under various conditions.¹⁸³ A common, yet understudied pathway for accessing persulfides, hydropolysulfides, and other closely related reactive sulfur species is the thiol-mediated reduction of organic polysulfides.

Polysulfides are a class of organosulfur species commonly found in nature,^{156, 184} that have unique biological properties.¹⁸⁵ Readily isolated from alliums such as garlic¹⁸⁶, diallyl trisulfide (**DATS**) is a simple, organic polysulfide which has been studied heavily in the field of biological sulfur chemistry. The commercial availability of **DATS** has led to its broad use as an H₂S donor and source of S⁰. For example, the cytotoxicity of **DATS** has been reported in a wide array of human cancer cell lines,¹⁸⁷ although we note the cytotoxicity of **DATS** appears to be directly correlated to S⁰ content as the analogous monosulfide and disulfide demonstrate minimal cytotoxicity.¹⁸⁸ Upon

examining the mechanism of action, **DATS** was found to suppress cell proliferation in human colon cancer cells (HCT-15) via *S*-allylation of Cys-12 β and Cys-354 β in β -tubulin rather than direct H₂S or persulfide release.¹⁸⁹ By contrast, the thiol-dependent release of H₂S from **DATS** in human red blood cells and the vasoactivity of garlic extract administration was found to be directly related to H₂S production.¹⁵² In the presence of thiols, **DATS** releases H₂S upon nucleophilic attack at the α -sulfur to generate allyl persulfide, which further reacts with a second equivalent of thiol to generate H₂S.¹⁵⁴ Despite the accessibility of other organic polysulfides, studies have been primarily limited to **DATS**. Alternatively, researchers have relied heavily on the use of inorganic polysulfides,¹⁹⁰ which spontaneously disproportionate under mild, aqueous conditions to yield complex mixtures.¹⁹¹ Recently, our group and others¹³⁶ have demonstrated the ability to access¹⁹² and utilize organic polysulfides beyond **DATS** for thiol-triggered H₂S delivery.¹³⁷ Aligned with our interests in studying S⁰-containing reactive sulfur species, we sought to expand the toolbox of available organic polysulfides and study the effect of varying S⁰ content in a single series of polysulfides. Herein, we demonstrate the thiol-mediated release of H₂S from benzyl trisulfide and benzyl tetrasulfide respectively. Additionally, we demonstrate the ability of S⁰-containing benzyl polysulfides to suppress cell proliferation in bEnd.3 cells in a S⁰ content-dependent manner.

5.2 Results and Discussion

To investigate the impacts of sulfur content in polysulfides, we chose to study benzyl polysulfides ranging from benzyl sulfide (**Bn₂S**) up to and including benzyl tetrasulfide (**Bn₂S₄**). Using previously reported conditions,¹⁹³ we synthesized **Bn₂S₄** in

89% yield via treatment of benzyl mercaptan with sulfur monochloride (S_2Cl_2) in the presence of pyridine at $-78\text{ }^\circ\text{C}$ (Figure 5.2a).

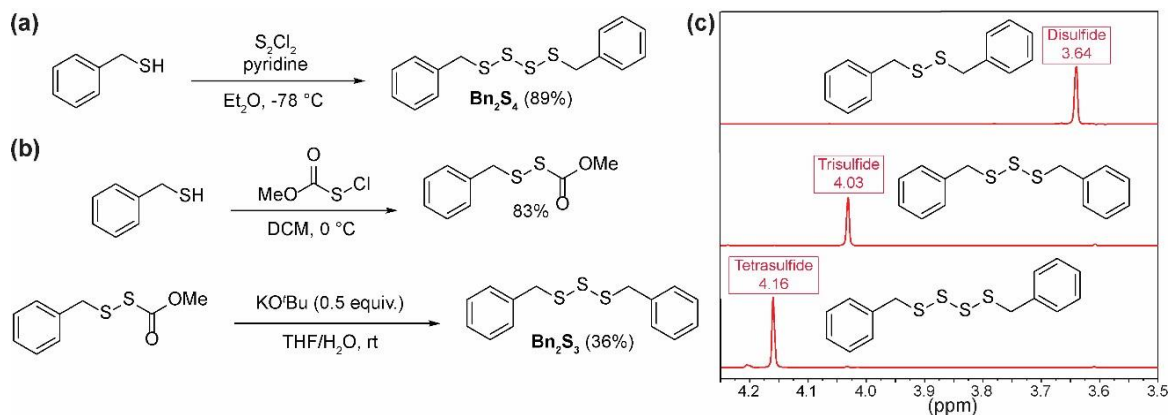


Figure 5.2 (a) Synthesis of **Bn₂S₄**. (b) Synthesis of **Bn₂S₃**. (c) Comparison of benzylic ^1H NMR (500 MHz) signals between **Bn₂S₂**, **Bn₂S₃**, and **Bn₂S₄** in CDCl_3 .

To access benzyl trisulfide (**Bn₂S₃**), we evaluated prior reports of symmetrical trisulfide synthesis. Most reports cite the use of sulfur dichloride (SCl_2), an unstable sulfur chloride reagent that exists in equilibrium with S_2Cl_2 . To avoid the use of SCl_2 , we were drawn to a report by Harpp and co-workers that used alkoxide-mediated decomposition of sulfenylthiocarbonates to access trisulfides.¹⁹⁴ Although treatment of methoxycarbonylsulfenyl chloride with benzyl mercaptan readily afforded the desired precursor in 83% yield, we found that further treatment with potassium tert-butoxide (KO^tBu) in methanol provided an inseparable mixture of benzyl disulfide (**Bn₂S₂**) and **Bn₂S₃**. The proposed reaction mechanism by Harpp and co-workers involves an initial nucleophilic attack by the tert-butoxide anion at the carbonyl to form a carbonate and release benzyl persulfide. Based on previous work from our group, treatment of BnSSH with different bases resulted in disproportionation to yield various benzyl polysulfides, which supports the formation of benzyl persulfide under the current reaction conditions.¹⁹⁵

Due to steric congestion and poor nucleophilicity, we viewed that nucleophilic attack by KO^tBu was unlikely and hypothesized that the active nucleophile in this reaction was hydroxide, which can be generated upon deprotonation of residual water in methanol by the tert-butoxide anion.

To test this hypothesis, we treated the benzyl sulfenylthiocarbonate precursor with ^tBuOK in a mixture of tetrahydrofuran and water. Consistent with our hypothesis, we were able to isolate **Bn₂S₃** in 36% yield (Figure 5.2b). Considering hydroxide as the active nucleophile, we have proposed a new reaction mechanism for the synthesis of symmetrical trisulfides via hydroxide-mediated decomposition of sulfenylthiocarbonates (Scheme E.1). In comparison to current methods of mild trisulfide synthesis, we note the use of hydroxide likely prevents the formation of symmetrical trisulfides containing base-sensitive functional groups. Using ¹H NMR spectroscopy, benzyl polysulfides can be identified by their respective peaks corresponding to benzylic protons which are unique to each polysulfide ranging from **Bn₂S₂** to benzyl pentasulfide in deuterated chloroform allowing for ease of characterization (Figure 5.2c).¹⁹⁶

With a series of benzyl polysulfides in hand, we next investigated the release of H₂S in the presence of cysteine and GSH. We anticipated that only **Bn₂S₃** and **Bn₂S₄** would release H₂S and that **Bn₂S₄** would release twice as much H₂S relative to **Bn₂S₃**. To test our hypothesis, dibenzyl polysulfides (25 μM) were treated with an excess of cysteine or GSH (500 μM, 20 equiv.) in PBS (10 mM, pH 7.4) at 25 °C and H₂S release was measured via the spectrophotometric methylene blue assay (Figure 5.3). As expected, we did not observe H₂S release from **Bn₂S** and **Bn₂S₂** in the presence of cysteine or GSH, consistent with a lack of S⁰ content. Additionally, we note that the lack of H₂S release from **Bn₂S₂** suggests

that nucleophilic attack by Cys or GSH at the benzylic carbon to generate a H₂S-releasing persulfide intermediate does not occur.⁶¹ For both GSH and Cys, we observed approximately twice as much H₂S released from **Bn₂S₄** than from **Bn₂S₃**, which is consistent with the higher S⁰ content of tetrasulfides when compared to trisulfides.

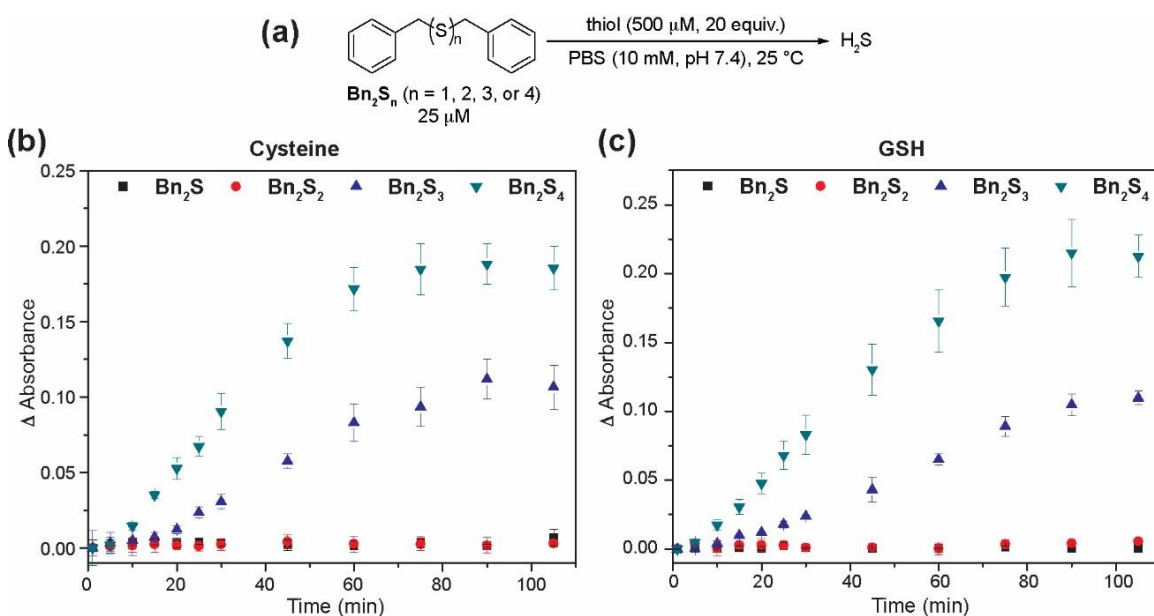


Figure 5.3 (a) Reaction conditions for thiol-triggered release of H₂S from **Bn₂S_n** (n = 1, 2, 3, or 4). (b) Release of H₂S in the presence of cysteine. (c) Release of H₂S in the presence of GSH.

In the presence of cysteine (500 μM, 20 equiv.), **Bn₂S₃** and **Bn₂S₄** released 8.6 (34% releasing efficiency) and 17.5 μM (35% releasing efficiency) H₂S respectively after 90 min. Similarly, we observed 4.3 μM (17% releasing efficiency) and 16 μM (32% releasing efficiency) H₂S released from **Bn₂S₃** and **Bn₂S₄** respectively in the presence of GSH (500 μM, 20 equiv.) after 90 min. To compare the release of H₂S from benzyl polysulfides to other commonly-used organic polysulfides, we measured the H₂S release from **DATS** under the reported conditions. By comparison, **DATS** is a faster H₂S donor than the benzyl polysulfides tested and yields approximately the same quantity of H₂S after

110 min as **Bn₂S₄**. To rationalize this observation, we compared the stability of the intermediate persulfides for each donor system (i.e. benzyl persulfide vs. allyl persulfide). To the best of our knowledge, allyl persulfide has never been isolated and is simply observed as a fleeting intermediate, which suggests that it may be significantly less stable than benzyl persulfide, which has been isolated, characterized, and studied previously. Additionally, a comparison of the H₂S releasing curves demonstrates a brief induction period for **Bn₂S₃** and **Bn₂S₄** which we attribute to a buildup of benzyl persulfide in solution. Taken together, these results demonstrate the significance of pendant alkyl groups in organic polysulfides and their overall effect on the chemical reactivity of downstream reactive sulfur species including persulfides. Relative to other synthetic H₂S donors, we note that organic polysulfides provide lower H₂S releasing efficiencies, which is likely a result of higher lipophilicity. We anticipate the design of water-soluble polysulfides should provide more efficient H₂S donors.¹⁸³

Further advancing our studies, we sought to examine the effect of benzyl polysulfides on cell proliferation in murine epithelial bEnd.3 cells to determine whether the different releasing efficiencies for tri- and tetra-sulfides in solution translated into cellular environments. Previously, studies have shown administration of sodium hydrosulfide (NaSH) led a pro-proliferative effect in bEnd.3 cells.¹⁹⁷ The reported organic polysulfide library provides us a unique opportunity to directly examine the effects of S⁰ within a single series of polysulfides. With these compounds in hand, we sought to determine the impact of increasing S⁰ delivery on cell proliferation following 24 h treatments (Figure 5.4). Use of synthetic H₂S donors such as AP39¹⁹⁸ and direct administration of H₂S via NaSH¹⁹⁹ has been shown to have cytoprotective effects on

bEnd.3 cells. To the best of our knowledge, the effect of polysulfide administration has not been studied in this specific cell line. Consistent with a lack of S^0 content, 24 h incubation with **Bn₂S** and **Bn₂S₂** (up to 200 μ M) did not reduce cell viability.

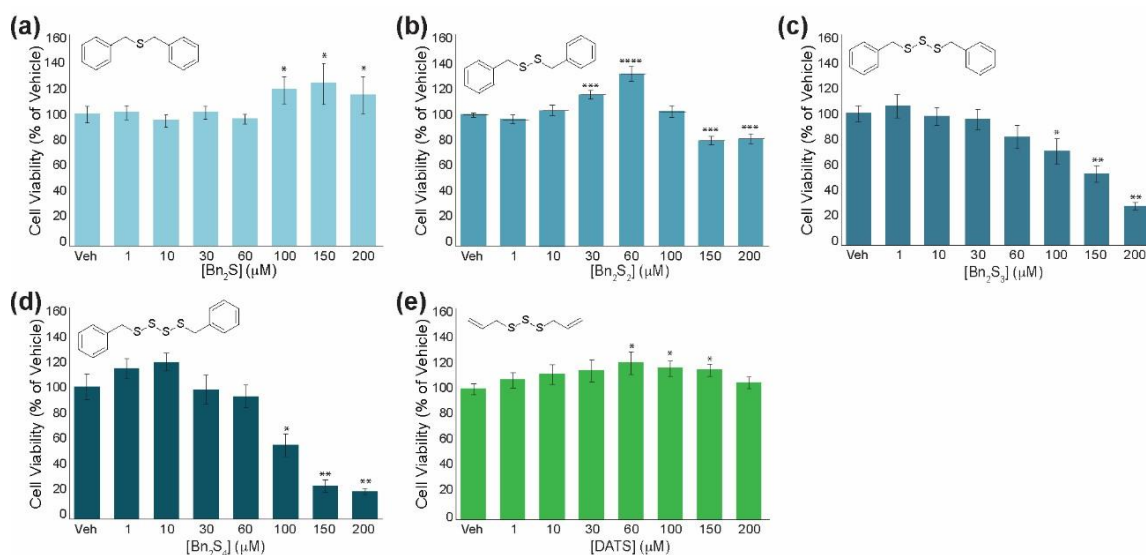


Figure 5.4 bEnd.3 cell viability after 24-h treatment of a series of organic polysulfides: (a) **Bn₂S**, (b) **Bn₂S₂**, (c) **Bn₂S₃**, (d) **Bn₂S₄**, and (e) **DATS**. * $p < 0.05$, ** $p < 0.01$, *** $p < 0.001$.

Interestingly, S^0 -containing **Bn₂S₃** and **Bn₂S₄** at concentrations of 100 μ M and higher demonstrated considerable cytotoxicity. Notably, **Bn₂S₄** appears to be significantly more cytotoxic than **Bn₂S₃**, which is consistent with the increased S^0 content in **Bn₂S₄** relative to **Bn₂S₃**. Because biological thiols react with the tri- and tetrasulfides to generate two equivalents of benzyl mercaptan as a byproduct, we also tested the cytotoxicity of benzyl mercaptan to confirm that the observed cytotoxicity was due to the S^0 content rather than the organic byproducts of the reaction. We elected to use *S*-benzyl ethanethioate (**BnSAc**) as a source of benzyl mercaptan to enhance cell permeability. We anticipated that hydrolysis of this ester under physiological conditions would generate benzyl

mercaptan and allow us to directly probe the effect of this thiol on cytotoxicity. Using treatment up to 400 μM , we did not observe significant cytotoxicity from **BnSAc** suggesting the observed cytotoxicity for benzyl polysulfides is a direct reflection of S^0 content, rather than organic byproducts of the reaction (Figure E.9). To compare our results with a well-known organic polysulfide, we examined the effect of **DATS** administration on cell proliferation in bEnd.3 cells under the same conditions. Interestingly, treatment of bEnd.3 cells with increasing concentrations of **DATS** did not demonstrate significant cytotoxicity and suggests pendant alkyl groups in organic polysulfides can directly alter biological activities. Taken together, these results demonstrate the effect of increasing S^0 content on cell proliferation in bEnd.3 cells and suggests organic polysulfides can afford varying biological activities independent of S^0 content.

5.3 Conclusions

The identification of key intermediates in sulfur biology responsible for physiological changes such as vasodilation and anti-inflammation is of utmost importance. Recent work has begun to suggest the importance of S^0 over H_2S in biology and modern synthetic techniques readily allow for access to simple organic polysulfides beyond **DATS**. Towards advancing our knowledge of reactive sulfur species in biology, we report our studies on examining S^0 content in a single series of organic polysulfides ranging from monosulfide up to and including tetrasulfide. In the presence of biological thiols including cysteine and GSH, we demonstrate the release of H_2S from **Bn₂S₃** and **Bn₂S₄** respectively under physiological conditions. Additionally, we

demonstrate the unique ability of **Bn₂S₃** and **Bn₂S₄** to suppress cell proliferation, whereas **DATS** has no effect in bEnd.3 cells. The results of this study warrant future investigations into the effects of various organic polysulfides and supports the significance of S⁰ in sulfur biology.

The results discussed in this Chapter demonstrate the H₂S-releasing efficacy of organic polysulfides with increasing S⁰ content and suggests intermediate persulfides govern the biological activity of this compounds. In parallel to expanding donor compounds which generate H₂S *via* intermediate reactive sulfur species, Chapter VI discusses the use of dithiasuccinoyl compounds as carbonyl sulfide-based H₂S donors in the presence of biological thiols.

5.4 Experimental Details

5.4.1 Materials and Methods

Reagents were purchased from Sigma-Aldrich, Tokyo Chemical Industry (TCI), and/or Cayman Chemical Company and used directly as received. Deuterated solvents were purchased from Cambridge Isotope Laboratories and used as received. ¹H and ¹³C ¹H NMR spectra were recorded on a Bruker 500 or 600 MHz instrument. Chemical shifts are reported relative to residual protic solvent resonances. Silica gel (SiliaFlash F60, Silicycle, 230–400 mesh) was used for column chromatography. All air-free manipulations were performed under an inert atmosphere using standard Schlenk technique or an Innovative Atmospheres N₂-filled glove box. UV–Vis spectra were acquired on an Agilent Cary 60 UV–Vis spectrophotometer equipped with a Quantum Northwest TC-1 temperature controller at 25 °C ± 0.05 °C.

H₂S Measurement Materials and Methods

Phosphate buffered saline (PBS) tablets (1×, CalBioChem) were used to prepare buffered solutions (140 mM NaCl, 3 mM KCl, 10 mM phosphate, pH 7.4) in deionized water. Buffer solutions were sparged with N₂ to remove dissolved oxygen and stored in an N₂-filled glovebox. Donor stock solutions (in DMSO) were freshly prepared inside an N₂-filled glovebox prior to an experiment. Thiol (cysteine or GSH) stock solutions (in PBS) were freshly prepared in an N₂-filled glovebox immediately before use.

General Procedure for Measuring H₂S Release via Methylene Blue Assay (MBA)

Scintillation vials containing 20 mL of PBS were prepared in an N₂-filled glovebox. To these solutions, 20 μL of 500 mM analyte stock solution (in PBS) was added for a final concentration of 500 μM. The solutions were allowed to thermally equilibrate while stirring in a heating block at the desired temperature for approximately 20–30 min. Immediately prior to donor addition, 0.5 mL solutions of the methylene blue cocktail were prepared in disposable 1.5 mL cuvettes. The methylene blue cocktail solution contained: 200 μL of 30 mM FeCl₃ in 1.2 M HCl, 200 μL of 20 mM *N,N*-dimethyl-*p*-phenylene diamine in 7.2 M HCl, and 100 μL of 1% (w/v) Zn(OAc)₂. To begin an experiment, 20 μL of the 25 mM donor stock solution (in DMSO) was added for a final concentration of 25 μM. At set time points after the addition of donor, 500 μL reaction aliquots were added to the methylene blue cocktail solutions and incubated for 1 h at room temperature shielded from light. Absorbance values were measured at 670 nm 1 h after addition of reaction aliquot. Each experiment was performed in quadruplicate unless stated otherwise.

MBA Calibration Curve

Solutions containing 0.5 mL of the methylene blue cocktail and 0.5 mL PBS containing 500 μ M thiol (cysteine or GSH) were freshly prepared in disposable cuvettes (1.5 mL). Under inert conditions, a 10 mM stock solution of NaSH (Strem Chemicals) in PBS was prepared and diluted to 1 mM. Immediately after dilution, 1 mM NaSH was added to 1.0 mL solutions for final concentrations of 10, 20, 30, 40, and 50 μ M. Solutions were mixed thoroughly, incubated at room temperature for 1 h, and shielded from light. Absorbance values at 670 nm were measured after 1 h.

Cell Culture

The murine brain endothelial cell line bEnd.3 was obtained by ATCC (CRL-2299) and cultured in phenol red DMEM containing 10% premium grade fetal bovine serum (FBS) and 1% penicillin-streptomycin (PS) (10,000 units/mL penicillin and 10,000 μ g/mL streptomycin). Cells were incubated at 37 °C under 5% CO₂.

Cell Proliferation Assay

bEnd.3 cells were seeded in Nunc® 96 well plates at 20,000 cells/well in 10% FBS, 1% PS DMEM and grown overnight. The next day, media was aspirated off and cells were rinsed in 1% PS-containing DMEM containing no FBS or phenol red. Media was replaced with the FBS-free DMEM containing either 0.5% DMSO (vehicle) or the tested compounds and cells were incubated under these conditions for 24 h before treatment with Cell Counting Kit-8 (CCK-8, Dojindo Molecular Technologies). No turbidity of the tested compounds was observed in DMEM up to the concentrations tested.

Statistical Analysis

Cell proliferation data is represented as a percentage viability compared to the vehicle (Veh). Data for each treatment condition were averaged from several trials using a pooled average. Error was pooled from the standard deviations for each treatment condition found in each of these trials. A two-tailed Student's *t*-test was then performed comparing each treatment condition to the vehicle.

5.4.2 Synthesis

SS-Benzyl O-methyl carbonodithioperoxoate

Methoxycarbonylsulfonyl chloride (2.6 mmol, 1.1 equiv.) was added to anhydrous CH₂Cl₂ (20 mL) and cooled to 0 °C in an ice bath under N₂. Once cooled, benzyl mercaptan (2.4 mmol, 1.0 equiv.) was added dropwise, and the reaction mixture was stirred for 1 h at 0 °C under N₂. After 1 h, the reaction was quenched with the addition of deionized H₂O (30 mL), and the organic layer was separated. The remaining aqueous layer was extracted with CH₂Cl₂ (2 × 30 mL), and the combined organic layers were washed with brine (x1) and dried over MgSO₄. After filtration, the solvent was removed under reduced pressure, and the desired product purified by column chromatography (10% EtOAc in hexanes, *R_f* = 0.46). The product was isolated as a clear liquid. Mass: 430 mg (83%) ¹H NMR (500 MHz, DMSO-*d*⁶) δ: 7.38–7.26 (m, 5H), 4.07 (s, 2H), 3.79 (s, 3H). ¹³C ¹H NMR (126 MHz, DMSO-*d*⁶) δ: 168.35, 136.13, 129.44, 128.41, 127.60, 55.77, 42.07. TOF MS EI+ (*m/z*) [M + H]⁺ calc'd for C₉H₁₀O₂S₂ 214.0122; found, 214.0120.

5.4.2.2 Benzyl tetrasulfide

Benzyl mercaptan (2.0 mmol, 1.0 equiv.) and pyridine (2.0 mmol, 1.0 equiv.) were added to anhydrous Et₂O (20 mL) and cooled to -78 °C over 1 h under N₂. Sulfur monochloride (1.2 mmol, 0.6 equiv.) was added dropwise, and the reaction mixture was stirred at -78 °C for 2 h. The reaction was quenched with the addition of dH₂O (30 mL) and diluted with CH₂Cl₂ (30 mL). The organic layer was removed, and the aqueous layer was extracted with CH₂Cl₂ (20 mL x 2). The combined organic layers were washed organic layers with brine (20 mL x 1), dried over MgSO₄, filtered, and evaporated under reduced pressure to yield the product as a yellow solid. Mass: 280 mg (89%). ¹H NMR (500 MHz, CDCl₃) δ 7.37–7.27 (m, 10H), 4.16 (s, 4H). ¹³C ¹H NMR (126 MHz, CDCl₃) δ 136.39, 129.64, 128.81, 127.87, 43.81. (HRMS experiments did not show the parent ion peak due to the weak internal S-S bond.)

5.4.2.3 S-Benzyl ethanethioate

Benzyl mercaptan (1.6 mmol, 1.1 equiv.) and triethylamine (1.6 mmol, 1.1 equiv.) were added to anhydrous CH₂Cl₂ (30 mL) and cooled to 0 °C in an ice bath under N₂. Once cooled, acetyl chloride (1.4 mmol, 1.0 equiv.) was added dropwise, and the reaction was stirred at 0 °C for 2 h under N₂. The reaction was quenched with the addition of deionized H₂O (20 mL), and the organic layer was separated. The remaining aqueous layer was extracted with CH₂Cl₂ (2 × 20 mL) and the combined organic extractions were washed with brine (1 × 20 mL) and dried over MgSO₄. After filtration, the solvent was removed under reduced pressure, and the desired product purified by column chromatography (20% CH₂Cl₂ in Hexanes, *R_f* = 0.25). The product was isolated as a clear liquid.

Mass: 126 mg (52%). ^1H NMR (600 MHz, CDCl_3) δ : 7.31–7.27 (m, 4H), 7.27–7.23 (m, 1H), 4.13 (s, 2H), 2.35 (s, 3H). ^{13}C ^1H NMR (151 MHz, CDCl_3) δ : 195.09, 137.56, 128.77, 128.60, 127.24, 33.42, 30.29. TOF MS (EI+) (m/z): $[\text{M} + \text{H}]^+$ calc'd for $\text{C}_9\text{H}_{10}\text{OS}$ 166.0452; found 166.0454.

CHAPTER VI

USE OF DITHIASUCCINOYL-CAGED AMINES ENABLES COS/H₂S RELEASE LACKING ELECTROPHILIC BYPRODUCTS

This chapter includes previously published and coauthored material from Cerda, M.M.; Mancuso, J.L.; Mullen, E.J.; Hendon, C.H.; Pluth, M.D. Use of Dithiasuccinoyl-Caged Amines Enables COS/H₂S Release Lacking Electrophilic Byproducts. *Chem. Eur. J.* **2020**, DOI: 10.1002/chem.201905577. This manuscript was written by Matthew M. Cerda with editorial assistance from Professor Michael D. Pluth. The project in this chapter was conceived by Matthew M. Cerda. The experimental work in this chapter was performed by Matthew M. Cerda and Emma J. Mullen. The computational work in this chapter was performed by Jenna L. Mancuso with assistance from Professor Christopher H. Hendon.

6.1 Introduction

Despite being a malodorous gas,²⁰⁰ hydrogen sulfide (H₂S) is an important biological signaling molecule often referred to as a gasotransmitter alongside carbon monoxide and nitric oxide.^{1c, 90} H₂S-mediated signaling is important in several physiological processes including vasodilation,²⁰¹ neurotransmission,²⁰² and inflammation.^{14b} These findings have led researchers to propose the use of H₂S as a potential therapeutic agent for a variety of conditions and pathologies.⁹² Toward this goal, researchers have relied heavily on the use of NaSH and Na₂S as sources of H₂S due to ease of handling and commercial availability; however, H₂S release from these salts is

considerably different relative to enzymatic H₂S generation.⁹⁶ To better mimic endogenous H₂S production, methods of generating H₂S at controlled rates under physiologically-relevant conditions are needed,^{127b} and the development of small molecule “H₂S donors” is an active research area aimed at addressing this need.²⁰³ Such compounds typically generate H₂S by passive hydrolysis^{33, 37} or activation in the presence of specific stimuli including light,⁷⁴ biological thiols,⁵² and cellular enzymes including esterases.¹⁷

Recently, an alternative approach to H₂S generation has utilized the hydrolysis of carbonyl sulfide (COS) by carbonic anhydrase (CA), a ubiquitous metalloenzyme.²⁰⁴ Existing in Nature as the most abundant sulfur-containing gas in the atmosphere,¹⁰⁰ COS is rapidly converted to H₂S and carbon dioxide (CO₂) in the presence of bovine carbonic anhydrase II ($k_{cat}/K_M=2.2\times 10^4\text{ m}^{-1}\text{ s}^{-1}$).²⁰⁵ In our initial approach, we were inspired by self-immolative carbamates, which release CO₂ as a byproduct upon activation,²⁰⁶ and developed analogous self-immolative thiocarbamates that function as tunable COS-based H₂S donors (Figure 6.1a).¹⁶

The high modularity of self-immolative COS-releasing motifs has enabled the rapid expansion of this approach by our group²⁰⁴ as well as others to prepare COS-based H₂S donors activated by various stimuli including acidic pH,⁴⁰ esterases,^{20-21, 207} reactive oxygen species,^{24, 208} and cysteine.⁶⁷⁻⁶⁸ This approach has also been extended to provide oligomeric COS-based H₂S donors.²⁰⁹ A critical, yet often overlooked component of this approach is the formation of a quinone methide byproduct, which is a potent electrophile and known Michael acceptor in biological systems.²¹⁰ Although we have not observed cytotoxicity from this byproduct in our studies, chronic exposure from therapeutic administration of

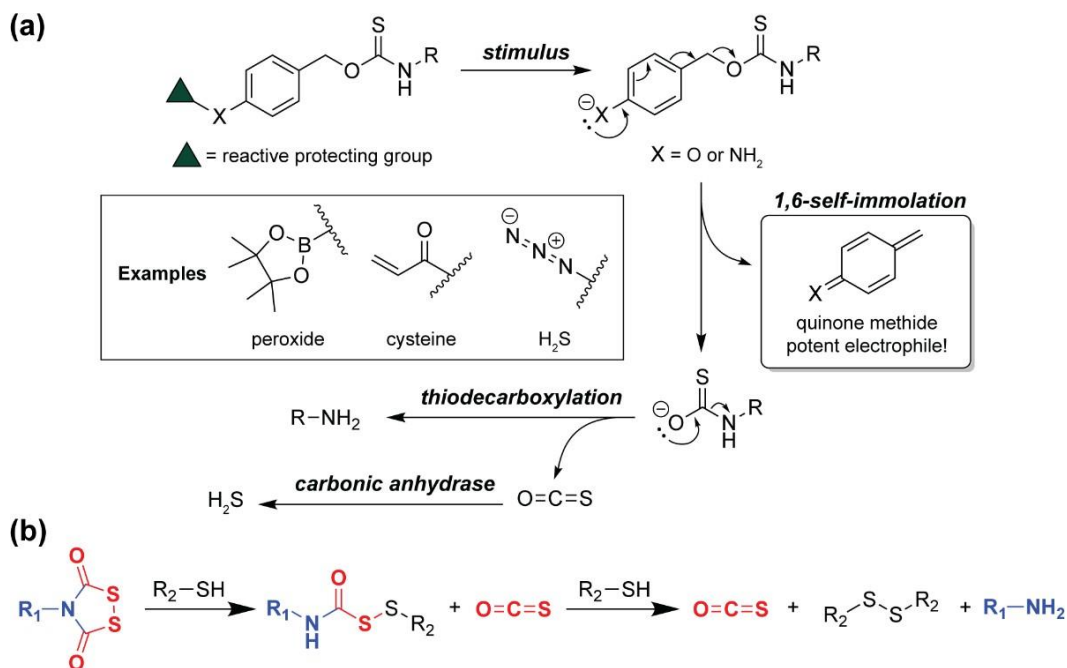


Figure 6.1 (a) Generalized reaction mechanism for COS release from self-immolative thiocarbamates and subsequent hydrolysis of COS to H₂S by carbonic anhydrase. (b) Overall reaction scheme of COS release from dithiasuccinoyl groups in the presence of thiols.

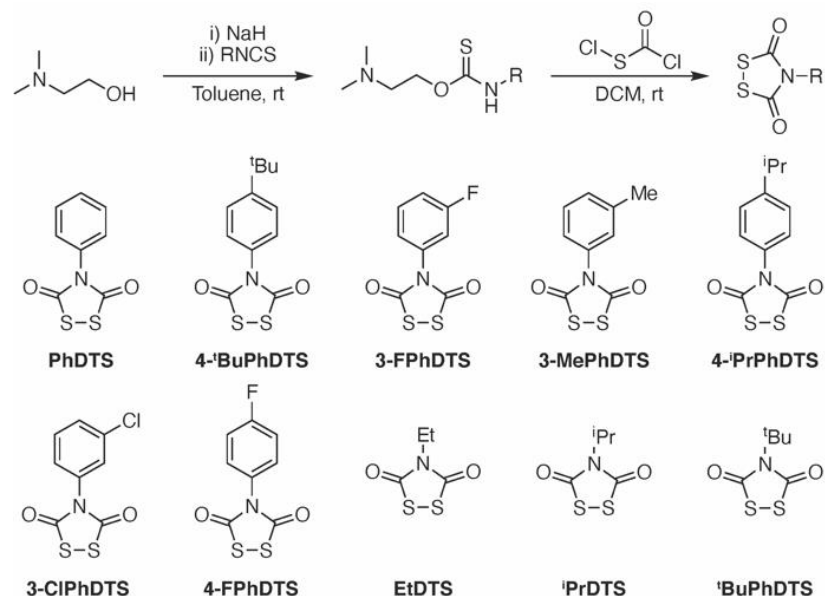
these compounds may induce electrophilic stress leading to long-term cytotoxicity.²¹¹ As an alternative approach, Matson and co-workers have reported both small molecule and polymeric *N*-thiocarboxyanhydrides (NTAs) as COS/H₂S donors, which only result in small peptide byproducts.^{15b, 87} These donor compounds, however, exhibit a relatively low H₂S-releasing efficiencies. To further develop COS-based H₂S donors as both research tools and potential pharmacological agents, alternative donor motifs are needed that lack electrophilic byproducts, maximize COS/H₂S release, and allow for simple tuning of release rates.

To address these needs, we focused on the reactivity of the dithiasuccinoyl (DTS) group, which has been used previously as a protecting group for amines in peptide synthesis.²¹² The DTS group is cleaved by thiols, which results in reduction to a symmetric disulfide, two equivalents of COS, and an amine (Figure 6.1b). We note that previous

studies on thiol-mediated reduction of DTS groups examined this reactivity in organic solvents using β -mercaptoethanol as the reductant and quantified reaction kinetics through the use of an amino acid analyzer without direct observation of COS.²¹³ We envisioned that this reactivity could be harnessed to prepare a library of COS-based H₂S donors that do not release electrophilic byproducts, but that readily release COS/H₂S under physiologically relevant conditions in the presence of CA. Herein, we demonstrate that DTS-caged amines function as versatile COS/H₂S donors activated by biological nucleophiles, including cysteine and reduced glutathione (GSH). Additionally, we use a combination of experimental and computational investigations to demonstrate that the rate of COS/H₂S release can be readily tuned by electronic modulation and subsequent stabilization of the COS-releasing thiocarbamic acid intermediate.

6.2 Results and Discussion

To prepare a small library of COS-based H₂S donors with tunable release rates, we treated alkyl and aryl isothiocyanates with *N,N*-dimethylethanolamine in the presence of sodium hydride to generate the desired thiocarbamate intermediate. Subsequent treatment with chlorocarbonylsulfonyl chloride afforded the desired DTS-caged compounds (Scheme 6.1). The amines chosen for this library included aryl amines with different electron donating/withdrawing properties, as well as alkyl amines with increasing steric bulk. To assess the viability of these compounds as COS/H₂S donors, we examined the release of H₂S from **PhDTS** (25 μ m) in the presence of biologically-relevant nucleophiles (500 μ m, 20 equiv) and CA (25 μ g mL⁻¹) using the methylene blue assay to measure H₂S generation (Figure 6.2).²¹⁴ Our expectation was that this donor functional group would be activated



Scheme 6.1 Synthesis of DTS-based COS/H₂S donors

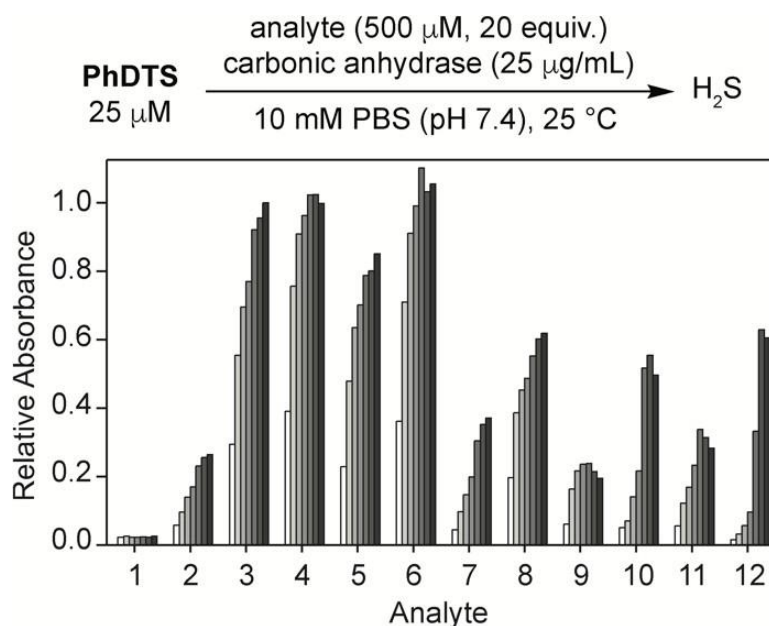


Figure 6.2 Activation profiles of H₂S release from **PhDTS** (25 μM) in the presence of different nucleophiles (500 μM, 20 equiv.) and carbonic anhydrase (25 μg mL⁻¹). Data were acquired at 1, 5, 10, 15, 30, 45, and 60 min. Methylene blue absorbance values are relative to the maximum absorbance value obtained from H₂S release in the presence of cysteine (3). Analytes: H₂O with no carbonic anhydrase (1), cysteine with no carbonic anhydrase (2), *N*-acetyl-l-cysteine (4), L-cysteine methyl ester (5), *N*-acetyl-l-cysteine methyl ester (6), homocysteine (7), reduced glutathione (8), serine (9), lysine (10), only carbonic anhydrase (11), *S*-methyl cysteine (12).

broadly by different nucleophiles rather than one specific biological nucleophile, thus broadening the scope of potential activation pathways.

In the absence of CA, we did not observe hydrolysis-mediated H₂S release from **PhDTS**. The addition of cysteine to **PhDTS** in the absence of CA resulted in slow, yet gradual H₂S release. We attribute this observation to the hydrolysis of COS at physiological pH, which has been reported previously to be slow.²¹⁵ Treatment of **PhDTS** with cysteine in the presence of CA resulted in significant H₂S generation. Using a calibration curve generated with known concentrations of NaSH, we measured 40 μM H₂S generation from 25 μM **PhDTS** in the presence of 500 μM cysteine, which corresponds to an H₂S releasing efficiency of 80% (Figure F.46). This observation not only highlights the high efficiency of H₂S release from DTS-caged compounds, but also supports that two equivalents of COS are released per DTS group.

In addition to COS/H₂S release, we also observed the formation of aniline following treatment of **PhDTS** with cysteine by HPLC, which further supports the proposed releasing mechanism (Figure S48). Protection of the amine and/or carboxylate groups on cysteine did not significantly impact the rate or quantity of COS/H₂S release from **PhDTS**, which supports a thiol-mediated releasing pathway. Interestingly, the use of *S*-methyl cysteine resulted in slow, yet considerable H₂S release suggesting a less favorable, thiol-independent reaction pathway. In previous studies, the direct reaction of amines at the carbonyl position of DTS groups has been observed and proposed to result in the generation of COS and sulfane sulfur.²¹³ We observed a similar rate of H₂S release in the presence of lysine, which further supports a minor, amine-mediated mechanism of H₂S release. We note an induction phase in the rate of amine activation and find that this reaction is slower

relative to the thiol-mediated reduction of DTS groups (Figure F.49). Together with the decreased nucleophilicity of amines due to protonation at physiological pH and lower biological concentrations relative to thiols, we expect this mechanism of activation to be negligible in a biological context. In the presence of homocysteine and GSH, we observed lower quantities of COS/H₂S released, which we attribute to the lower nucleophilicity of these thiols as a function of thiolate/thiol speciation at physiological pH.^{108, 216} We failed to observe COS/H₂S release in the presence of serine, which implies that alcohol-mediated mechanisms are not a significant activation pathway.

In the presence of CA, but absence of any added nucleophiles, we did observe slight H₂S production. We hypothesized that this release could be due to coordination of **PhDTS** to the Zn²⁺ center in CA, which would facilitate hydrolysis by carbonyl activation. To probe this reactivity, we pre-incubated CA with the CA inhibitor acetazolamide (5 μM) and measured H₂S release from **PhDTS** (Figure F.47). Under these conditions, we failed to observe H₂S generation, which supports the hypothesis of a minor CA/Zn²⁺-mediated hydrolysis mechanism. Alternatively, this could also be due to minor background DTS hydrolysis followed by COS conversion to H₂S by CA. Further experiments using a catalytic amount of Zn(OAc)₂ (5 μM) did not result in COS/H₂S release from **PhDTS**, which suggests the need for the protein microenvironment present in CA for activation of **PhDTS** (Figure F.48).²¹⁷ Similar to the reactivity with amines, the rate of CA/Zn²⁺-mediated hydrolysis is slower than the thiol-mediated reduction. Taken together, these results demonstrate the validity of **PhDTS** and related compounds to serve as COS/H₂S donors under physiologically relevant conditions in the presence of thiols and CA.

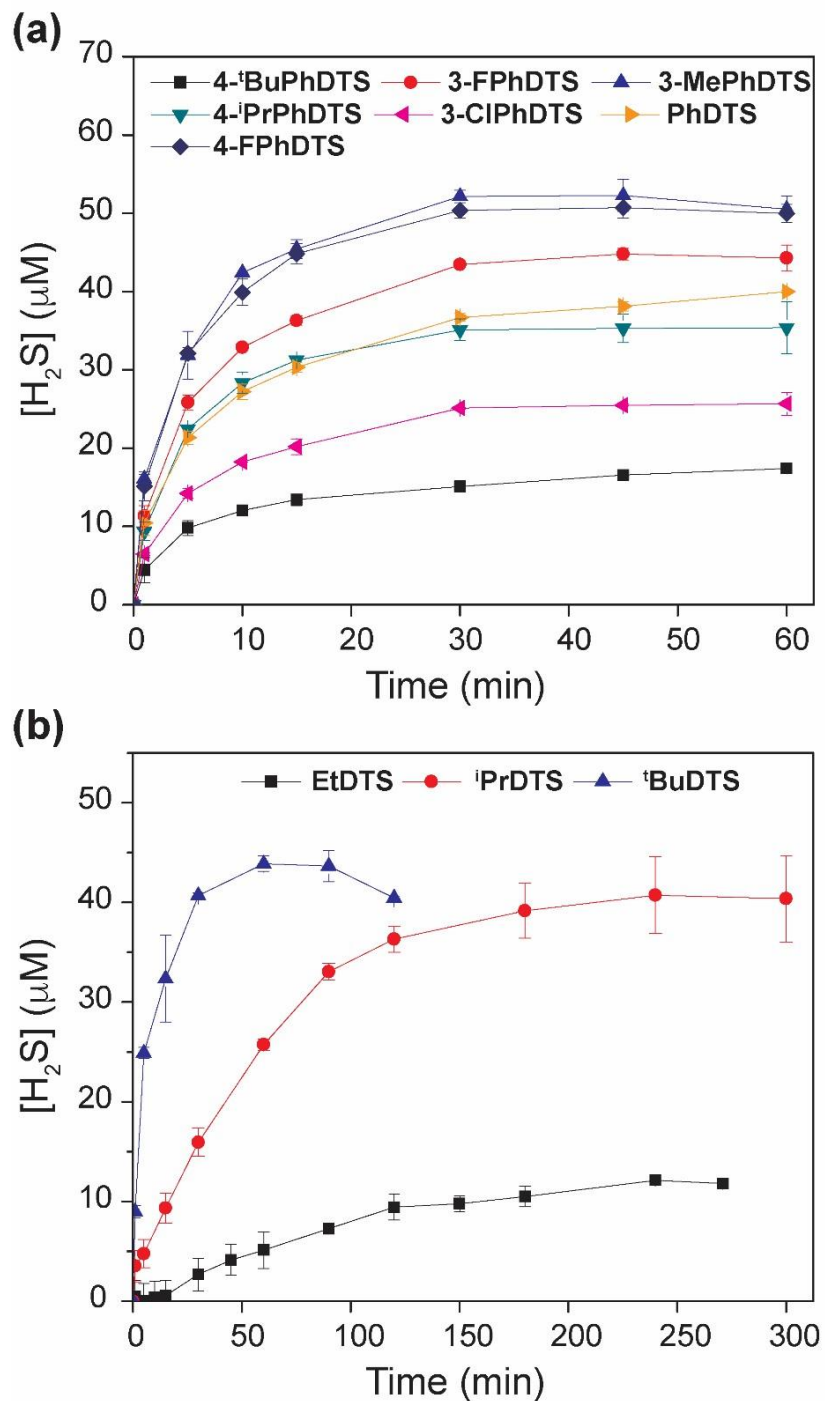
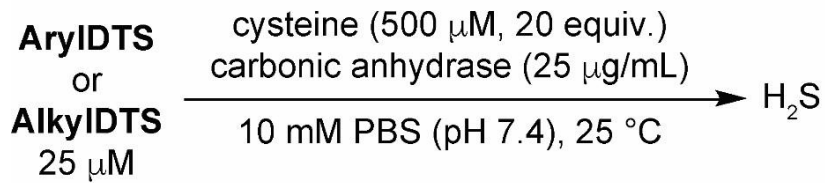


Figure 6.3 (a) H_2S release from aryl-based DTS compounds. (b) H_2S release from alkyl-based DTS compounds.

With a small library of DTS-based donors in hand, we next examined the effect of the amine payload on COS/H₂S release using each donor (25 μM) in the presence of cysteine (500 μM, 20equiv.) and CA (25 μg mL⁻¹) at physiological pH (Figure 6.3). We hypothesized that DTS-caging of functionalized anilines would allow COS/H₂S release rates to be tuned based on prior work aimed at solvent-dependent linear free energy relationship investigations into the phosphine-mediated sulfur extrusion from DTS.²¹⁸ Additionally, we expected that the caging of alkyl amines would lead to stabilization of the COS-releasing thiocarbamic acid intermediate and subsequently decrease the rate of H₂S release relative to that observed for DTS-caged anilines. In the presence of cysteine and CA, we observed varying rates and quantities of H₂S release from the reported aryl-based DTS compounds with **3-MePhDTS** and **4-*t*BuPhDTS** displaying the fastest and slowest rates of H₂S release, respectively (Figure 6.3a). The releasing curves from the DTS-caged anilines did not fit cleanly to first-order exponential decay, which we attribute to competing COS-releasing and DTS consumption pathways, such as direct thiol activation versus CA-mediated activation. Additionally, previous work has reported the formation of isothiocyanates from sufficiently acidic thiocarbamates, which likely further complicates the rates of release from DTS-caged anilines containing electron-withdrawing groups.²¹⁹ Overall, the functionalization of caged anilines directly alters rates of COS/H₂S release from DTS-based donors, and the ability to control tuning of these releasing kinetics merits future investigation. By contrast, we observed the caging of alkyl amines resulted in significantly slower rates of H₂S release relative to DTS-caged anilines with ***t*BuDTS** and **EtDTS** displaying the fastest and slowest rates of H₂S release, respectively (Figure 6.3b). We reasoned that inductively donating alkyl amines likely

stabilize the COS-releasing thiocarbamic intermediates leading to a decrease in H₂S-releasing kinetics.

To further investigate the differences between aryl and alkyl amine substitution, we used density functional theory (DFT) to examine the potential energy surface for COS release from **PhDTS** and **AlkylDTS** compounds. In these systems, we used methyl thiol (**MeSH**) to simplify possible protonation states of non-participating functional groups during the reaction. Calculations were performed using Gaussian 09 at the B3LYP/6-311++G(d,p) level of theory applying the IEF-PCM water solvation model (Figure 6.4).

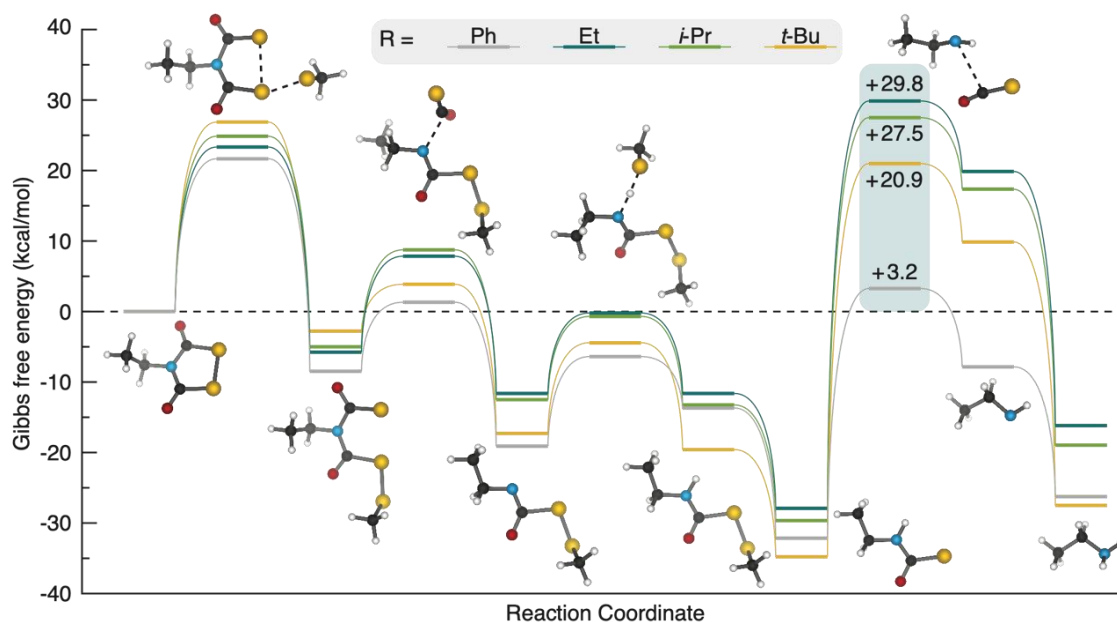


Figure 6.4 Potential energy surface for COS release from **PhDTS** and **AlkylDTS** compounds. Calculations were performed using Gaussian 09 at the B3LYP/6-311++G(d,p) level of theory applying the IEF-PCM water solvation model. **MeSH** was used as the thiol nucleophile to simplify accessible protonation states of non-participating functional groups on the thiol nucleophile.

For **PhDTS**, we found that the initial nucleophilic attack by the thiolate was the highest barrier (21.7 kcal mol⁻¹) on the reaction coordinate and dethiocarboxylation of the thiocarbamic acid intermediate was only moderately endothermic (+3.2 kcal mol⁻¹) with

respect to the starting materials. By contrast, although the **AlkylDTS** compounds showed similar activation barriers for the initial attack by thiolate (23.5–26.8 kcal mol⁻¹), the activation barrier for the final dethiocarboxylation varied significantly as a function of the alkyl group. The highest activation barrier for dethiocarboxylation was found for the **EtDTS** compound (+29.8 kcal mol⁻¹), but this barrier decreased with the increasing donating ability of ***i*PrDTS** (+27.5 kcal mol⁻¹), and ***t*BuDTS** (+20.9 kcal mol⁻¹); all of which were competitive with the activation barriers for initial thiol attack on the DTS motif. These relative energetic barriers are consistent with the observed rates of COS/H₂S release from the **AlkylDTS** compounds. Moreover, these results suggest that the inductive contributions, rather than the steric bulk differences of the alkyl substituents, have a larger impact on the release of COS from thiocarbamic acid intermediates. Taken together, the combination of experimental and computational data demonstrates the ability to tune H₂S/COS release from this scaffold by simple structural modifications. More broadly, these results provide guidance for controlling the COS/H₂S release rate from donor motifs that proceed through a thiocarbamic acid intermediate prior to COS extrusion.

6.3 Conclusions

We demonstrated the use of DTS-based compounds to serve as COS/H₂S donors in the presence of thiols without the formation of electrophilic byproducts. Reactivity studies using **PhDTS** as a model compound were used to investigate COS/H₂S release as a function of biological nucleophiles and thiol identity. By modifying the structure of the amine payloads, we also demonstrated that the rate of COS/H₂S release from DTS-based donors can be modified by simple structural modifications. The results from DFT

calculations has shed light on the impact of amine identity on COS release from thiocarbamic acids and provides a foundation to guide future work on this reactive intermediate. Specifically, this work directly elaborates on the observed reactivity differences between aryl and alkyl thiocarbamates as COS-releasing motifs, which provides fundamental information upon which to expand the utility of these donors. The simple synthetic conditions and unique reactivity of this donor scaffold would readily allow for the incorporation amine-based payloads including fluorophores²²⁰ and known therapeutics²²¹ to provide COS-based H₂S fluorescent donors and prodrugs.

The chemistry described in Chapter VI provides a modular platform for the development of COS-based H₂S donors with no electrophilic byproducts and potential prodrug applications. Aligned with our interests in the potential signaling properties of COS independent of H₂S, there exists a need to develop a method of selective COS detection. The work in Chapter VII describes the validity of a colorimetric and fluorescent probe for selective detection of COS over carbon dioxide and carbon disulfide.

6.4 Experimental Details

6.4.1 Materials and Methods

Reagents were purchased from Sigma-Aldrich, Tokyo Chemical Industry, or VWR and used directly as received. Deuterated solvents were purchased from Cambridge Isotope Laboratories and used as received. ¹H, ¹³C ¹H, and ¹⁹F NMR spectra were recorded on a Bruker 500 MHz instrument. Chemical shifts were reported relative to residual protic solvent resonances. MS data was collected on a Xevo G2-XS QToF (Waters) instrument. Silica gel (SiliaFlash F60, Silicycle, 230–500 mesh) was used for column chromatography.

All air-free manipulations were performed under an inert atmosphere using standard Schlenk technique.

H₂S Detection Materials and Methods

Phosphate buffered saline (PBS) tablets (1X, CalBioChem) were used to prepare buffered solutions (140 mm NaCl, 3 mm KCl, 10 mm phosphate, pH 7.4) in deionized water. Buffer solutions were sparged with nitrogen to remove dissolved oxygen and stored in an Innovative Atmosphere nitrogen-filled glovebox. Donor stock solutions (in acetonitrile) were prepared inside a nitrogen-filled glovebox immediately before use. Trigger stock solutions (in PBS) were freshly prepared in an N₂-filled glovebox immediately before use. CA stock solutions (in PBS) were freshly prepared in a nitrogen-filled glovebox immediately before use.

General Procedure for Measuring H₂S Release via Methylene Blue Assay (MBA)

Scintillation vials containing 20 mL of 10 mm PBS (pH 7.4) were prepared in a nitrogen-filled glovebox. To these solutions, 20 μ L of 500 mm analyte stock solution and 50 μ L of 10 mg mL⁻¹ CA were added for final concentrations of 500 μ m and 25 μ g mL⁻¹ respectively. While stirring, solutions were allowed to thermally equilibrate in heating block set at 25 °C for approximately 20–30 min. Immediately prior to donor addition, 0.5 mL solutions of methylene blue cocktail were prepared in disposable 1.5 mL cuvettes. The methylene blue cocktail solution contains: 200 μ L of 30 mm FeCl₃ in 1.2 m HCl, 200 μ L of 20 mm *N,N*-dimethyl-*p*-phenylene diamine in 7.2 m HCl, and 100 μ L of 1% (w/v) Zn(OAc)₂. To begin an experiment, 20 μ L of 25 mm donor stock solution

was added for a final concentration of 25 μM . At set time points after the addition of donor, 500 μL reaction aliquots were added to the methylene blue cocktail solutions and incubated for 1 h at room temperature shielded from light. Absorbance values at 670 nm were measured 1 h after addition of reaction aliquot. Each experiment was performed in quadruplicate unless stated otherwise. UV/Vis spectra were acquired on an Agilent Cary 60 UV/Vis spectrophotometer equipped with a Quantum Northwest TC-1 temperature controller set at 25 ± 0.05 $^{\circ}\text{C}$.

MBA Calibration Curve

Solutions containing 0.5 mL of methylene blue cocktail and 0.5 mL PBS (pH 7.4) containing 500 μM cysteine and 25 $\mu\text{g}/\text{mL}$ CA were freshly prepared in disposable 1.5 mL cuvettes. Under inert conditions, a 10 mM stock solution of NaSH (Strem Chemicals) in PBS was prepared and diluted to 1 mM. Immediately after dilution, 1 mM NaSH was added to 1.0 mL solutions for final concentrations of 10, 20, 30, 40, 50, and 60 μM . Solutions were mixed thoroughly, incubated at room temperature for 1 h, and shielded from light. Absorbance values at 670 nm were measured after 1 h.

Computational Methods

All structures were initially constructed, and optimized using the UFF force field as implemented, in Avogadro.²²² The resultant structures were further optimized using the unrestricted hybrid GGA functional, B3LYP, as implemented in Gaussian 09,²²³ with a triple zeta basis set that includes diffuse and polarization functions on heavy atoms, 6-311+G*. A pseudosolvent polarizable continuum model for water was used to account for

solvation effects. Attacking thiols were modeled as methyl thiol to reduce computational expense.

Transition state searches were carried out at the same level of theory as ground state structures. First, a potential energy surface scan of the active reaction coordinate was used to obtain a good starting point for the ultimate transition state search algorithm. Vibrational analysis confirmed a single imaginary frequency corresponding to the direction of bond formation or breaking for each activated complex. No transition state was found for thiol disulfide exchange, which could indicate a barrierless transition, or a shallow potential energy surface with a loose transition state. Biologically relevant thiols, such as cysteine, may undergo a more sterically hindered attack when compared to the methyl thiol employed in this model and may experience a more defined transition state and activation barrier.

6.4.2 Synthesis

General procedure for the synthesis of thiocarbamates

This procedure has been modified from a previous report.²¹⁸

In a flame-dried round bottom flask under nitrogen, sodium hydride (1.25 equiv) and *N,N*-dimethylethanolamine were added to anhydrous toluene (20 mL). After stirring briefly until gas evolution ceased, the desired isothiocyanate (1.0 equiv) was added dropwise (if liquid) or in a single portion (if solid). The reaction was stirred at room temperature for 3 h under nitrogen, quenched with deionized H₂O (30 mL), and extracted with ethyl acetate (3×15 mL). The combined organic extractions were washed with brine (1×20 mL), dried over MgSO₄, and concentrated under reduced pressure. The desired product was obtained

following purification by column chromatography. All NMR data for these compounds was obtained at 60 °C due to hindered rotation of thiocarbamates at room temperature. We note the alkyl thiocarbamates displayed hindered rotation at 60 °C giving rise to two sets of peaks corresponding to the *E* and *Z* isomers.

O-(2-(Dimethylamino)ethyl) phenylcarbamothioate (**PhTC**)

Slightly yellow oil, 339 mg (68%) $R_f = 0.30$ (5% MeOH in DCM)

^1H NMR (500 MHz, DMSO- d^6) δ : 7.50 (br s, 2 H), 7.37 – 7.26 (m, 2 H), 7.23 – 7.06 (m, 1 H), 4.56 (t, $J = 5.7$ Hz, 2 H), 2.65 (t, $J = 5.8$ Hz, 2 H), 2.22 (s, 6 H). $^{13}\text{C}\{^1\text{H}\}$ NMR (126 MHz, DMSO- d^6) δ : 187.48, 137.98, 128.29, 124.55, 122.17, 67.88, 56.80, 44.98.

TOF MS (ASAP⁺) (m/z): $[\text{M} + \text{H}]^+$ calc'd for $\text{C}_{11}\text{H}_{17}\text{N}_2\text{OS}$ 225.1062; found 225.1047

O-(2-(Dimethylamino)ethyl) (4-(*tert*-butyl)phenyl)carbamothioate (**4-^tBuPhTC**)

Slightly yellow oil, 368 mg (84%) $R_f = 0.43$ (5% MeOH in DCM)

^1H NMR (500 MHz, DMSO- d^6) δ : 10.85 (br s, 1 H), 7.41 (br s, 2 H), 7.34 (d, $J = 8.5$ Hz, 2 H), 4.55 (t, $J = 5.8$ Hz, 2 H), 2.65 (t, $J = 5.8$ Hz, 2 H), 2.23 (s, 6 H), 1.28 (s, 9 H).

$^{13}\text{C}\{^1\text{H}\}$ NMR (126 MHz, DMSO- d^6) δ : 187.25, 147.09, 135.45, 124.90, 121.80, 56.79, 54.51, 44.96, 33.83, 30.86. TOF MS (ASAP⁺) (m/z): $[\text{M} + \text{H}]^+$ calc'd for $\text{C}_{15}\text{H}_{25}\text{N}_2\text{OS}$ 281.1688; found 281.1707

O-(2-(Dimethylamino)ethyl) (3-fluorophenyl)carbamothioate (**3-FPhTC**)

White powder, 395 mg (83%) $R_f = 0.34$ (5% MeOH in DCM)

^1H NMR (500 MHz, DMSO- d^6) δ : 7.51 (br s, 1 H), 7.44 – 7.25 (m, 2 H), 6.95 (dt, $J = 9.0$, 4.5 Hz, 1 H), 4.58 (t, $J = 5.7$ Hz, 2 H), 2.66 (t, $J = 5.6$ Hz, 2 H), 2.24 (s, 6 H). ^{19}F NMR (471 MHz, DMSO- d^6) δ : -112.32. $^{13}\text{C}\{^1\text{H}\}$ NMR (126 MHz, DMSO- d^6) δ : 187.40, 161.72 (d, $J = 242.0$ Hz), 139.60, 129.85 (d, $J = 9.4$ Hz), 117.42, 110.85 (d, $J = 20.9$ Hz), 108.66 (d, $J = 25.9$ Hz), 67.99, 56.70, 44.88. TOF MS (ASAP⁺) (m/z): $[\text{M} + \text{H}]^+$ calc'd for $\text{C}_{11}\text{H}_{16}\text{FN}_2\text{OS}$ 243.0967; found 243.0969

O-(2-(Dimethylamino)ethyl) *m*-tolylcarbamothioate (**3-MePhTC**)

Slightly yellow oil, 403 mg (84%) $R_f = 0.50$ (10% MeOH in DCM)

^1H NMR (500 MHz, DMSO- d^6) δ : 10.84 (br s, 1 H), 7.43 – 7.24 (m, 2 H), 7.20 (t, $J = 7.7$ Hz, 1 H), 6.96 (d, $J = 7.3$ Hz, 1 H), 4.55 (t, $J = 5.7$ Hz, 2 H), 2.64 (t, $J = 5.7$ Hz, 2 H), 2.29 (s, 3 H), 2.23 (s, 6 H). $^{13}\text{C}\{^1\text{H}\}$ NMR (126 MHz, DMSO- d^6) δ : 187.39, 137.90, 137.58, 128.06, 125.17, 122.66, 119.09, 68.04, 56.79, 44.93, 20.72. TOF MS (ASAP⁺) (m/z): $[\text{M} + \text{H}]^+$ calc'd for $\text{C}_{12}\text{H}_{19}\text{N}_2\text{OS}$ 239.1218; found 239.1200

O-(2-(Dimethylamino)ethyl) (4-isopropylphenyl)carbamothioate (**4-ⁱPrPhTC**)

Slightly yellow oil, 350 mg (78%) $R_f = 0.45$ (10% MeOH in DCM)

^1H NMR (500 MHz, DMSO- d_6) δ : 10.84 (br s, 1 H), 7.40 (br s, 2 H), 7.19 (d, $J = 8.5$ Hz, 2 H), 4.55 (t, $J = 5.8$ Hz, 2 H), 2.87 (hept, $J = 6.9$ Hz, 1 H), 2.64 (t, $J = 5.8$ Hz, 2 H), 2.22 (s, 6 H), 1.20 (d, $J = 6.9$ Hz, 6 H). $^{13}\text{C}\{^1\text{H}\}$ NMR (126 MHz, DMSO- d_6) δ : 187.34, 144.82, 135.80, 126.01, 122.41, 67.66, 48.33, 44.98, 32.60, 23.50. TOF MS (ASAP⁺) (m/z): $[\text{M} + \text{H}]^+$ calc'd for C₁₄H₂₃N₂OS 267.1531; found 267.1540

O-(2-(Dimethylamino)ethyl) (3-chlorophenyl)carbamothioate (**3-CIPhTC**)

Faint yellow powder, 331 mg (72%) $R_f = 0.51$ (10% MeOH in DCM)

^1H NMR (500 MHz, DMSO- d_6) δ : 7.72 (s, 1 H), 7.45 (s, 1 H), 7.34 (t, $J = 8.1$ Hz, 1 H), 7.18 (d, $J = 7.9$ Hz, 1 H), 4.57 (t, $J = 5.6$ Hz, 2 H), 2.65 (t, $J = 5.6$ Hz, 2 H), 2.24 (s, 6 H). $^{13}\text{C}\{^1\text{H}\}$ NMR (126 MHz, DMSO- d_6) δ : 187.46, 139.36, 132.70, 129.88, 124.09, 121.49, 120.14, 68.03, 56.71, 44.90. TOF MS (ASAP⁺) (m/z): $[\text{M} + \text{H}]^+$ calc'd for C₁₁H₁₆ClN₂OS 259.0672; found 259.0681

O-(2-(Dimethylamino)ethyl) (4-fluorophenyl)carbamothioate (**4-FPhTC**)

Yellow oil, 324 mg (68%) $R_f = 0.34$ (5% MeOH in DCM)

^1H NMR (500 MHz, DMSO- d_6) δ : 10.92 (s, 1 H), 7.52 (s, 2 H), 7.14 (t, $J = 8.9$ Hz, 2 H), 4.55 (t, $J = 5.7$ Hz, 2 H), 2.64 (t, $J = 5.7$ Hz, 2 H), 2.22 (s, 6 H). ^{19}F NMR (471 MHz, DMSO- d_6) δ : -117.76. $^{13}\text{C}\{^1\text{H}\}$ NMR (126 MHz, DMSO- d_6) δ : 187.57, 158.90 (d, $J = 242.2$ Hz), 134.34, 124.29, 114.88 (d, $J = 22.4$ Hz), 67.77, 56.75, 44.93. TOF MS (ASAP⁺) (m/z): $[\text{M} + \text{H}]^+$ calc'd for C₁₁H₁₆FN₂OS 243.0967; found 243.0952

O-(2-(Dimethylamino)ethyl) ethylcarbamothioate (**EtTC**)

Yellow oil, 805 mg (80%) $R_f = 0.20$ (5% MeOH in DCM)

^1H NMR (500 MHz, DMSO- d^6) δ : 8.95 (s, 1H), 4.42 (t, $J = 5.8$ Hz, 2H), 3.39 (p, $J = 7.0$ Hz, 2H), 2.55 (t, $J = 5.8$ Hz, 2H), 2.20 (s, 6H), 1.10 (t, $J = 7.3$ Hz, 3H). ^{13}C NMR (500 MHz, DMSO- d^6) δ : 189.01, 66.60, 57.05, 44.99, 36.95, 13.06 TOF MS (ASAP⁺) (m/z): [M + H]⁺ calc'd for C₇H₁₇N₂OS 177.1062; found 177.1048

O-(2-(Dimethylamino)ethyl) isopropylcarbamothioate (**ⁱPrTC**)

Yellow oil, 354 mg (64%) $R_f = 0.46$ (5% MeOH in DCM)

^1H NMR (500 MHz, DMSO- d^6) δ : 8.87 (s, 1H), 4.41 (t, $J = 5.8$ Hz, 2H), 4.20 (m, $J = 6.7$ Hz, 1H), 2.56 (t, $J = 5.9$ Hz, 2H), 2.20 (s, 6H), 1.13 (d, $J = 6.6$ Hz, 6H) ^{13}C NMR (500 MHz, DMSO- d^6) δ : 187.95, 66.40, 57.06, 46.38, 44.98, 20.99 TOF MS (ASAP⁺) (m/z): [M + H]⁺ calc'd for C₈H₁₉N₂OS 191.1218; found 191.1206

O-(2-(Dimethylamino)ethyl) *tert*-butylcarbamothioate (**^tBuTC**)

Yellow oil, 418 mg (47%) $R_f = 0.41$ (5% MeOH in DCM)

^1H NMR (500 MHz, DMSO- d^6) δ : 8.50 (s, 1H), 4.48 (t, $J = 5.9$ Hz, 2H), 2.59 (t, $J = 5.8$ Hz, 2H), 2.20 (s, 6H), 1.29 (s, 9H) ^{13}C NMR (500 MHz, DMSO- d^6) δ : 188.75, 67.86, 57.07, 53.50, 45.00, 28.71 TOF MS (ASAP⁺) (m/z): [M + H]⁺ calc'd for C₉H₂₁N₂OS 205.1375; found 205.1363

General procedure for the synthesis of dithiasuccinoyls

This procedure has been modified from a previous report.²¹⁸

To a flame-dried round bottom flask under N₂, chlorocarbonylsulfonyl chloride (1.0 equiv) was added to anhydrous DCM (20 mL). In a separate vial, the desired thiocarbamate (1.0 equiv) was dissolved in anhydrous DCM (1 mL) and added dropwise to the reaction. The reaction mixture was stirred at room temperature for 1 h, after which it was quenched with 1 M HCl (15 mL). The organic layer was separated and washed with deionized water (2×20 mL) and brine (1×20 mL). The resultant solution was dried over MgSO₄ and concentrated under reduced pressure. The desired product obtained by purification via preparative thin layer chromatography.

4-Phenyl-1,2,4-dithiazolidine-3,5-dione (**PhDTS**)

White solid, 70 mg (49%) R_f = 0.43 (40% Hexanes in DCM)

¹H NMR (500 MHz, CD₃CN) δ : 7.60 – 7.47 (m, 3 H), 7.42 – 7.26 (m, 2 H). ¹³C NMR (126 MHz, CD₃CN) δ : 169.01, 136.01, 130.93, 130.68, 129.04. TOF MS (ASAP⁺) (m/z): [M + H]⁺ calc'd for C₈H₆NO₂S₂ 211.9840; found 211.9842

4-(4-(*tert*-Butyl)phenyl)-1,2,4-dithiazolidine-3,5-dione (**4-^tBuPhDTS**)

White powder, 70 mg (41%) R_f = 0.42 (1:1 Hexanes/DCM)

¹H NMR (500 MHz, CD₃CN) δ : 7.60 (d, J = 8.7 Hz, 2 H), 7.27 (d, J = 8.7 Hz, 2 H), 1.35 (s, 9 H). ¹³C{¹H} NMR (126 MHz, CD₃CN) δ : 169.08, 154.25, 133.42, 128.57, 127.69, 35.55, 31.40. TOF MS (ASAP⁺) (m/z): [M + H]⁺ calc'd for C₁₂H₁₄NO₂S₂ 268.0466; found 268.0478

4-(3-Fluorophenyl)-1,2,4-dithiazolidine-3,5-dione (**3-FPhDTS**)

White solid, 80 mg (56%) $R_f = 0.28$ (1:1 Hexanes:DCM)

^1H NMR (500 MHz, CD_3CN) δ : 7.58 (td, $J = 8.2, 6.2$ Hz, 1 H), 7.30 (tdd, $J = 8.6, 2.6, 0.9$ Hz, 1 H), 7.22 (ddd, $J = 8.0, 2.0, 0.9$ Hz, 1 H), 7.18 (dt, $J = 9.3, 2.3$ Hz, 1 H). ^{19}F NMR (471 MHz, CD_3CN) δ -112.52 (td, $J = 8.9, 6.2$ Hz). $^{13}\text{C}\{^1\text{H}\}$ NMR (126 MHz, CD_3CN) δ : 168.74, 164.59, 162.63, 137.05 (d, $J = 10.5$ Hz), 132.18 (d, $J = 9.0$ Hz), 125.32 (d, $J = 3.3$ Hz), 117.98 (d, $J = 21.1$ Hz), 116.51 (d, $J = 24.5$ Hz). TOF MS (ASAP⁺) (m/z): $[\text{M} + \text{H}]^+$ calc'd for $\text{C}_8\text{H}_5\text{FNO}_2\text{S}_2$ 229.9746; found 229.9728

4-(*m*-Tolyl)-1,2,4-dithiazolidine-3,5-dione (**3-MePhDTS**)

White solid, 70 mg (46%) $R_f = 0.40$ (1:1 Hexanes/DCM)

^1H NMR (500 MHz, CD_3CN) δ : 7.43 (t, $J = 7.8$ Hz, 1 H), 7.35 (d, $J = 7.7$ Hz, 1 H), 7.21–7.09 (m, 2 H), 2.39 (s, 3 H). $^{13}\text{C}\{^1\text{H}\}$ NMR (126 MHz, CD_3CN) δ : 168.99, 141.06, 135.99, 131.62, 130.50, 129.41, 126.02, 21.25. TOF MS (ASAP⁺) (m/z): $[\text{M} + \text{H}]^+$ calc'd for $\text{C}_9\text{H}_8\text{NO}_2\text{S}_2$ 225.9996; found 225.9988

4-(4-Isopropylphenyl)-1,2,4-dithiazolidine-3,5-dione (**4-ⁱPrPhDTS**)

White solid, 20 mg (14%) $R_f = 0.37$ (1:1 Hexanes:DCM)

^1H NMR (500 MHz, CD_3CN) δ : 7.43 (d, $J = 8.3$ Hz, 2 H), 7.26 (d, $J = 8.5$ Hz, 2 H), 3.00 (hept, $J = 6.9$ Hz, 1 H), 1.27 (d, $J = 6.9$ Hz, 6 H). $^{13}\text{C}\{^1\text{H}\}$ NMR (126 MHz, CD_3CN) δ : 169.08, 152.08, 133.67, 128.92, 128.68, 34.72, 24.08. TOF MS (ASAP⁺) (m/z): $[\text{M} + \text{H}]^+$ calc'd for $\text{C}_{11}\text{H}_{12}\text{NO}_2\text{S}_2$ 254.0309; found 254.0316

4-(3-Chlorophenyl)-1,2,4-dithiazolidine-3,5-dione (**3-CIPhDTS**)

White solid, 60 mg (42%) $R_f = 0.28$ (1:1 Hexanes/DCM)

^1H NMR (500 MHz, CD_3CN) δ : 7.58 – 7.52 (m, 2 H), 7.45 – 7.38 (m, 1 H), 7.37 – 7.28 (m, 1 H). $^{13}\text{C}\{^1\text{H}\}$ NMR (126 MHz, CD_3CN) δ : 168.74, 136.94, 135.32, 132.05, 131.08, 129.15, 127.81. TOF MS (ASAP⁺) (m/z): $[\text{M} + \text{H}]^+$ calc'd for $\text{C}_8\text{H}_5\text{ClNO}_2\text{S}_2$ 245.9450; found 245.9432

4-(4-Fluorophenyl)-1,2,4-dithiazolidine-3,5-dione (**4-FPhDTS**)

White solid, 71 mg (53%) $R_f = 0.32$ (3:2 DCM/Hexanes)

^1H NMR (500 MHz, CD_3CN) δ : 7.43 – 7.35 (m, 2 H), 7.33 – 7.24 (m, 2 H). ^{19}F NMR (471 MHz, CD_3CN) δ : -112.38 – -112.54 (m). $^{13}\text{C}\{^1\text{H}\}$ NMR (126 MHz, CD_3CN) δ : 168.99, 163.94 (d, $J = 248.0$ Hz), 131.94 (d, $J = 3.2$ Hz), 131.29 (d, $J = 9.1$ Hz), 117.58 (d, $J = 23.6$ Hz). TOF MS (ASAP⁺) (m/z): $[\text{M} + \text{H}]^+$ calc'd for $\text{C}_8\text{H}_5\text{FNO}_2\text{S}_2$ 229.9746; found 229.9752

4-Ethyl-1,2,3-dithiazolidine-3,5-dione (**EtDTS**)

Yellow oil, 54 mg (35%) $R_f = 0.33$ (50% DCM in hexanes)

^1H NMR (500 MHz, CDCl_3) δ : 3.85 (q, $J = 7.1$ Hz, 2H), 1.27 (t, $J = 7.1$ Hz, 3H) ^{13}C NMR (500 MHz, CDCl_3) δ : 167.54, 41.76, 12.88 TOF MS (ASAP⁺) (m/z): $[\text{M} + \text{H}]^+$ calc'd for $\text{C}_4\text{H}_6\text{NO}_2\text{S}_2$ 163.9831; found 163.9840

4-Isopropyl-1,2,3-dithiazolidine-3,5-dione (**ⁱPrDTS**)

White solid, 32 mg (22%) $R_f = 0.42$ (50% DCM in hexanes)

^1H NMR (500 MHz, CDCl_3) δ : 4.68 (hept, $J = 6.9$ Hz, 1H), 1.47 (d, $J = 6.9$ Hz, 6H) ^{13}C

NMR (500 MHz, CDCl_3) δ : 167.70, 52.19, 18.84 TOF MS (ASAP⁺) (m/z): $[\text{M} + \text{H}]^+$ calc'd for $\text{C}_5\text{H}_8\text{NO}_2\text{S}_2$ 177.9996; found 177.9985

4-(*tert*-Butyl)-1,2,3-dithiazolidine-3,5-dione (**^tBuDTS**)

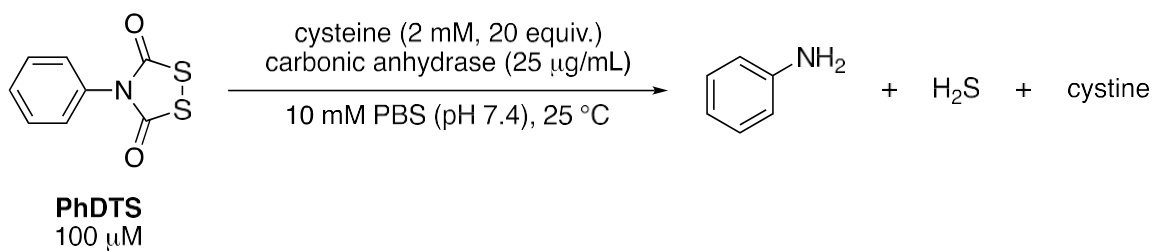
White solid, 35 mg (21%) $R_f = 0.50$ (50% DCM in hexanes)

^1H NMR (500 MHz, CDCl_3) δ : 1.68 (s, 9H) ^{13}C NMR (500 MHz, CDCl_3) δ : 168.73, 67.31,

28.46. TOF MS (ASAP⁺) (m/z): $[\text{M} + \text{H}]^+$ calc'd for $\text{C}_6\text{H}_{10}\text{NO}_2\text{S}_2$ 192.0153; found

192.0099

HPLC Reaction Analysis



Scheme 6.2 Reaction analysis products of PhDTS in the presence of cysteine

To a 20 mL solution of 10 mM PBS (pH 7.4) containing 2 mM L-cysteine, 20 mL of 100 mM **PhDTS** in MeCN was added and stirred at room temperature. After 1 h, 1.0 mL reaction aliquot was analyzed by HPLC. HPLC analysis was performed on an Agilent 1260 HPLC instrument with a Poroshell 120 EC-C18 4.6x100 mm column and monitored at 230

nm. Solvent A: Solvent A: 95% H₂O, 5% MeOH, Solvent B: 100% MeCN. Gradient: 35% Solvent A/65% Solvent B for 2 min. Change to 100% Solvent B over 4 min and hold for 6.5 min. Change to 35% Solvent A/65% Solvent B over 0.5 min and hold for 4.5 min. Flow Rate: 0.5 mL/min, 2 μ L injection.

CA Inhibition Experiment

A 5 mM stock solution of acetazolamide (AAA) in DMSO was prepared in an N₂-filled glovebox immediately prior to use. To 20 mL solutions containing 10 mM PBS (pH 7.4), 20 μ L of 5 mM AAA and 50 μ L of 10 mg/mL CA were added for final concentrations of 5 μ M and 25 μ g/mL respectively. While stirring, solutions were allowed to thermally equilibrate in a heating block set at 25 $^{\circ}$ C for approximately 20-30 min. To begin the experiment, 20 μ L of 25 mM **PhDTS** was added for a final concentration of 25 μ M. At set time points after the addition of donor, 0.5 mL reaction aliquots were added to the methylene blue cocktail solutions and incubated for 1 h at room temperature shielded from light. Absorbance values at 670 nm were measured 1 h after addition of reaction aliquot.

Zn²⁺-Mediated Hydrolysis Experiment

A 5 mM stock solution Zn(OAc)₂ in PBS was prepared in an N₂-filled glovebox immediately prior to use. To 20 mL solutions containing 10 mM PBS (pH 7.4), 20 μ L of 5 mM Zn(OAc)₂ was added for a final concentration of 5 μ M. While stirring, solutions were allowed to thermally equilibrate in a heating block set at 25 $^{\circ}$ C for approximately 20-30 min. To begin the experiment, 20 μ L of 25 mM **PhDTS** was added for a final concentration of 25 μ M. At set time points after the addition of donor, 500 μ L reaction aliquots were

added to the methylene blue cocktail solutions and incubated for 1 h at room temperature shielded from light. Absorbance values at 670 nm were measured 1 h after addition of reaction aliquot.

CHAPTER VII

COLORIMETRIC AND FLUORESCENT DETECTION OF CARBONYL SULFIDE

This chapter includes unpublished and coauthored material. This manuscript was written by Matthew M. Cerda with editorial assistance from Professor Michael D. Pluth. The project in this chapter was conceived by Matthew M. Cerda. The experimental work in this chapter was performed by Matthew M. Cerda, Julia M. Fehr, and Dr. Tobias J. Sherbow.

7.1 Introduction

Carbonyl sulfide (COS) is an important organosulfur species in the global sulfur cycle²²⁴ that is generated during the burning of biomass²²⁵ combustion of biofuels,²²⁶ and in different production processes in the pulp and paper industries.²²⁷ In addition, geochemical production of COS arises from volcanic activity, emission from hot springs, and deep sea thermal vents.²²⁸ Although the chemical properties and reactivity of COS have long been established,²²⁹ the biological implications of COS have only recently begun to emerge.¹⁰⁰ As an example, treatment of α -amino acids with COS under prebiotic reaction conditions results in the formation of dipeptides, demonstrating the potential role of COS in origin of life chemical ligation.²³⁰ Aligned with our interests in studying biological reactive sulfur species,¹⁷² our group has recently advanced the use of COS-releasing compounds for the controlled release of hydrogen sulfide (H₂S) due to the rapid catalyzed hydrolysis of COS by carbonic anhydrase, a ubiquitous metalloenzyme.²⁰⁴

Although enzymatic pathways for endogenous COS production in mammals remain undiscovered, COS has been detected in porcine cardiovascular tissues²³¹ and exhaled breath from cystic fibrosis patients²³² by using gas chromatography mass spectrometry (GC-MS). More recently, in our investigation of esterase-sensitive COS-based H₂S donors in human lung epithelial (BEAS2B) cells, we observed COS-dependent inhibition of mitochondrial bioenergetics. This finding suggests that COS may possess biological activities and properties akin to H₂S.²⁰ As the potential roles of COS in biological systems and investigations into COS releasing compounds expand, a currently unmet need to further such investigations is the development of minimally invasive and sensitive methods for COS detection. Based on the significant impacts of colorimetric and fluorescent activity-based probes for the detection of reactive sulfur species (RSS), such as cysteine, reduced glutathione, and H₂S, we envisioned that analogous platforms could be developed for COS detection.²³³

Based on the electrophilicity and structural similarities between carbon dioxide (CO₂), carbon disulfide (CS₂), and COS,²²⁹ we anticipated that a nucleophilic platform could be used to develop chemical tools for COS detection. For example, *N*-heterocyclic carbenes can insert into heterocumulenes, which has been demonstrated separately for CO₂,²³⁴ CS₂,²³⁵ and COS,²³⁶ respectively. Bridging the gap to heterocumulene detection, the vast majority of work has aimed at the spectroscopic²³⁷ or electrochemical detection²³⁸ of CO₂. Of these reported methods, we were drawn to the prior use of a fluorescent, colorimetric benzobisimidazolium probe (**TBBI**) for CO₂ detection.²³⁹ In this system, treatment of **TBBI** with tetra-*n*-butylammonium fluoride (TBAF) produces a “carbene-like” intermediate²⁴⁰ that readily reacts with CO₂ through carbene insertion into CO₂ and

subsequent hydrolysis to form bicarbonate (Figure 7.1). This reactivity was also investigated for CS₂ by ¹³C NMR spectroscopy and shown to result in the generation of an imidazolium-dithiocarboxylate betaine through carbene insertion into CS₂ (Figure 1b). Building from structural similarities between these compounds, we hypothesized the treatment of **TBBI** with COS in the presence of fluoride would provide a unique spectroscopic response for COS that would be distinguishable from that of CO₂ and CS₂. Based on this motivation, we report here the first demonstration of selective COS detection by UV-Vis and fluorescence spectroscopy.

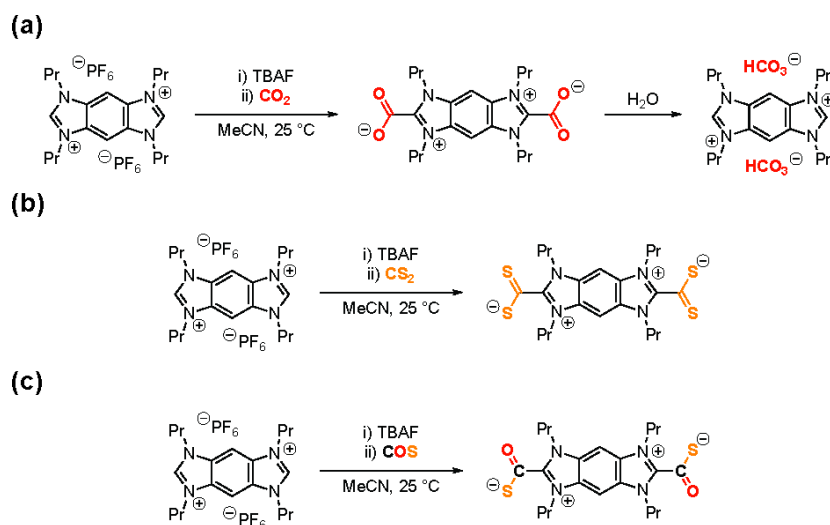


Figure 7.1 (a) Reaction of CO₂ and **TBBI** in the presence of fluoride. (b) Reaction between CS₂ and **TBBI** in the presence of fluoride. (c) Proposed reaction between COS and **TBBI** in the presence of fluoride.

7.2 Results and Discussion

One challenge when working with COS is that commercial sources often contain H₂S as a common impurity. To overcome this challenge, we have previously prepared COS through the acidic hydrolysis of KSCN using modifications of known methods (Figure 7.2a).²⁴¹ Based on the growing interest in various aspects of COS chemistry, including

delivery, organometallic chemistry, and chemical biology, we have included this method here and in the Supporting Information (Appendix G). A key requirement when preparing COS is purification of the product, which can be accomplished by sparging through aqueous KOH, aniline in anhydrous ethanol, ice water, and neat H₂SO₄. The purified COS can be collected and stored in a gas storage flask or added directly into a solution or NMR tube for use as a reactant or reagent (Figure 7.2b). COS has a characteristic ¹³C chemical shift at $\delta = 154.3$ ppm (CD₃CN) and IR stretch at 2927, 2909 cm⁻¹, which matches prior reports.²⁴²

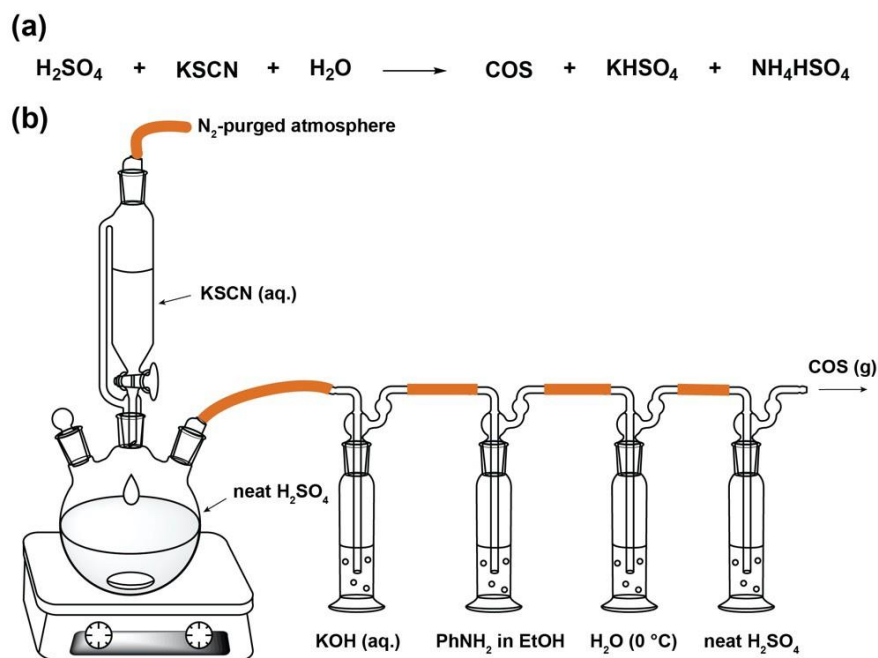


Figure 7.2 (a) Acid-mediated hydrolysis of KSCN to generate COS. (b) Schematic of laboratory-scale COS synthesis and purification.

To investigate the strategy of carbene insertion for COS detection, we prepared **TBBI**²³⁹ and monitored its reactivity toward COS in the presence of TBAF by UV-Vis spectroscopy (Figure 7.3b). The parent **TBBI** compound (15 μM in MeCN containing 1% (v/v) H₂O) has an absorption band centered at 290 nm, which shifts to 344 nm upon

addition of TBAF (6.0 equiv.). This change in absorbance is consistent with the previous report of hydrogen bond formation between the C1-H in **TBBI** and F⁻.²³⁹ Subsequent addition of COS in 0.5 mL increments resulted in a decrease in the 344 nm absorbance and concomitant increase of a new absorbance at 321 nm. We note that this observed reaction with COS did not occur if anhydrous MeCN was used, which highlights that residual H₂O is required. The new absorbance at 321 nm is unique to COS and is not observed upon reaction of **TBBI** with CO₂ or CS₂ in the presence of TBAF.

Building from this observation, we next investigated the reaction by fluorescence spectroscopy. The parent **TBBI** compound (15 μM, MeCN containing 1% (v/v) H₂O) showed negligible fluorescence when excited at 321 nm, but addition of TBAF (6.0 equiv.) resulted in the appearance of a broad emission centered at 434 nm, which we attribute to formation of the hydrogen bonded **TBBI** intermediate. Subsequent addition of COS in 0.5 mL increments led to a clean ratiometric response, with a decrease at the 434 nm emission and concomitant increase at 354 nm (Figure 7.3c). The product formed upon COS addition is persistent, unlike in the case for CO₂ in which rapid hydrolysis to bicarbonate is observed. Taken together, these results demonstrate that **TBBI** can be used to spectroscopically distinguish between CO₂, CS₂, and COS in the presence of the fluoride.

The stability and unique spectroscopic properties of product formed upon COS addition prompted us to investigate whether this **TBBI** system could be used for naked-eye optical detection of COS. The recognition of CS₂ by 10 mM **TBBI** in the presence of fluoride was previously reported to generate a color change from clear to yellow red and form an imidazolium-dithiocarboxylate betaine.²³⁹ To further investigate this reactivity, we charged series of cuvettes with 10 mM **TBBI** and 60 mM TBAF in MeCN containing 1%

CO₂ yielded a white precipitate corresponding to the bicarbonate salt of **TBBI**, whereas the cuvette containing CS₂ yielded a pale orange solution. The reaction between **TBBI** and COS yielded a teal green color and transitioned to a dark forest green upon standing for an extended period of time. These results demonstrate the unique ability of **TBBI** to serve as a versatile platform for distinct recognition of CO₂, COS, and CS₂ by naked eye detection.

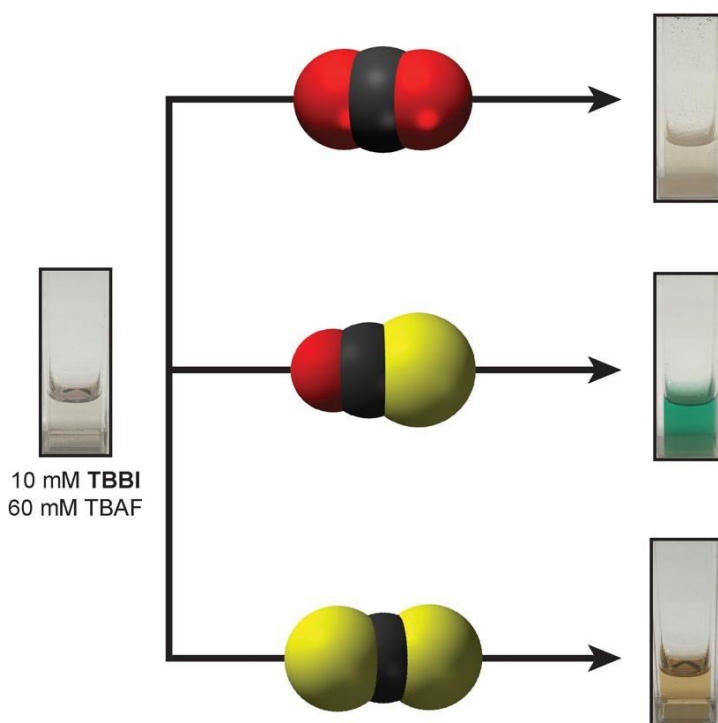


Figure 7.4 Naked-eye detection and differentiation of CO₂, CS₂, and COS using **TBBI** (10 mM) in the presence of TBAF (60 mM).

7.3 Conclusions

In summary, we have demonstrated that the **TBBI** platform can be used for the colorimetric and fluorescent detection of COS. Importantly, these spectroscopic responses for COS are distinct from those generated by CO₂ or CS₂. We view that these advances provide a first step toward developing chemical tools that can be used to investigate the growing evidence for a biological role of COS in complex systems.

7.4 Concluding Remarks

In this dissertation, I have discussed contributions to the development of chemical tools capable to generating reactive sulfur species including H₂S, COS, and persulfides in the presence of biological thiols such as cysteine and GSH. The chemical reactivity between thiocarbonyl-based compounds and free cysteine described in Chapters II and III could be extended to the development of cysteine selective probes and synthesis of dihydrothiazoles under mild reaction conditions. The basic research on H₂S release from organic polysulfides discussed in Chapters IV and V highlights the potential impact of persistence persulfides on the biological activity of organic polysulfides and merits future investigation. The chemical tools for studying COS discussed in Chapter VI and VII provide researchers with key tools to further elucidate the biological implications of COS. Overall, the development of chemical tools to study reactive sulfur species is an area of rapidly expanding research which will likely contribute to our fundamental understanding of these compounds in biology, physiology, and medicine.

7.5 Experimental Details

7.5.1 Materials and Methods

Reagents were purchased from Sigma-Aldrich, TCI, Fisher Scientific, or Combi-Blocks and used as received. Non-fritted gas washing bottles were purchased from ChemGlass (CG-1112). UV- Vis spectra were acquired on a Cary 100 spectrophotometer equipped with a Quantum Northwest TLC-42 dual cuvette temperature controller set at 25.00 ± 0.05 °C. Fluorescence spectra were obtained on a Quanta Master 40 spectrofluorometer (Photon

Technology International) equipped with a Quantum Northwest TLC-50 temperature controller set at 25.00 ± 0.05 °C.

General Procedure for UV-Vis Measurements

A septum-sealed cuvette was charged with 3.00 mL of MeCN containing 1% (v/v) deionized H₂O and 20 μ L of 2.5 mM **TBBI** in anhydrous MeCN for a final concentration of 15 μ M **TBBI**. An initial UV-Vis absorbance spectrum was recorded (250-450 nm). A 6.75 mM solution of TBAF in anhydrous MeCN was prepared via dilution of 1.0 M TBAF in THF and 40 μ L was added to the cuvette solution for a final concentration of 90 μ M TBAF (6.0 equiv.) Another UV-Vis absorbance spectrum was recorded (250-450 nm). A 5.0 mL gastight Hamilton syringe was charged with COS (g) and added in 0.5 mL increments to the cuvette solution. A UV-Vis absorbance spectrum was recorded (250-450 nm) between additions.

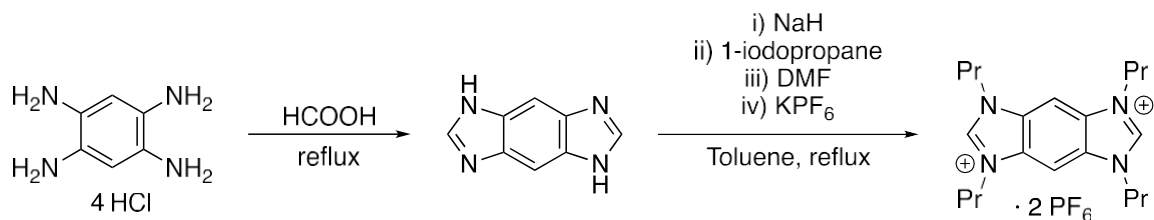
General Procedure for Fluorescent Intensity Measurements

A septum-sealed cuvette was charged with 3.00 mL of MeCN containing 1% (v/v) deionized H₂O and 20 μ L of 2.5 mM **TBBI** in anhydrous MeCN for a final concentration of 15 μ M **TBBI**. An initial fluorescence spectrum was recorded ($\lambda_{\text{ex}} = 321$ nm, $\lambda_{\text{em}} = 330$ -600 nm). A 6.75 mM solution of TBAF in anhydrous MeCN was prepared via dilution of 1.0 M TBAF in THF and 40 μ L was added to the cuvette solution for a final concentration of 90 μ M TBAF (6.0 equiv.) Another fluorescence spectrum was recorded ($\lambda_{\text{ex}} = 321$ nm, $\lambda_{\text{em}} = 330$ -600 nm). A 5.0 mL gastight Hamilton syringe was charged with COS (g) and

added in 0.5 mL increments to the cuvette solution. A fluorescence measurement was recorded ($\lambda_{\text{ex}} = 321 \text{ nm}$, $\lambda_{\text{em}} = 330\text{-}600 \text{ nm}$) between additions.

7.5.2 Synthesis of **TBBI**

This compound was prepared as previously described.²³⁹



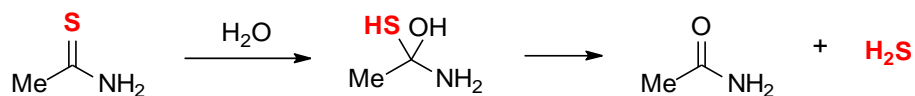
Scheme 7.1 Synthesis of **TBBI**

APPENDIX A

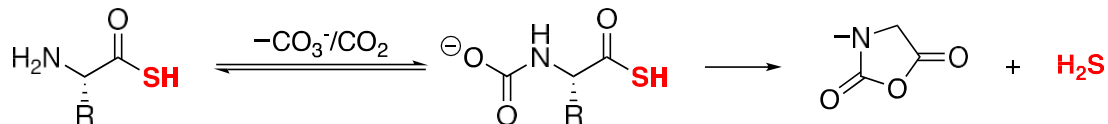
SUPPLEMENTARY INFORMATION FOR CHAPTER I

Appendix A is the supplementary appendix for Chapter I of this dissertation. It includes the general H₂S-releasing mechanisms of the various compounds reported in Chapter I.

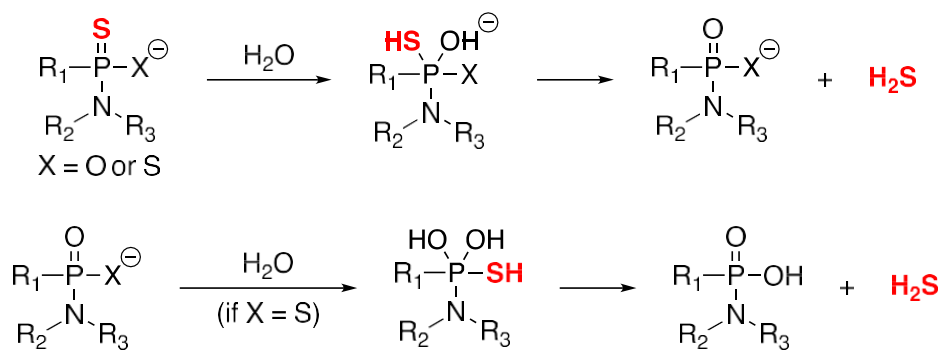
Hydrolysis-Activated Donors



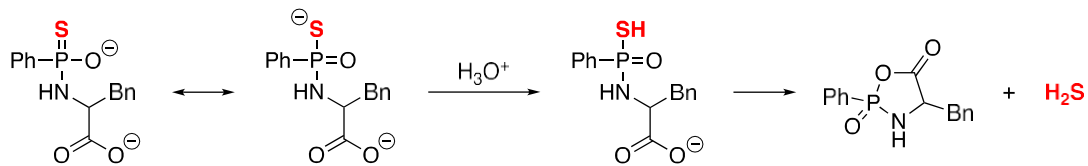
Scheme A.1 Mechanism of hydrolysis-mediated H₂S release from thioacetamide



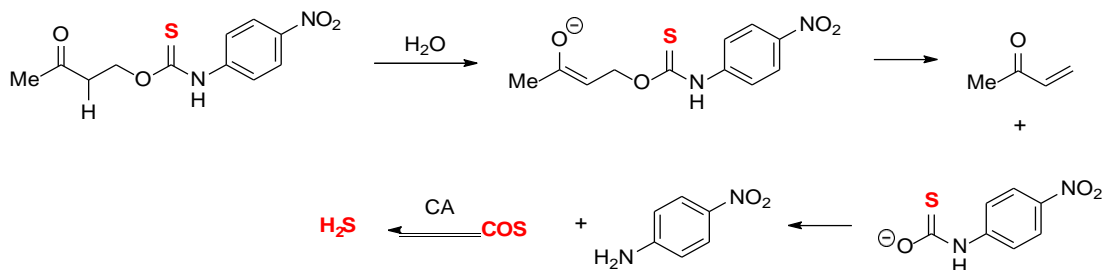
Scheme A.2 Mechanism of H₂S release from thioaminoacids (R = Me or H) in the presence of bicarbonate (HCO₃⁻)



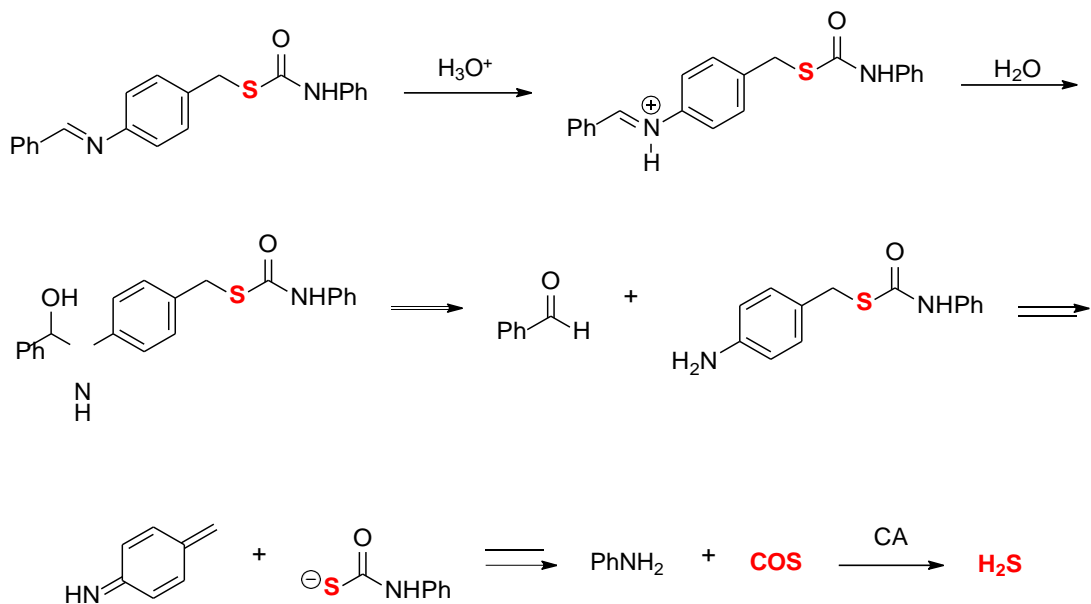
Scheme A.3 Generalized hydrolysis mechanism of H₂S release from **GY4137**, phosphorodithioates, and **FW1256**



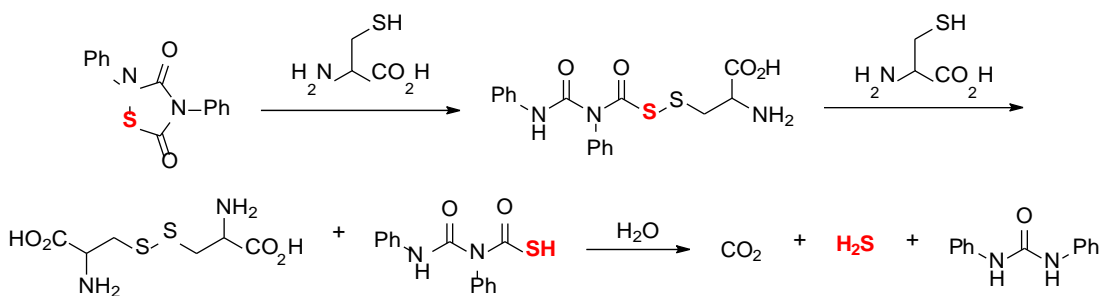
Scheme A.4 Mechanism of acid-mediated H₂S release from **JK-2**



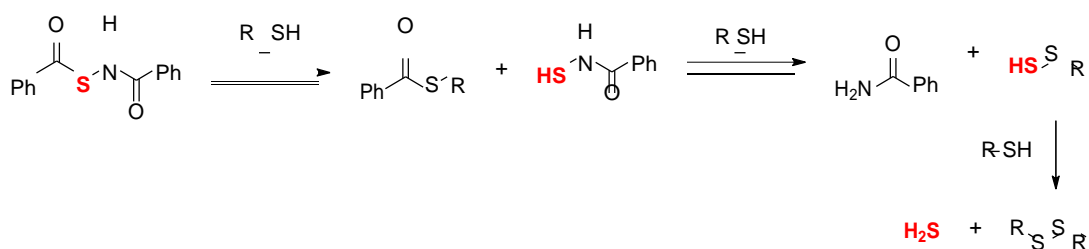
Scheme A.5 Mechanism of COS/H₂S release from γ -KetoTCM-1 in the presence of carbonic anhydrase (CA)



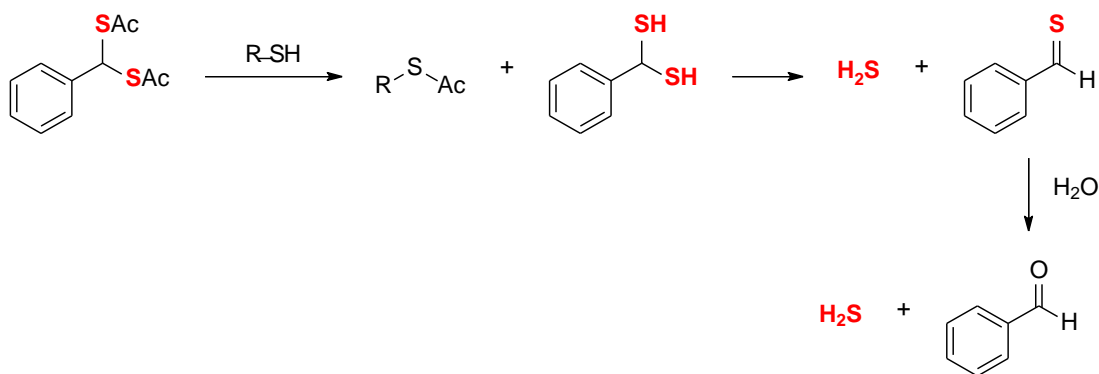
Scheme A.6 Mechanism of COS/H₂S release from **S-pHTCM** *via* imine hydrolysis in the presence of carbonic anhydrase (CA)



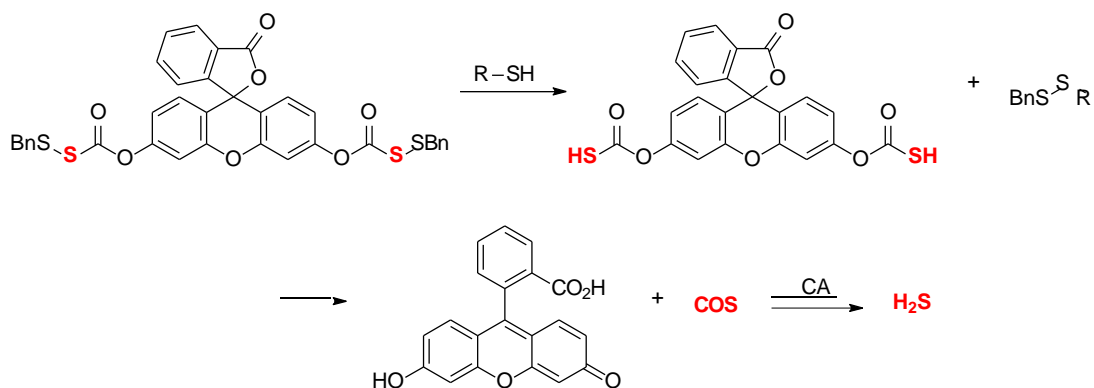
Scheme A.12 Proposed mechanism of H₂S release from 1,2,4-thiadiazolidine-3,5-diones in the presence of cysteine



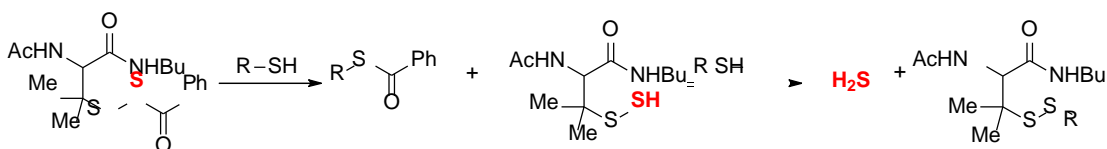
Scheme A.13 Mechanism of H₂S release from “N-mercapto donors” in the presence of thiols



Scheme A.14 Mechanism of H₂S release from acylated geminal dithiols in the presence of thiols



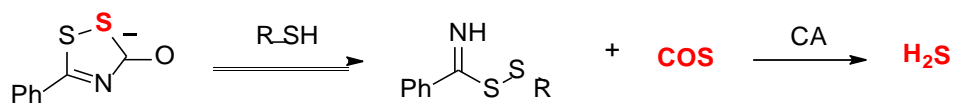
Scheme A.15 Mechanism of COS/H₂S release from **FLD-1** in the presence of thiols and carbonic anhydrase (CA)



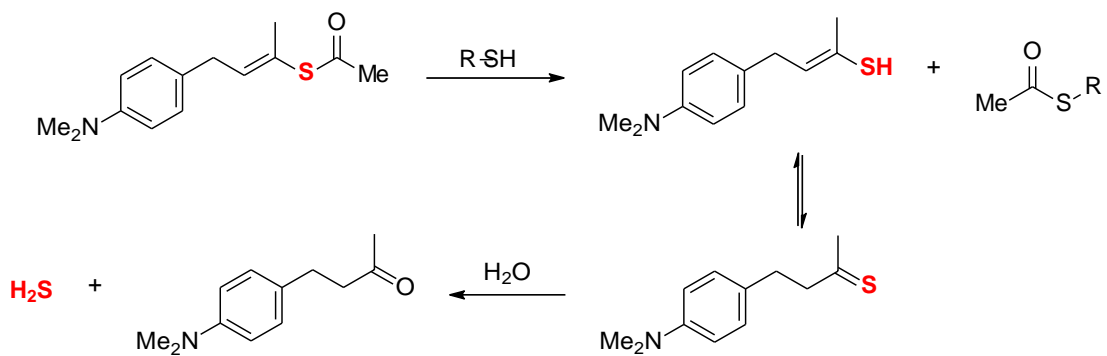
Scheme A.16 Mechanism of H₂S release from acylated persulfides in the presence of thiols



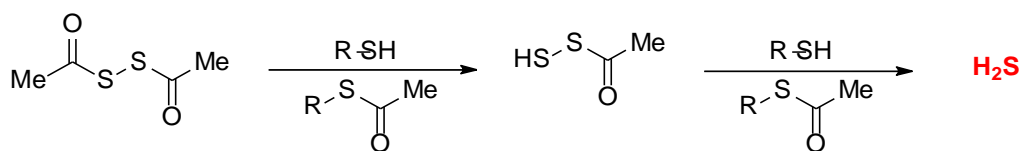
Scheme A.17 Mechanism of H₂S release from organic polysulfides including **DATS** in the presence of thiols. We note the presence of a pendant allyl group likely complicates the mechanism of H₂S release from **DATS**.



Scheme A.18 Mechanism of thiol-mediated COS/H₂S release from cyclic sulfenylthiocarbamates in the presence of carbonic anhydrase (CA)

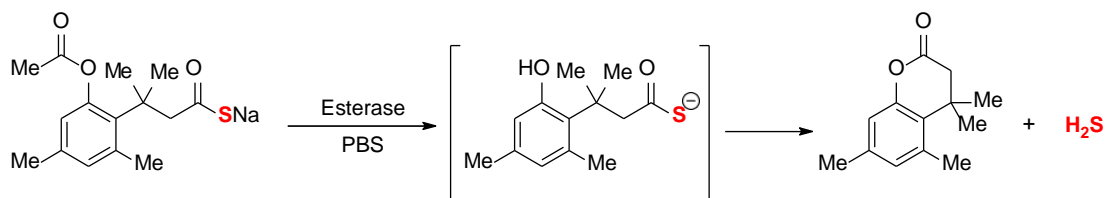


Scheme A.19 Mechanism of H₂S release from protected thioenols in the presence of thiols

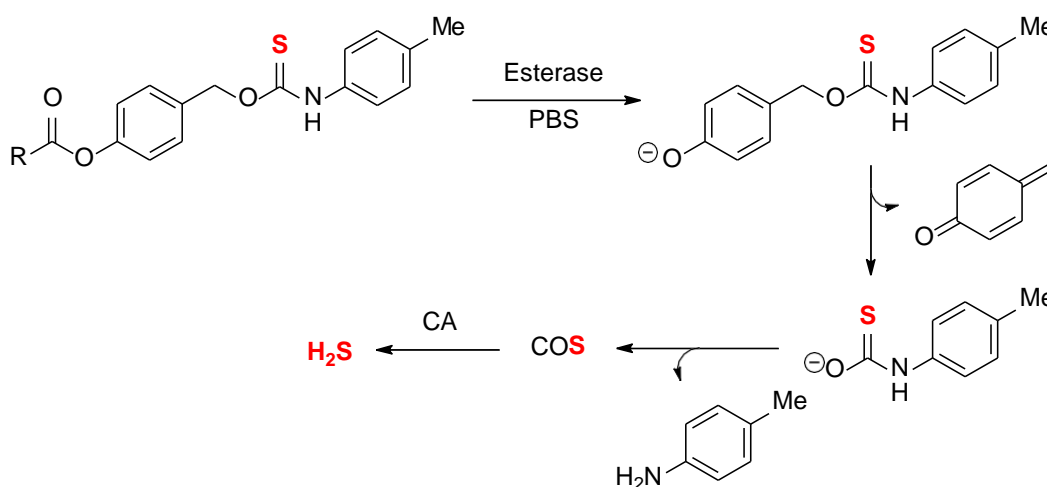


Scheme A.20 Mechanism of H₂S release from dithioperoxyanhydrides in the presence of thiols

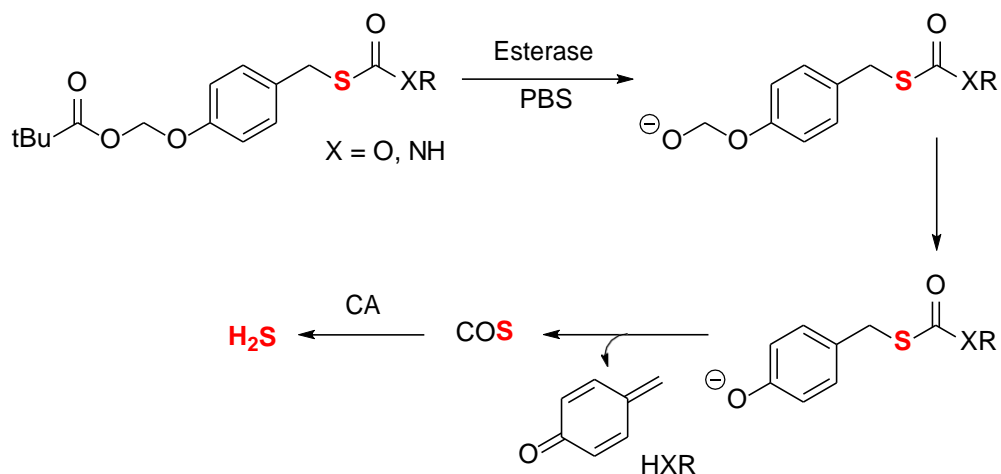
Enzyme-Activated Donors



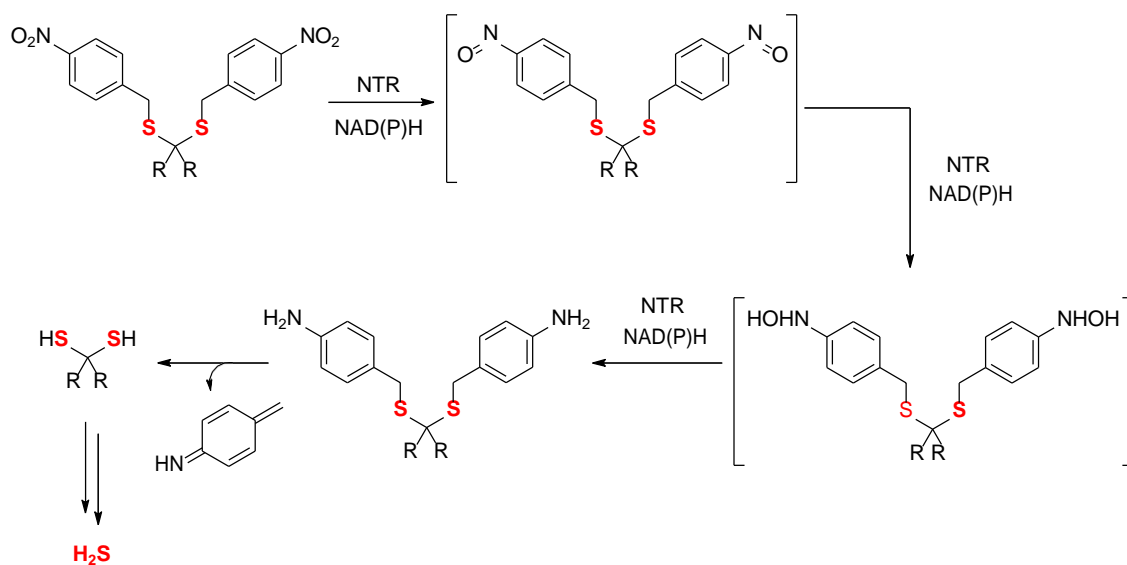
Scheme A.21 Mechanism of H₂S release from **HP-101** in the presence of esterase



Scheme A.22 Mechanism of H₂S release from **Esterase-TCM-OA** in the presence of esterase and carbonic anhydrase

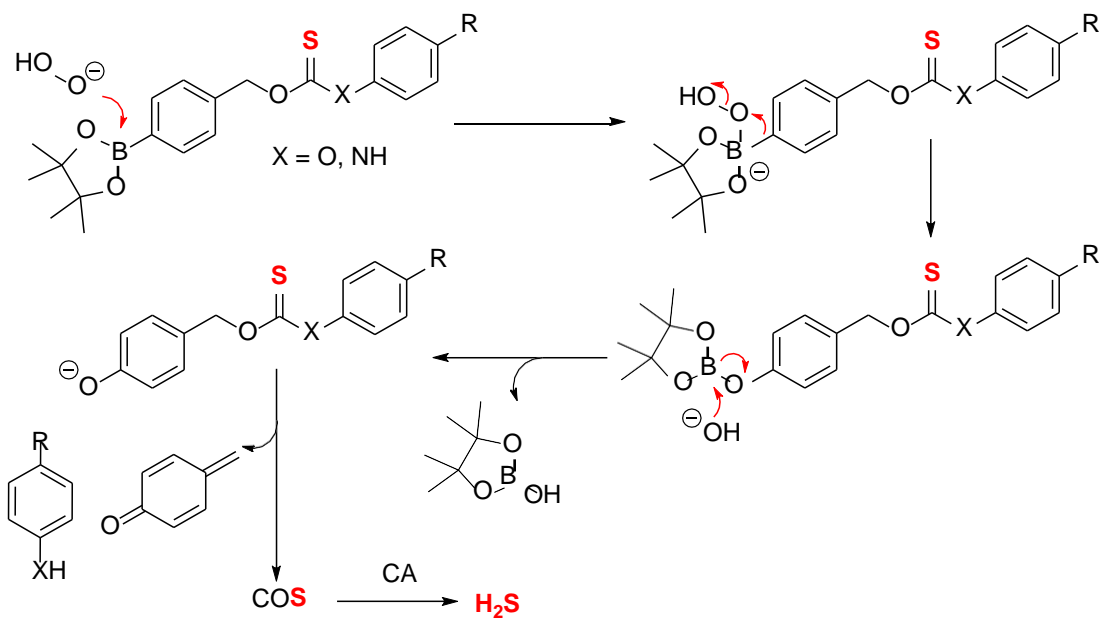


Scheme A.23 Mechanism of H₂S release from **Esterase-TCM-SA** in the presence of esterase and carbonic anhydrase



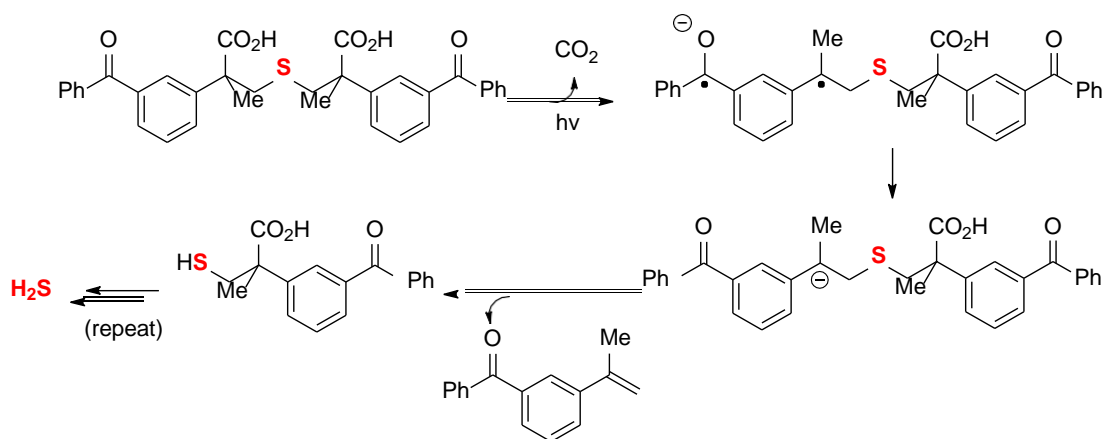
Scheme A.24 Mechanism of H₂S release from **NTR-H2S** in the presence of nitroreductase

H₂O₂-Activated Donors

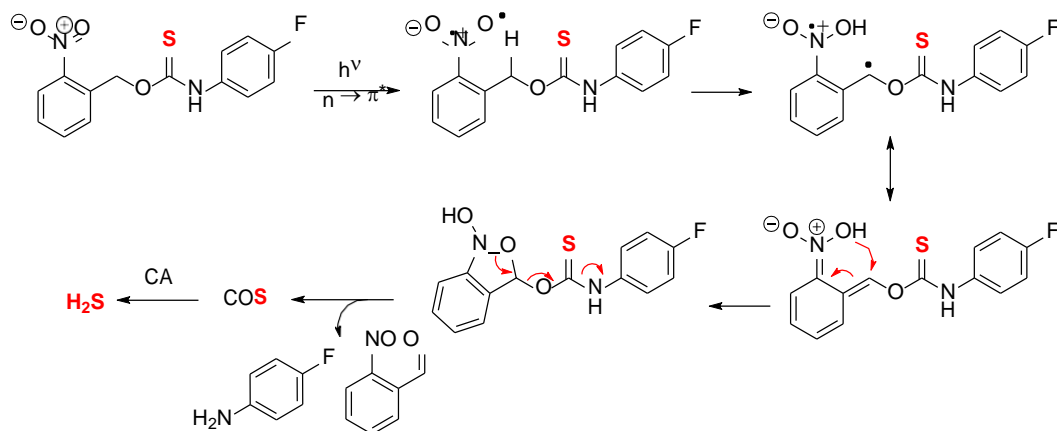


Scheme A.25 Mechanism of H₂S release from H₂O₂-triggered thiocarbamates and thiocarbonates in the presence of carbonic anhydrase

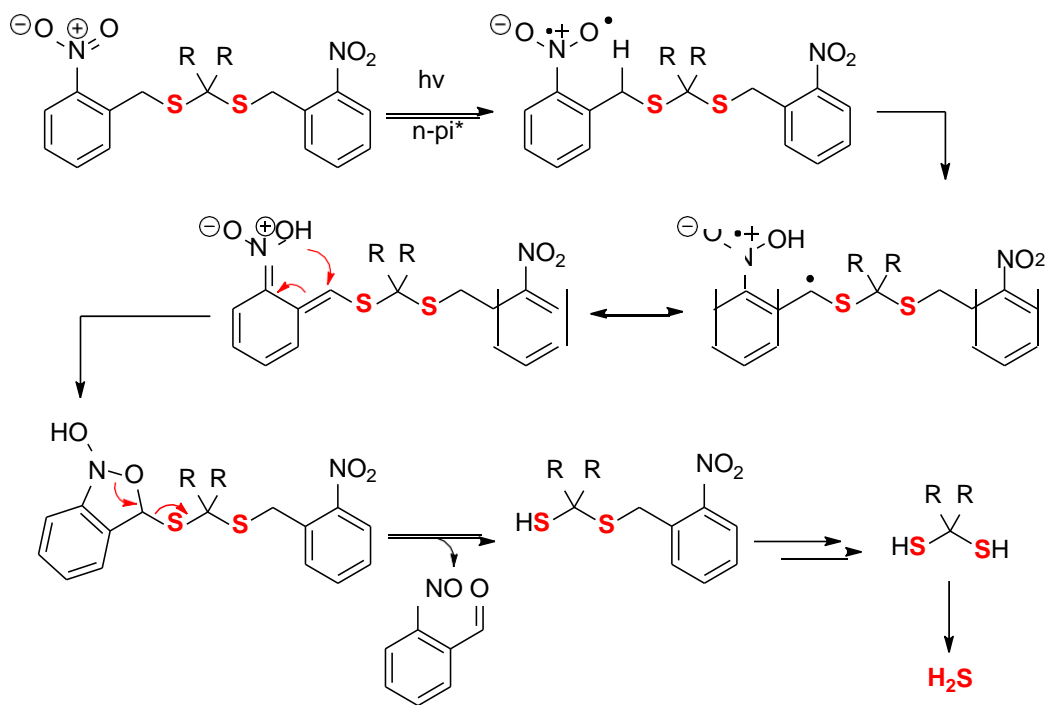
Photoactivated Donors



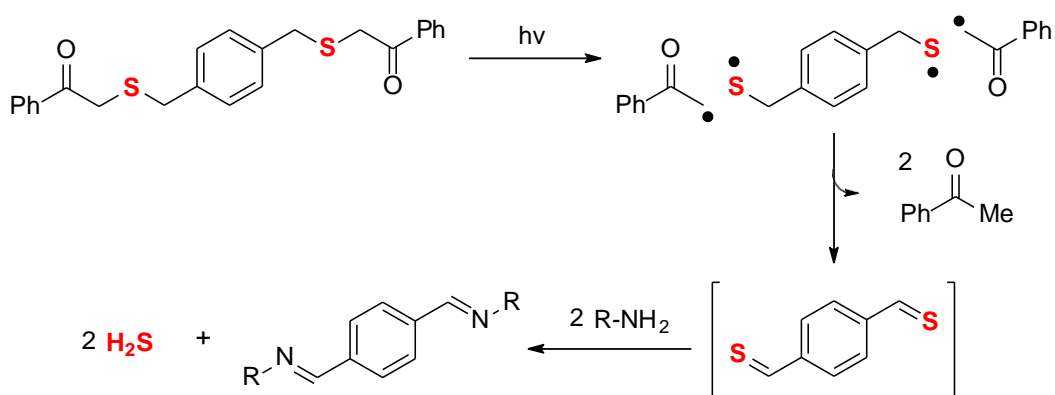
Scheme A.26 Mechanism of H_2S release from photolabile ketoprofenate-caged thioethers



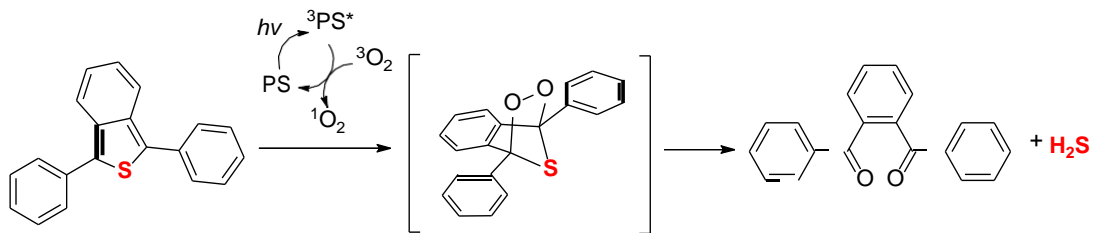
Scheme A.27 Mechanism of H_2S release from ortho-nitrophenyl thiocarbamates **PhotoTCM-1** in the presence of carbonic anhydrase



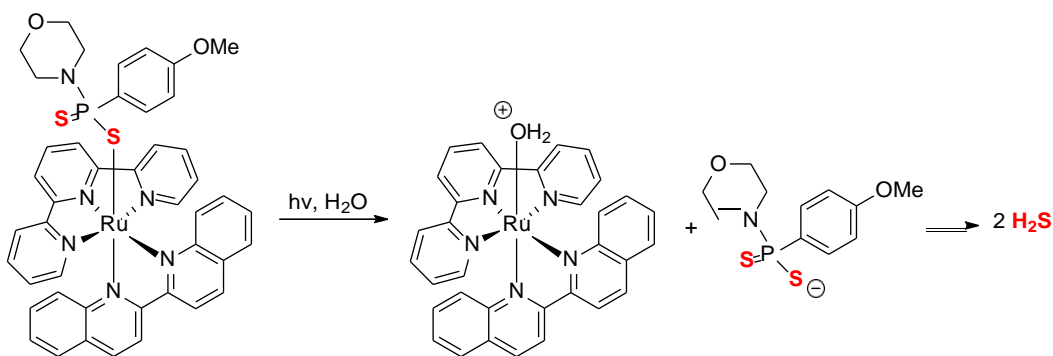
Scheme A.28 Mechanism of H₂S release from ortho-nitrophenyl caged **Photo-gem-dithiol**



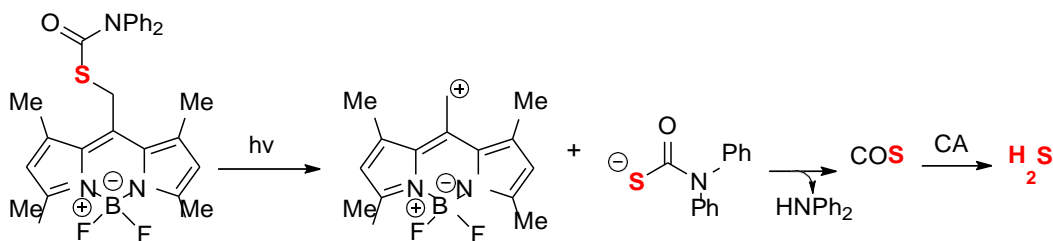
Scheme A.29 Mechanism of H₂S release from photo-caged thiobenzaldehydes in the presence of amines



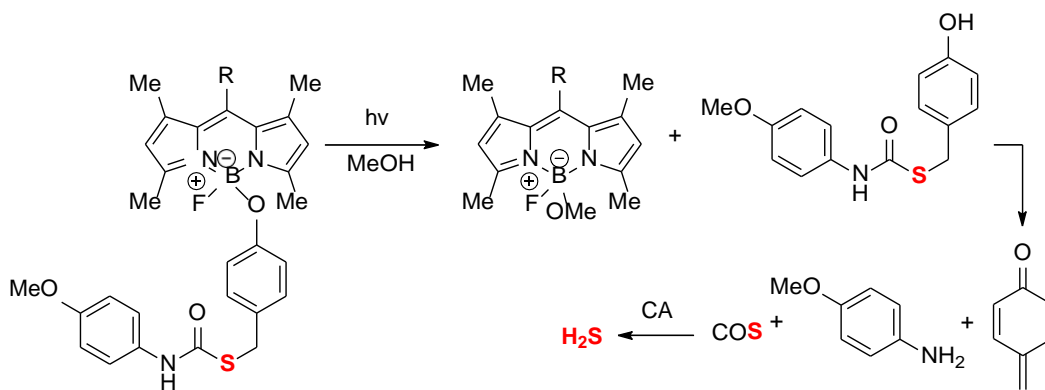
Scheme A.30 Mechanism of H_2S release from **DPBT** in the presence of a photosensitizer (PS) and oxygen. The protons in the generated H_2S originate from the water in the aqueous reaction conditions.



Scheme A.31 Mechanism of H_2S release from **Ru-GYY**



Scheme A.32 Mechanism of H_2S release from **BODIPY-TCM-2** in the presence of CA



Scheme A.33 Mechanism of H_2S release from **BODIPY-TCM-1** in the presence of CA

APPENDIX B

SUPPLEMENTARY INFORMATION FOR CHAPTER II

Appendix B is the supplementary information for Chapter II of this dissertation. It includes spectra and experimental data relevant to the content in Chapter II.

NMR Spectra

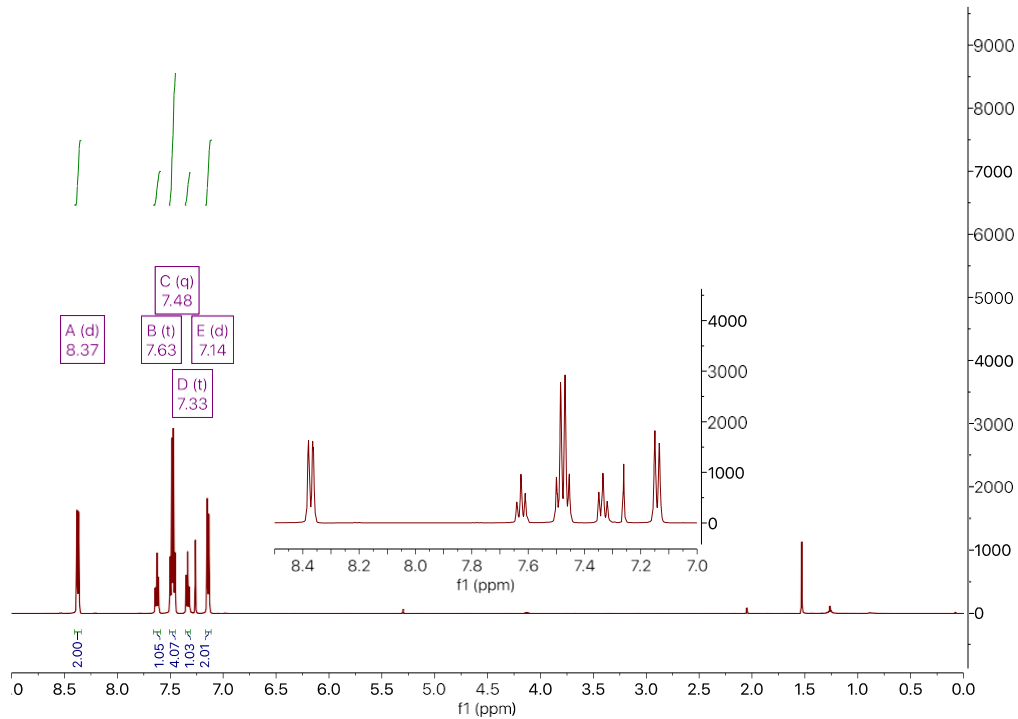


Figure B.1 ^1H NMR (500 MHz, CDCl_3) spectrum of DPTE.

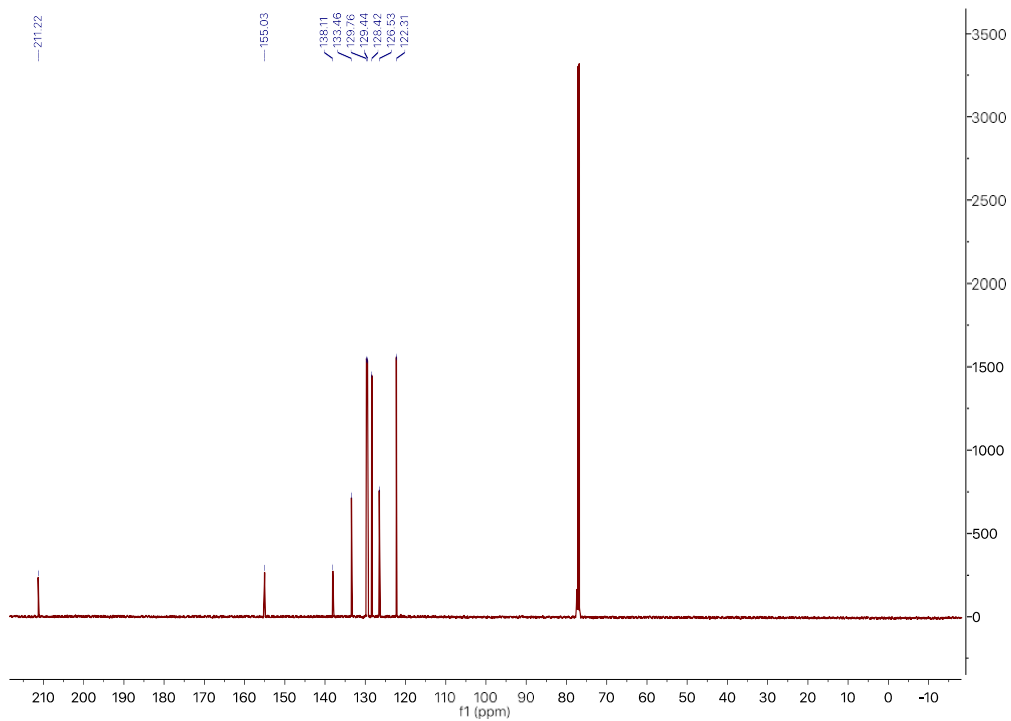


Figure B.2 $^{13}\text{C}\{^1\text{H}\}$ NMR (126 MHz, CDCl_3) spectrum of DPTE.

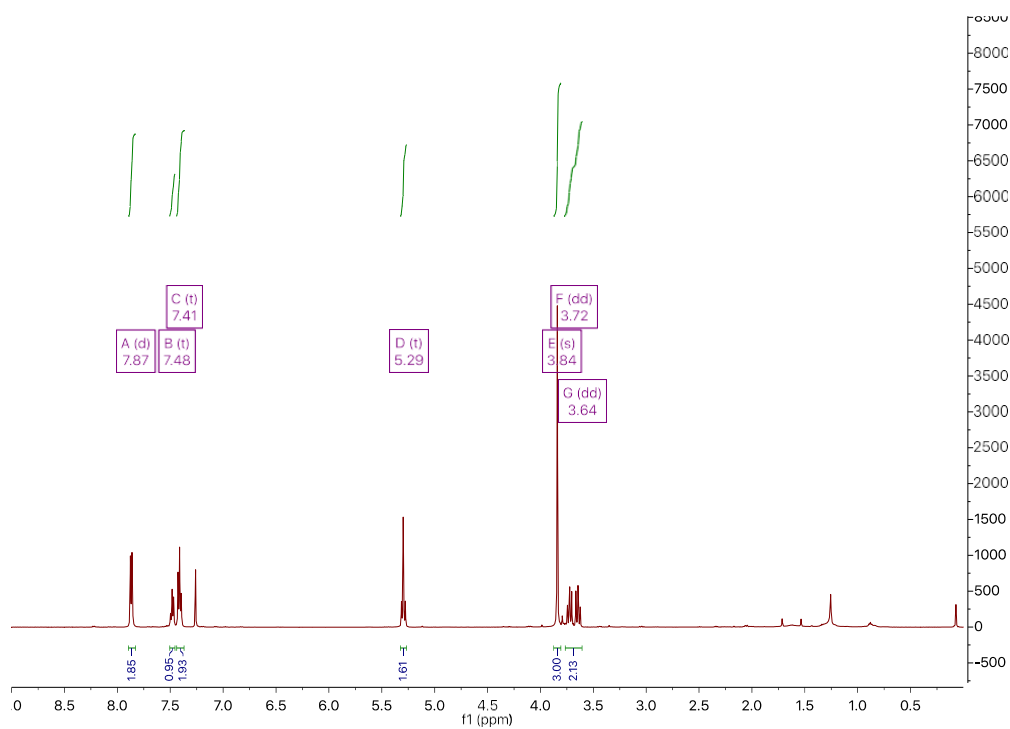


Figure B.3 ^1H NMR (500 MHz, CDCl_3) spectrum of isolated CysDHT

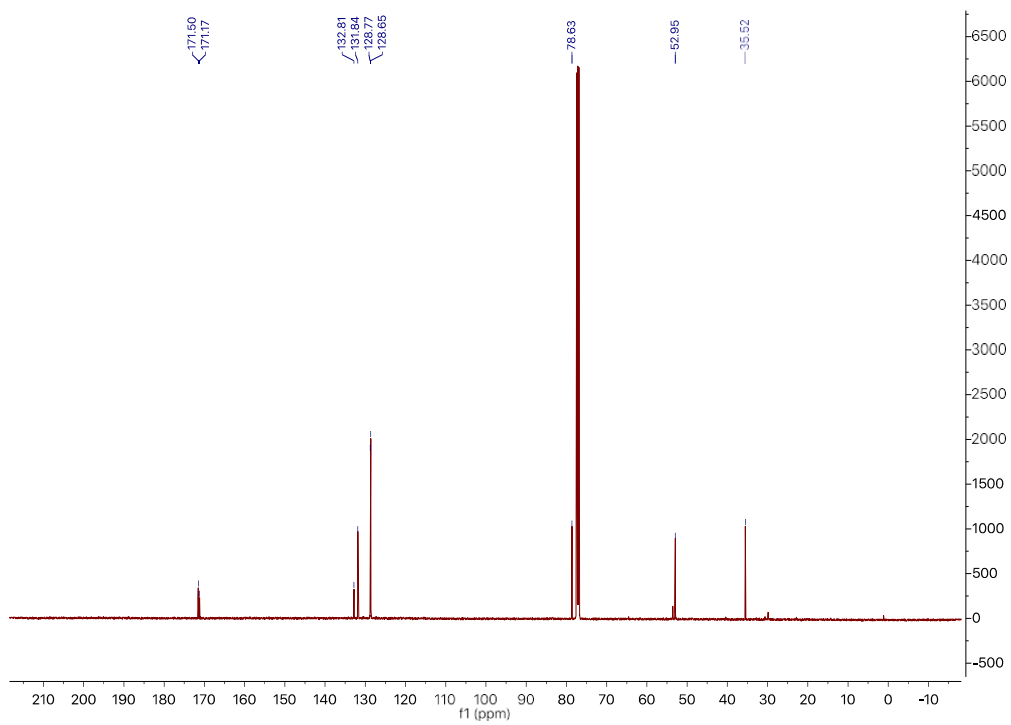


Figure B.4 $^{13}\text{C}\{^1\text{H}\}$ NMR (126 MHz, CDCl_3) spectrum of isolated CysDHT

HPLC Data

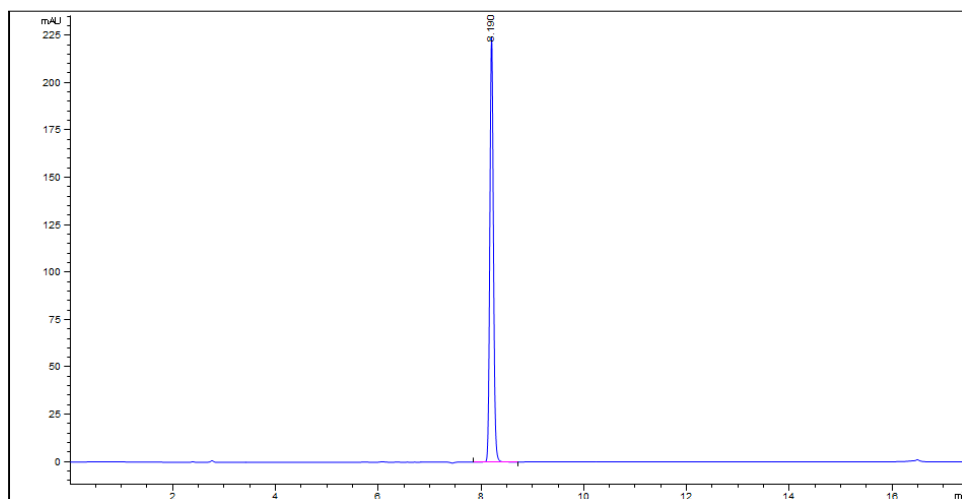


Figure B.5 HPLC trace of DPTE

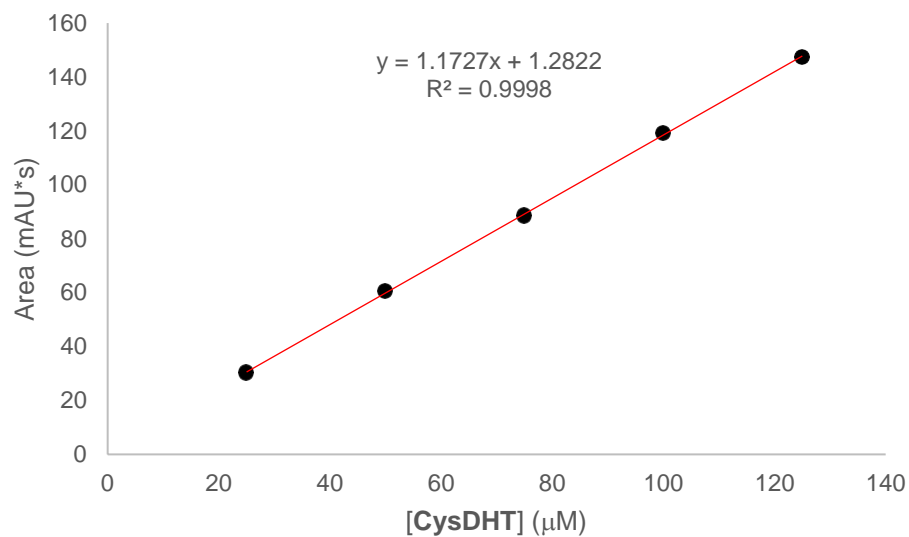


Figure B.6 HPLC calibration curve of CysDHT

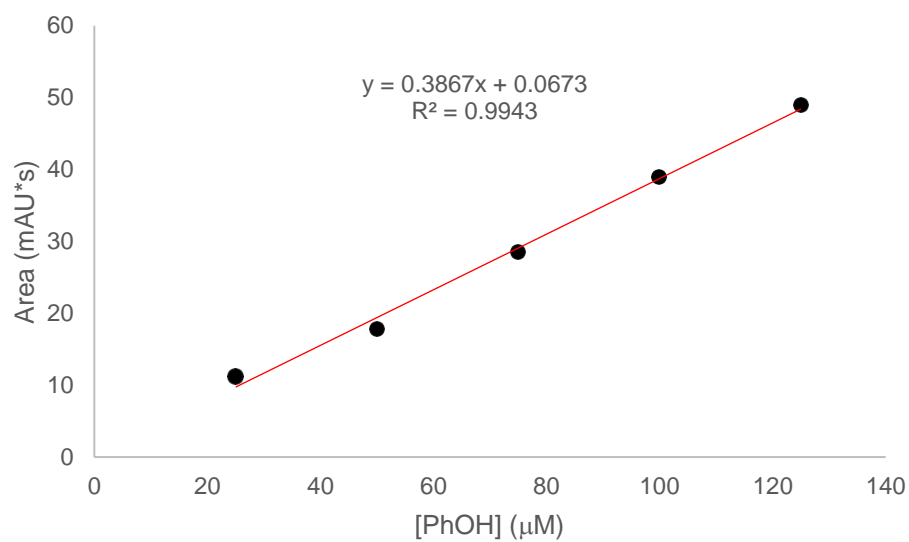


Figure B.7 HPLC calibration curve of phenol

MBA Calibration Curve

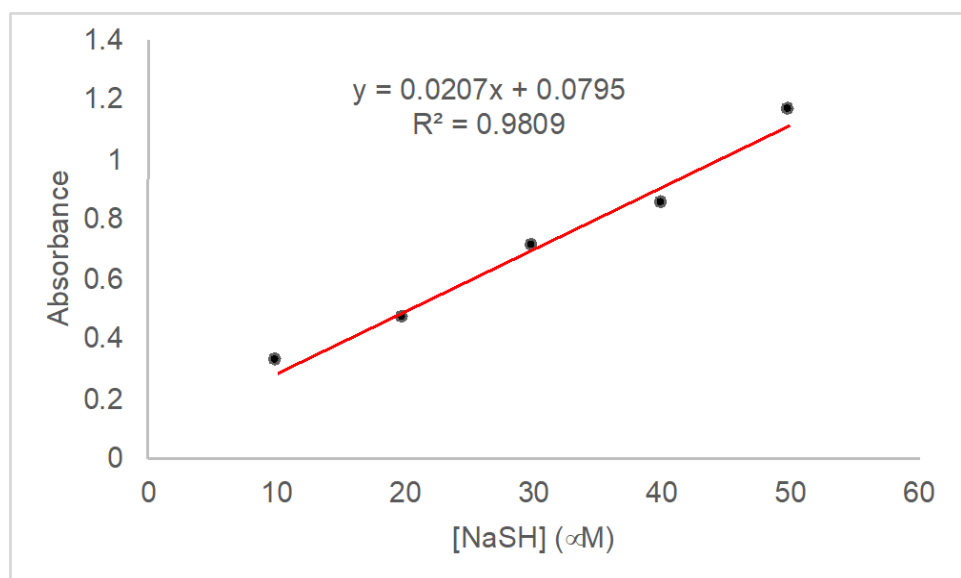


Figure B.8 MBA calibration curve generated using known concentrations of NaSH.

APPENDIX C

SUPPLEMENTARY INFORMATION FOR CHAPTER III

Appendix C is the supplementary information for Chapter III of this dissertation. It includes spectra and experimental data relevant to the content in Chapter III.

NMR Spectra

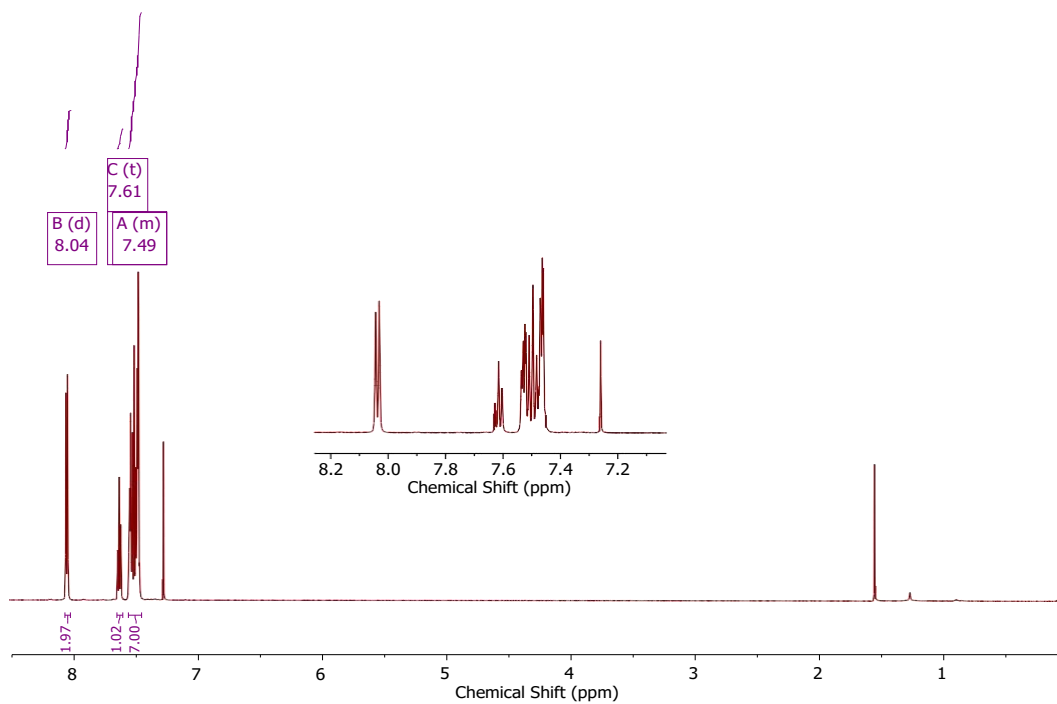


Figure C.1 ¹H NMR (600 MHz, CDCl₃) spectrum of S-phenyl benzothioate

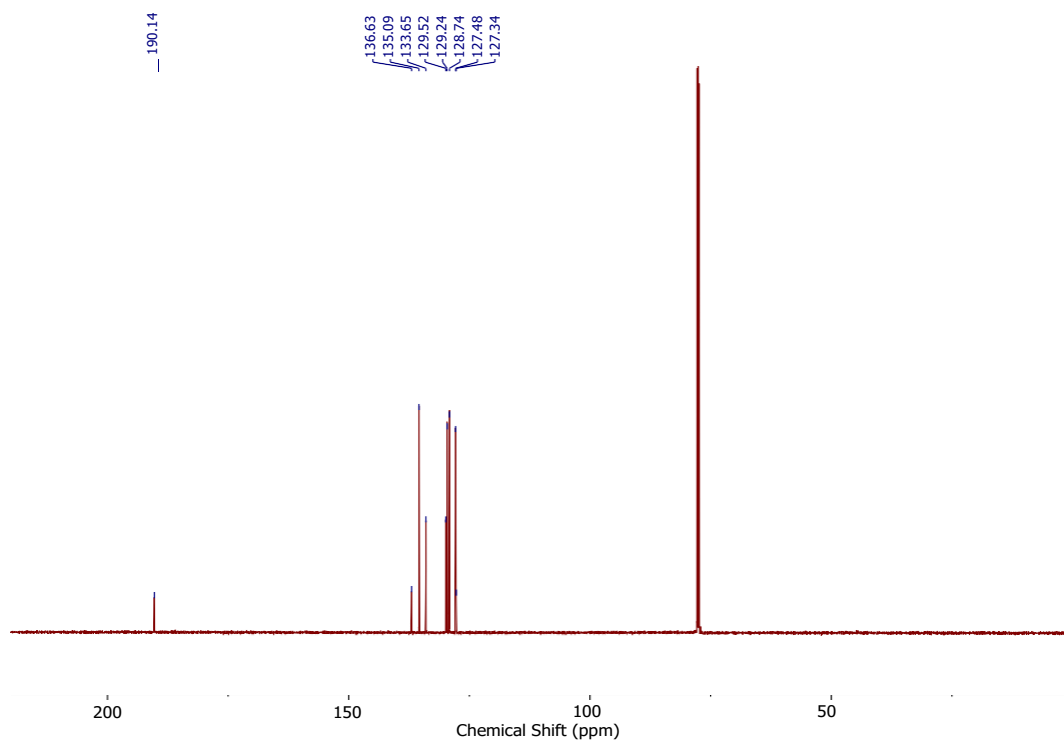


Figure C.2 $^{13}\text{C}\{^1\text{H}\}$ NMR (151 MHz, CDCl_3) spectrum of *S*-phenyl benzothioate

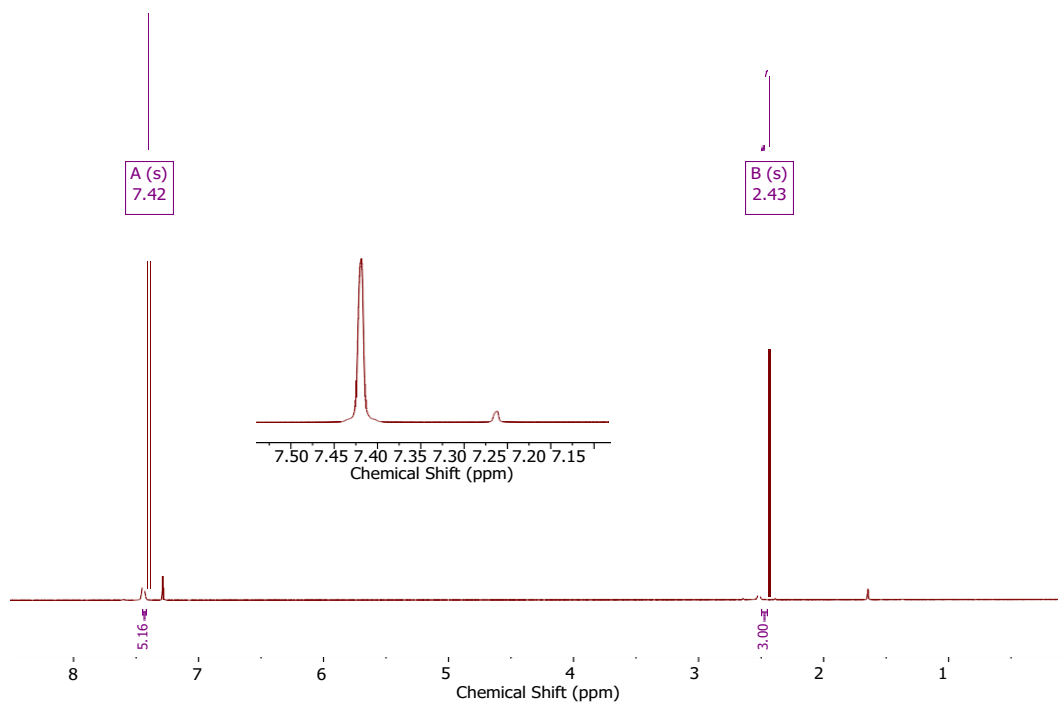


Figure C.3 ^1H NMR (500 MHz, CDCl_3) spectrum of *S*-phenyl ethanethioate

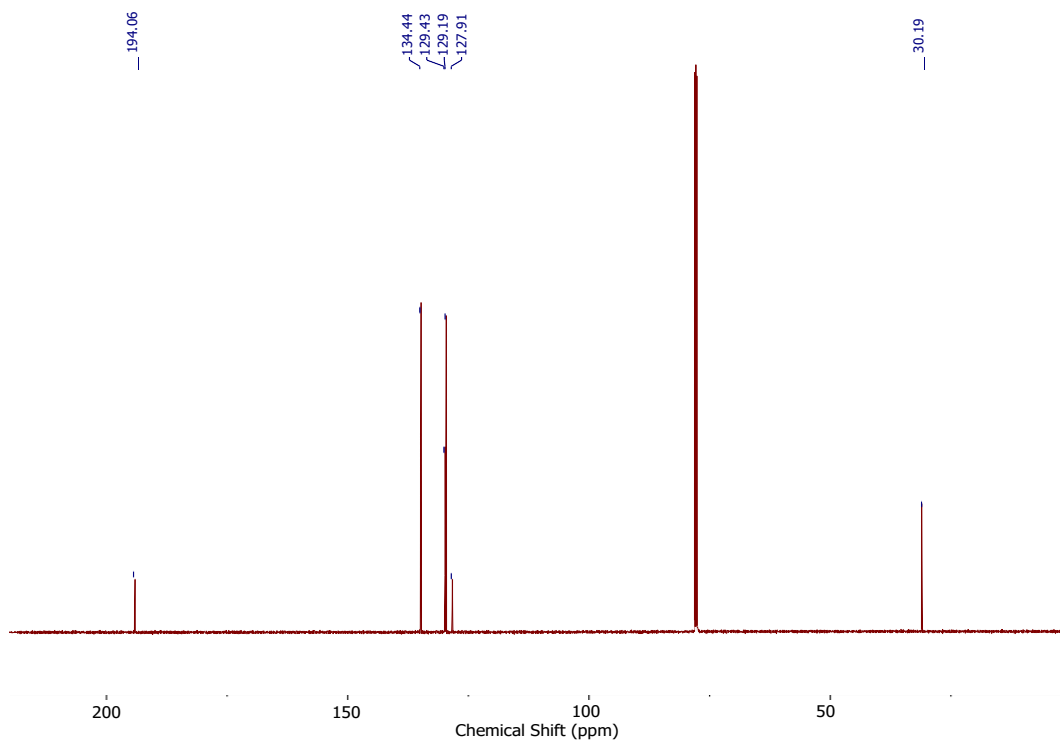


Figure C.4 $^{13}\text{C}\{^1\text{H}\}$ NMR (151 MHz, CDCl_3) spectrum of *S*-phenyl ethanethioate

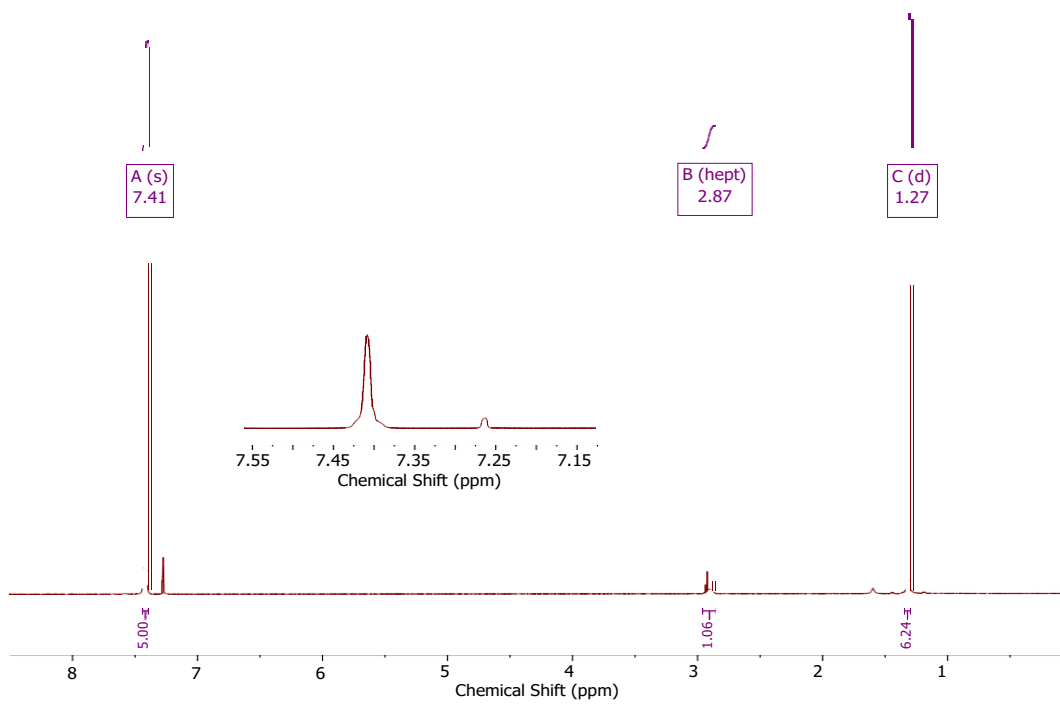


Figure C.5 ^1H NMR (500 MHz, CDCl_3) spectrum of *S*-phenyl 2-methylpropanethioate

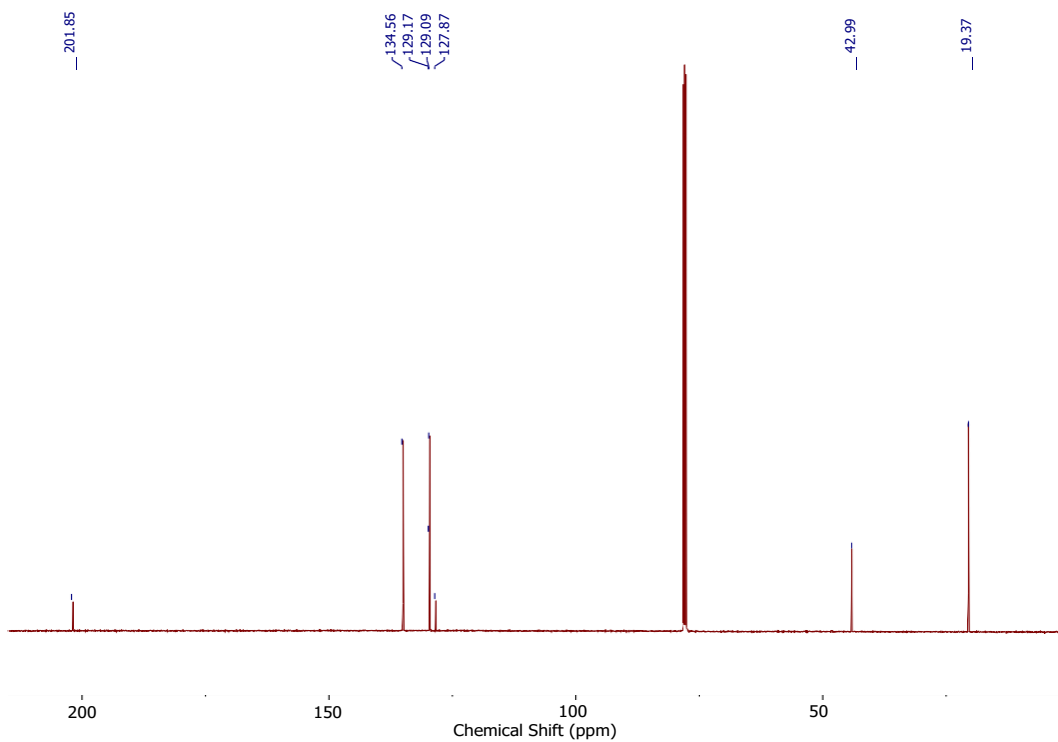


Figure C.6 $^{13}\text{C}\{^1\text{H}\}$ NMR (126 MHz, CDCl_3) spectrum of *S*-phenyl 2-methylpropanethioate

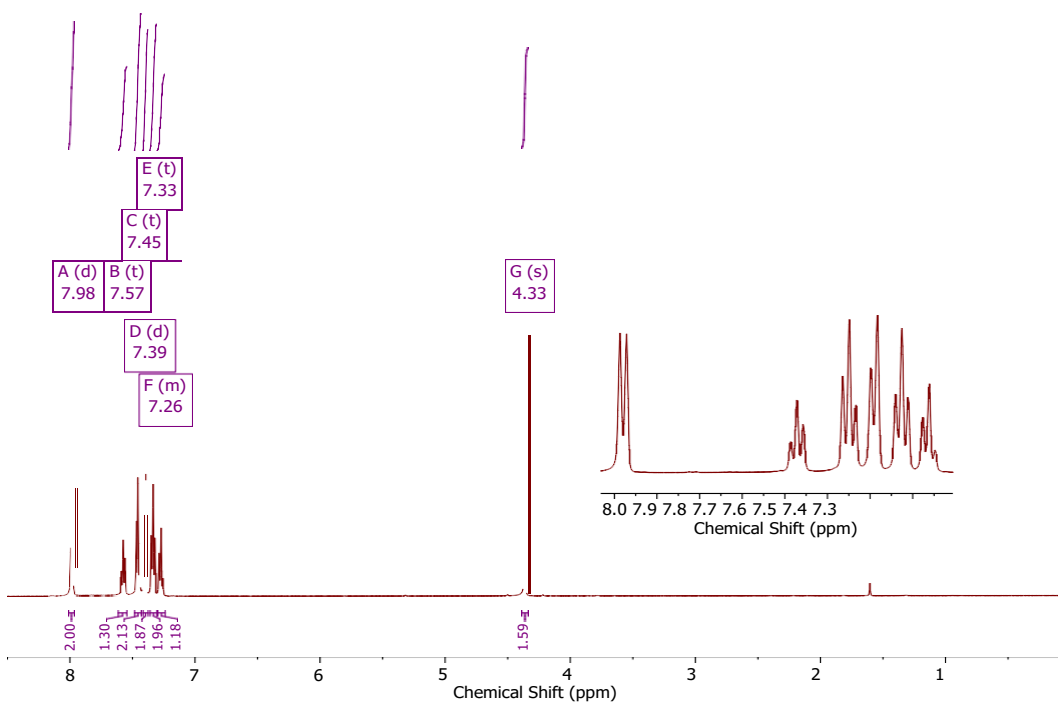


Figure C.7 ^1H NMR (500 MHz, CDCl_3) spectrum of *S*-benzyl benzothioate

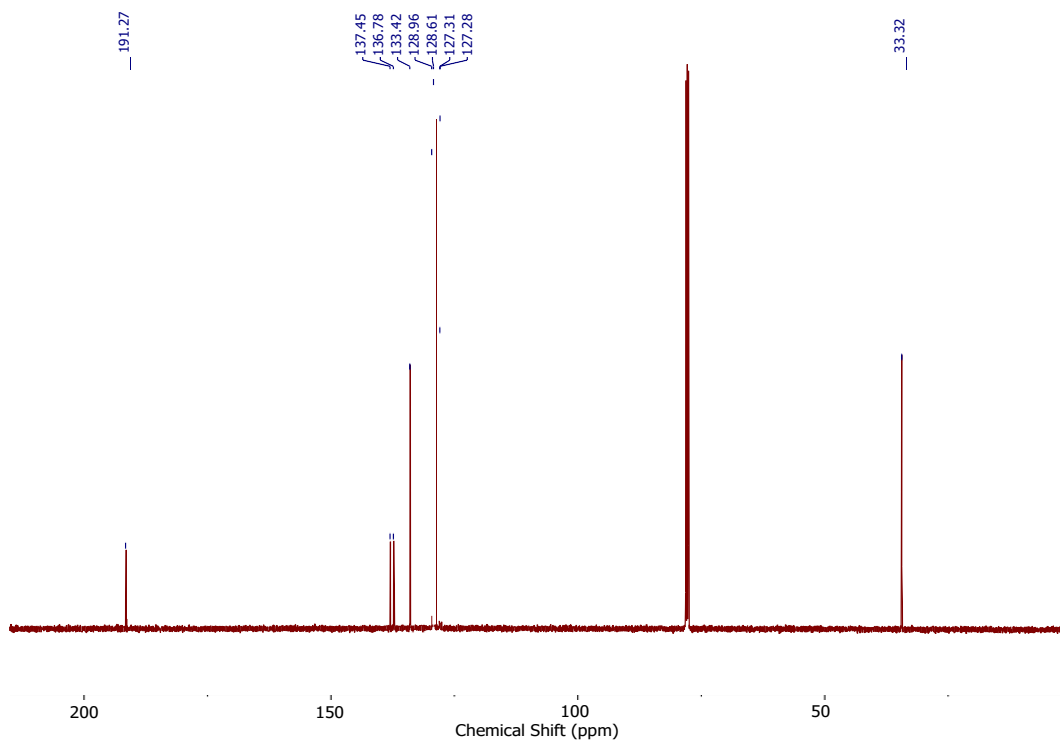


Figure C.8 $^{13}\text{C}\{^1\text{H}\}$ NMR (126 MHz, CDCl_3) spectrum of *S*-benzyl benzothioate

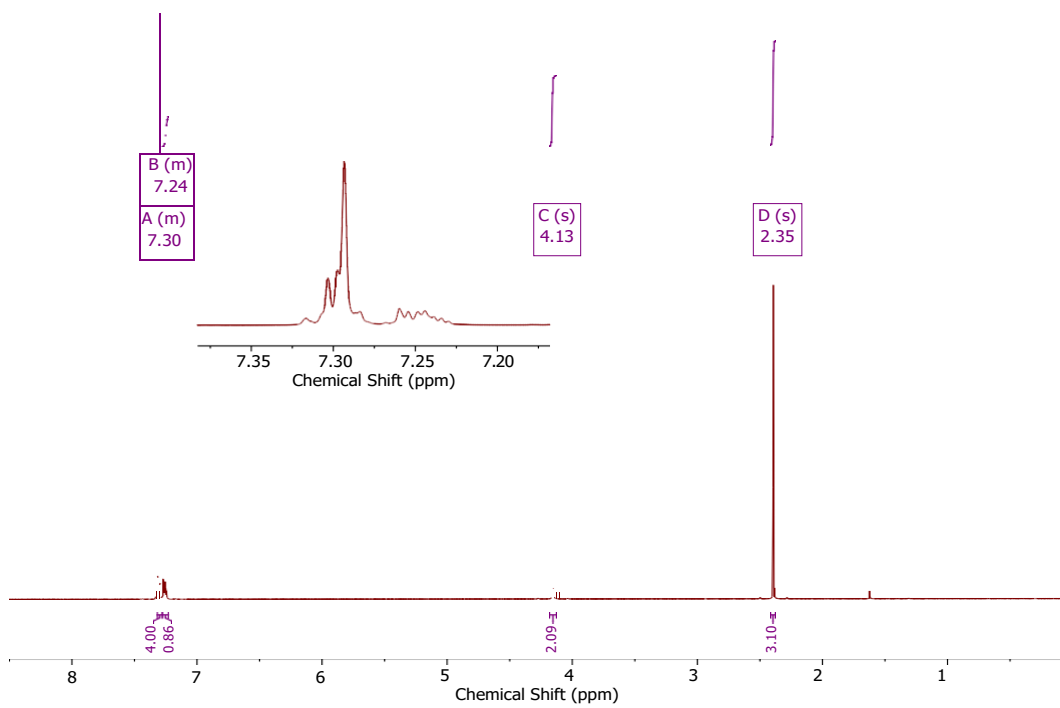


Figure C.9 ^1H NMR (600 MHz, CDCl_3) spectrum of *S*-benzyl ethanethioate

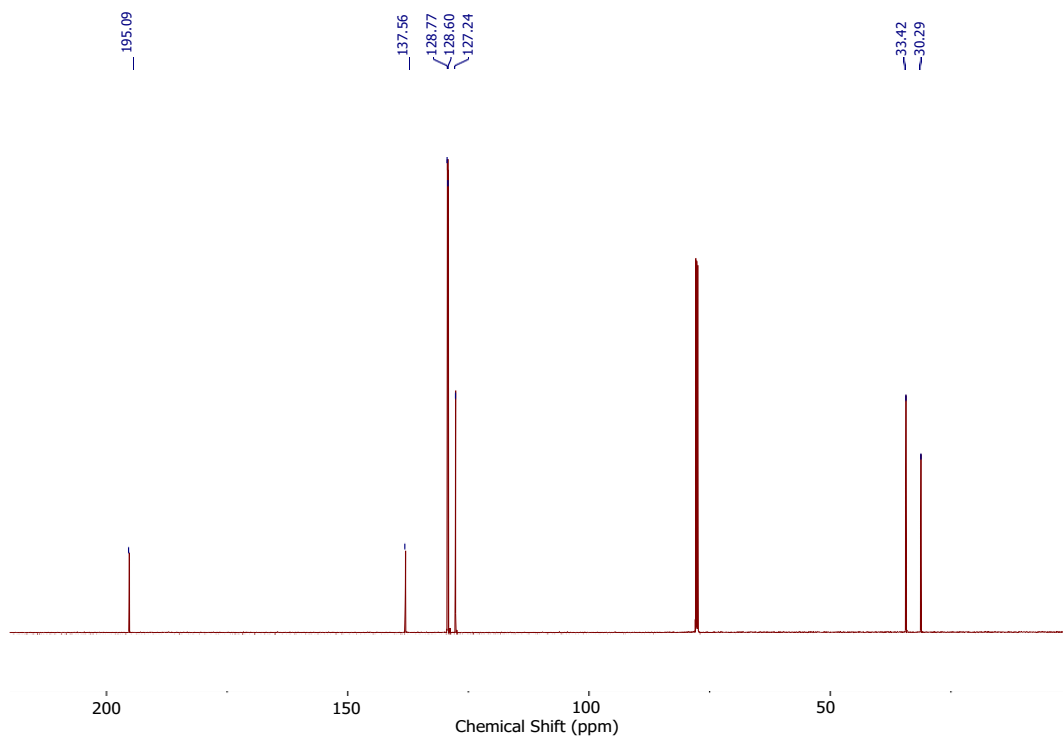


Figure C.10 $^{13}\text{C}\{^1\text{H}\}$ NMR (151 MHz, CDCl_3) spectrum of *S*-benzyl ethanethioate

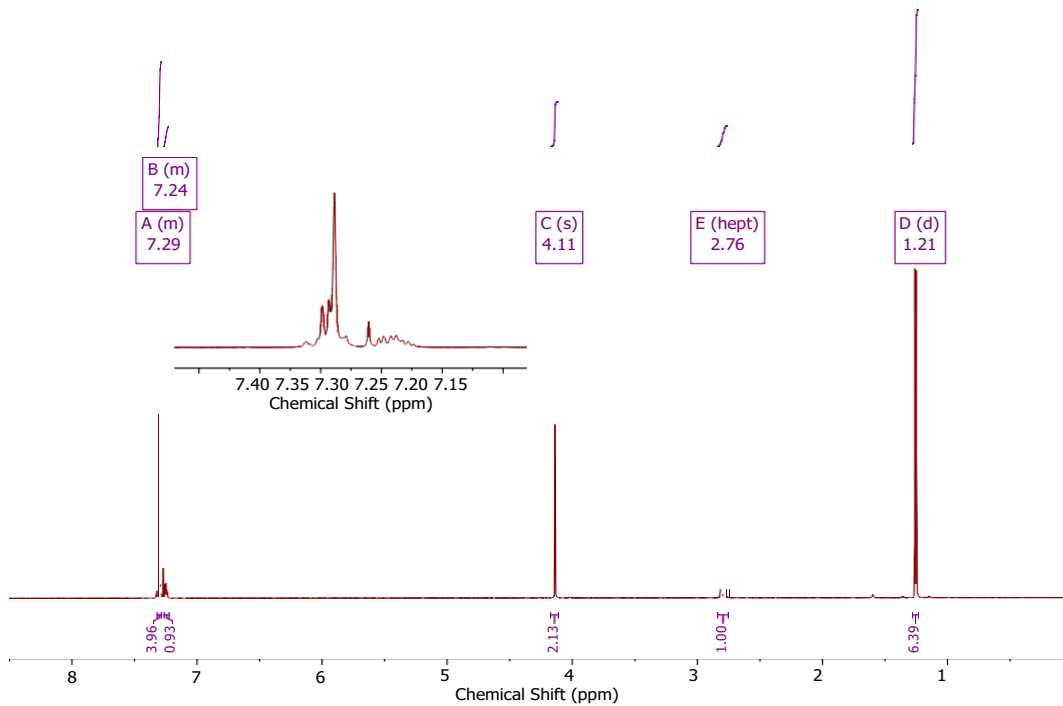


Figure C.11 ^1H NMR (600 MHz, CDCl_3) spectrum of *S*-benzyl 2-methylpropanethioate

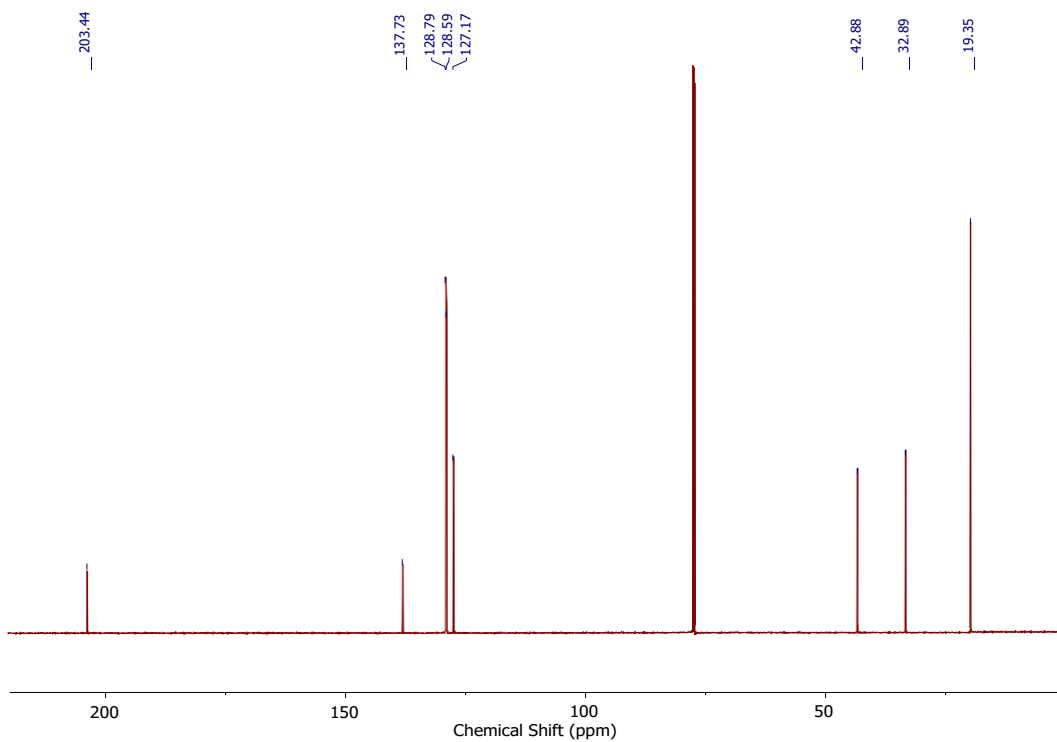


Figure C.12. $^{13}\text{C}\{^1\text{H}\}$ NMR (151 MHz, CDCl_3) spectrum of *S*-benzyl 2-methylpropanethioate

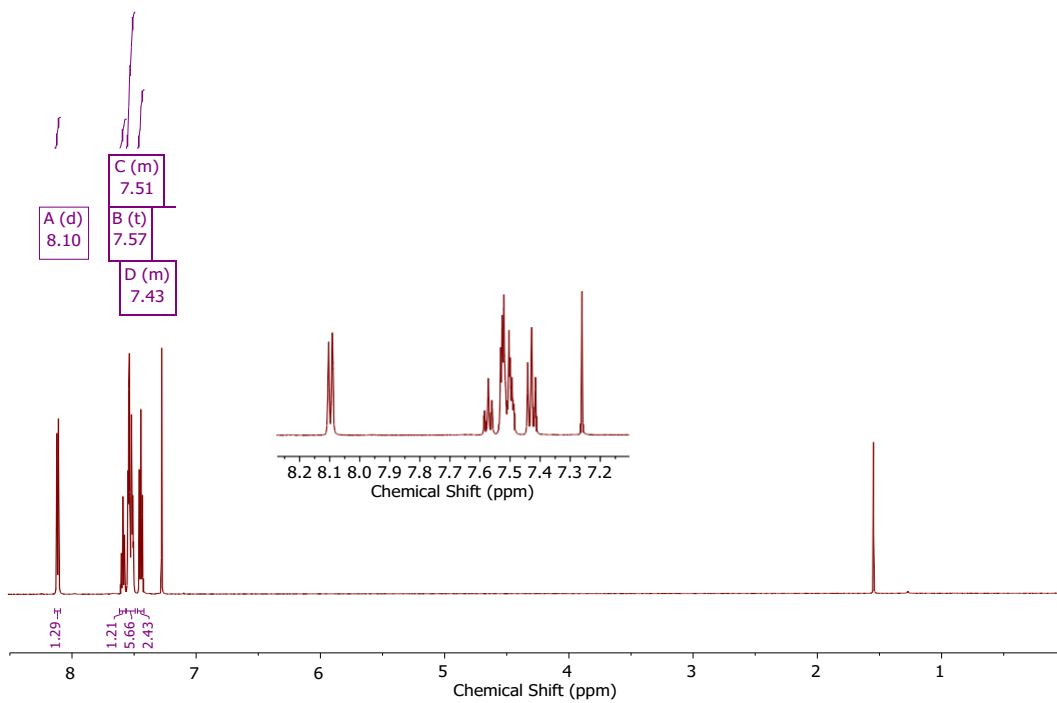


Figure C.13 ^1H NMR (600 MHz, CDCl_3) spectrum of PDTE

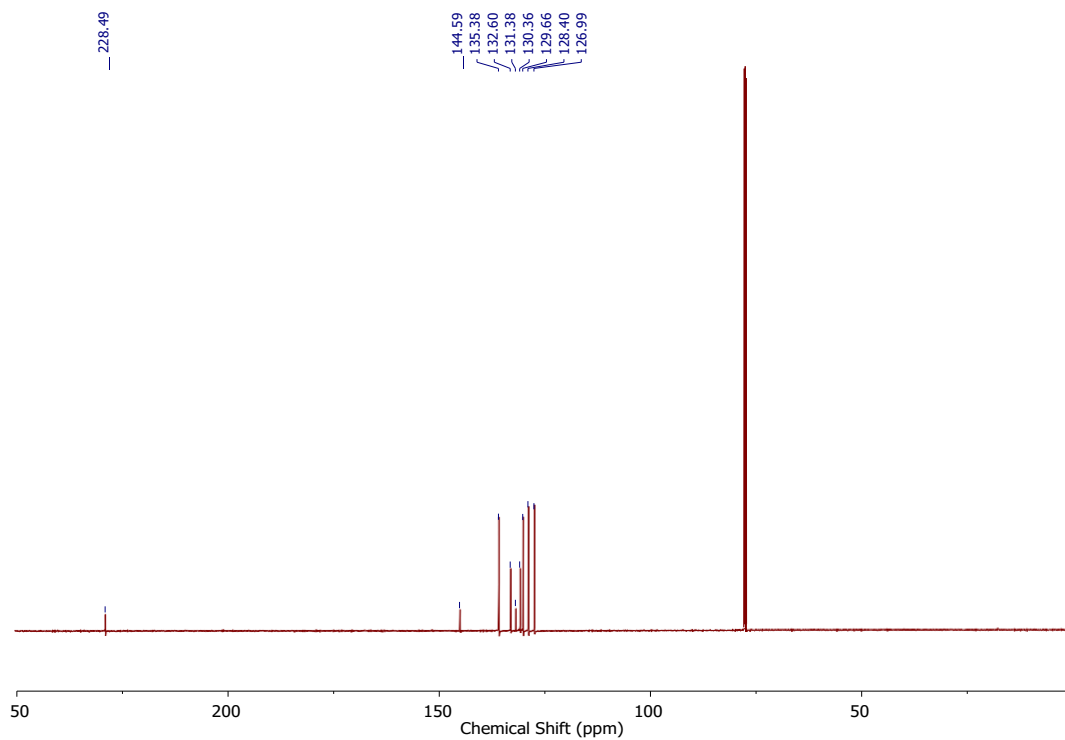


Figure C.14 $^{13}\text{C}\{^1\text{H}\}$ NMR (151 MHz, CDCl_3) spectrum of **PDTE**

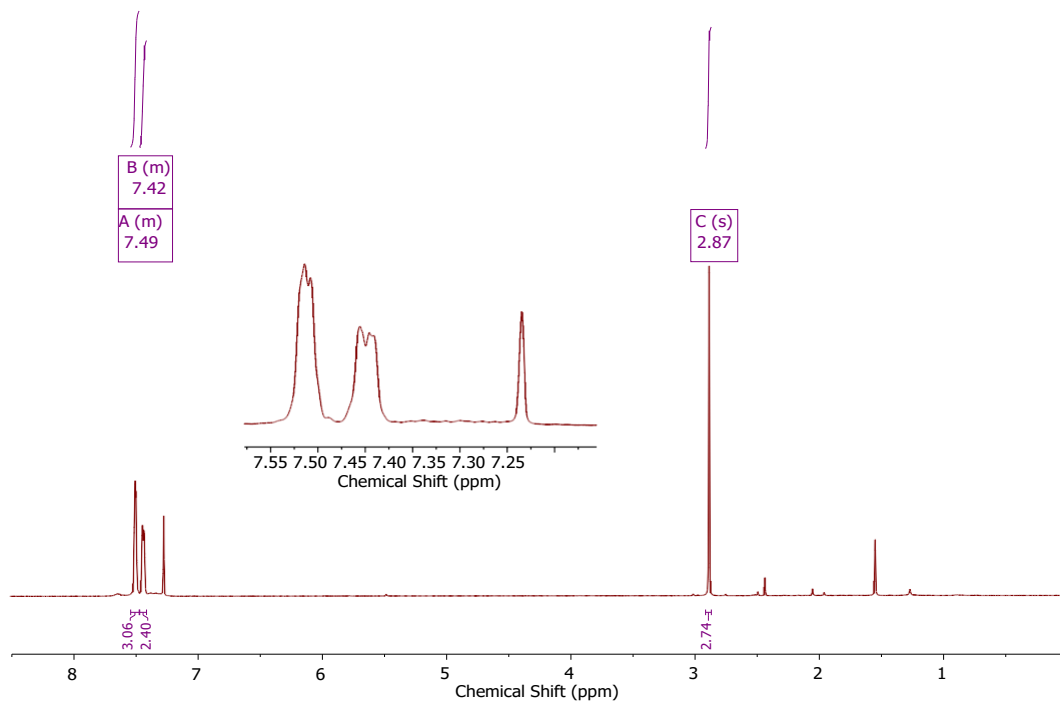


Figure C.15 ^1H NMR (500 MHz, CDCl_3) spectrum of **MPDTE**

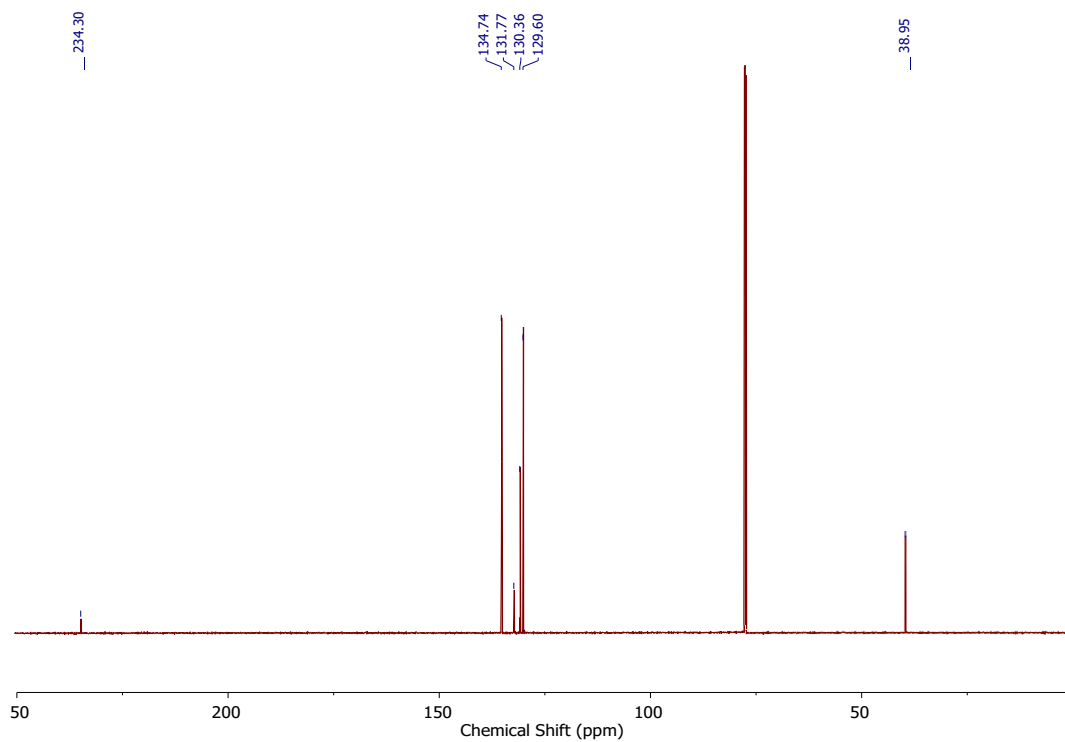


Figure C.16 $^{13}\text{C}\{^1\text{H}\}$ NMR (151 MHz, CDCl_3) spectrum of **MPDTE**

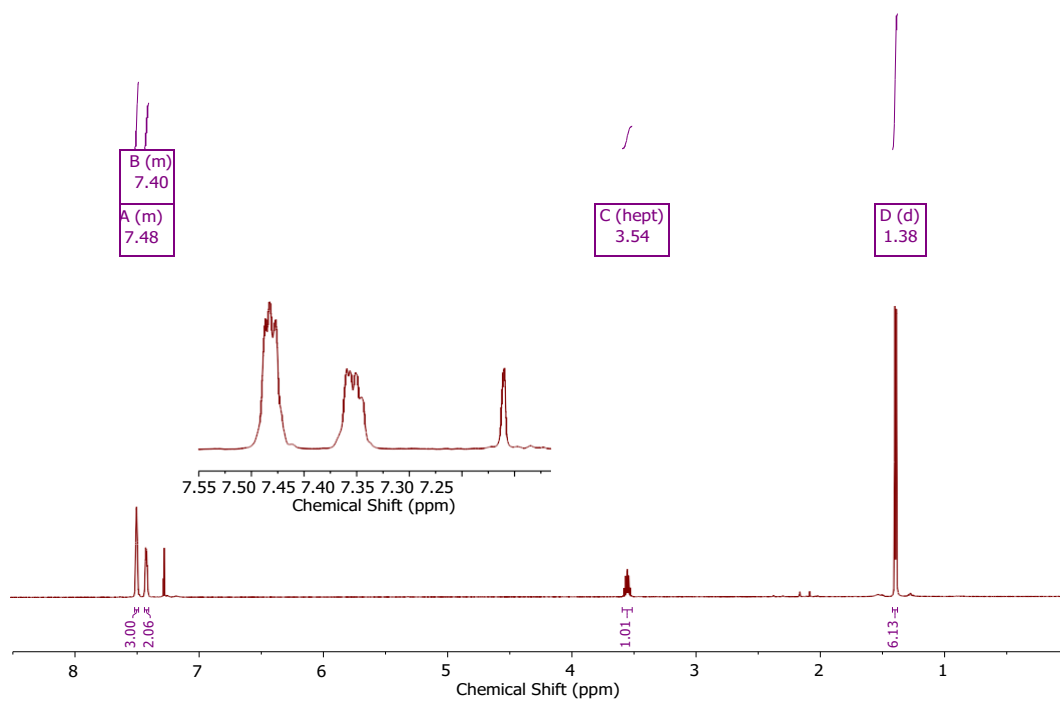


Figure C.17 ^1H NMR (600 MHz, CDCl_3) spectrum of **iPPDTE**

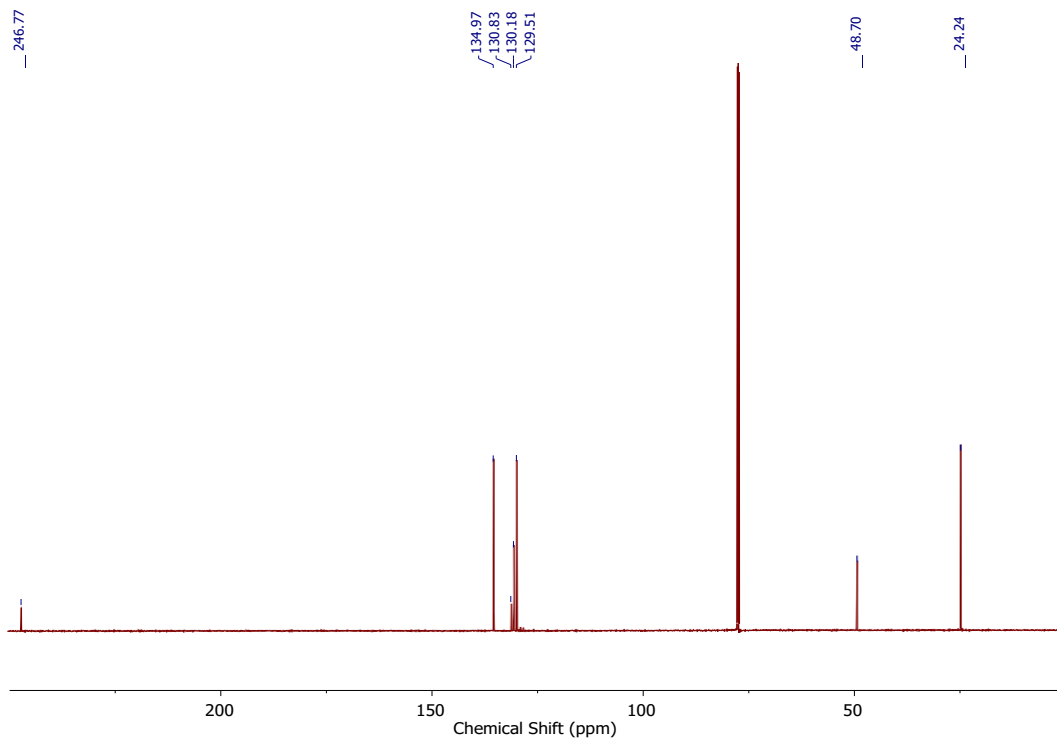


Figure C.18 $^{13}\text{C}\{^1\text{H}\}$ NMR (151 MHz, CDCl_3) spectrum of **iPPDTE**

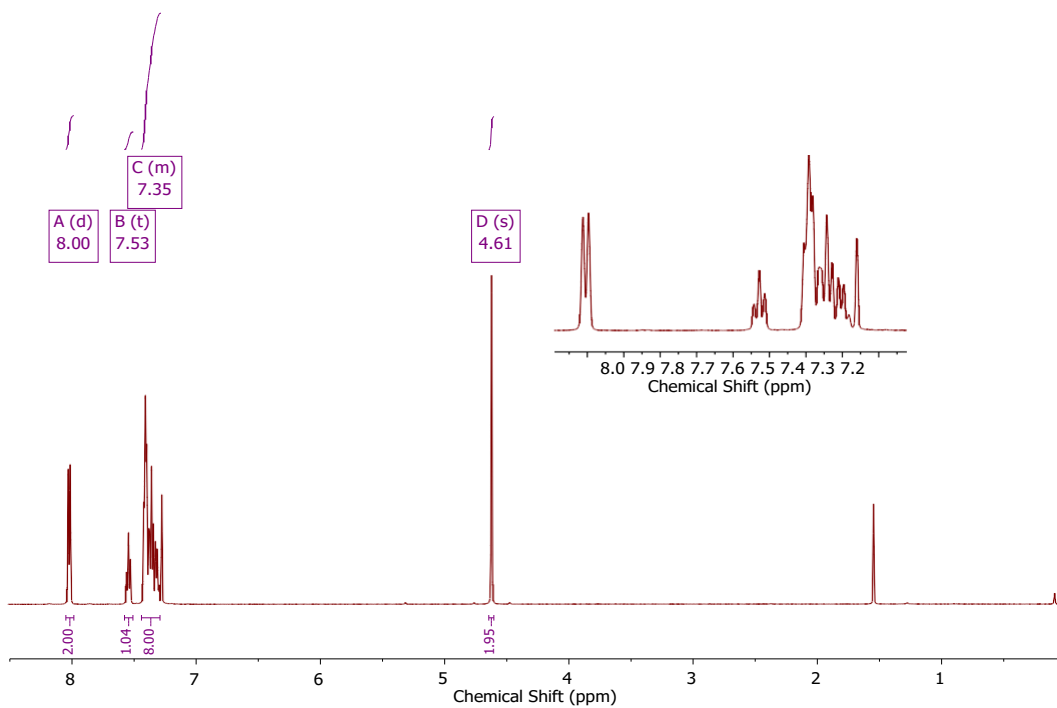


Figure C.19 ^1H NMR (500 MHz, CDCl_3) spectrum of **PBDTE**

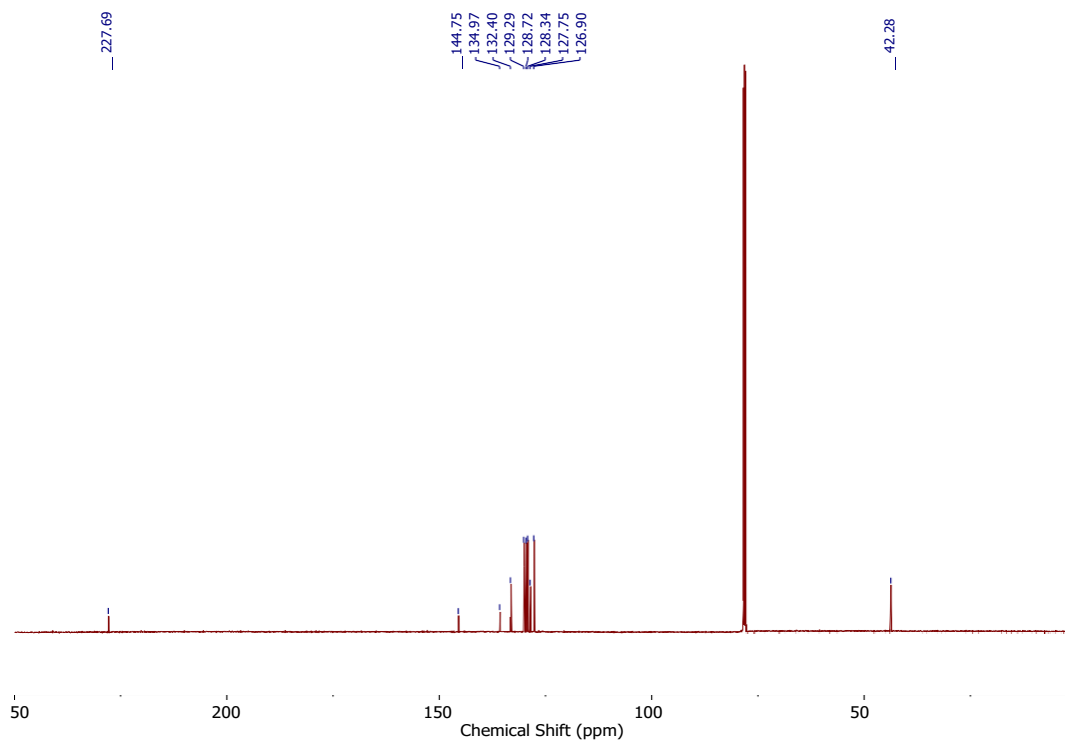


Figure C.20 $^{13}\text{C}\{^1\text{H}\}$ NMR (126 MHz, CDCl_3) spectrum of **PBDTE**

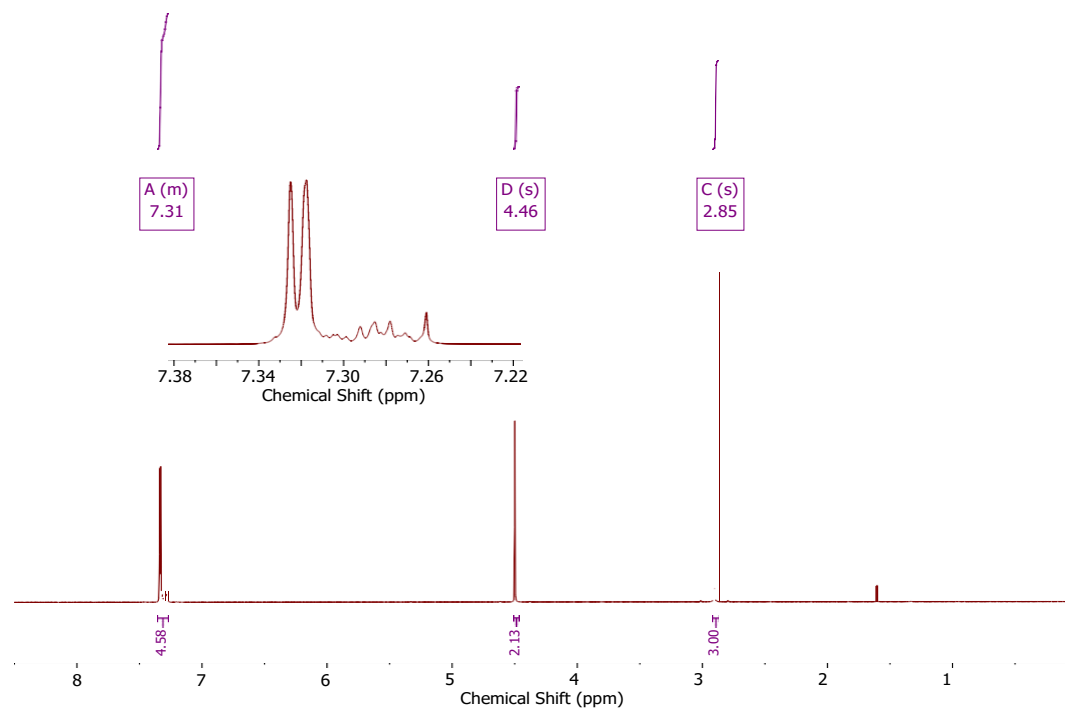


Figure C.21 ^1H NMR (600 MHz, CDCl_3) spectrum of **MBDTE**

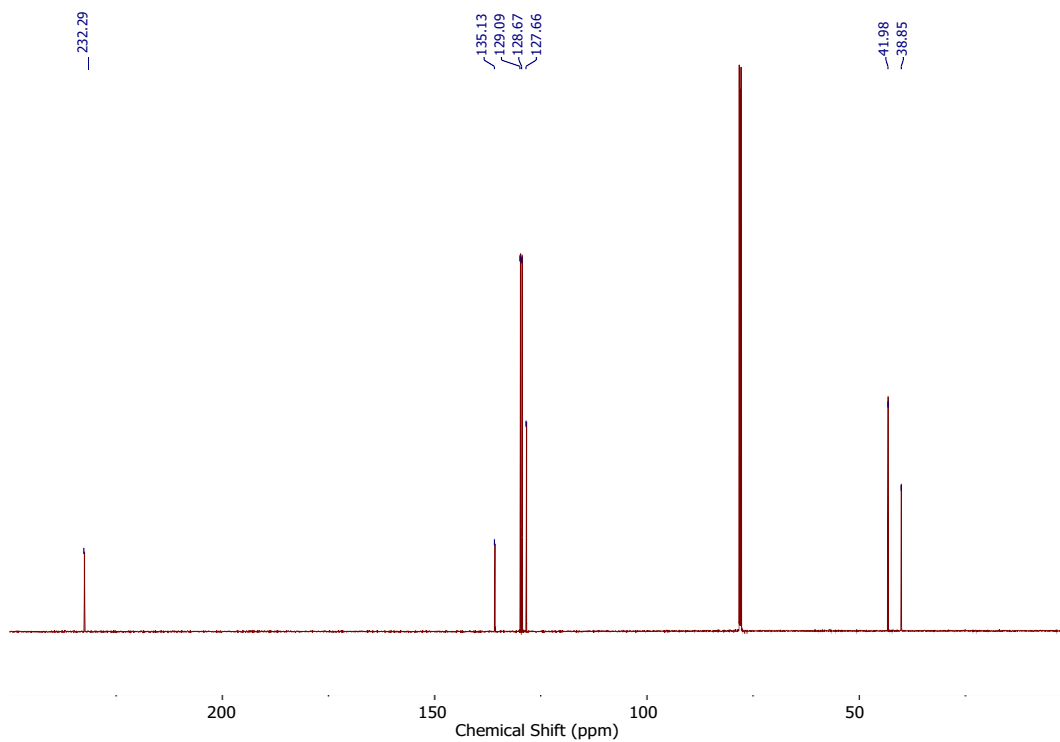


Figure C.22 $^{13}\text{C}\{^1\text{H}\}$ NMR (151 MHz, CDCl_3) spectrum of MBDTE

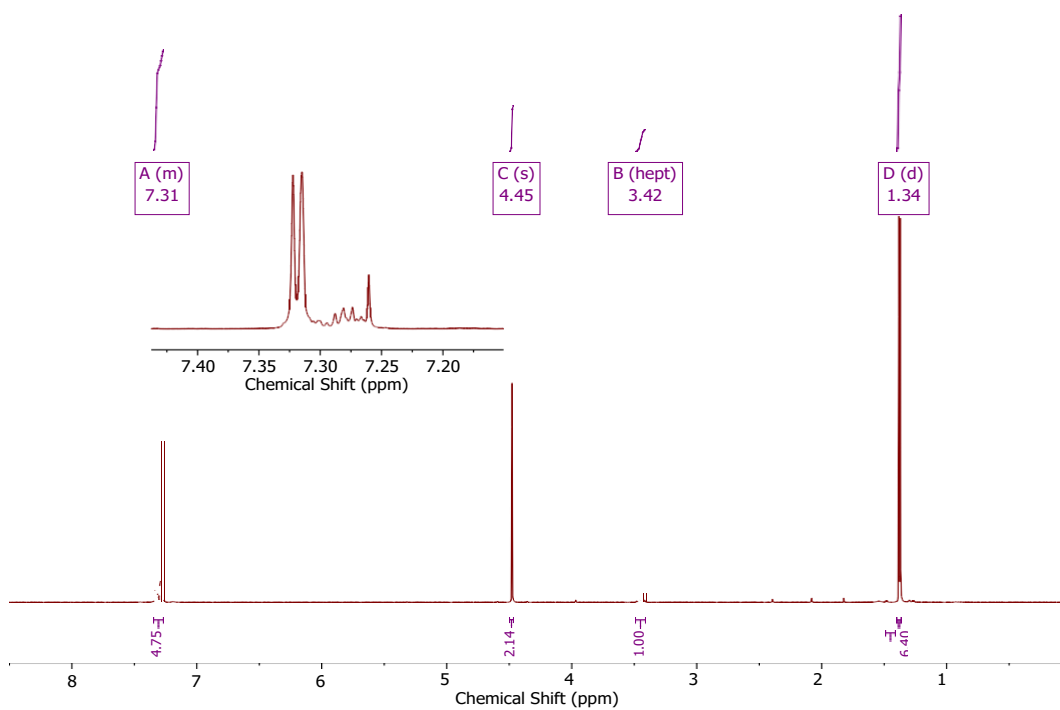


Figure C.23 ^1H NMR (600 MHz, CDCl_3) spectrum of iPBDTE

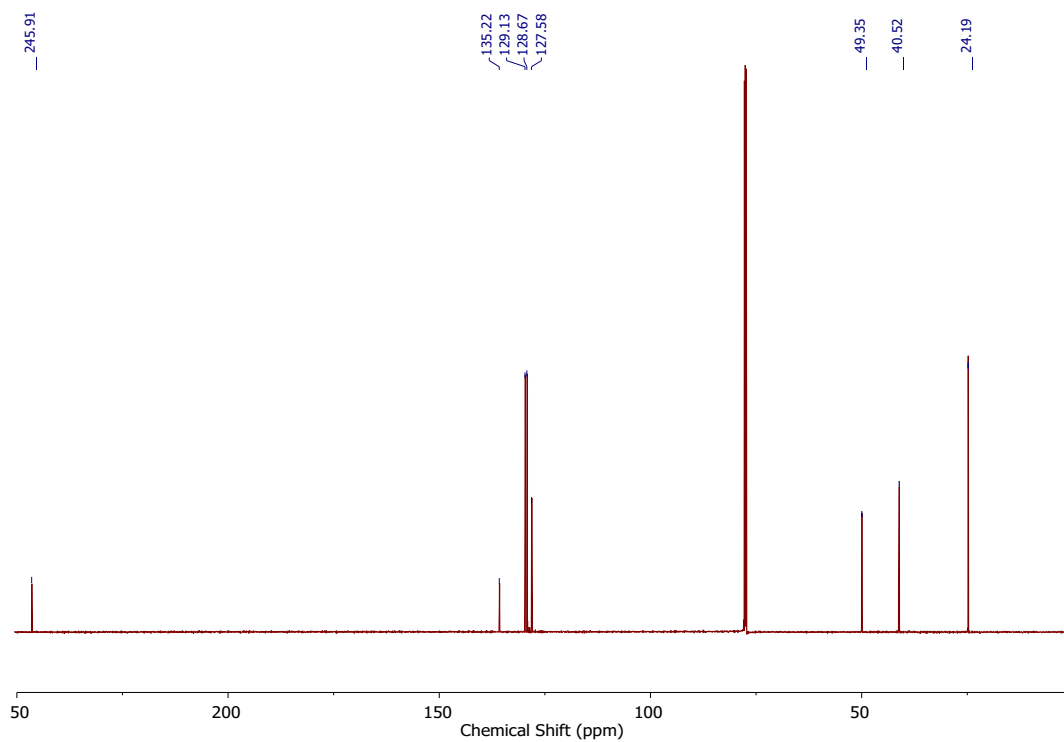


Figure C.24 $^{13}\text{C}\{^1\text{H}\}$ NMR (151 MHz, CDCl_3) spectrum of **iPBDE**

HPLC Data

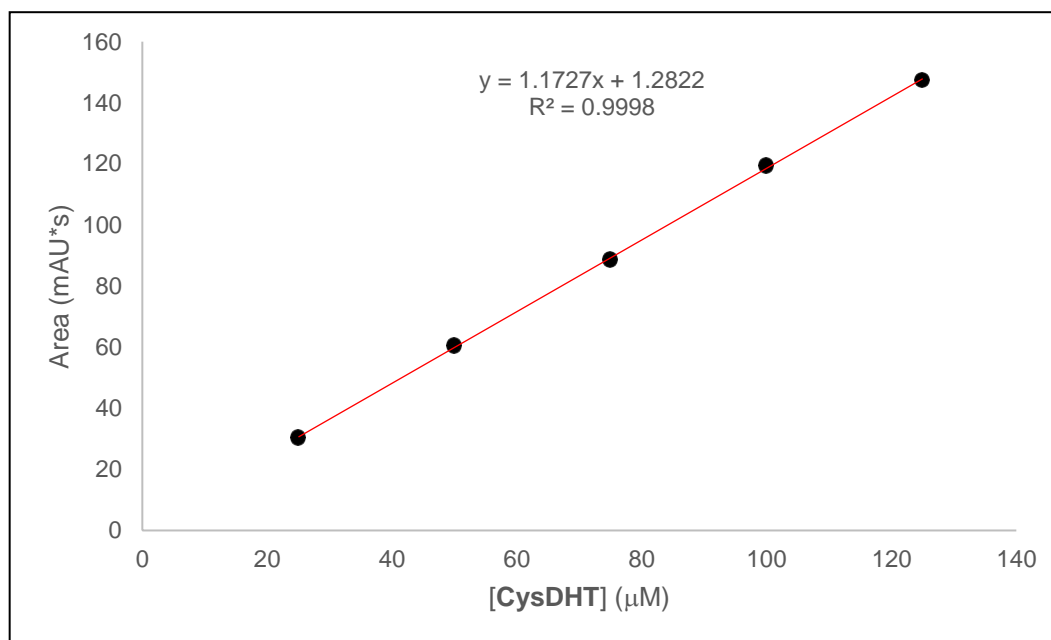


Figure C.25 HPLC Calibration Curve of **CysDHT**

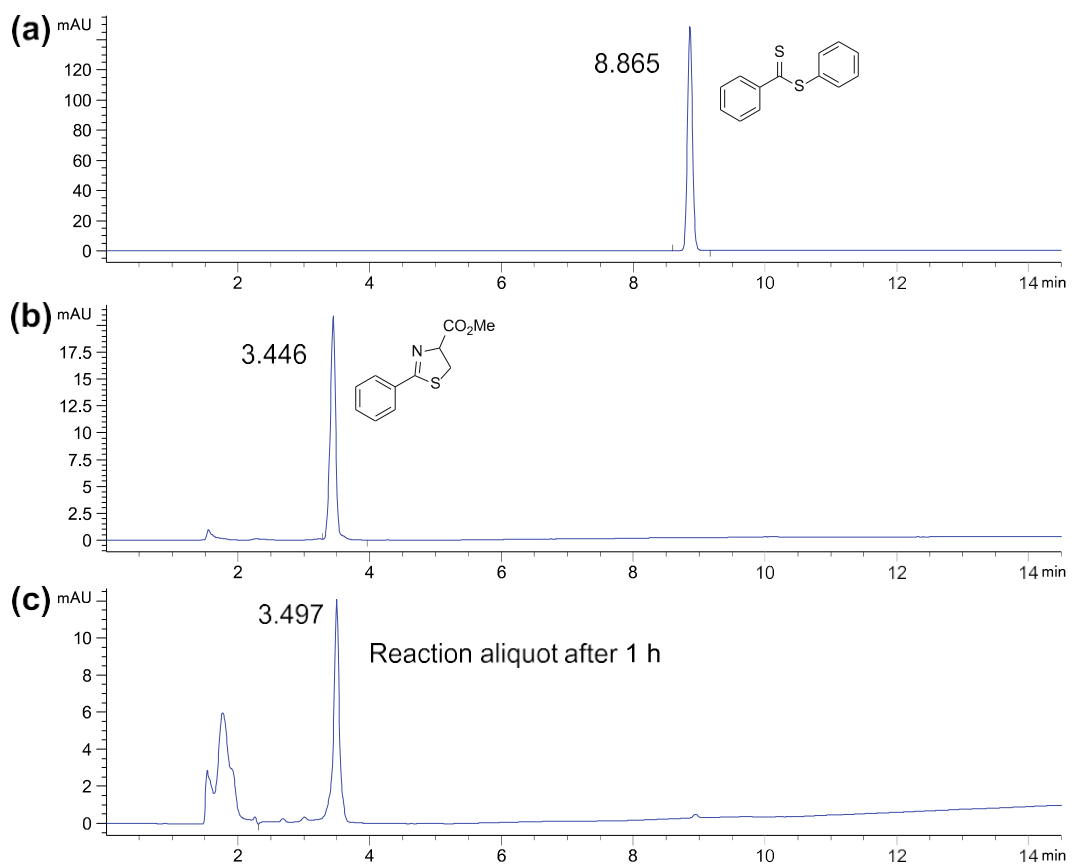


Figure C.26 a) 100 ppm PDTE in Hexanes b) 100 μ M CysDHT in 10 mM PBS (pH 7.4) with 10% THF c) Reaction aliquot after 1 h.

MBA Calibration Curve

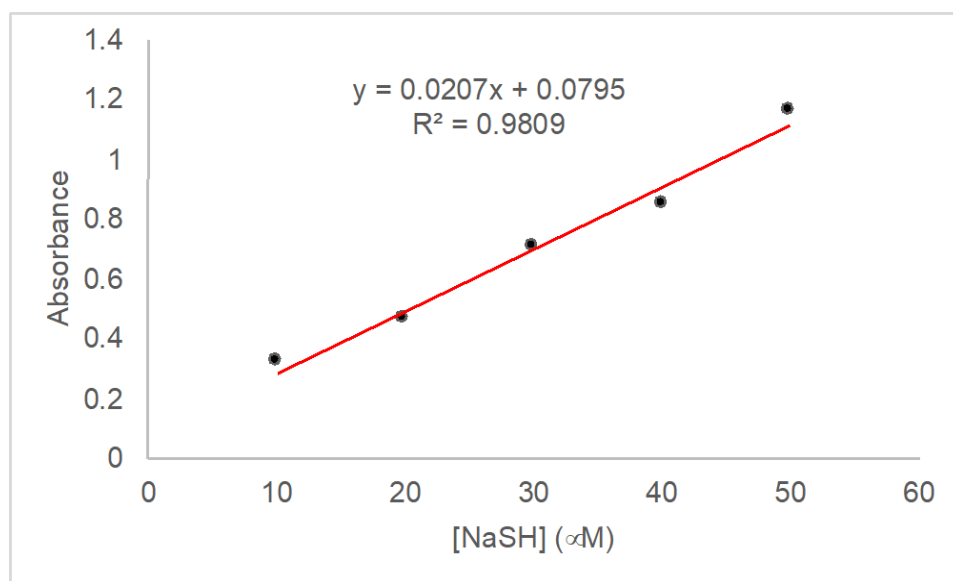


Figure C.27 MBA calibration curve generated using known concentrations of NaSH.

APPENDIX D

SUPPLEMENTARY INFORMATION FOR CHAPTER IV

Appendix D is the supplementary information for Chapter IV of this dissertation. It includes spectra and experimental data relevant to the content in Chapter IV.

NMR Spectra

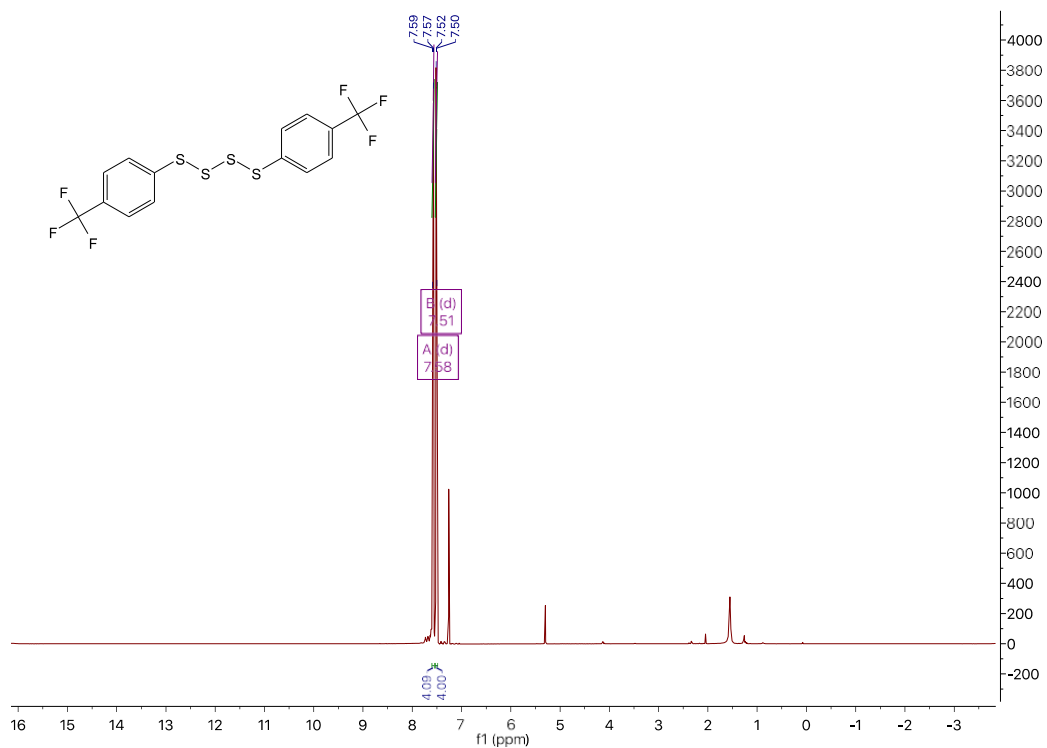


Figure D.1 ¹H NMR (500 MHz, CDCl₃) spectrum of **1**



Figure D.2 ^{19}F NMR (471 MHz, CDCl_3) spectrum of **1**

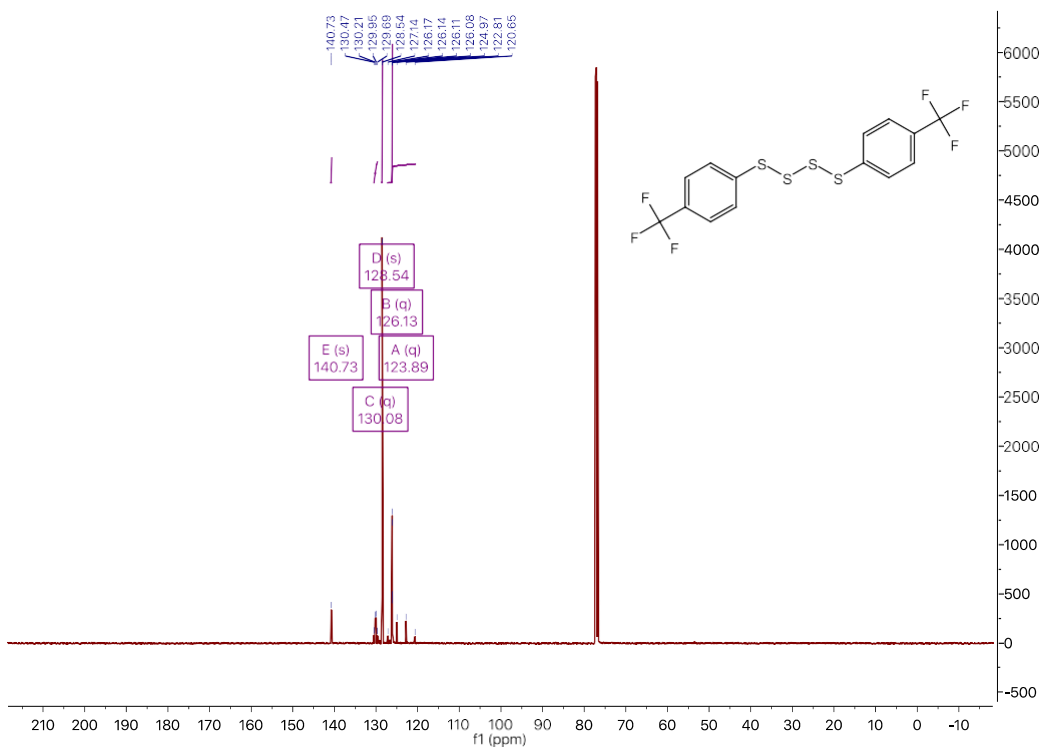


Figure D.3 $^{13}\text{C}\{^1\text{H}\}$ NMR (126 MHz, CDCl_3) spectrum of **1**

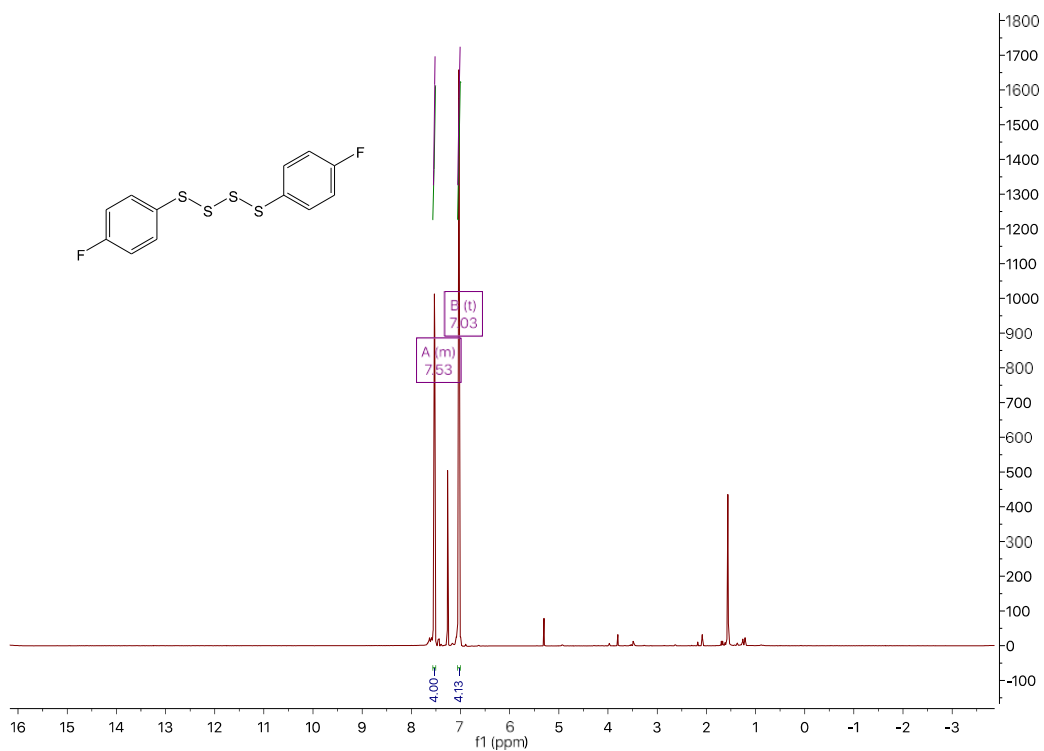


Figure D.4 ^1H NMR (600 MHz, CDCl_3) spectrum of **2**

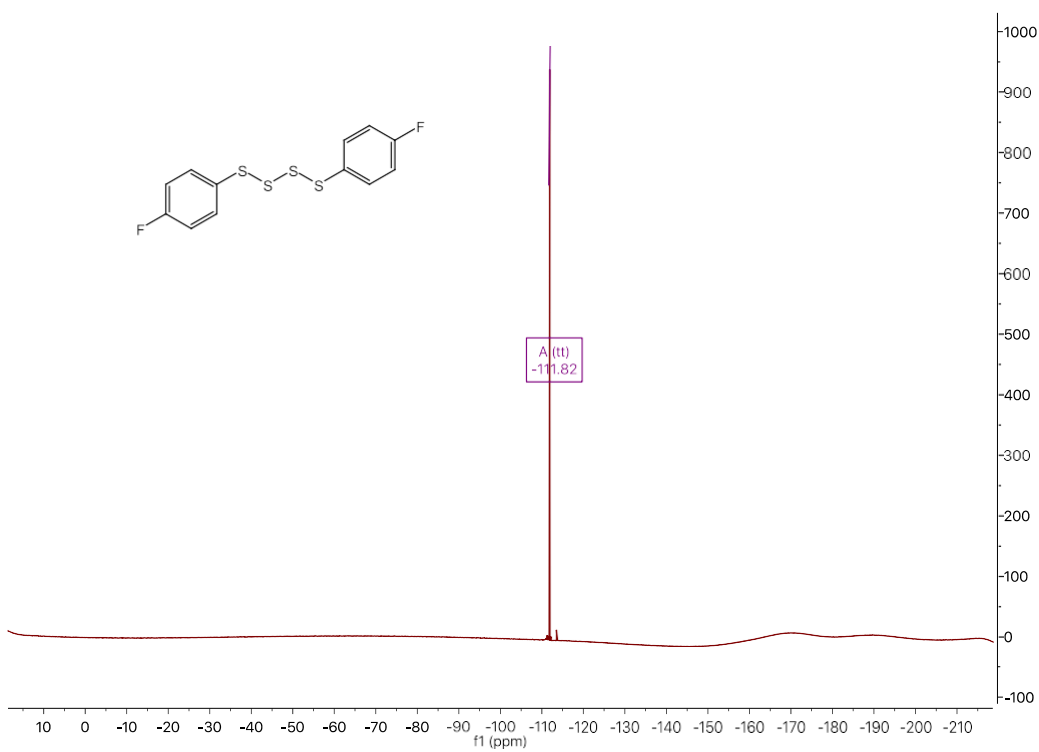


Figure D.5 ^{19}F NMR (565 MHz, CDCl_3) spectrum of **2**



Figure D.6 $^{13}\text{C}\{^1\text{H}\}$ NMR (151 MHz, CDCl_3) spectrum of **2**

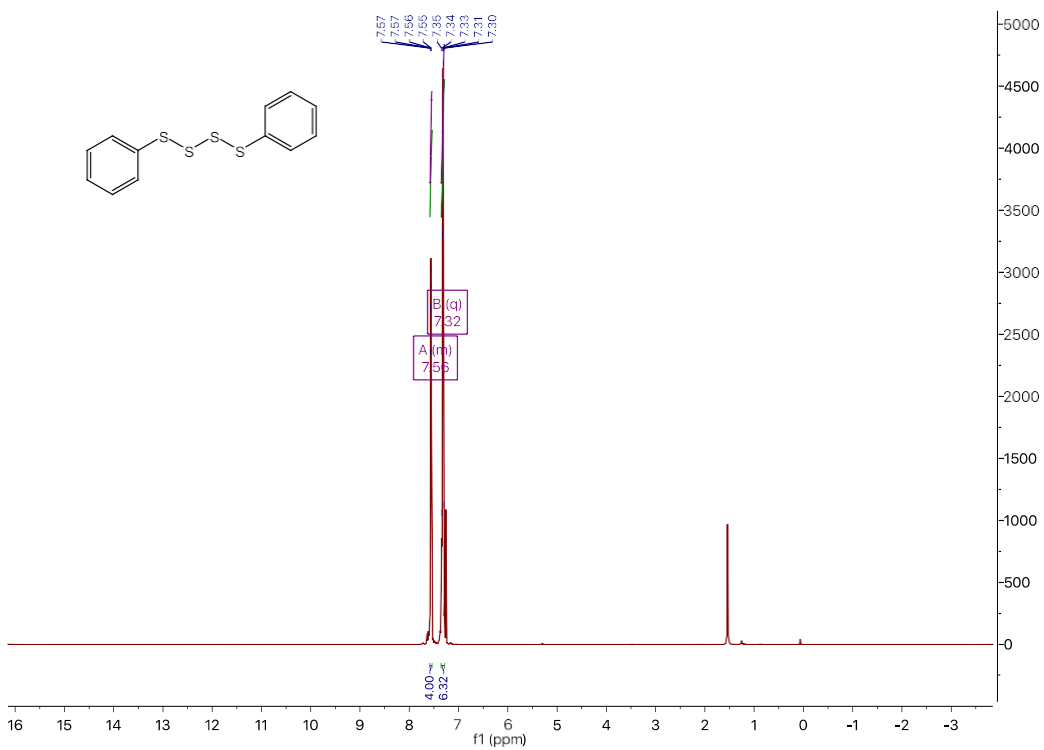


Figure D.7 ^1H NMR (500 MHz, CDCl_3) spectrum of **3**

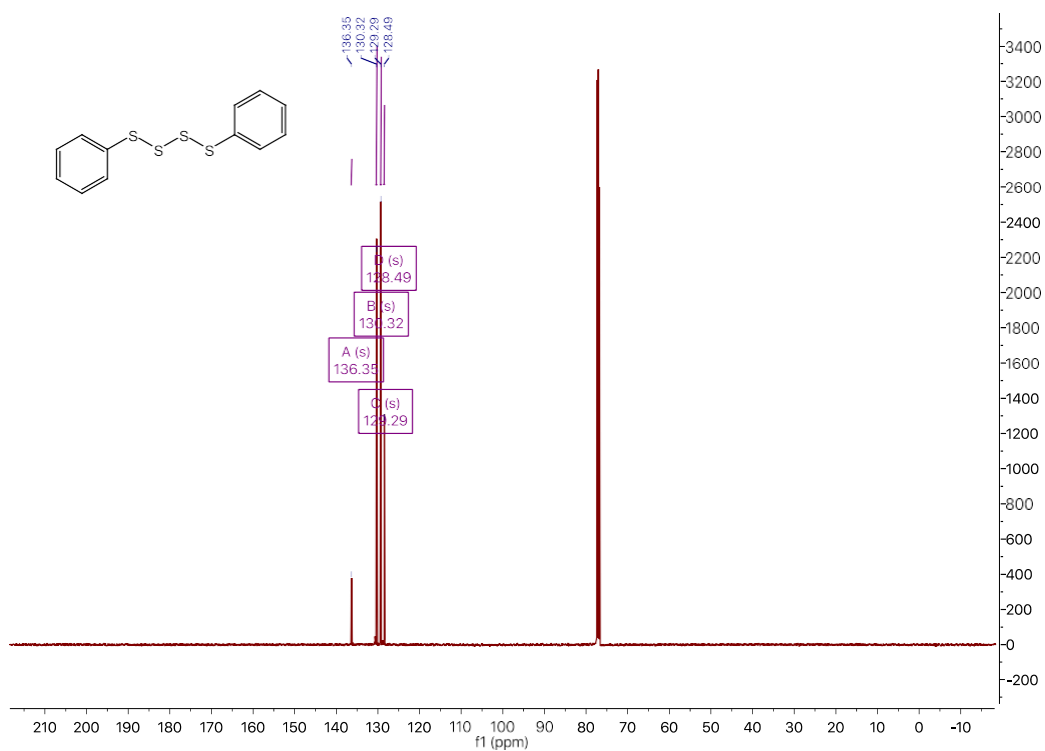


Figure D.8 $^{13}\text{C}\{^1\text{H}\}$ NMR (126 MHz, CDCl_3) spectrum of **3**

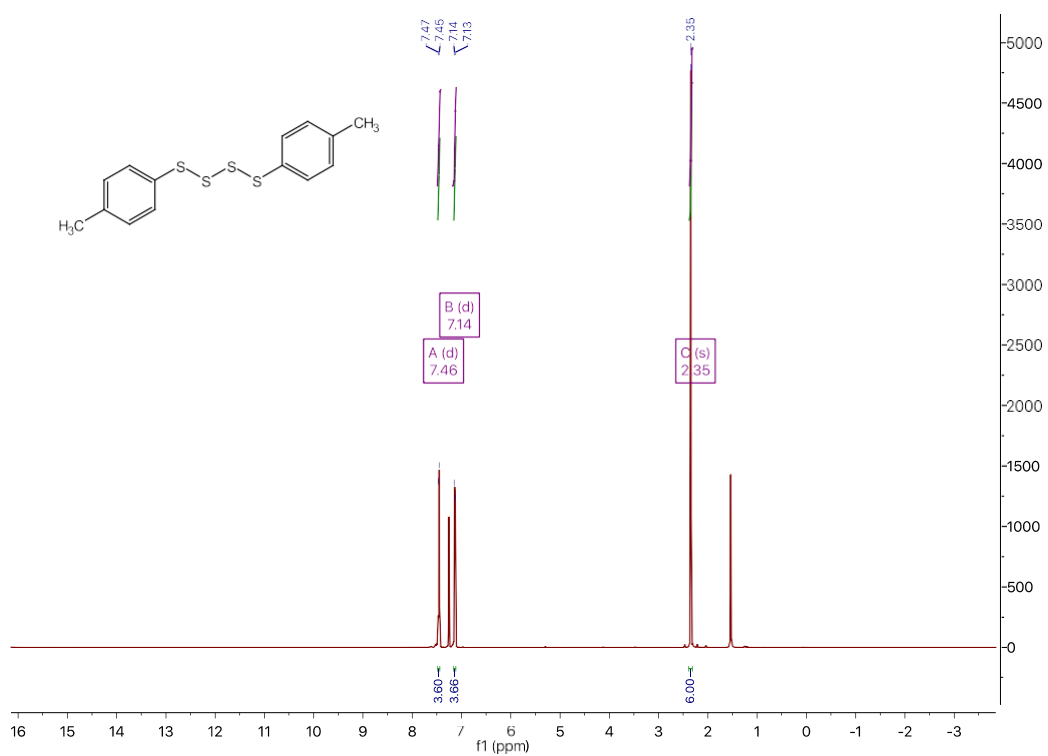


Figure D.13 ^1H NMR (500 MHz, CDCl_3) spectrum of **4**

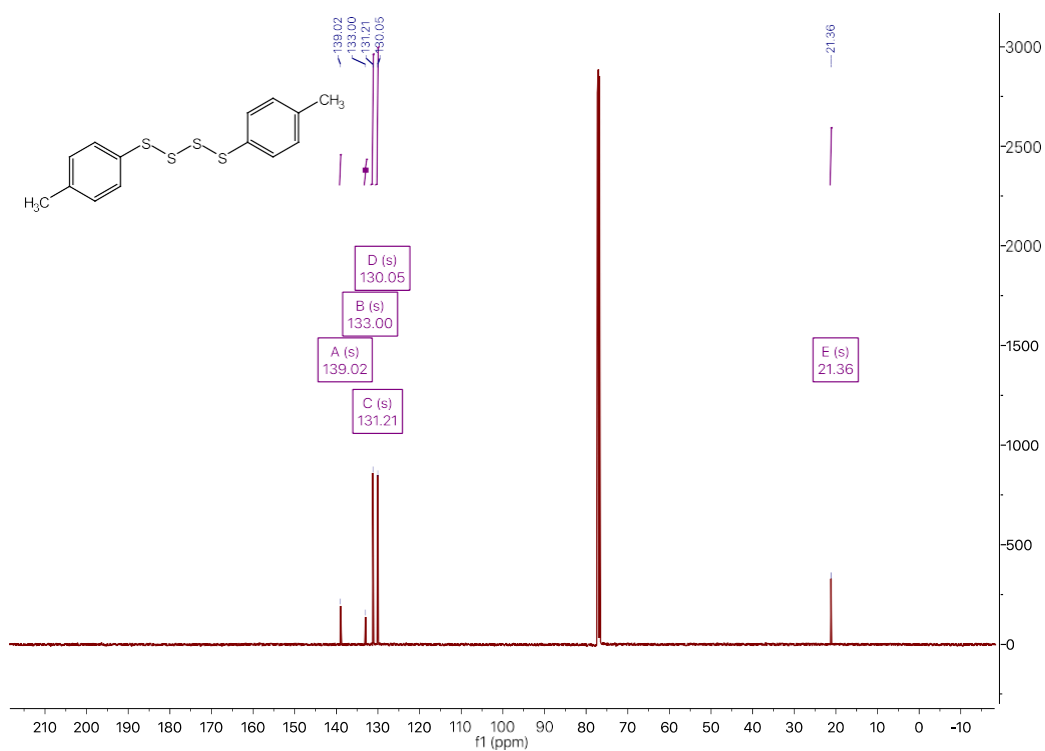


Figure D.10 $^{13}\text{C}\{^1\text{H}\}$ NMR (126 MHz, CDCl_3) spectrum of **4**

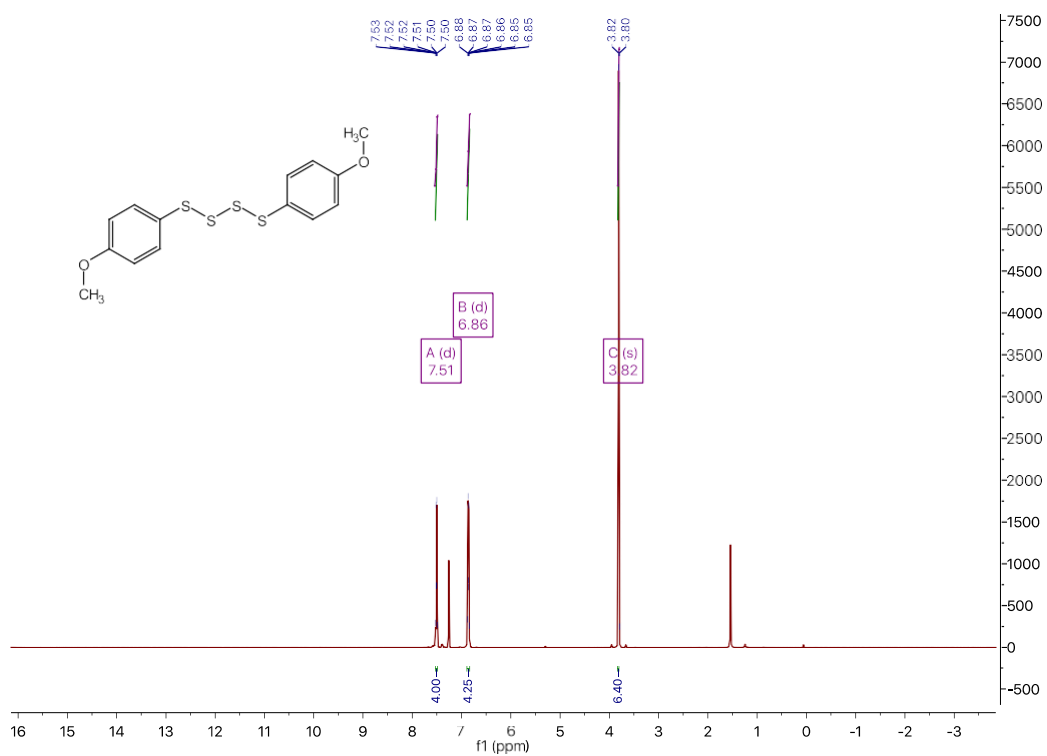


Figure D.13 ^1H NMR (500 MHz, CDCl_3) spectrum of **5**

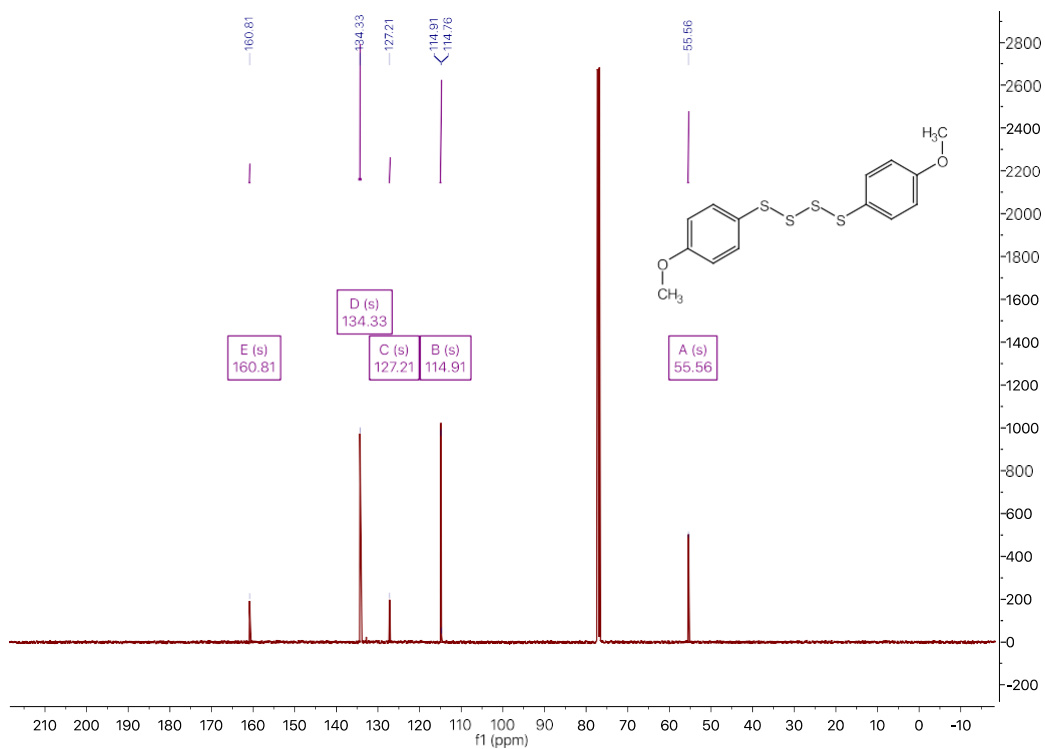


Figure D.12 $^{13}\text{C}\{^1\text{H}\}$ NMR (126 MHz, CDCl_3) spectrum of **5**

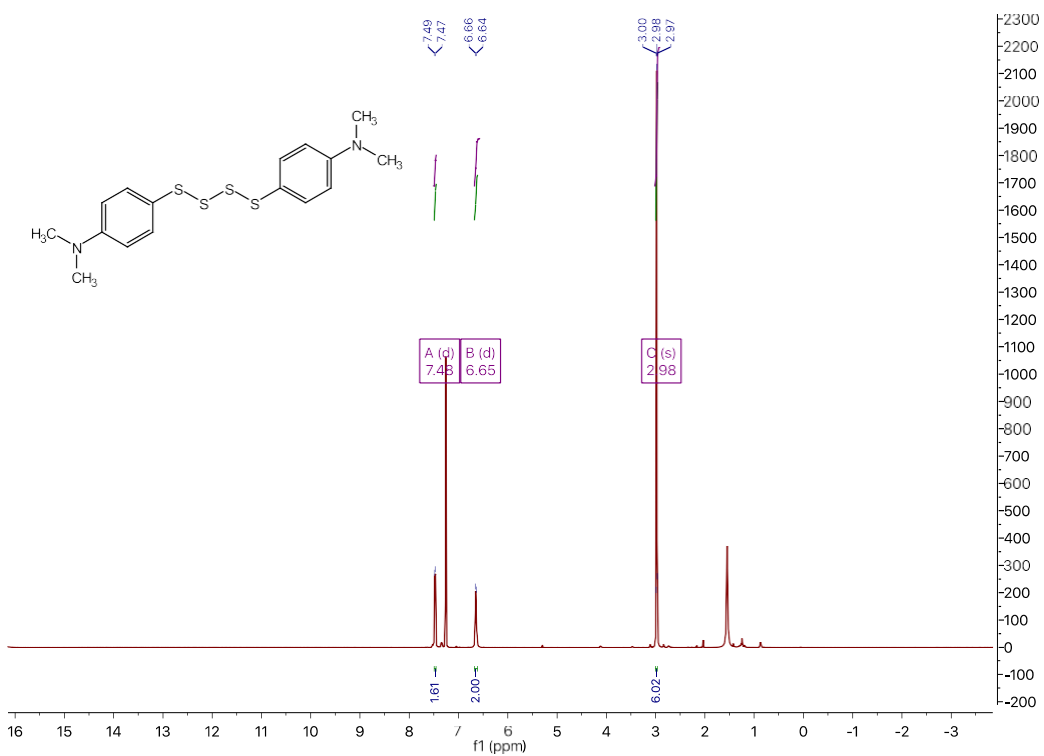


Figure D.13 ^1H NMR (500 MHz, CDCl_3) spectrum of **6**

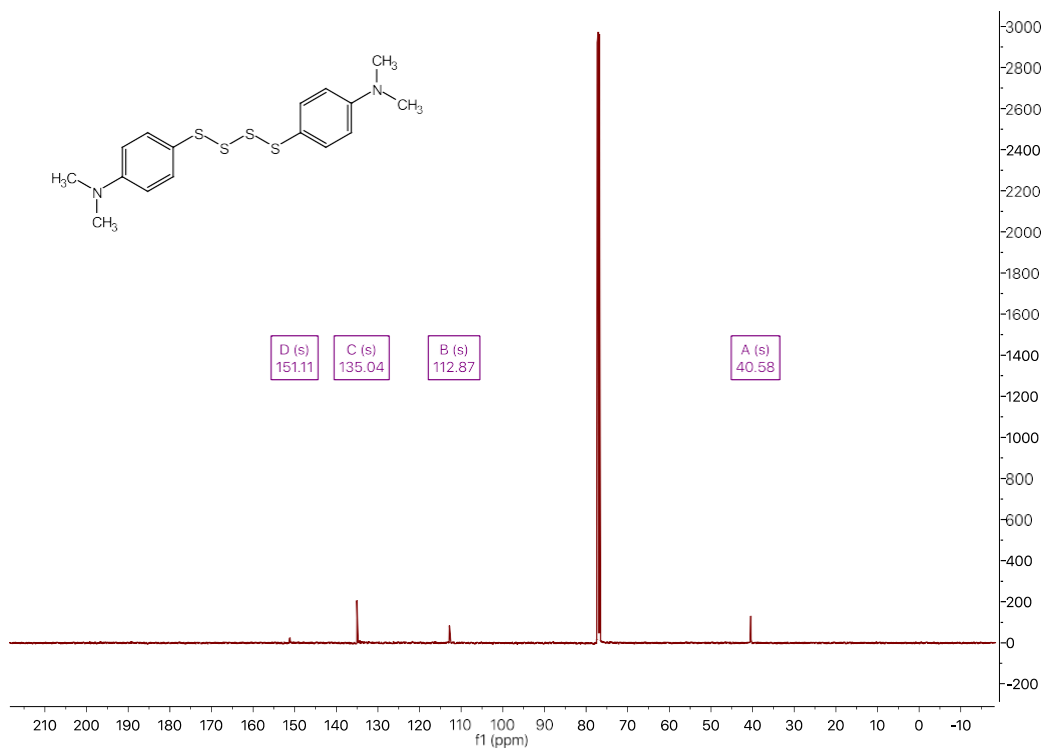


Figure D.14 $^{13}\text{C}\{^1\text{H}\}$ NMR (126 MHz, CDCl_3) spectrum of **6**

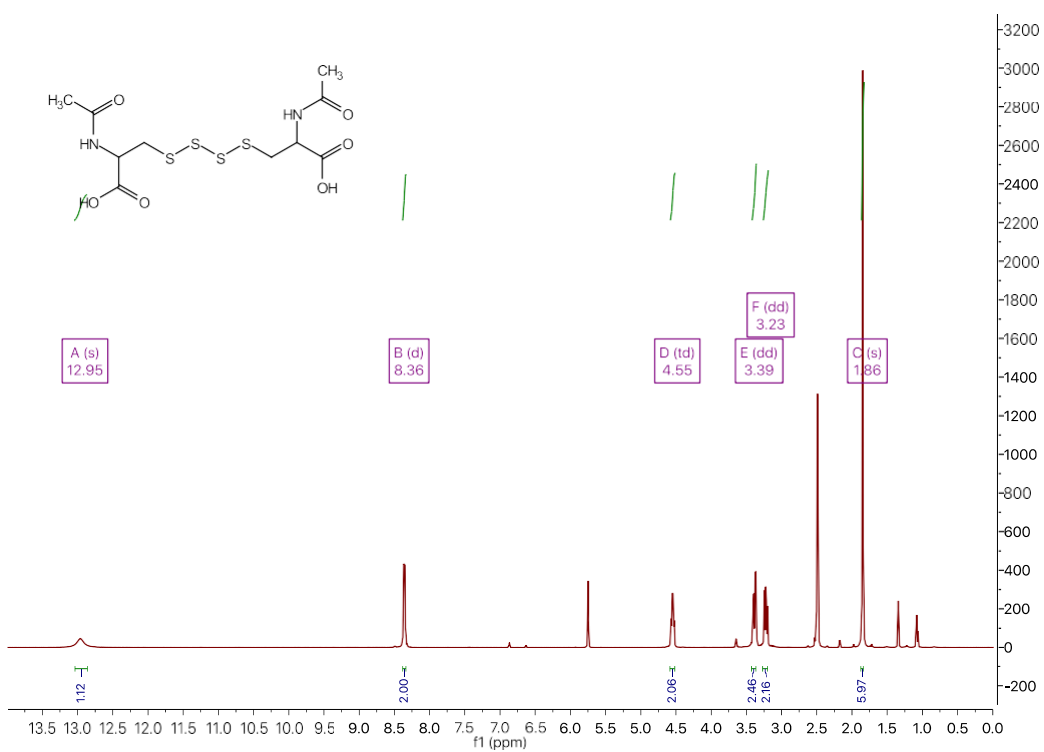


Figure D.15 ^1H NMR (500 MHz, d_6 -DMSO) spectrum of **7**

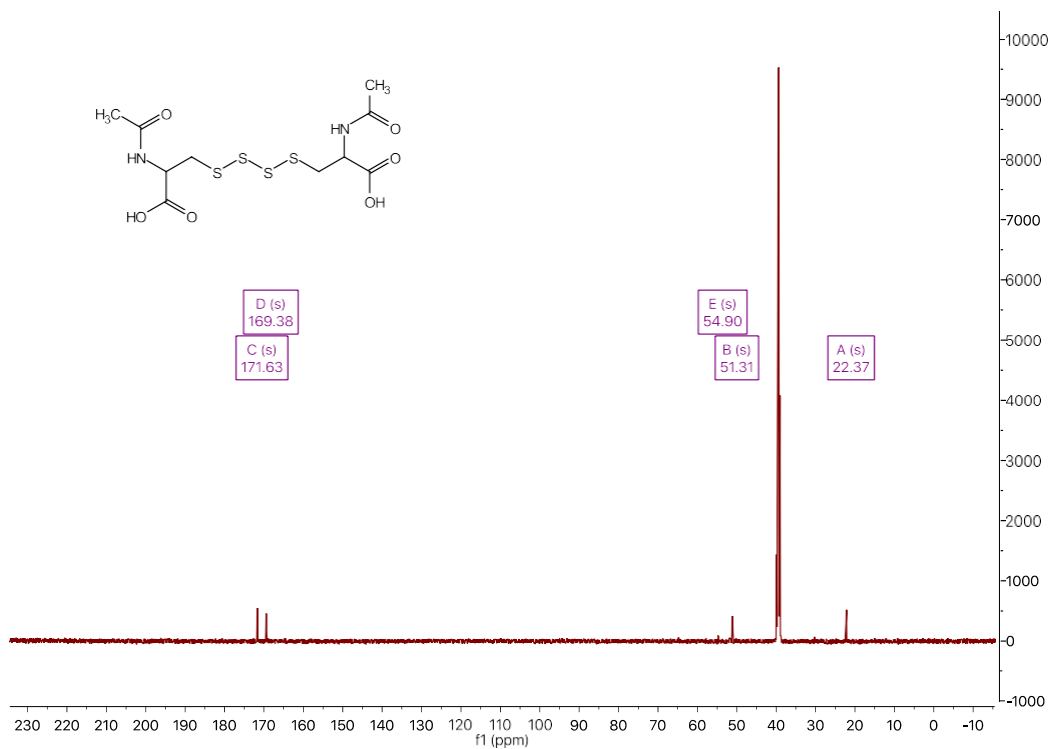


Figure D.16 $^{13}\text{C}\{^1\text{H}\}$ NMR (126 MHz, d^6 -DMSO) spectrum of 7

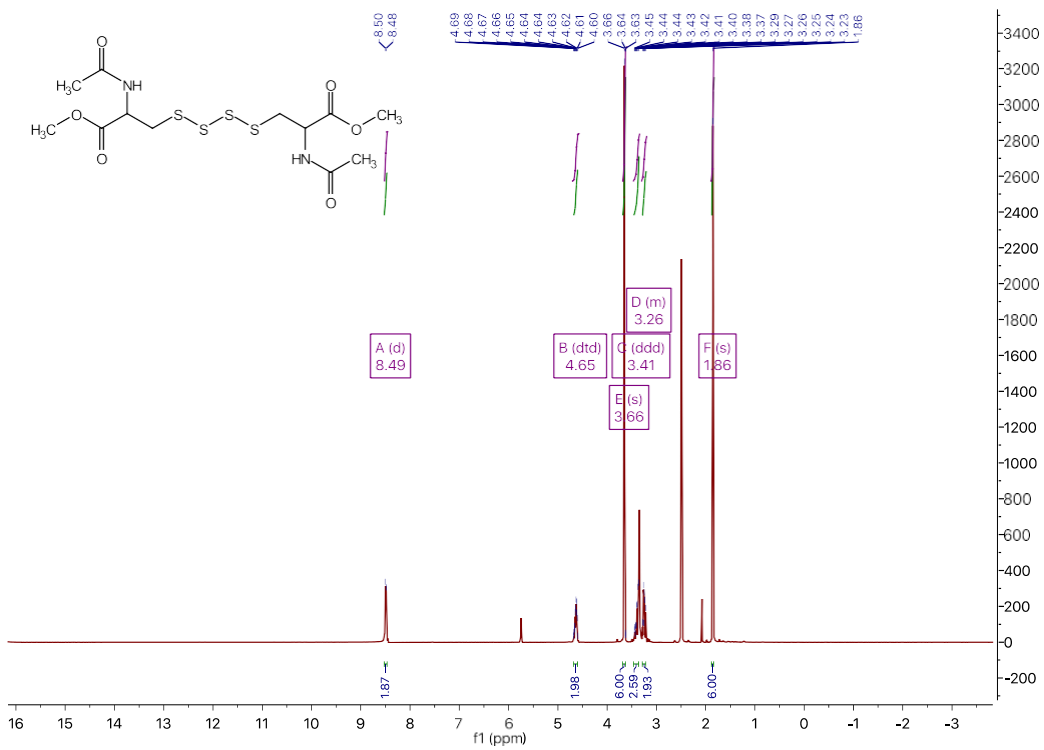


Figure D.15 ^1H NMR (500 MHz, d^6 -DMSO) spectrum of 8

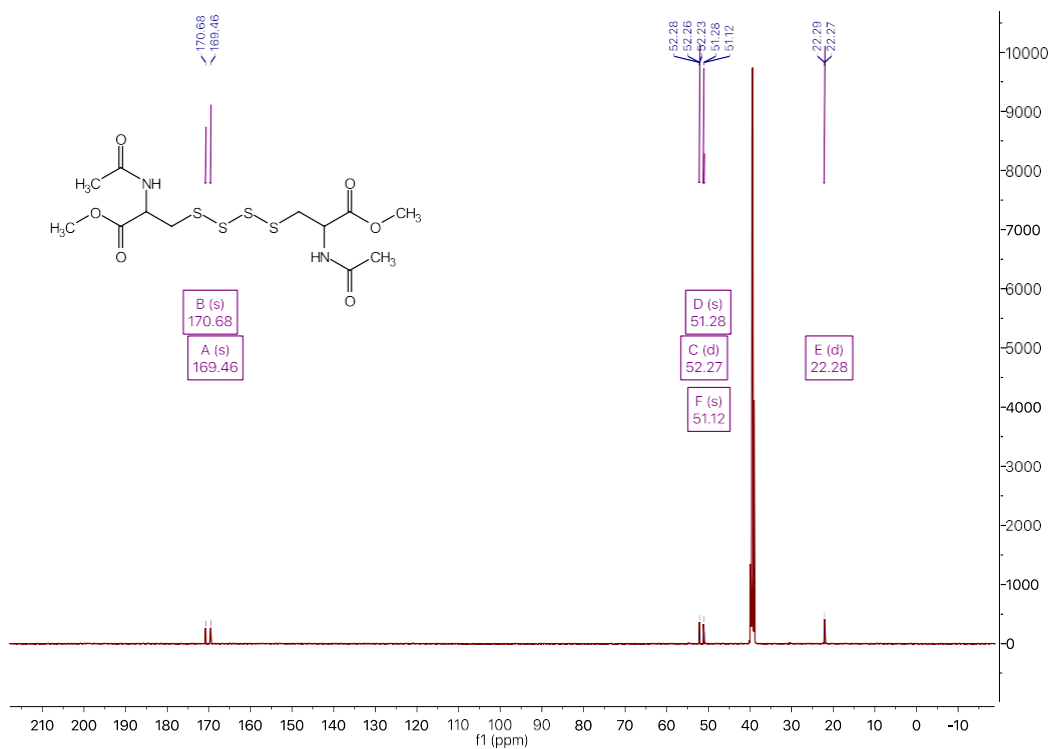


Figure D.18 $^{13}\text{C}\{^1\text{H}\}$ NMR (126 MHz, d^6 -DMSO) spectrum of **8**

HPLC Data

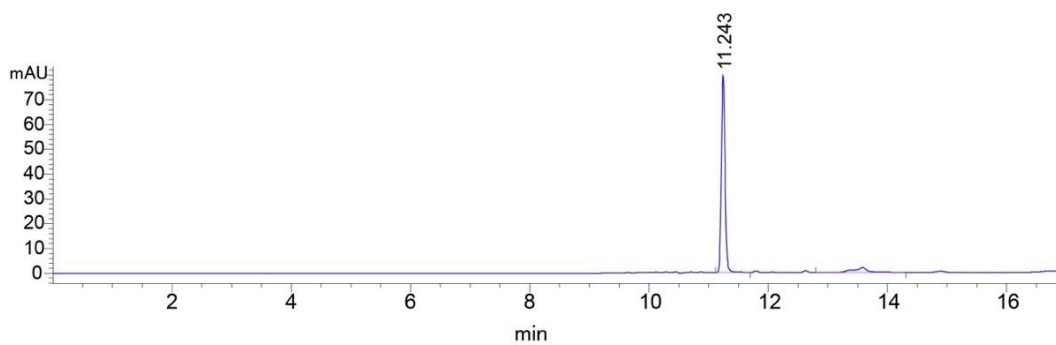


Figure D.19 HPLC Trace of **3**

Hammett Plot Data

Donor	R	σ
1	-CF ₃	0.54
2	-F	0.06
3	-H	0
4	-Me	-0.17
5	-OMe	-0.27
6	-NMe ₂	-0.83

Table D.1 Hammett σ parameters

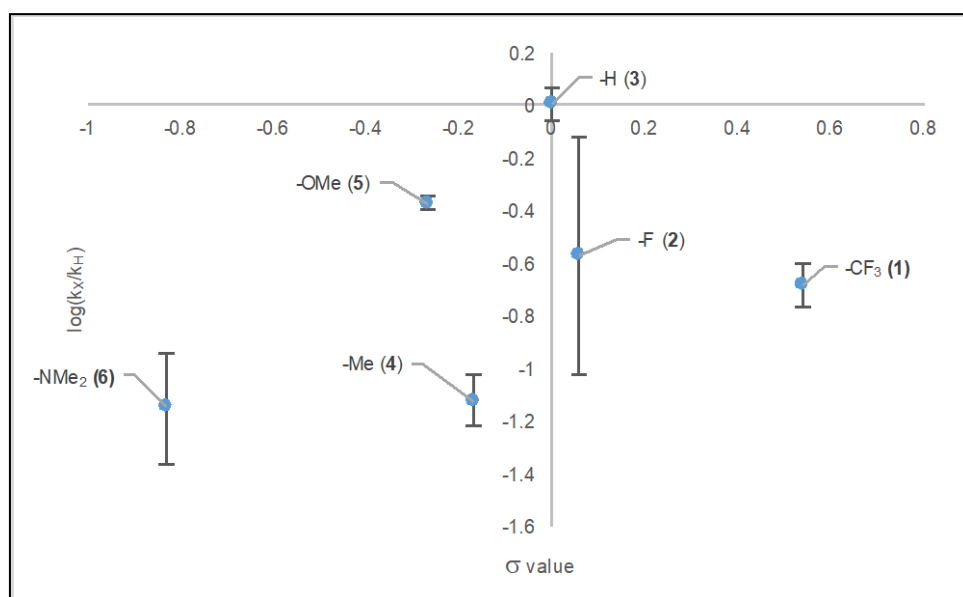


Figure D.20 Hammett plot for H₂S release from tetrasulfides

Donor	Initial Rate (nA/s)	Relative Rate
1	0.01128 ± 0.002	5.1
2	0.0151 ± 0.009	6.8
3	0.0547 ± 0.008	24.7
4	0.0041 ± 0.0009	1.9
5	0.0231 ± 0.001	10.4
6	0.0038 ± 0.002	1.7
7	0.0032 ± 0.0008	1.5
8	0.0033 ± 0.0002	1.5
DATS	0.0022 ± 0.0003	1.0

Table D.2 Tabulated initial rates for tetrasulfides (1-8) and **DATS** ($n = 3$)

APPENDIX E

SUPPLEMENTARY INFORMATION FOR CHAPTER V

Appendix E is the supplementary information for Chapter V of this dissertation. It includes spectra and experimental data relevant to the content in Chapter V.

NMR Spectra

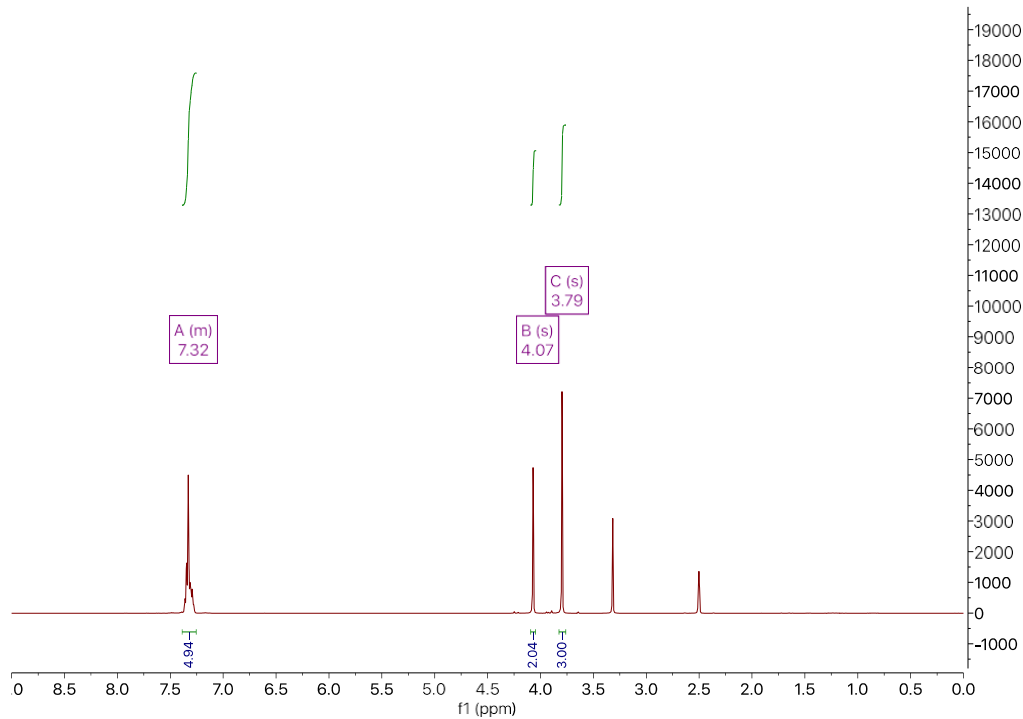


Figure E.1 ¹H NMR (500 MHz, DMSO-d₆) spectrum of *SS*-benzyl *O*-methyl carbono(dithioperoxoate)

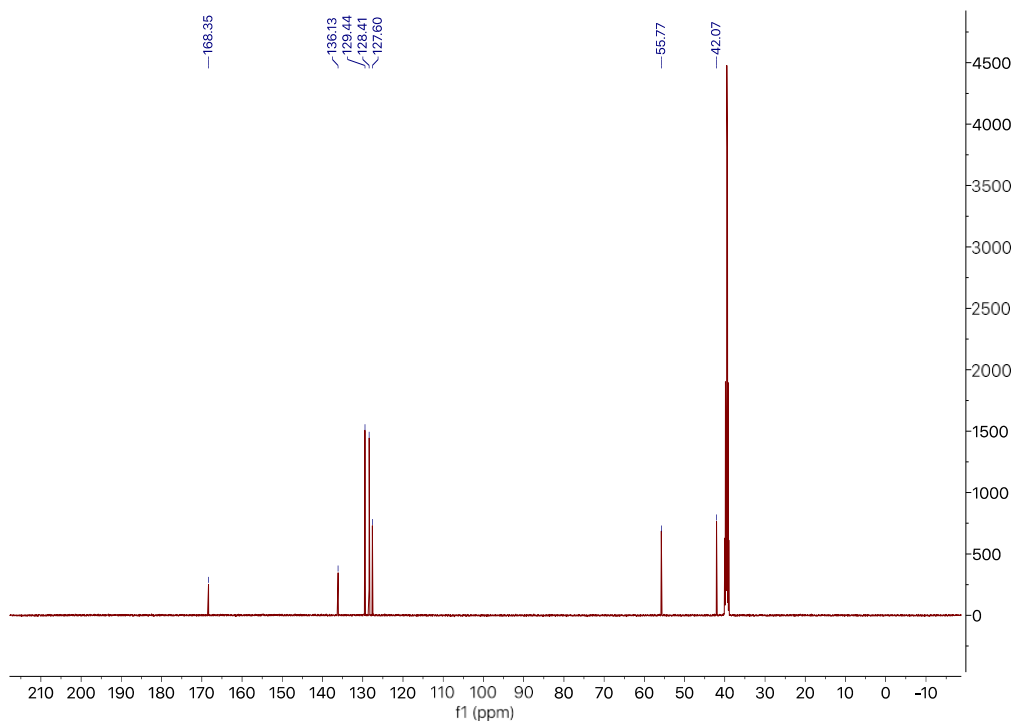


Figure E.2 $^{13}\text{C}\{^1\text{H}\}$ NMR (126 MHz, DMSO-d_6) spectrum of SS-benzyl O-methyl carbonodithioperoxoate)

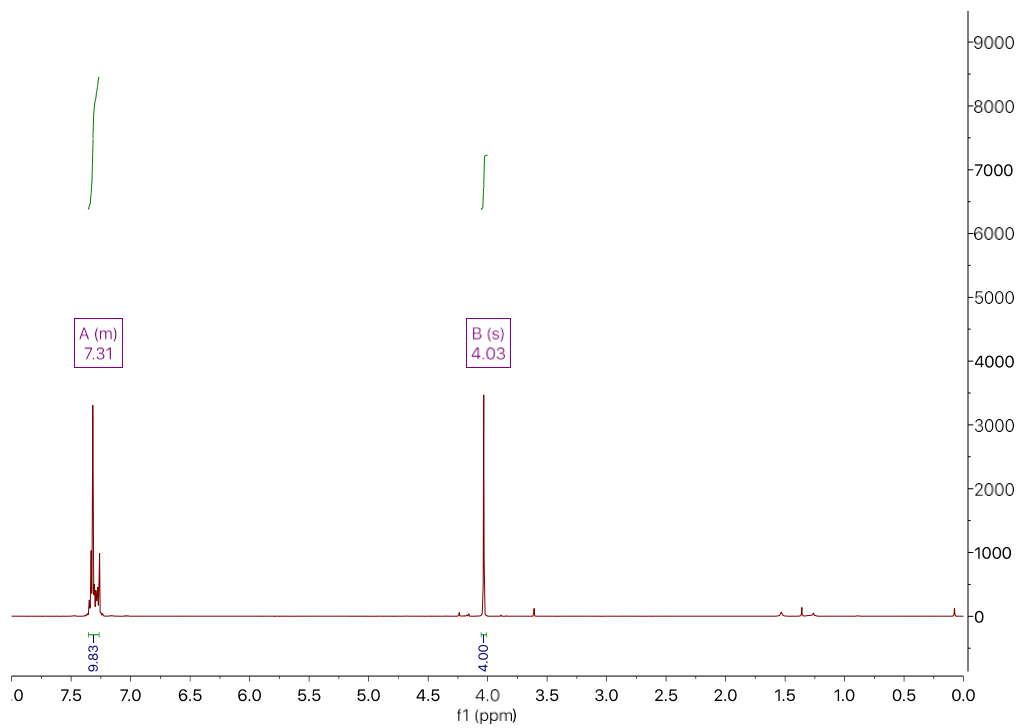


Figure E.3 ^1H NMR (500 MHz, CDCl_3) spectrum of Bn_2S_3

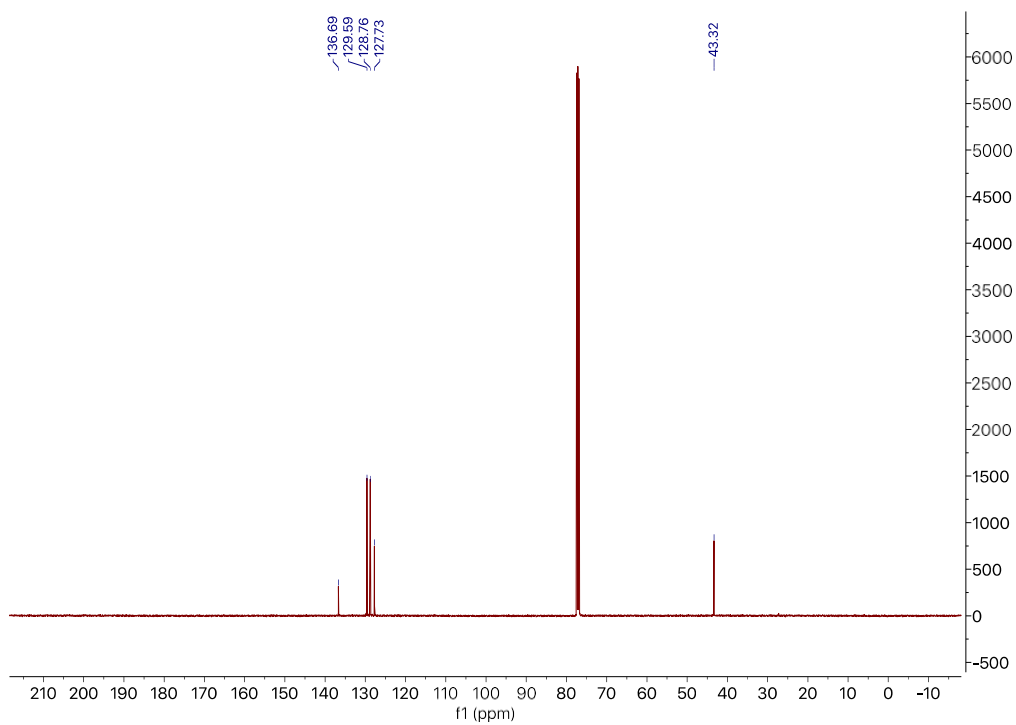


Figure E.4 $^{13}\text{C}\{^1\text{H}\}$ NMR (126 MHz, CDCl_3) spectrum of **Bn₂S₃**

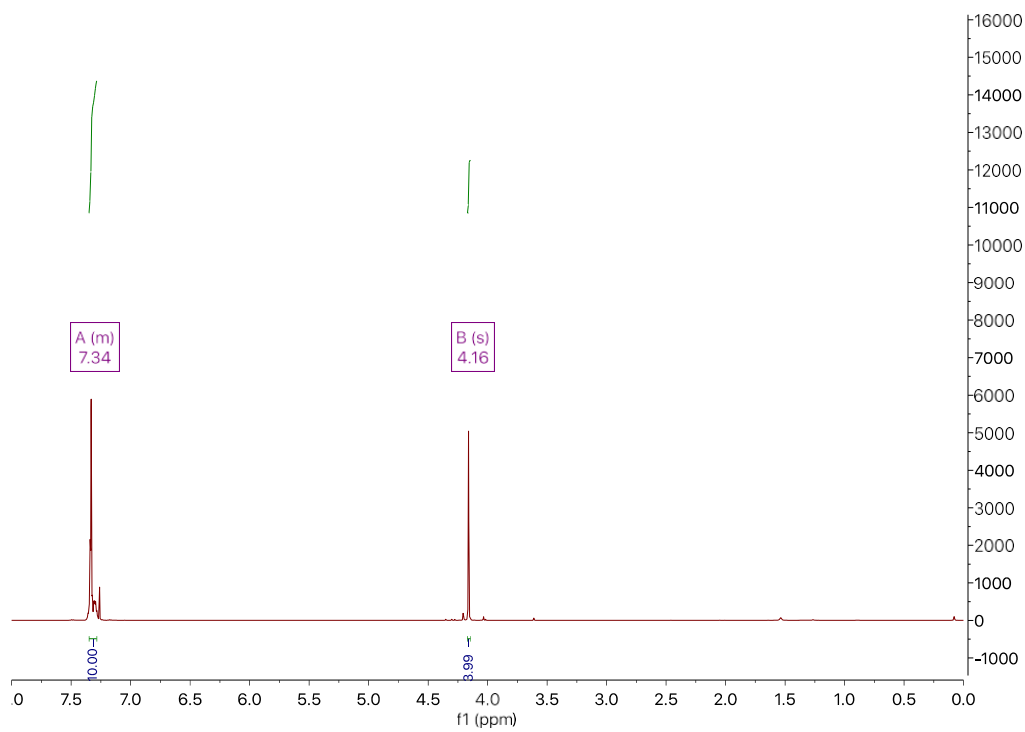


Figure E.3 ^1H NMR (500 MHz, CDCl_3) spectrum of **Bn₂S₄**

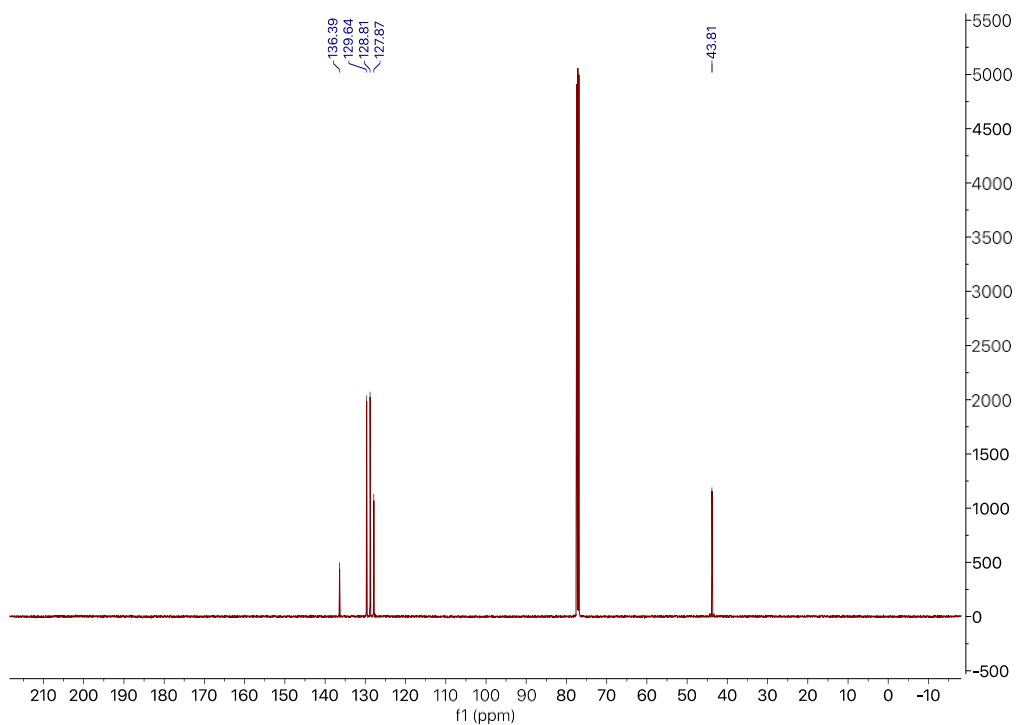


Figure E.6 $^{13}\text{C}\{^1\text{H}\}$ NMR (126 MHz, CDCl_3) spectrum of Bn_2S_4

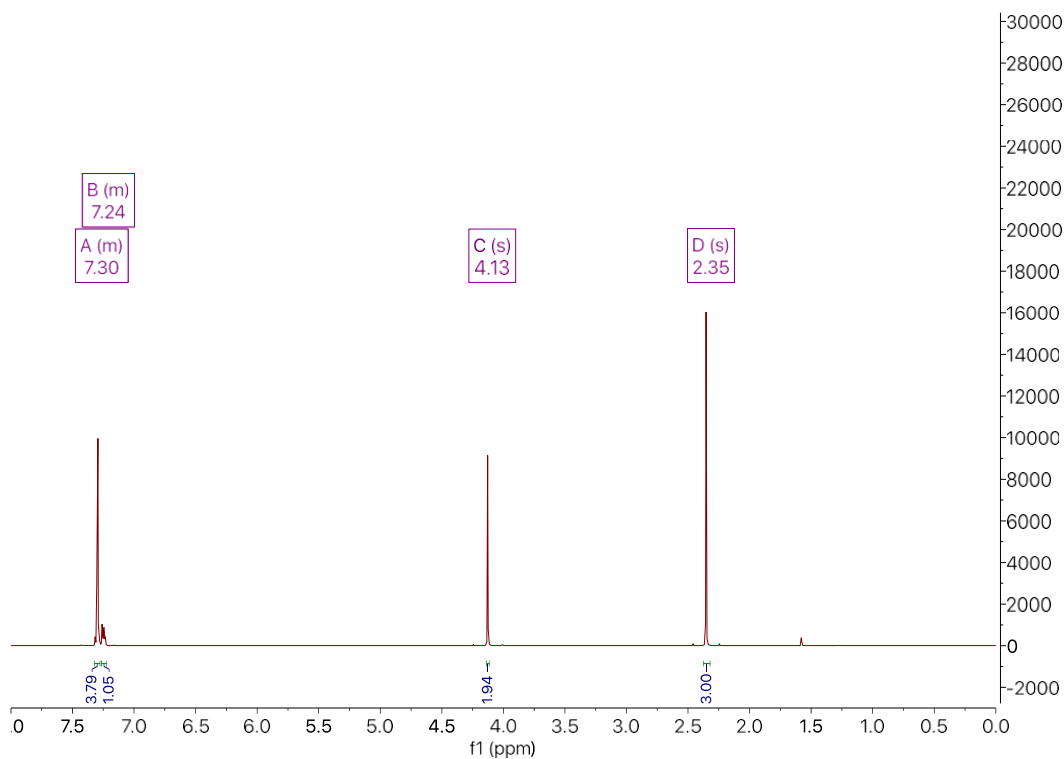


Figure E.7 ^1H NMR (600 MHz, CDCl_3) spectrum of *S*-benzyl ethanethioate

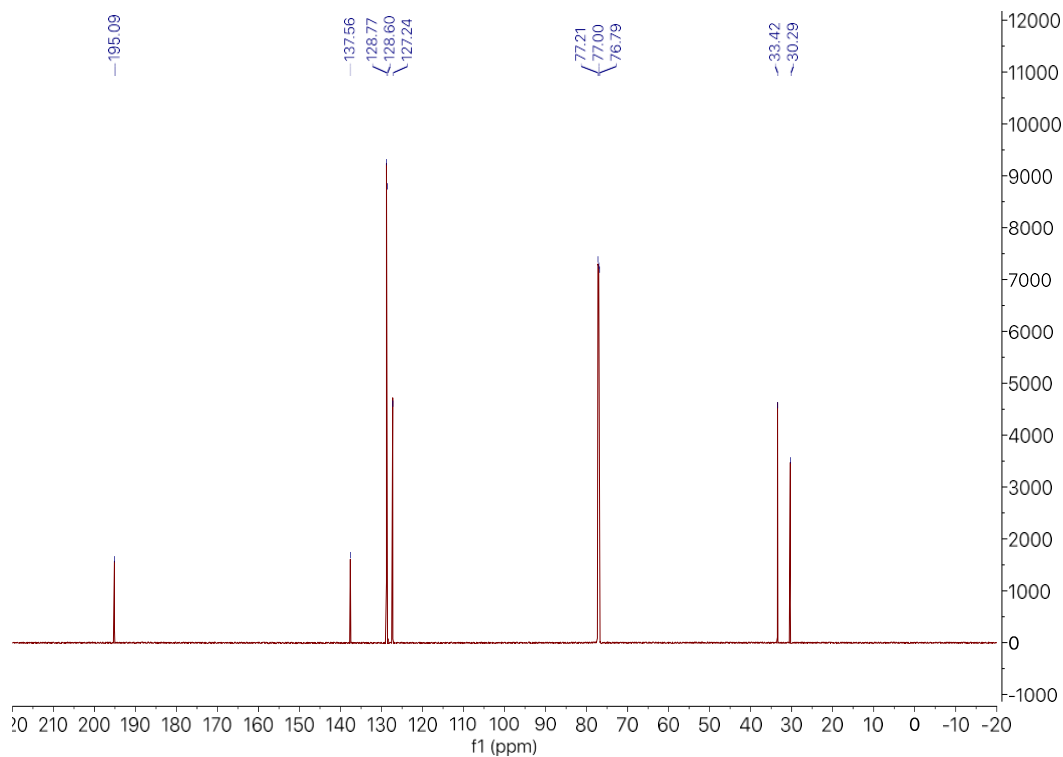


Figure E.8 $^{13}\text{C}\{^1\text{H}\}$ NMR (126 MHz, CDCl_3) spectrum of *S*-benzyl ethanethioate

Cell Proliferation Data

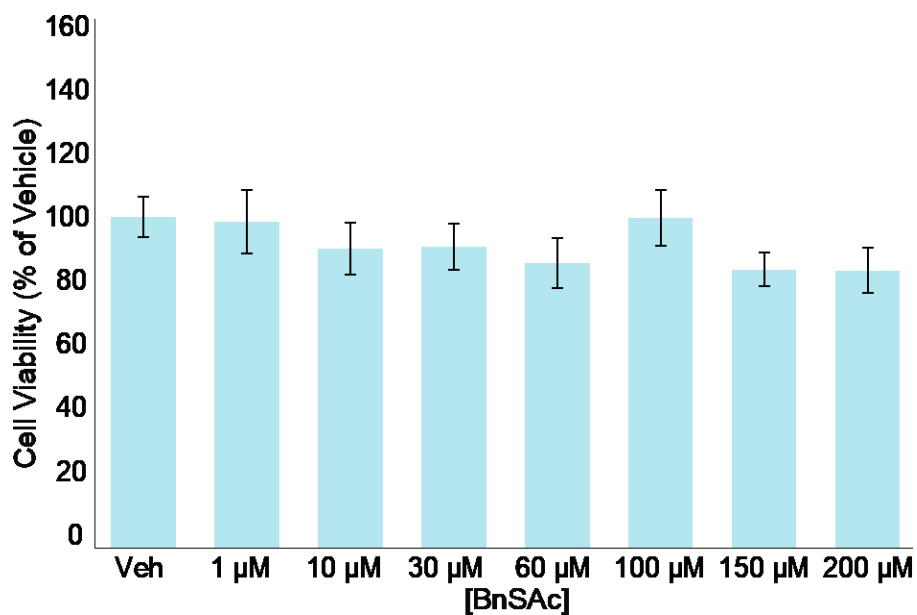


Figure E.9 Pooled average of cell proliferation data under **BnSAc** treatment. (n = 2)

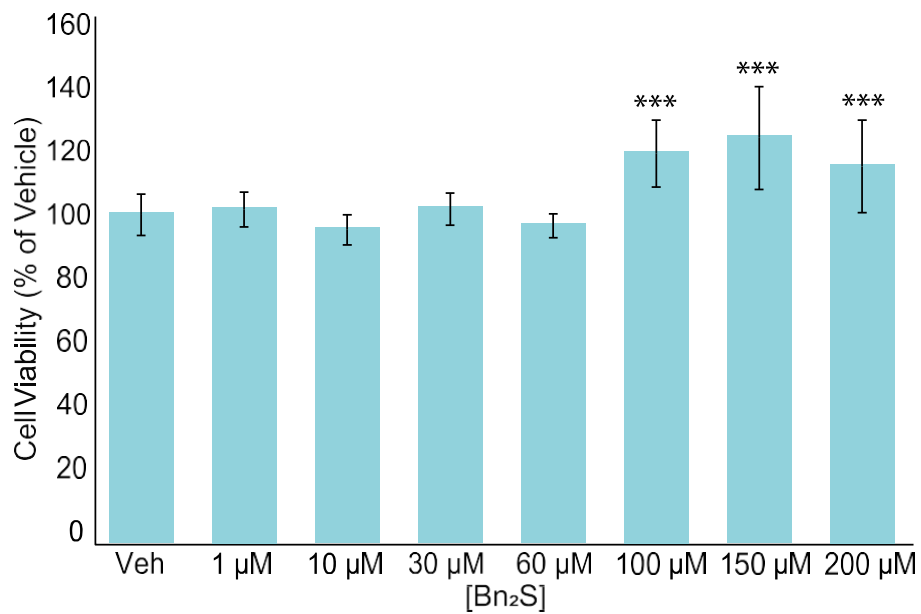


Figure E.10 Pooled average of cell proliferation data under **Bn₂S** treatment. (n=4)

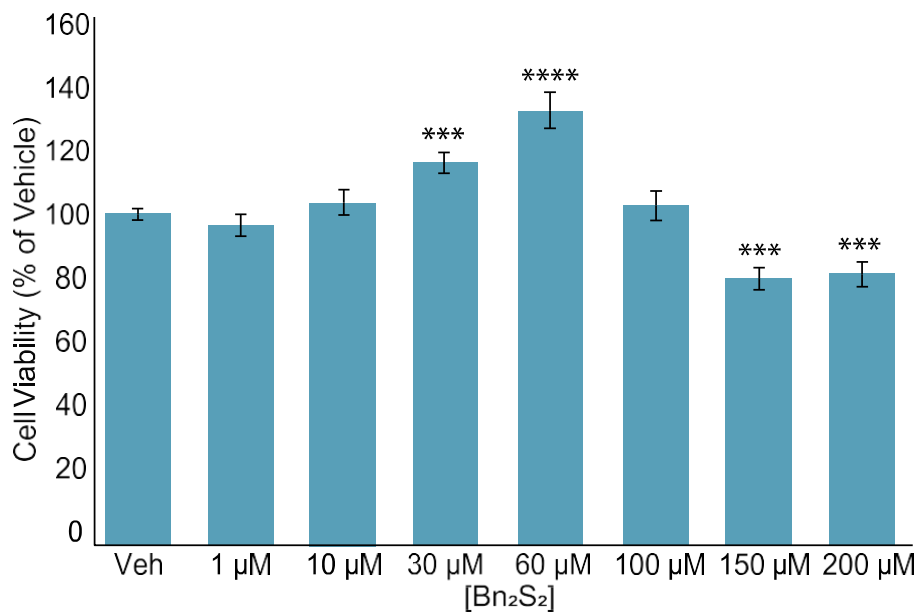


Figure E.11 Pooled average of cell proliferation data under **Bn₂S₂** treatment. (n=5)

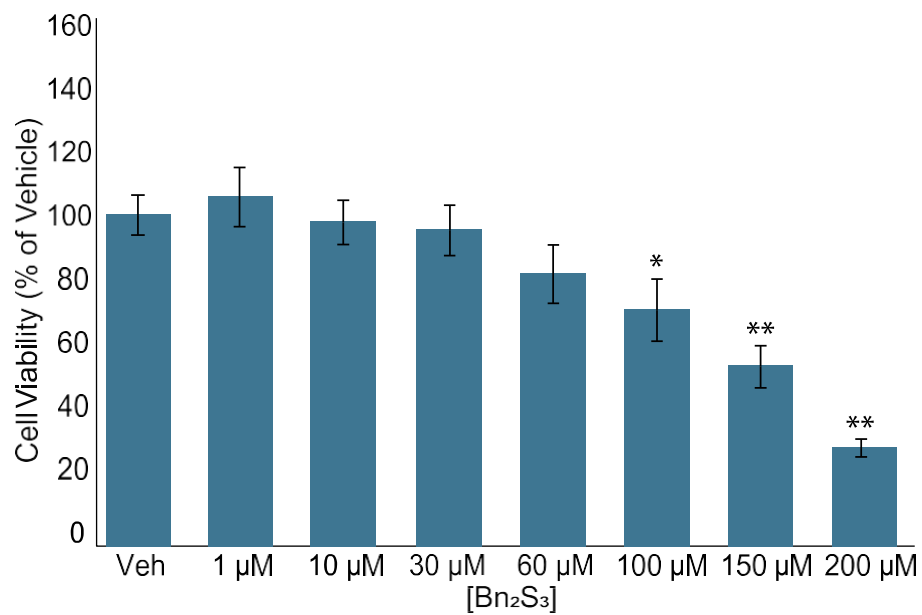


Figure E.12 Pooled average of cell proliferation data under Bn_2S_3 treatment. (n=3)

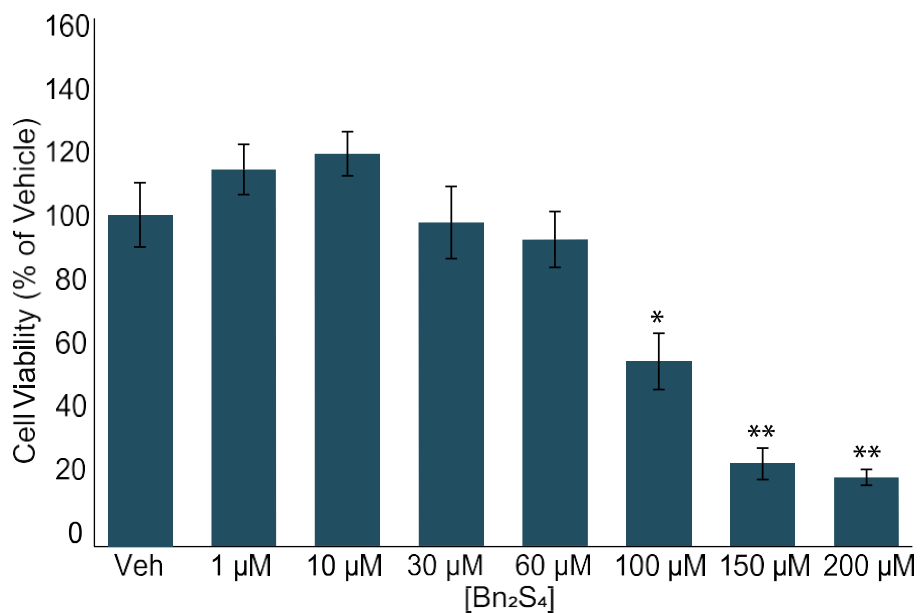


Figure E.13 Pooled average of cell proliferation data under Bn_2S_4 treatment. (n=3)

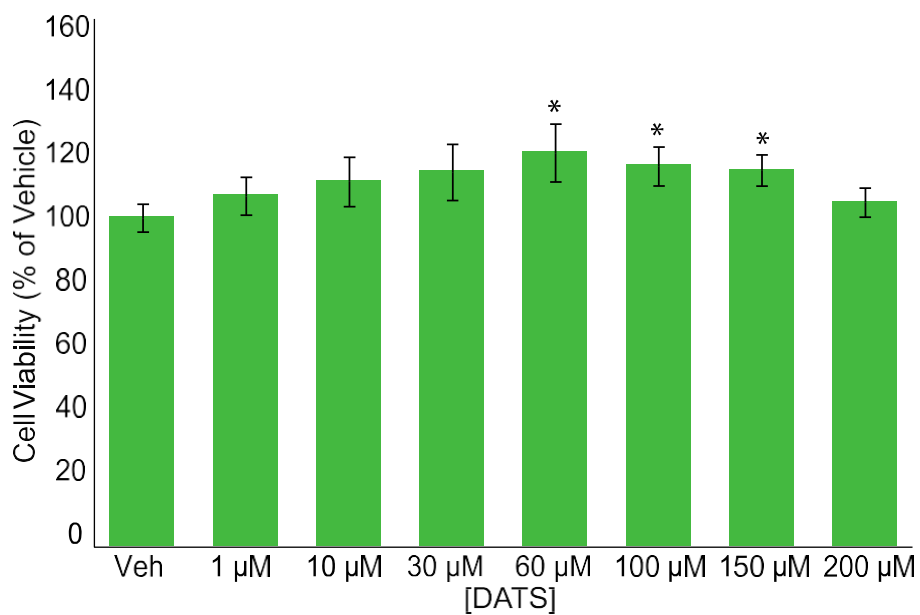


Figure E.14 Pooled average of cell proliferation data under **DATS** treatment. (n=4)

MBA Calibration Curves

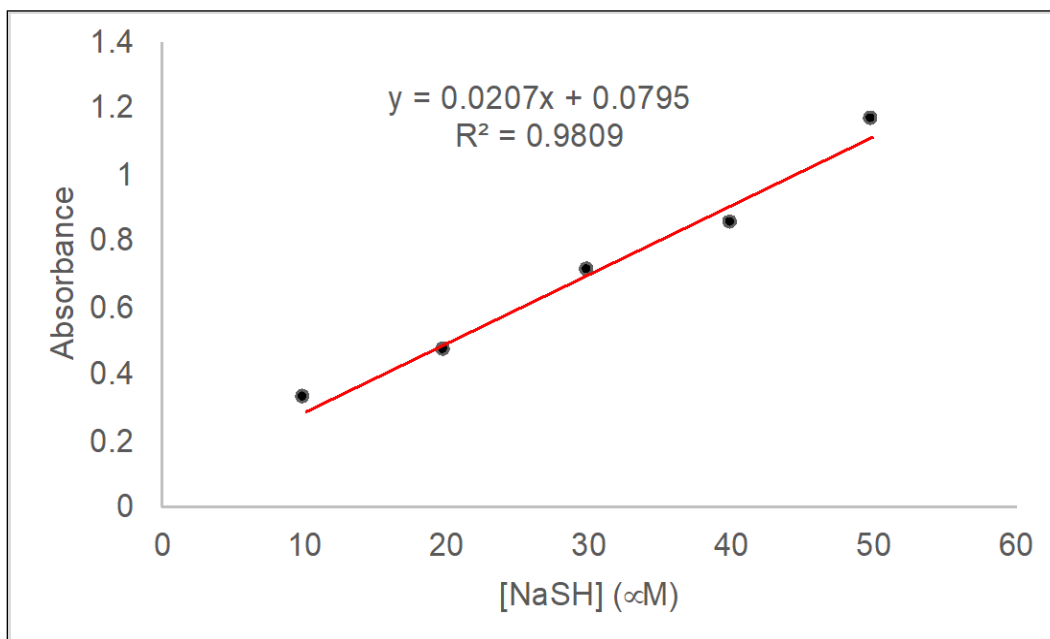


Figure E.15 MBA calibration curve generated using known concentrations of NaSH in the presence of 500 μM cysteine.

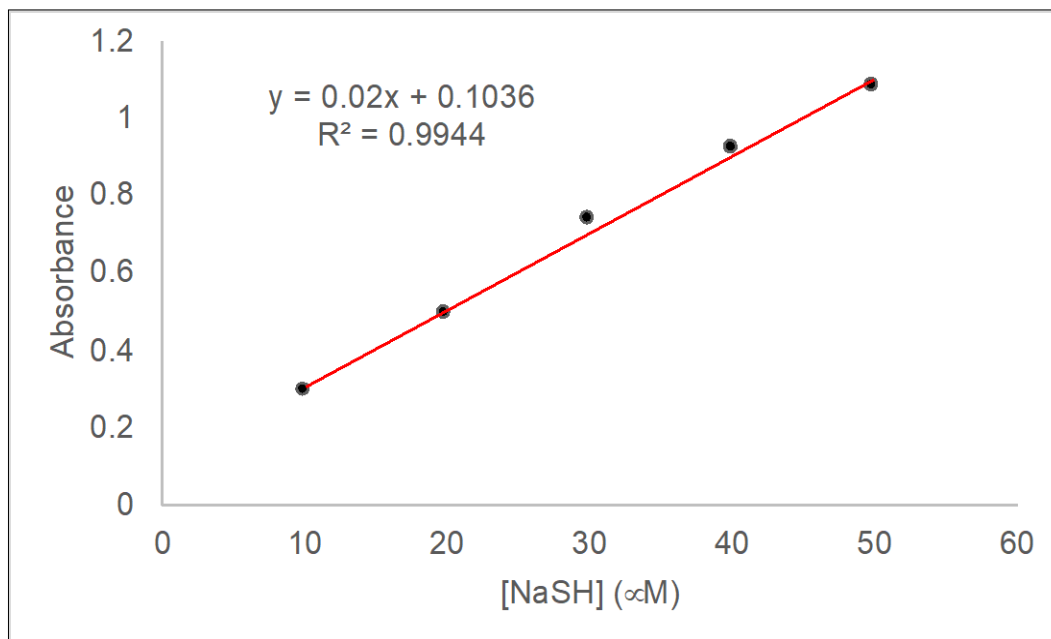
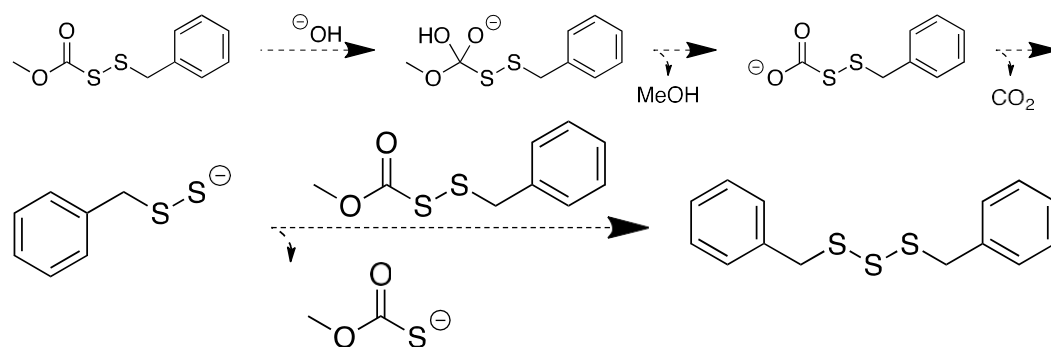


Figure E.16 MBA calibration curve generated using known concentrations of NaSH in the presence of 500 μM GSH.

Proposed Reaction Mechanism for Bn_2S_3 Synthesis



Scheme E.1 Proposed reaction mechanism for trisulfide synthesis via hydroxide-mediated decomposition of sulfenyl thiocarbonates.

APPENDIX F

SUPPLEMENTARY INFORMATION FOR CHAPTER VI

Appendix F is the supplementary information for Chapter VI of this dissertation. It includes spectra and experimental data relevant to the content in Chapter VI.

NMR Spectra

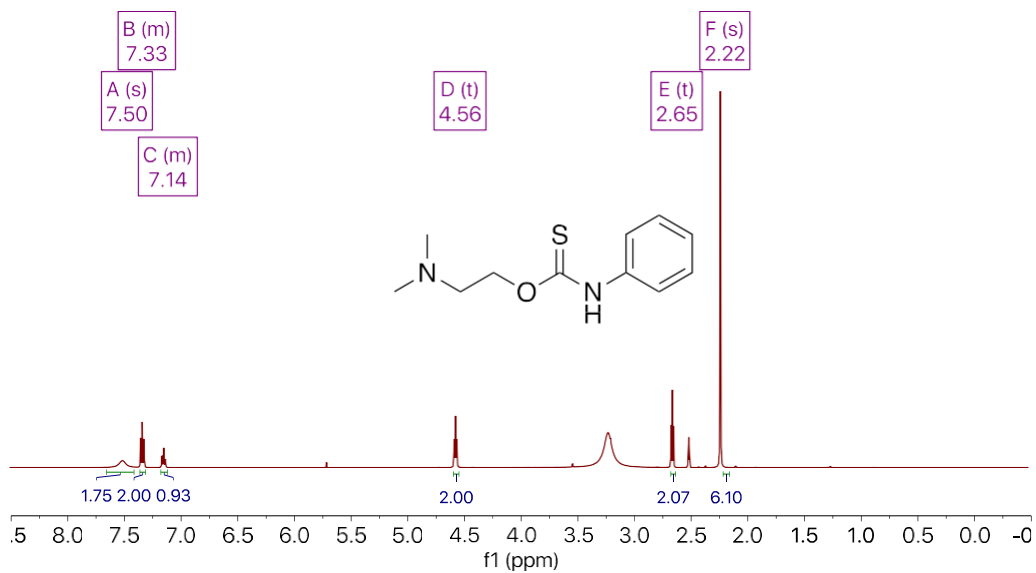


Figure F.1 ¹H NMR (500 MHz, DMSO-*d*₆) spectrum of **PhTC** at 60 °C

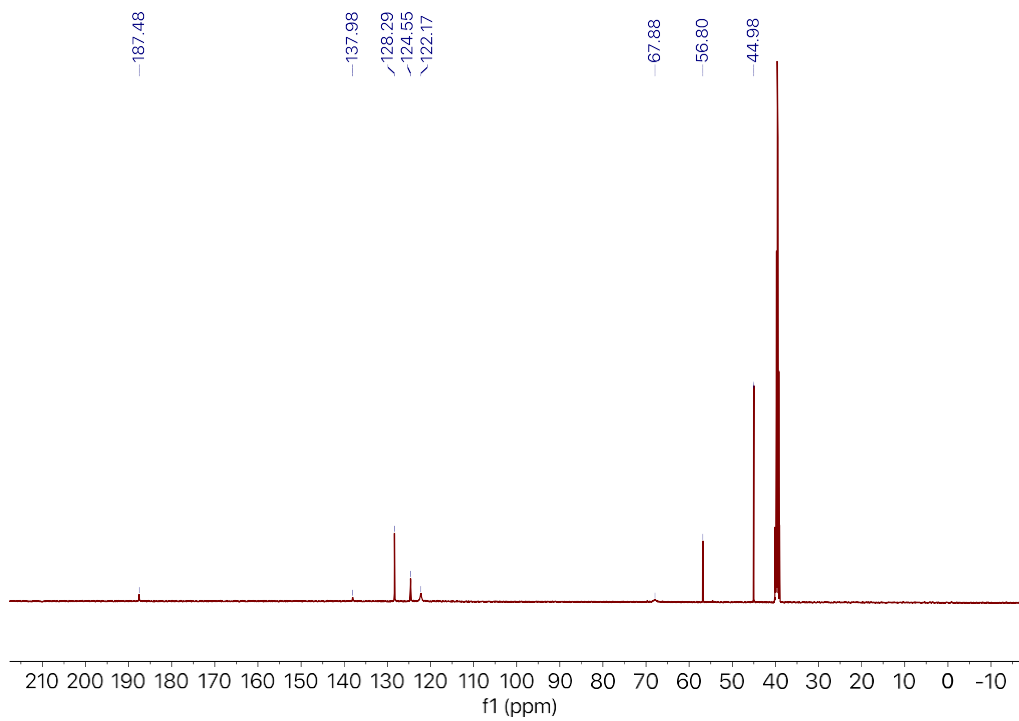


Figure F.2 $^{13}\text{C}\{^1\text{H}\}$ NMR (126 MHz, $\text{DMSO-}d^6$) spectrum of **PhTC** at 60 °C

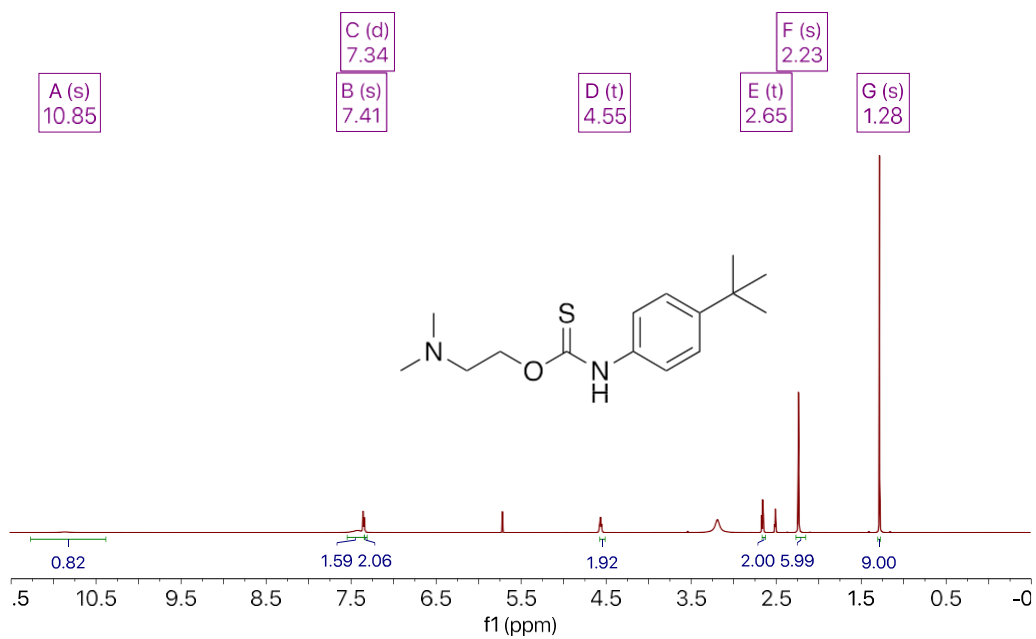


Figure F.3 ^1H NMR (500 MHz, $\text{DMSO-}d^6$) spectrum of **4-^tBuPhTC** at 60 °C

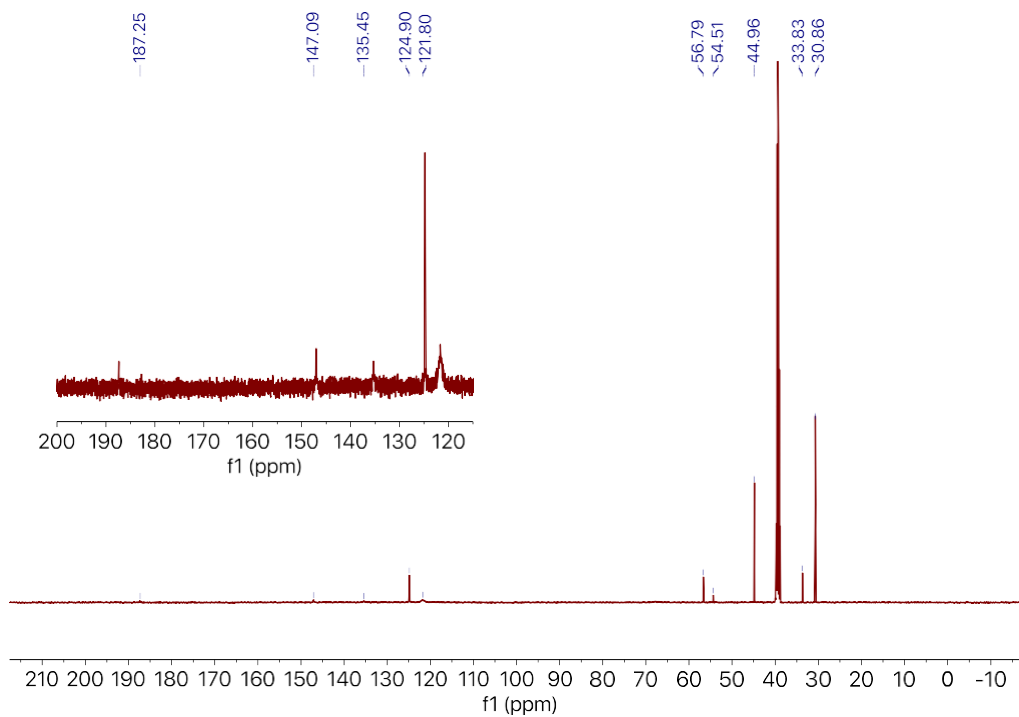


Figure F.4 $^{13}\text{C}\{^1\text{H}\}$ NMR (126 MHz, $\text{DMSO-}d^6$) spectrum of **4-BuPhTC** at 60 °C

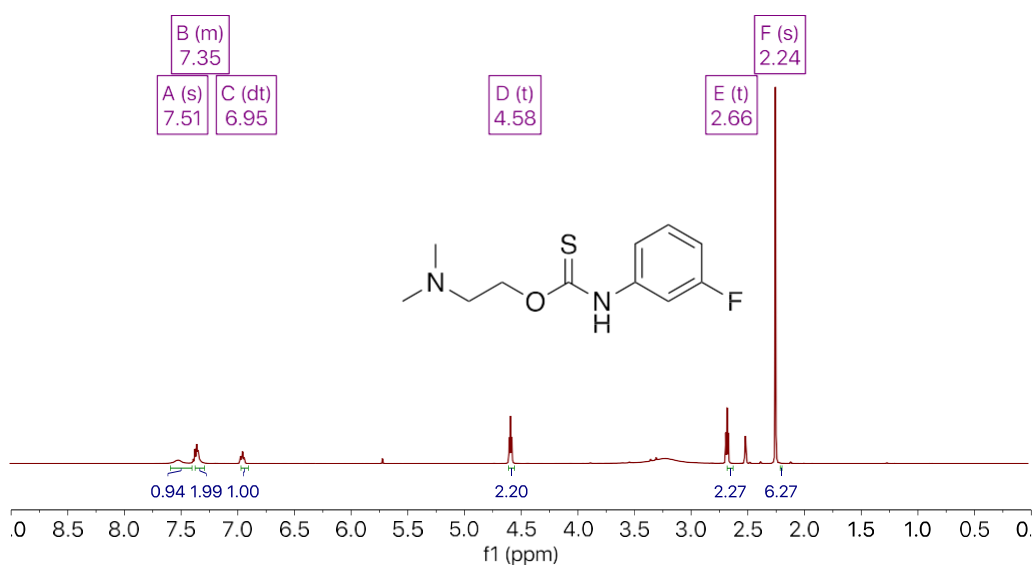


Figure F.5 ^1H NMR (500 MHz, $\text{DMSO-}d^6$) spectrum of **3-FPhTC** at 60 °C

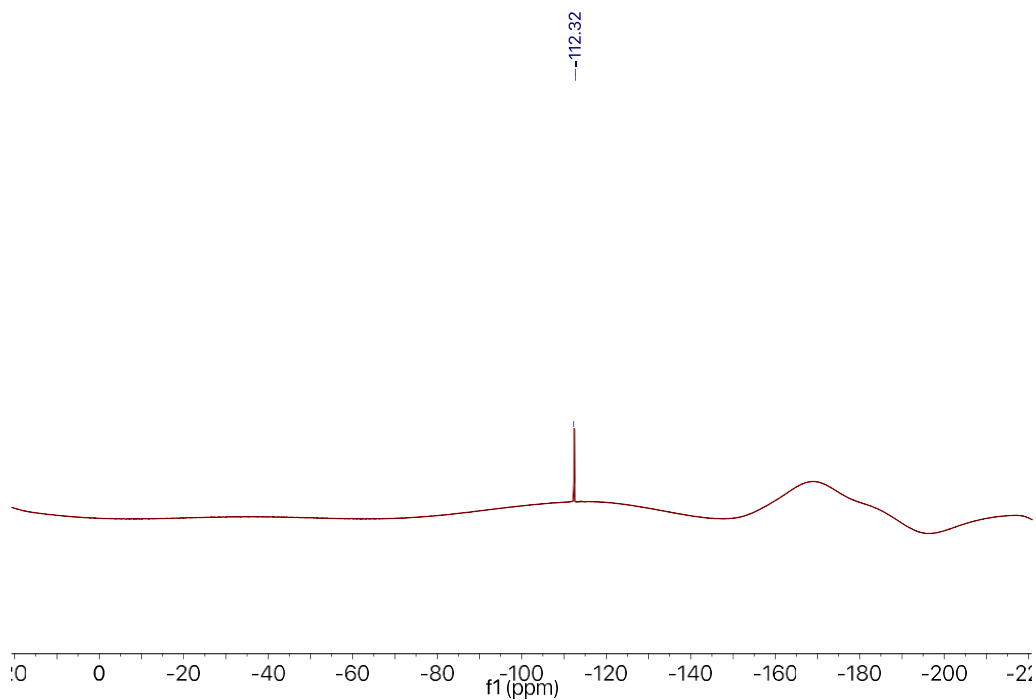


Figure F.6 ^{19}F NMR (471 MHz, $\text{DMSO-}d_6$) spectrum of **3-FPhTC** at 60 °C

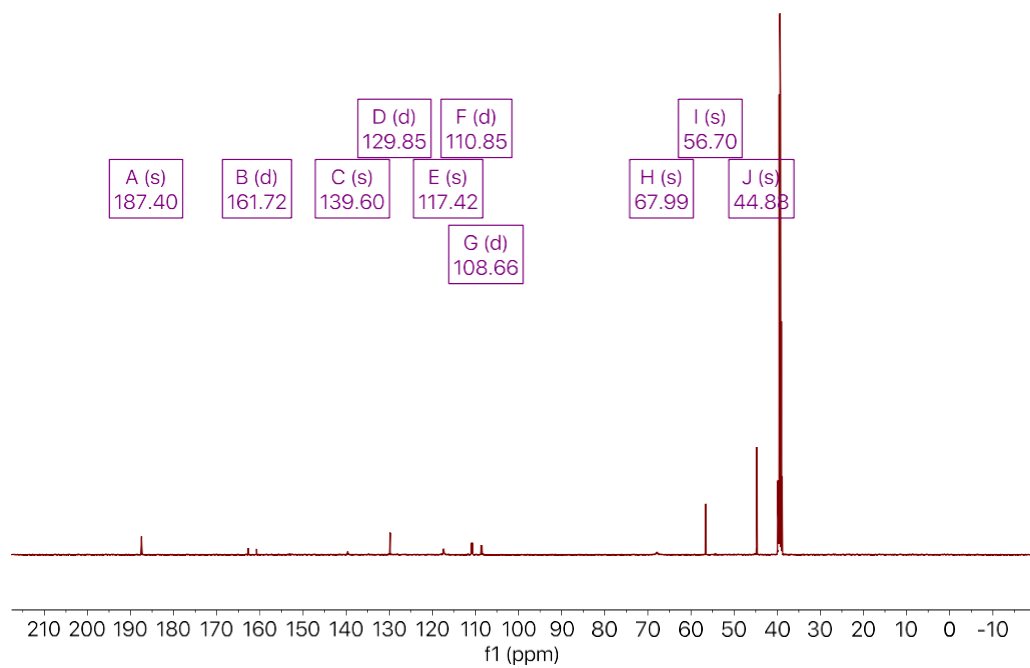


Figure F.7 $^{13}\text{C}\{^1\text{H}\}$ NMR (126 MHz, $\text{DMSO-}d_6$) spectrum of **3-FPhTC** at 60 °C

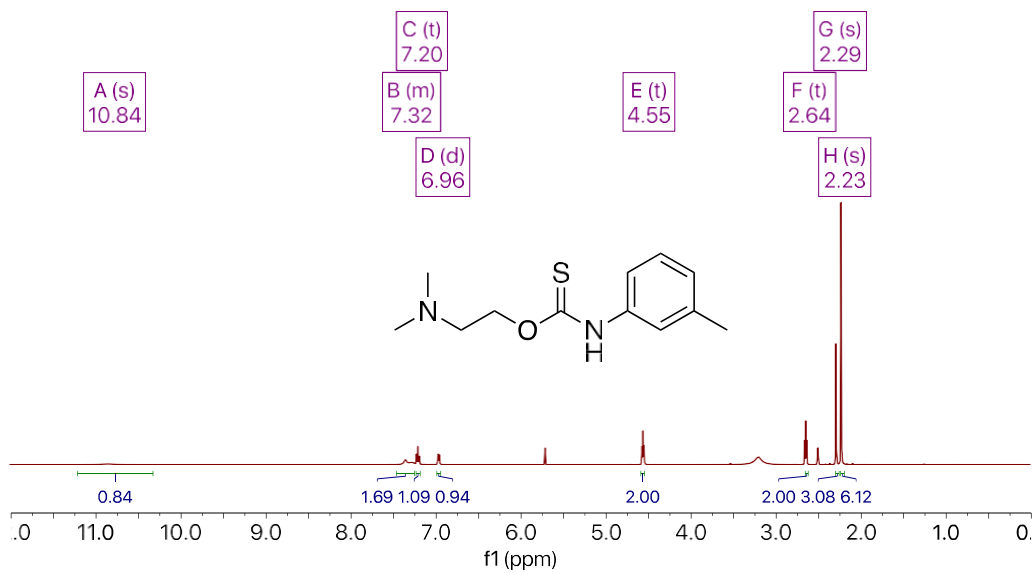


Figure F.8 ^1H NMR (500 MHz, $\text{DMSO-}d_6$) spectrum of **3-MePhTC** at 60 °C

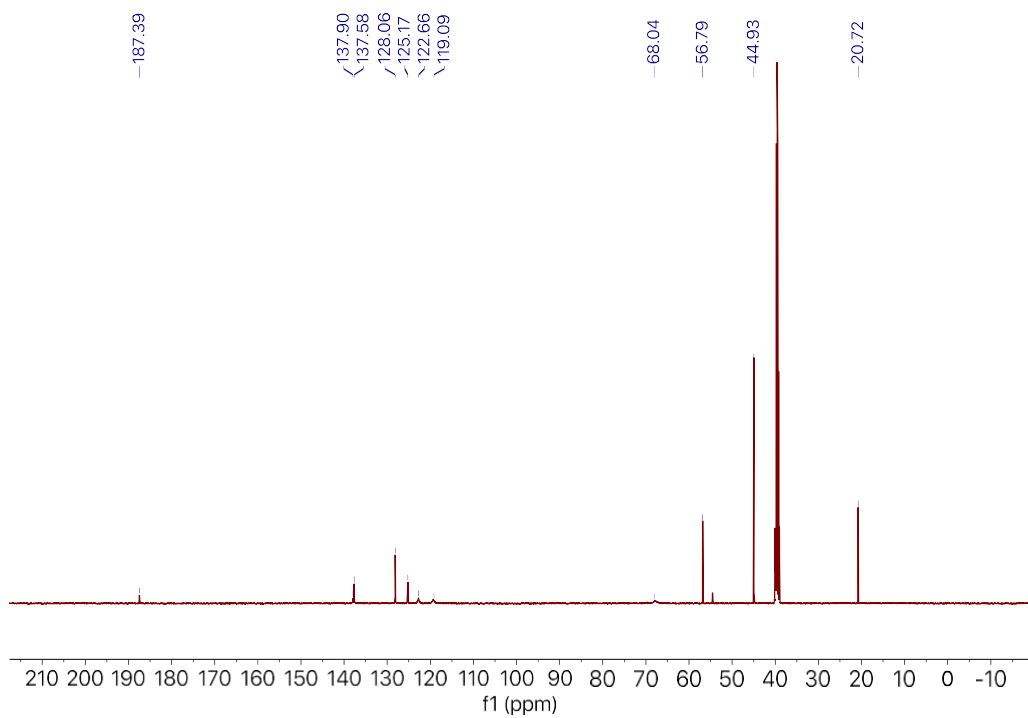


Figure F.9 $^{13}\text{C}\{^1\text{H}\}$ NMR (126 MHz, $\text{DMSO-}d_6$) spectrum of **3-MePhTC** at 60 °C

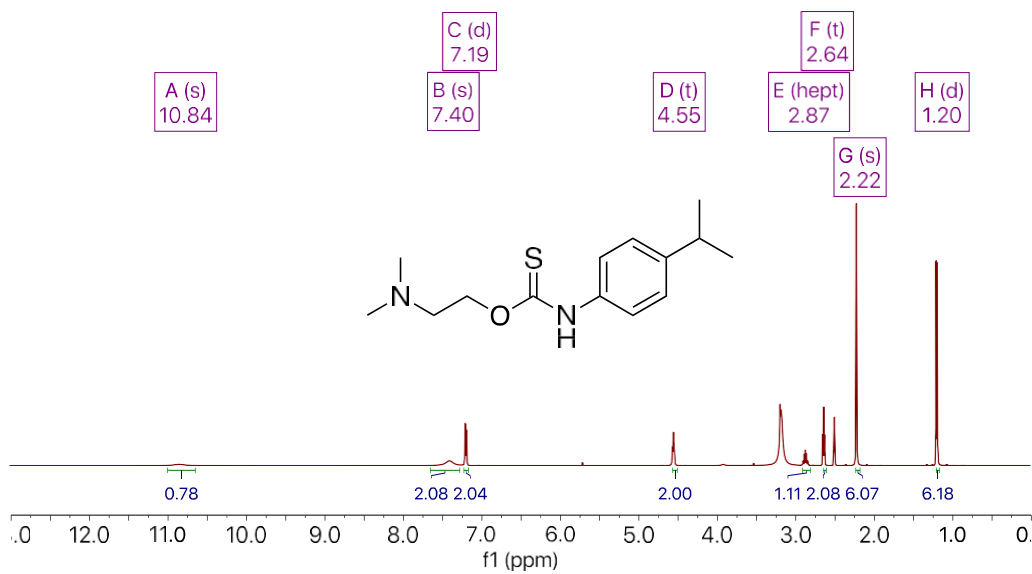


Figure F.10 ^1H NMR (500 MHz, $\text{DMSO-}d^6$) spectrum of **4-iPrPhTC** at 60 °C

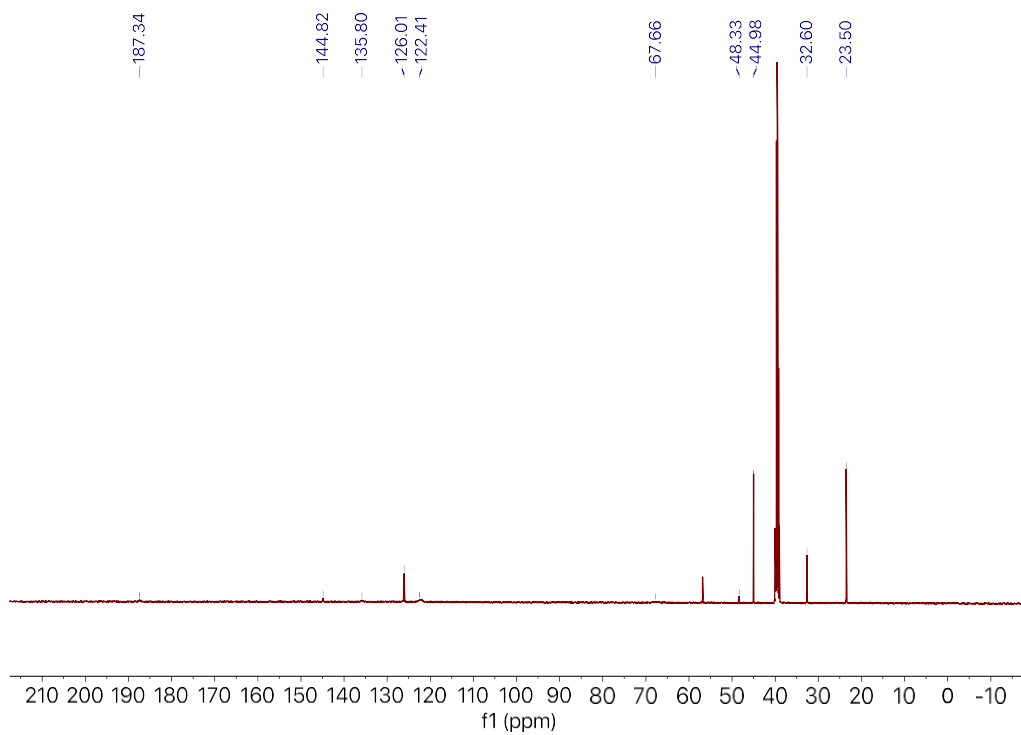


Figure F.11 $^{13}\text{C}\{^1\text{H}\}$ NMR (126 MHz, $\text{DMSO-}d^6$) spectrum of **4-iPrPhTC** at 60 °C

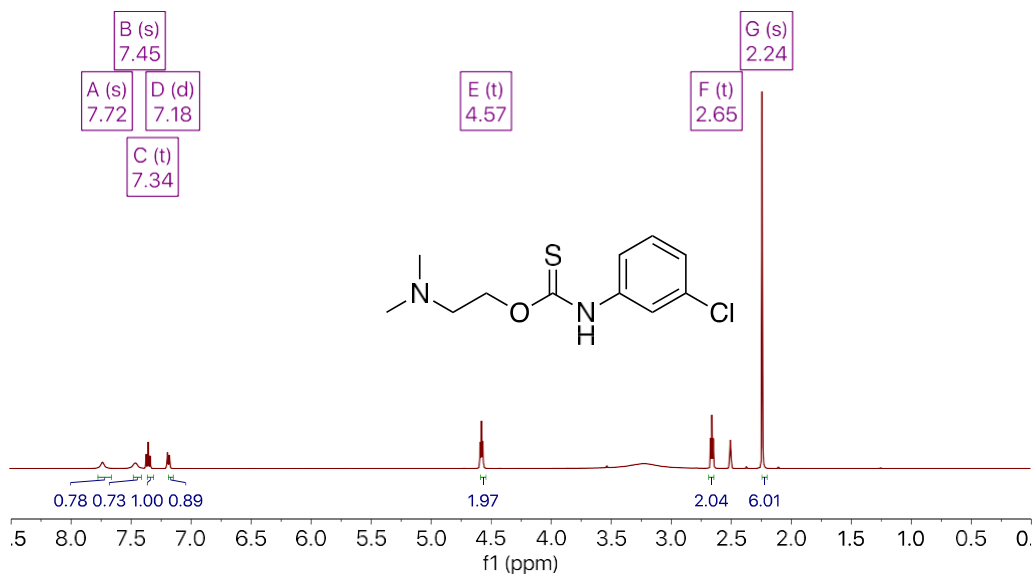


Figure F.12 ^1H NMR (500 MHz, $\text{DMSO-}d^6$) spectrum of **3-CIPhTC** at 60 °C

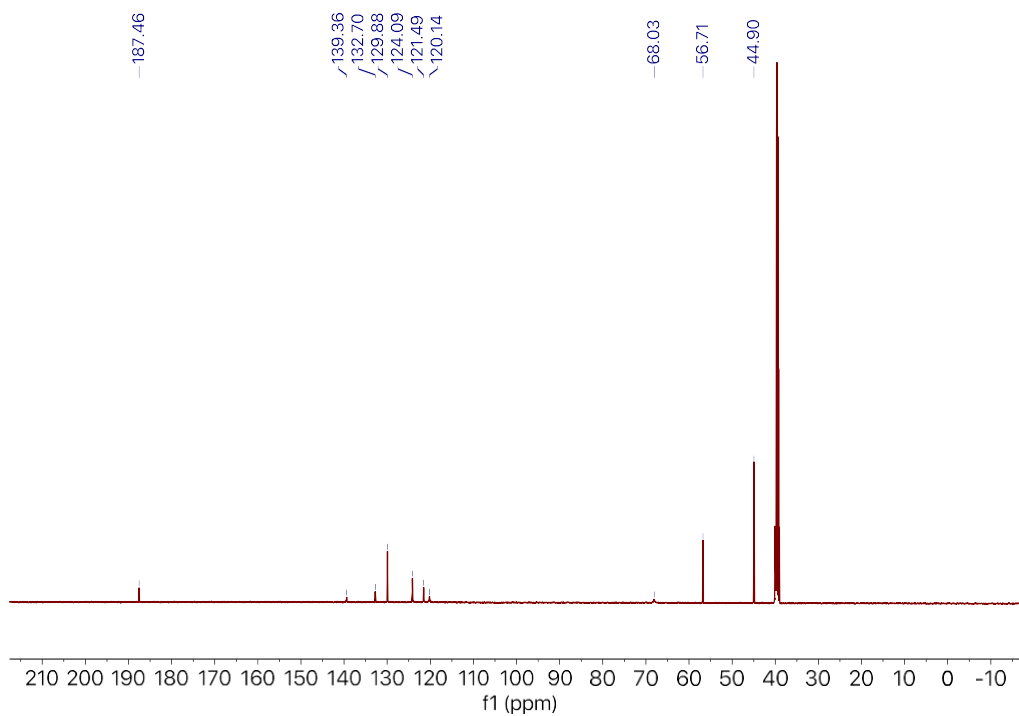


Figure F.13 $^{13}\text{C}\{^1\text{H}\}$ NMR (126 MHz, $\text{DMSO-}d^6$) spectrum of **3-CIPhTC** at 60 °C

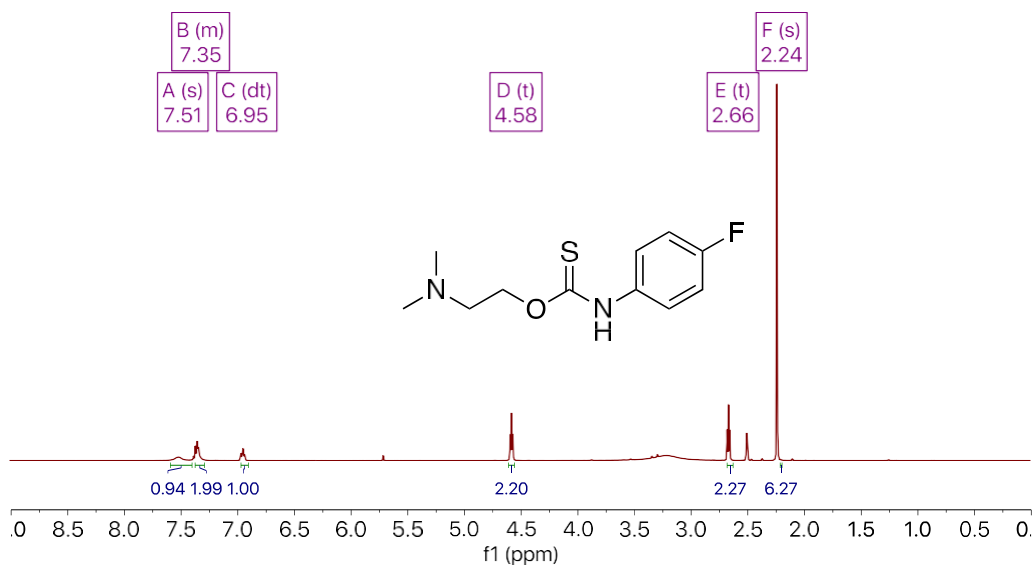


Figure F.14 ^1H NMR (500 MHz, $\text{DMSO-}d^6$) spectrum of **4-FPhTC** at 60 °C

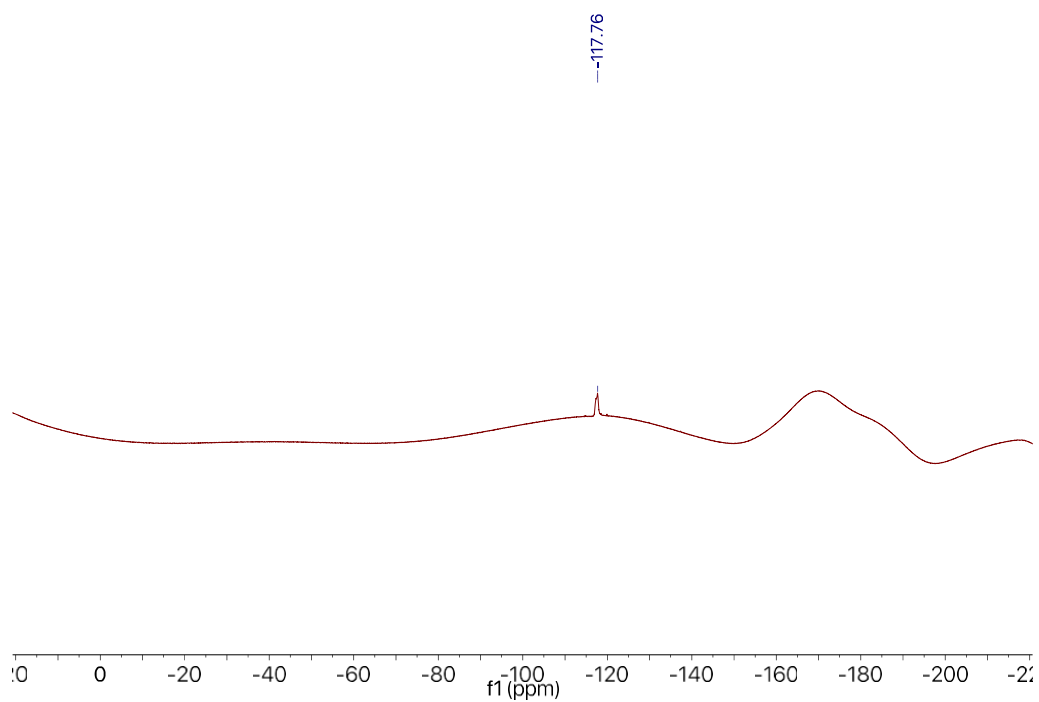


Figure F.15 ^{19}F NMR (471 MHz, $\text{DMSO-}d^6$) spectrum of **4-FPhTC** at 60 °C

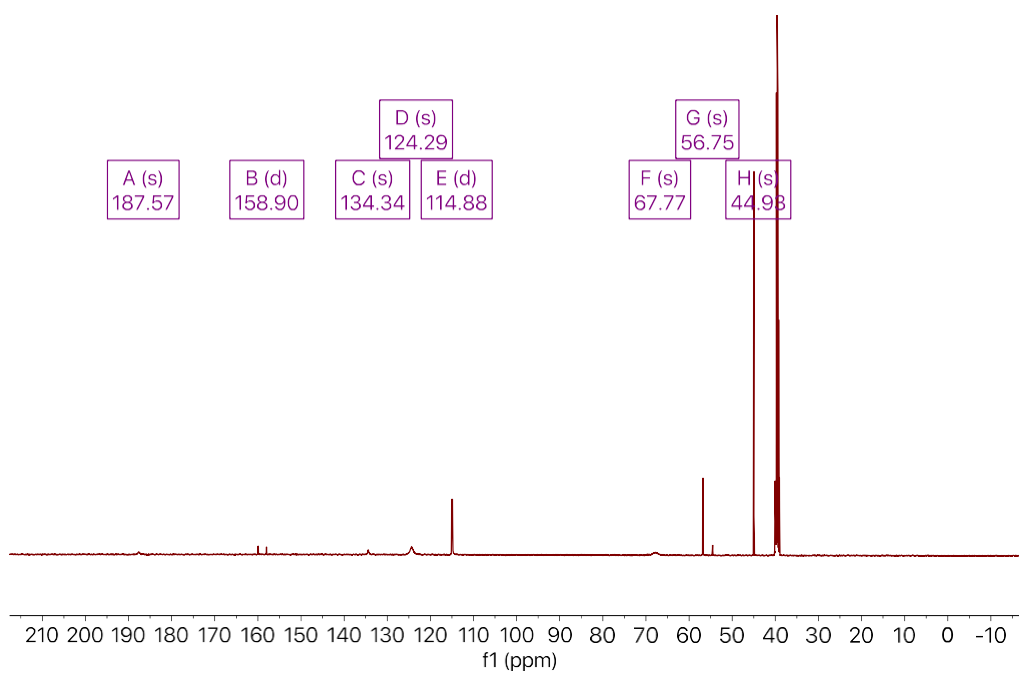


Figure F.16 $^{13}\text{C}\{^1\text{H}\}$ NMR (126 MHz, $\text{DMSO-}d^6$) spectrum of **4-FPhTC** at 60 °C

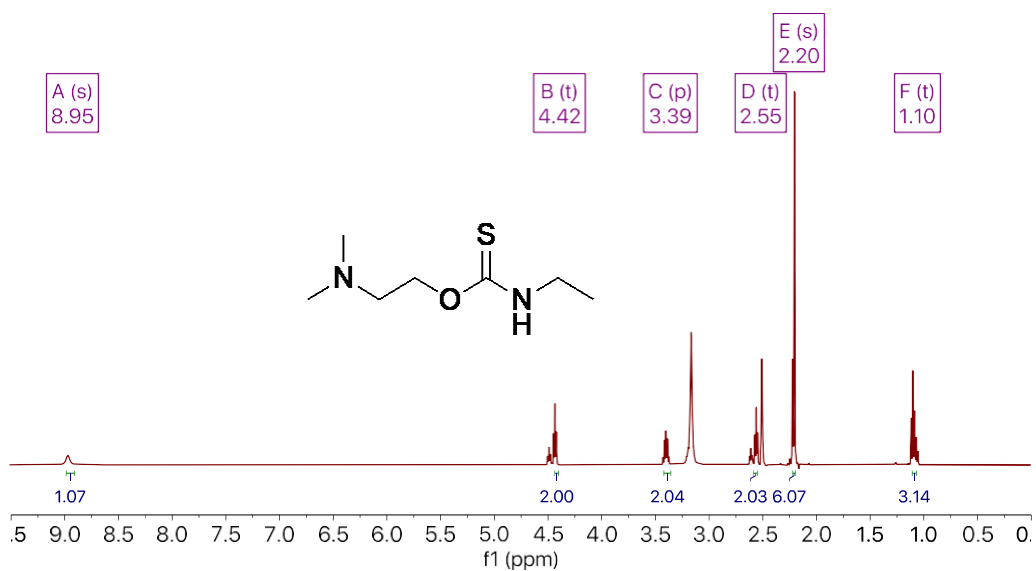


Figure F.17 ^1H NMR (500 MHz, $\text{DMSO-}d^6$) spectrum of **EtTC** at 60 °C

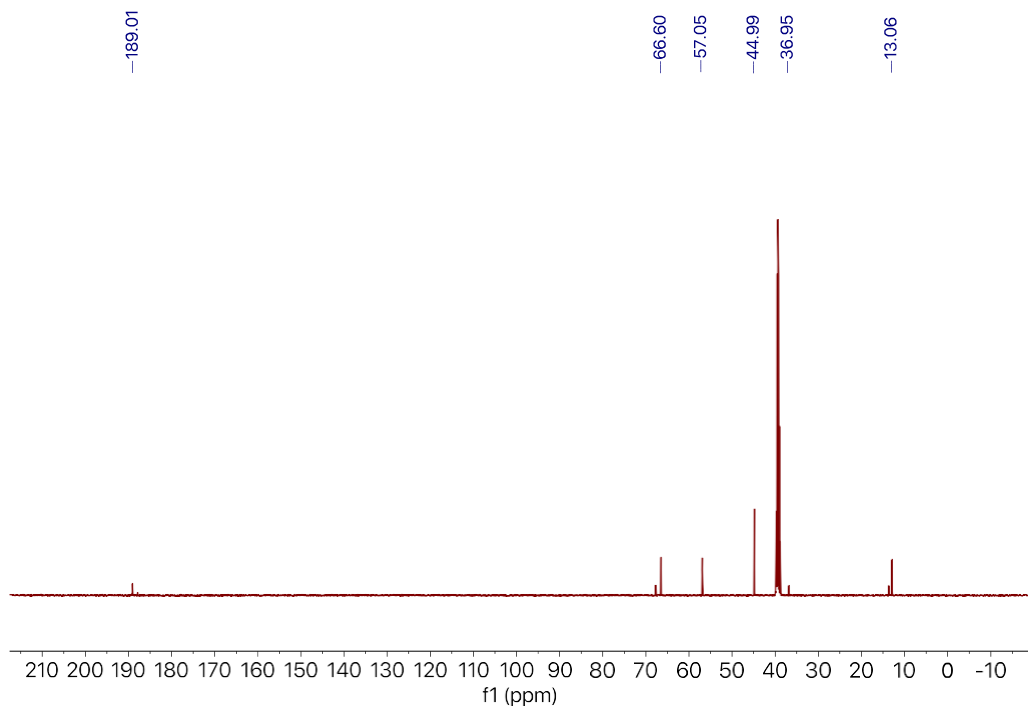


Figure F.18 $^{13}\text{C}\{^1\text{H}\}$ NMR (126 MHz, $\text{DMSO-}d^6$) spectrum of **EtTC** at 60 °C

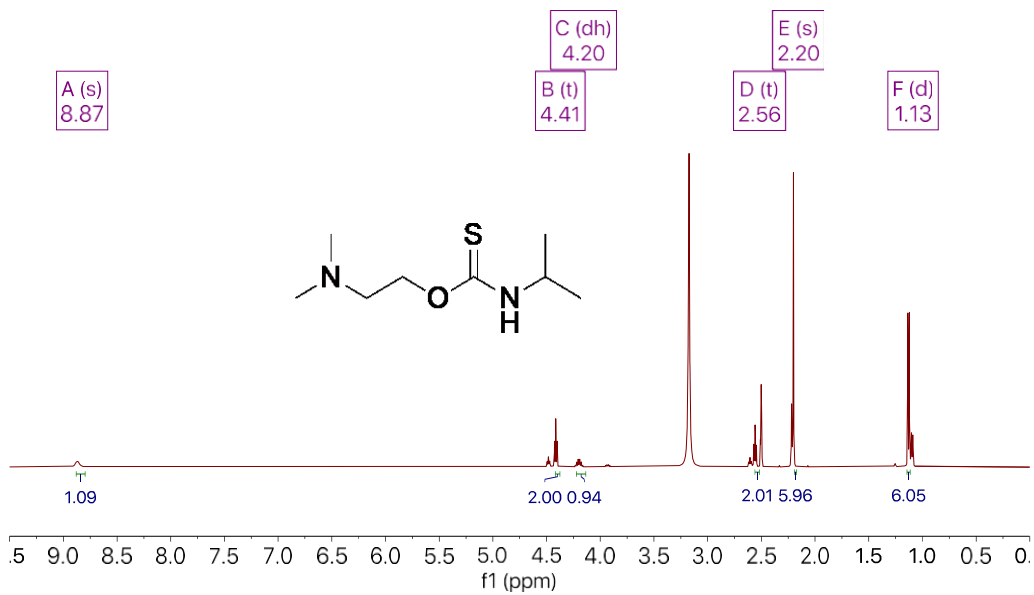


Figure F.19 ^1H NMR (500 MHz, $\text{DMSO-}d^6$) spectrum of **iPrTC** at 60 °C

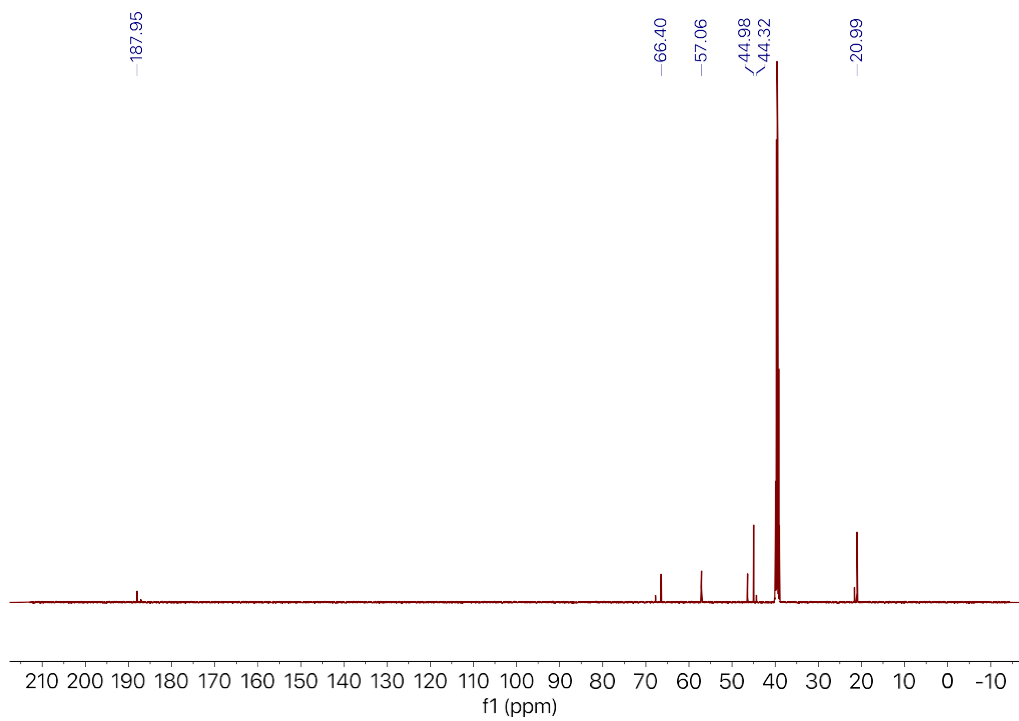


Figure F.20 $^{13}\text{C}\{^1\text{H}\}$ NMR (126 MHz, $\text{DMSO-}d_6$) spectrum of **iPrTC** at 60 °C

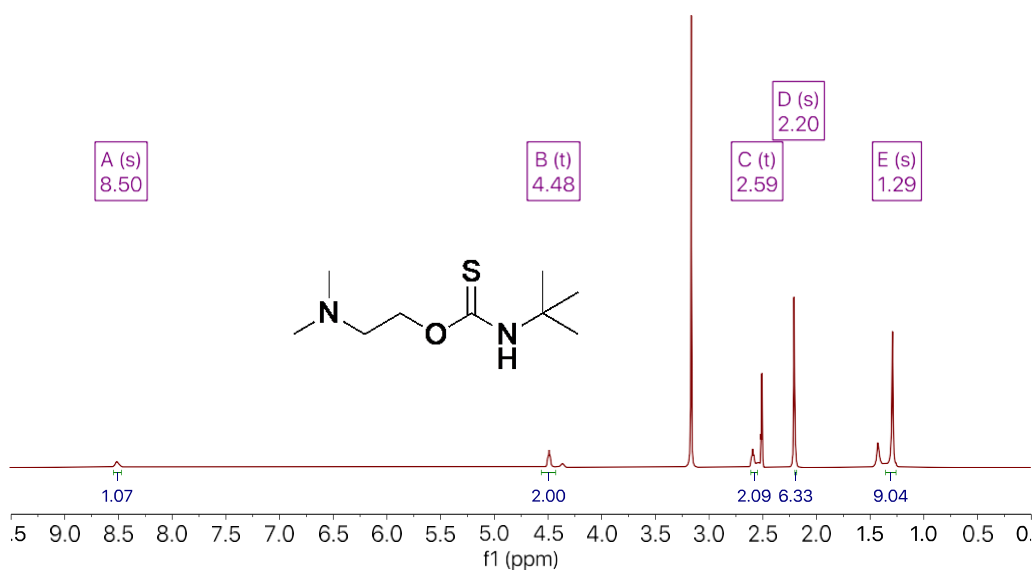


Figure F.21 ^1H NMR (500 MHz, $\text{DMSO-}d_6$) spectrum of **iBuTC** at 60 °C

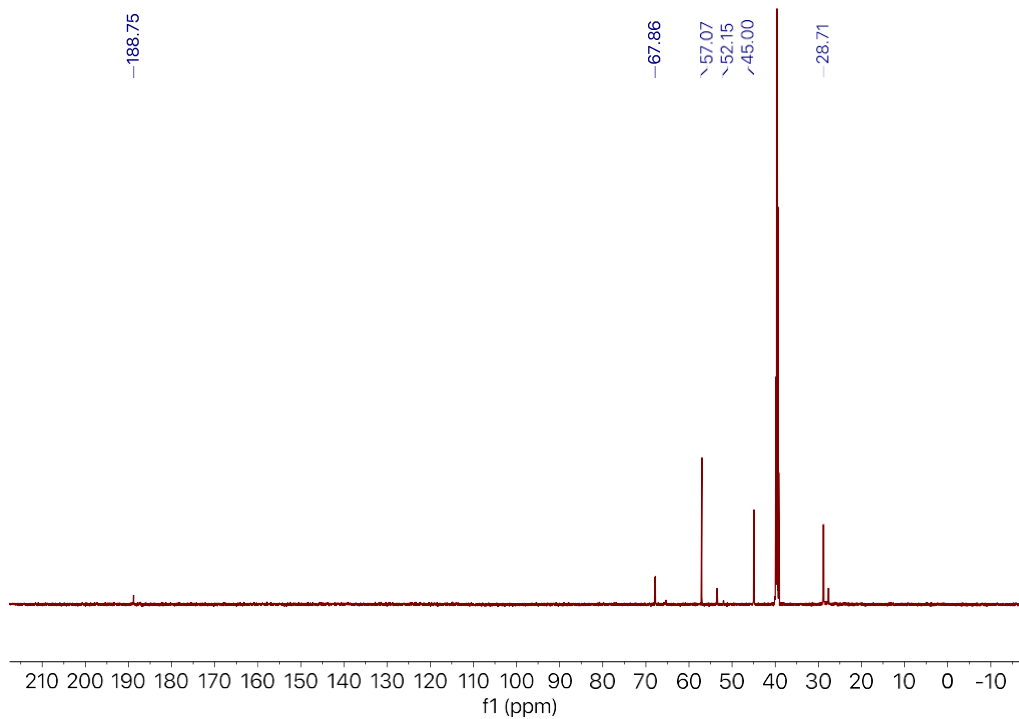


Figure F.22 $^{13}\text{C}\{^1\text{H}\}$ NMR (126 MHz, $\text{DMSO-}d_6$) spectrum of **tBuTC** at 60 °C

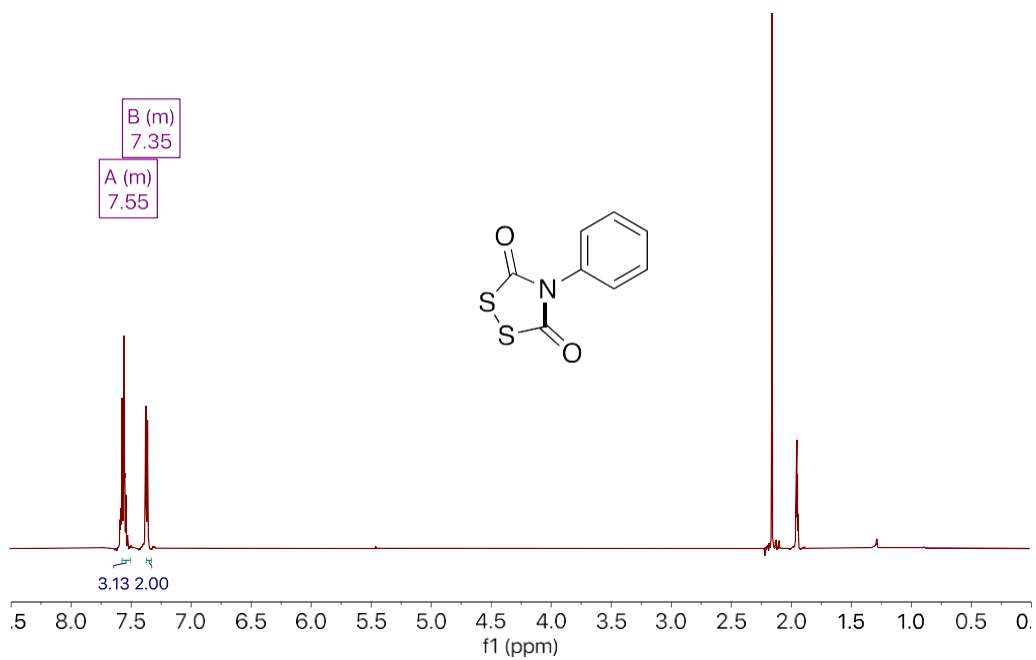


Figure F.23 ^1H NMR (500 MHz, CD_3CN) spectrum of **PhDTS**

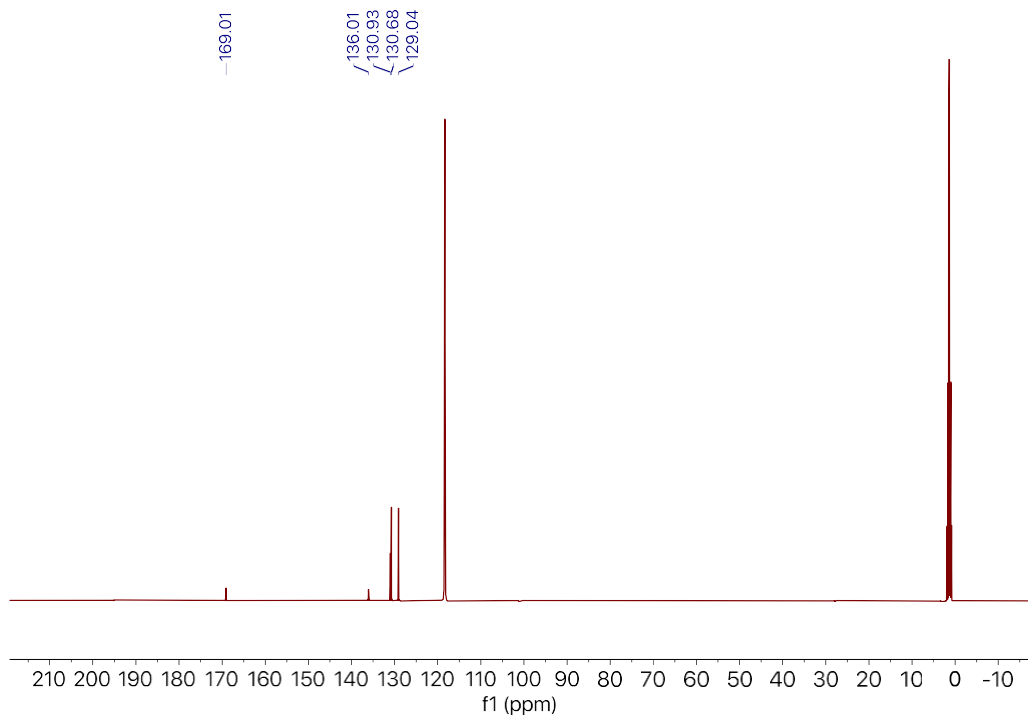


Figure F.24 $^{13}\text{C}\{^1\text{H}\}$ (126 MHz, CD_3CN) spectrum of **PhDTS**

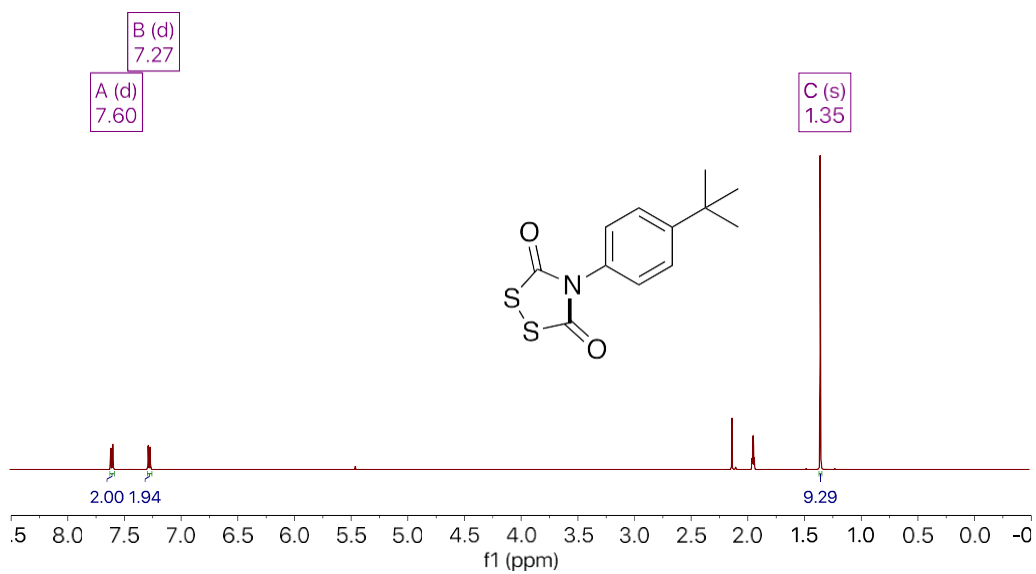


Figure F.25 ^1H NMR (500 MHz, CD_3CN) spectrum of **4-^tBuPhDTS**

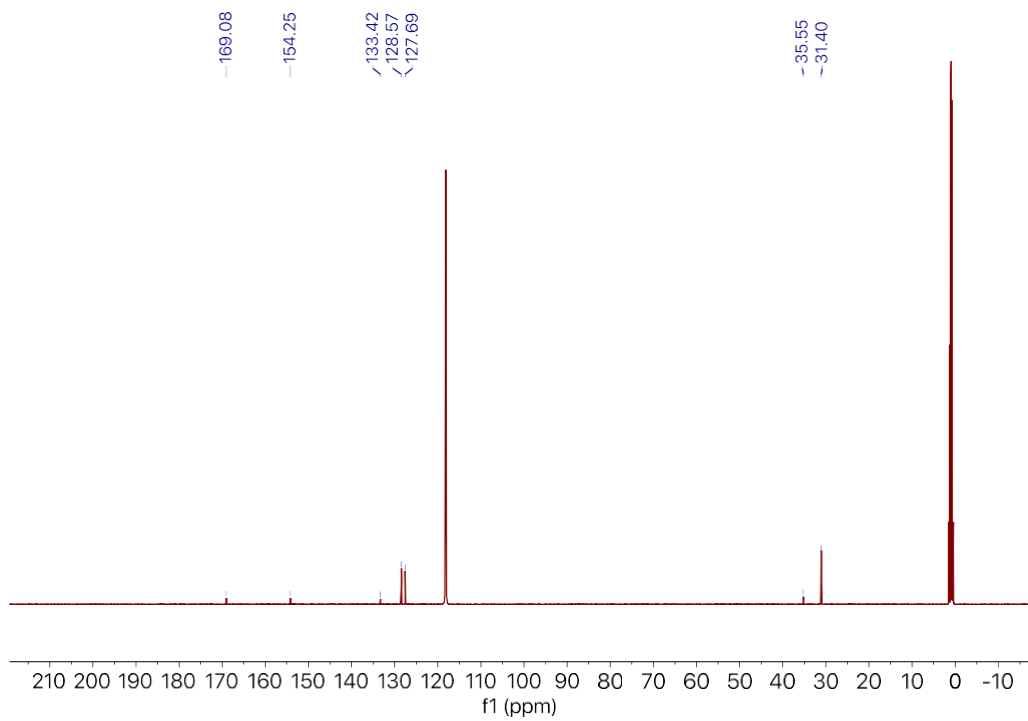


Figure F.26 $^{13}\text{C}\{^1\text{H}\}$ (126 MHz, CD_3CN) spectrum of **4-BuPhDTS**

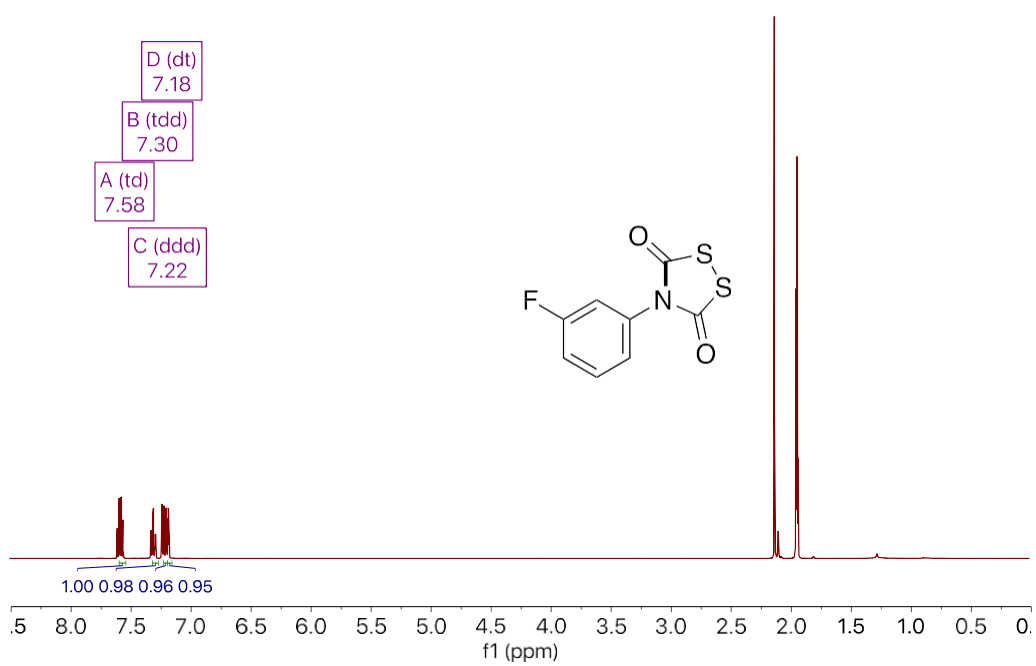


Figure F.27 ^1H NMR (500 MHz, CD_3CN) spectrum of **3-FPhDTS**

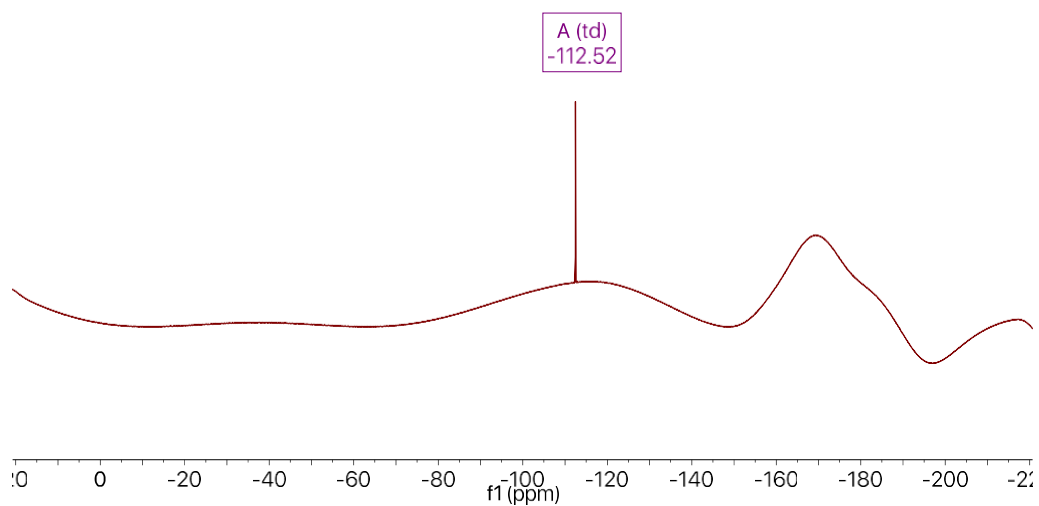


Figure F.28 ^{19}F NMR (471 MHz, CD_3CN) spectrum of **3-FPhDTS**

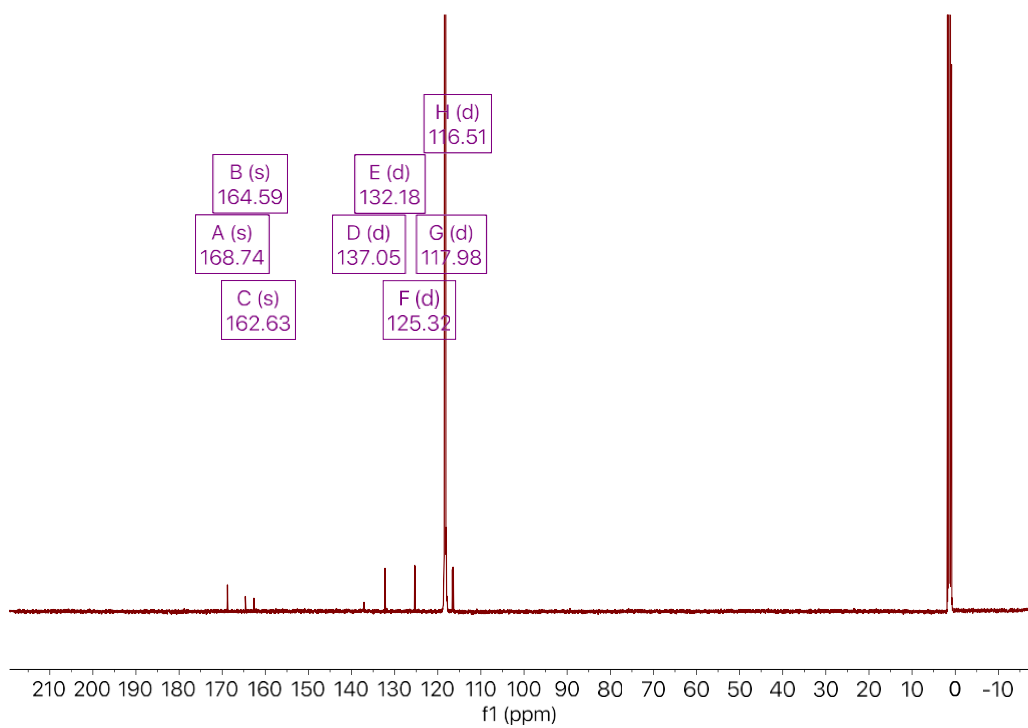


Figure F.29 ^{13}C { ^1H } NMR (126 MHz, CD_3CN) spectrum of **3-FPhDTS**

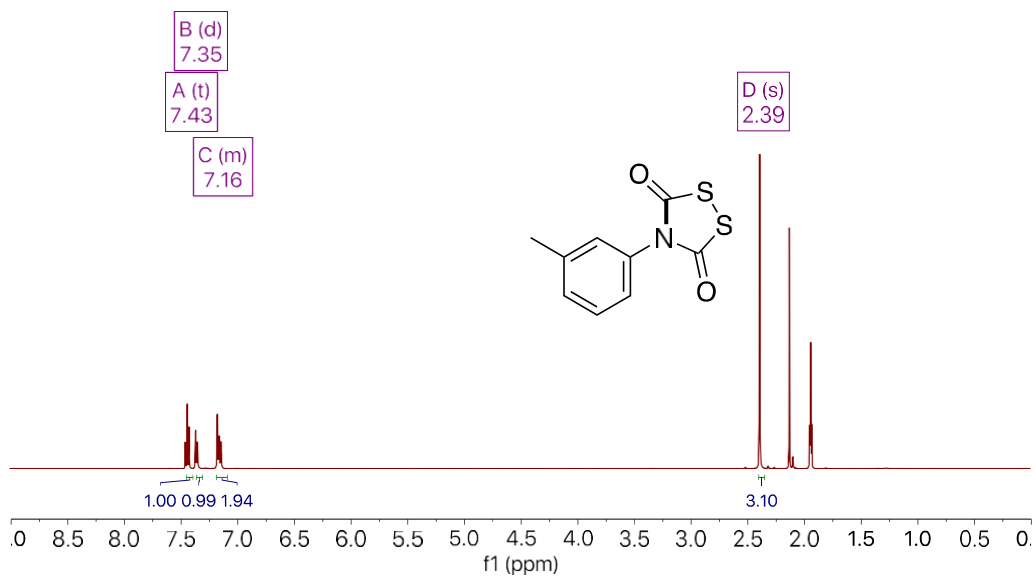


Figure F.30 ^1H NMR (500 MHz, CD_3CN) spectrum of **3-MePhDTS**

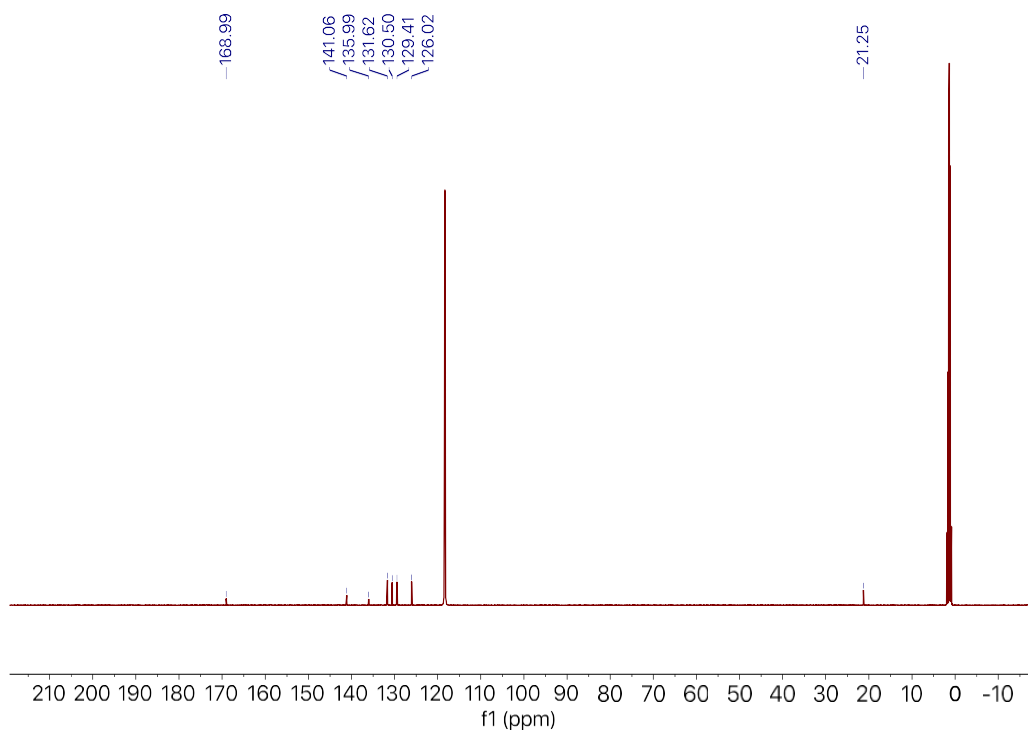


Figure F.31 $^{13}\text{C}\{^1\text{H}\}$ NMR (126 MHz, CD_3CN) spectrum of **3-MePhDTS**

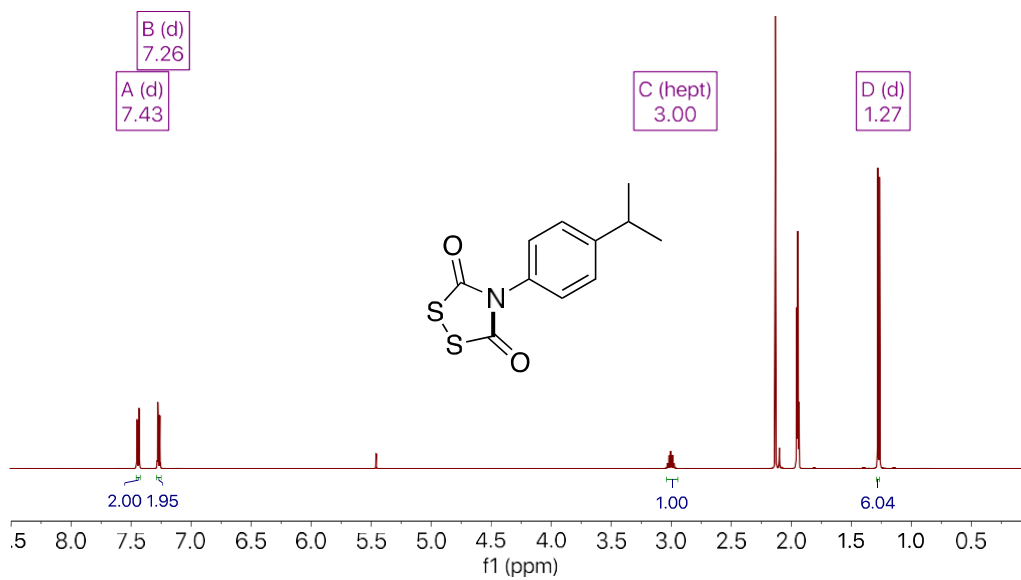


Figure F.32 ^1H NMR (500 MHz, CD_3CN) spectrum of **4-*i*PrPhDTS**

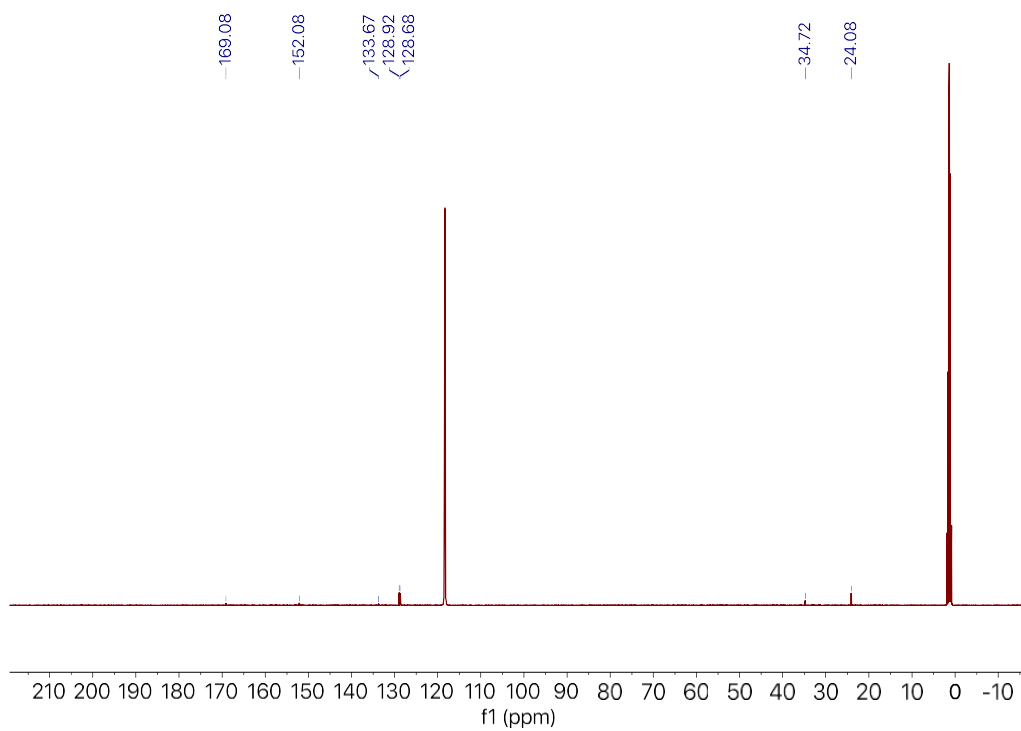


Figure F.33 $^{13}\text{C}\{^1\text{H}\}$ NMR (126 MHz, CD_3CN) **4-*i*PrPhDTS**

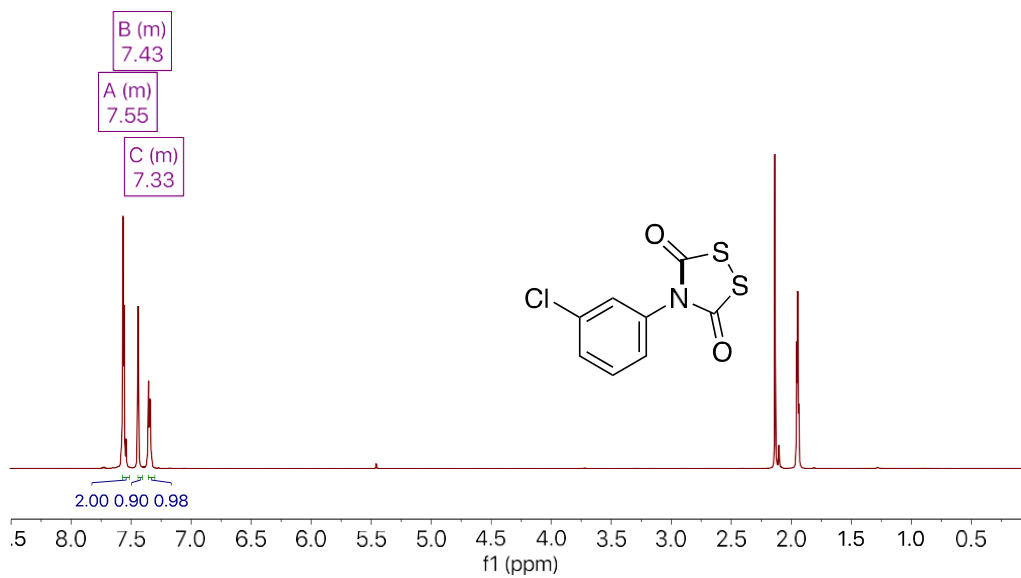


Figure F.34 ^1H NMR (500 MHz, CD_3CN) spectrum of 3-CIPhDTS

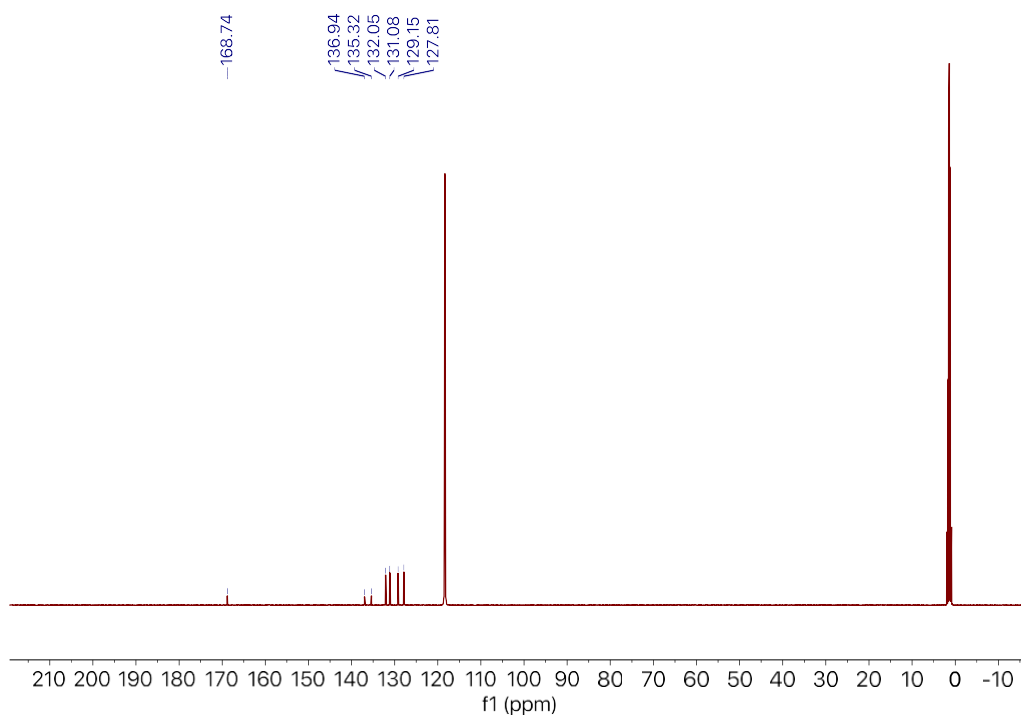


Figure F.35 $^{13}\text{C}\{^1\text{H}\}$ NMR (126 MHz, CD_3CN) spectrum of 3-CIPhDTS

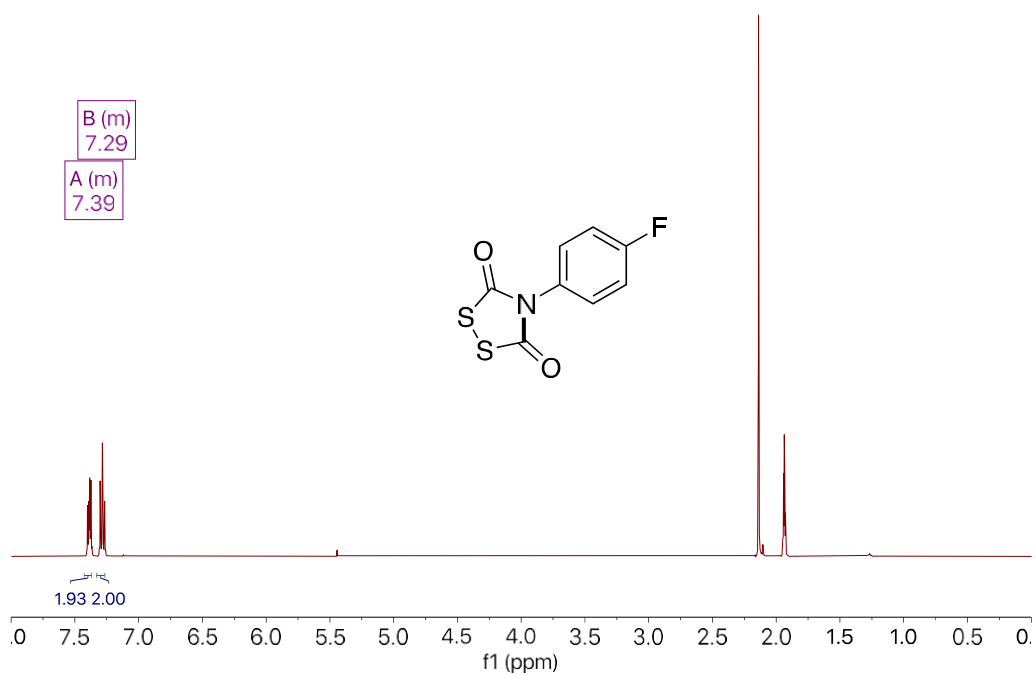


Figure F.36 ^1H NMR (500 MHz, CD_3CN) spectrum of **4-FPhDTS**

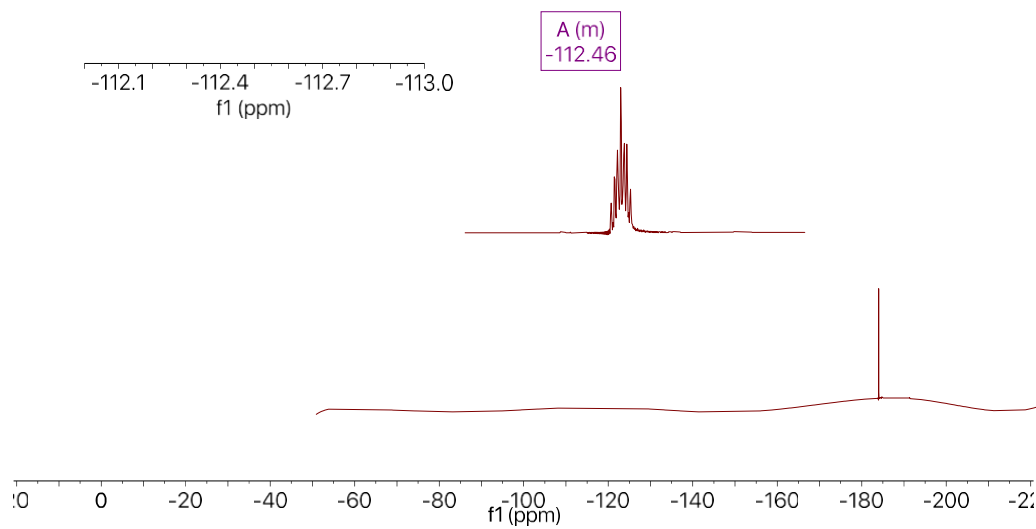


Figure F.37 ^{19}F NMR (471 MHz, CD_3CN) spectrum of **4-FPhDTS**

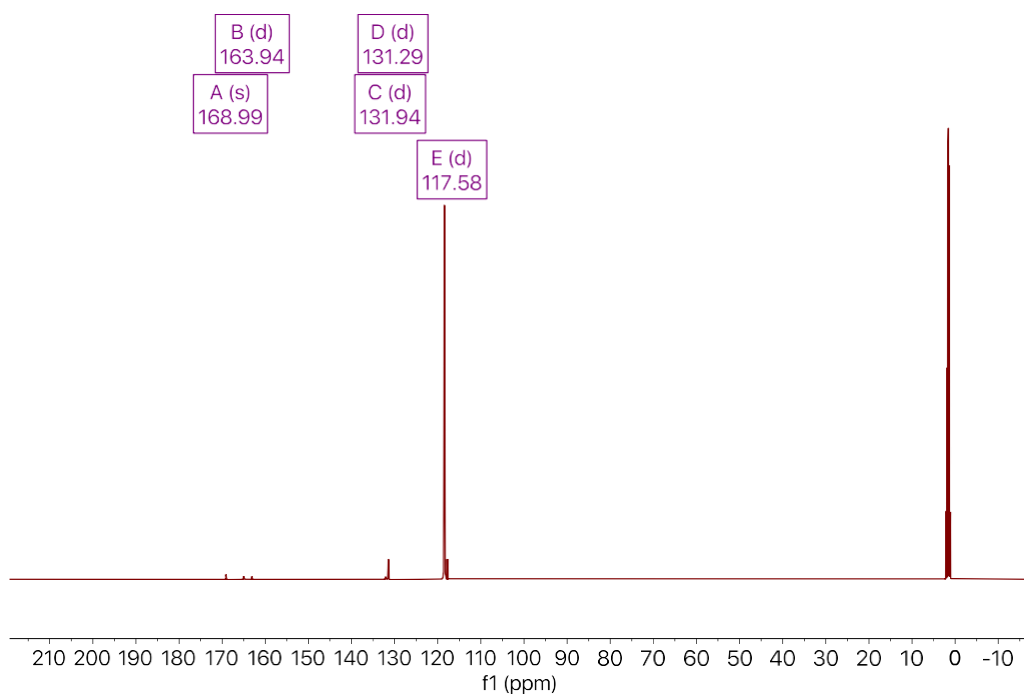


Figure F.38 ¹³C{¹H} NMR (126 MHz, CD₃CN) spectrum of **4-FPhDTS**

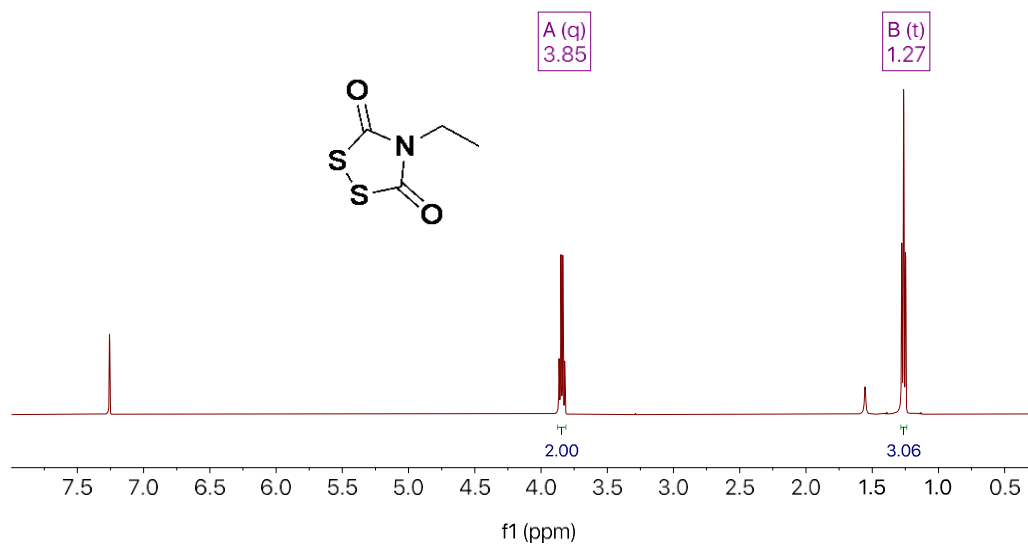


Figure F.39 ¹H NMR (500 MHz, CDCl₃) spectrum of **EtDTS**

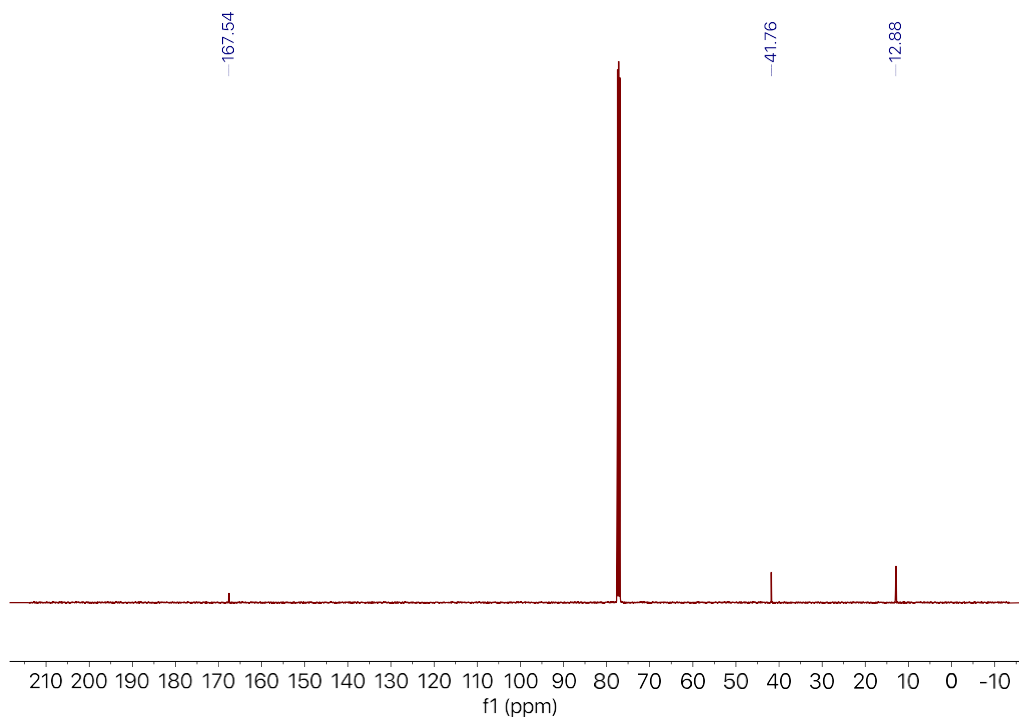


Figure F.40 $^{13}\text{C}\{^1\text{H}\}$ NMR (126 MHz, CDCl_3) spectrum of **EtDTS**

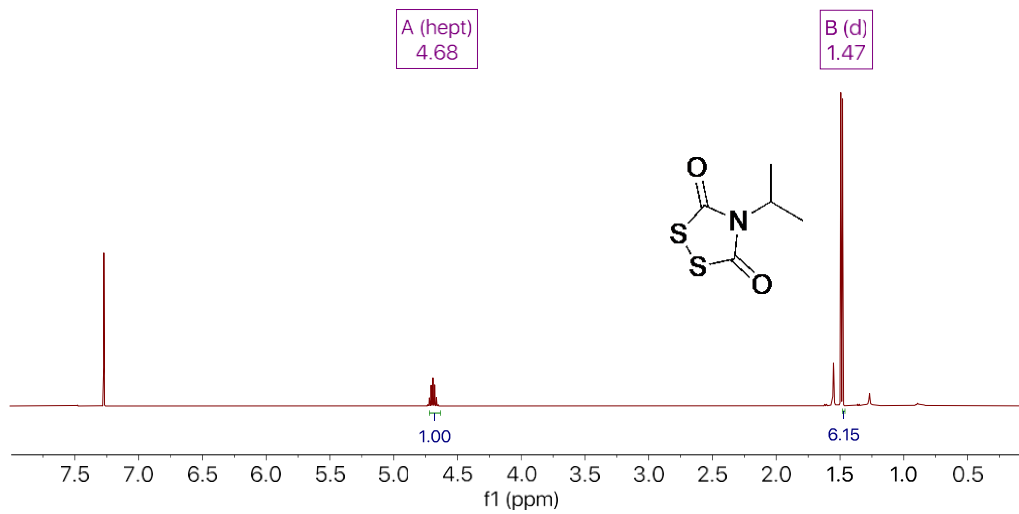


Figure F.41 ^1H NMR (500 MHz, CD_3CN) spectrum of **iPrDTS**

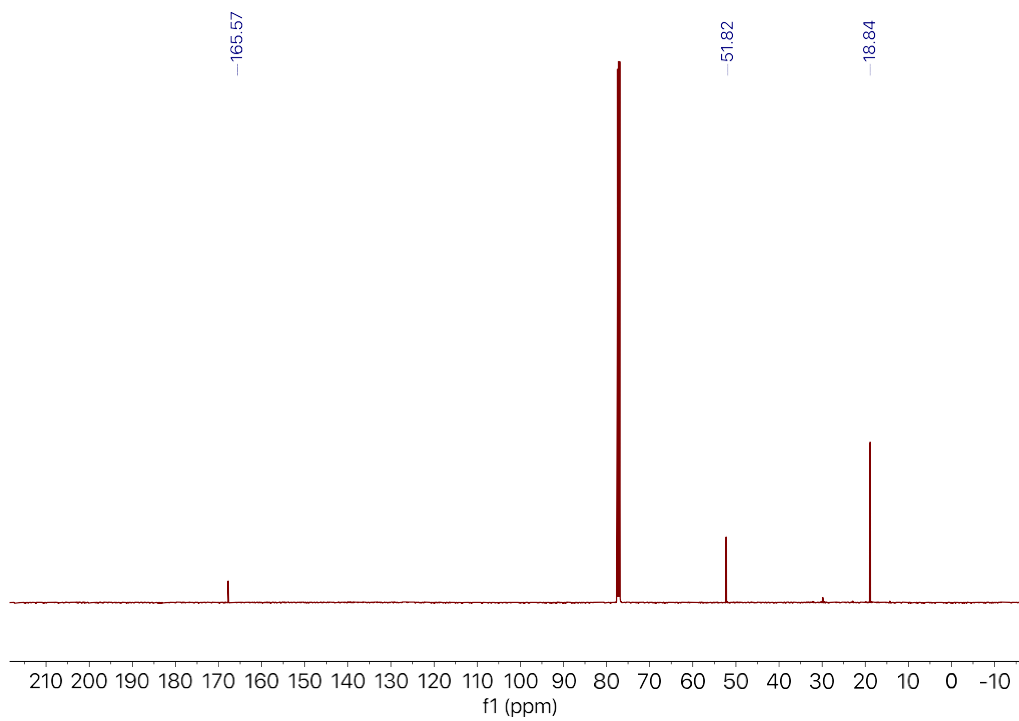


Figure F.42 $^{13}\text{C}\{^1\text{H}\}$ NMR (126 MHz, CD_3CN) spectrum of **iPrDTS**

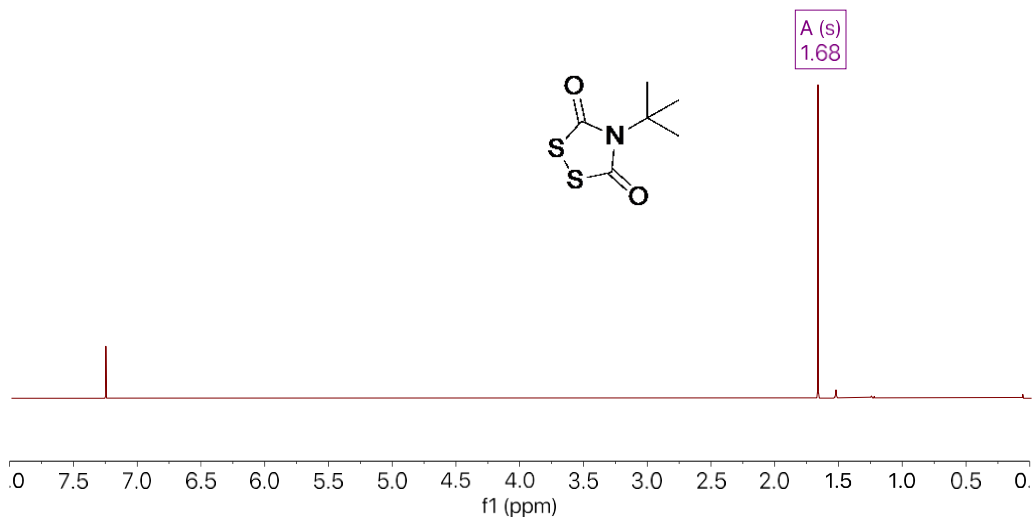


Figure F.43 ^1H NMR (500 MHz, CD_3CN) spectrum of **BuPhDTS**

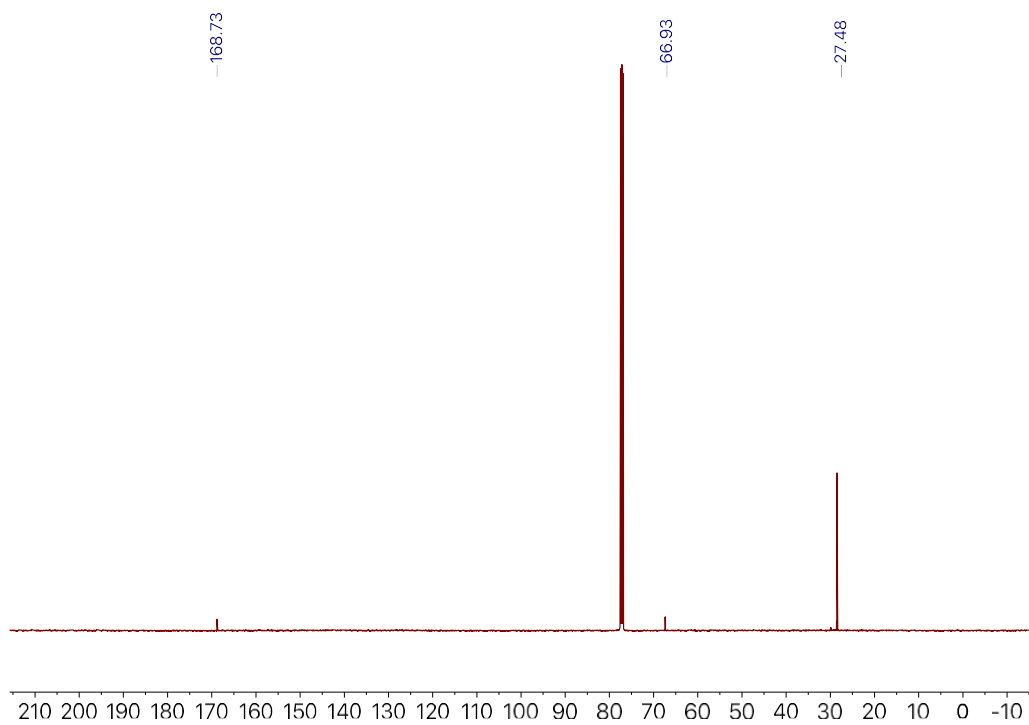


Figure F.44 $^{13}\text{C}\{^1\text{H}\}$ NMR (126 MHz, CD_3CN) spectrum of **$t\text{BuPhDTS}$**

HPLC Data

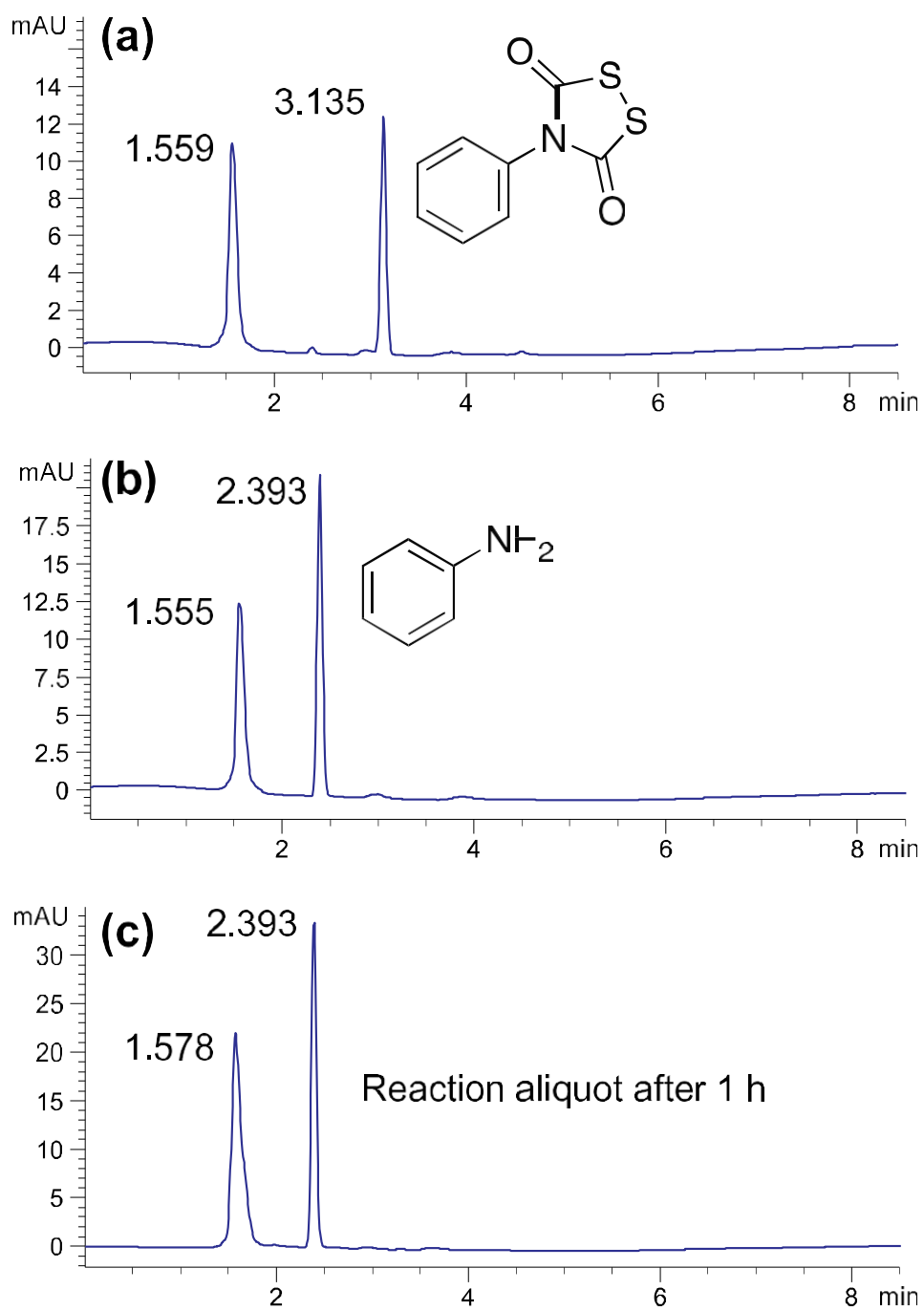


Figure F.45 a) 100 μM PhDTS in 10 mM PBS (pH 7.4) with 0.1% MeCN (b) 50 μM aniline in 10 mM PBS (pH 7.4) with 0.1% MeCN (c) Reaction aliquot after 1 h

MBA Calibration Curve

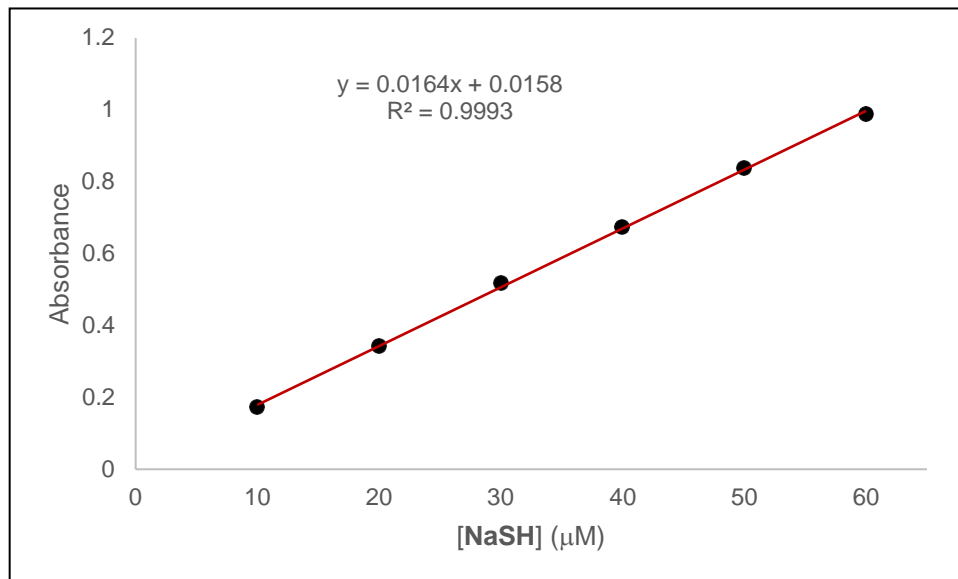


Figure F.46 MBA calibration curve generated using known concentrations of NaSH

CA Inhibition Experiment

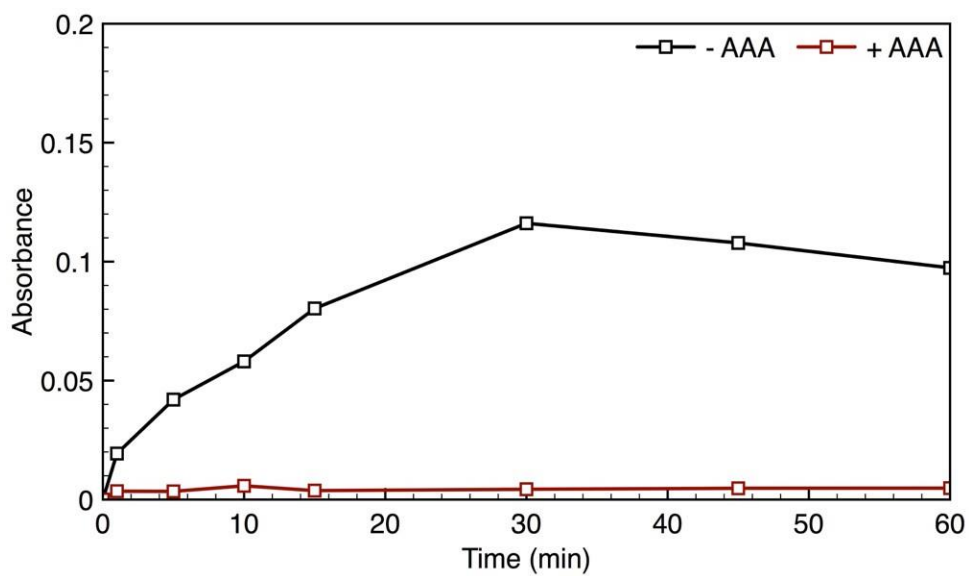


Figure F.47 Effect of AAA on CA-mediated H₂S release from **PhDTS** (25 μM)

Zn^{2+} -mediated Hydrolysis Experiment

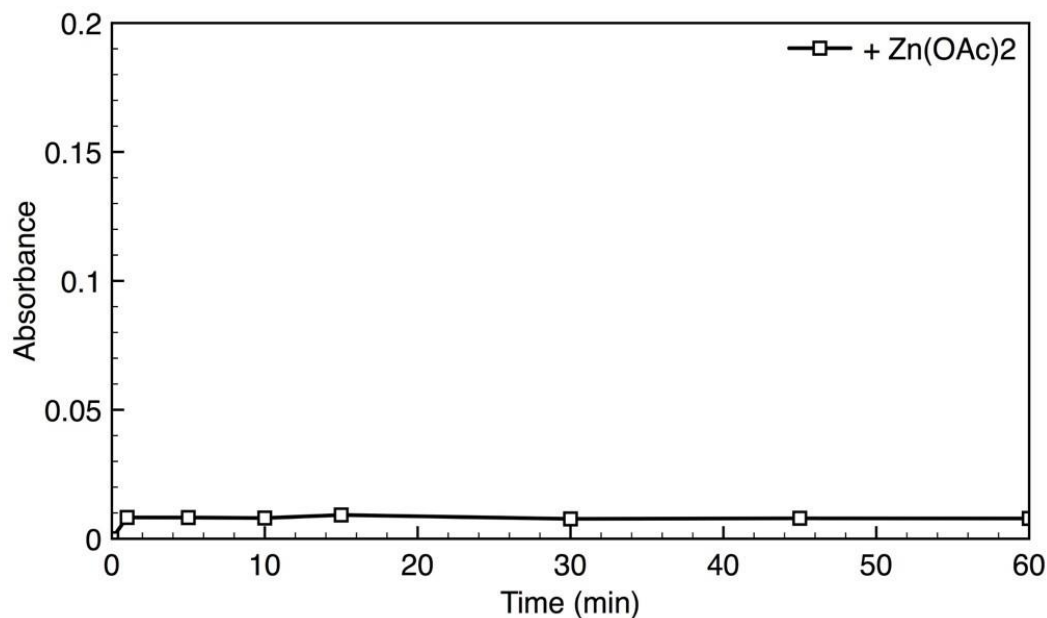
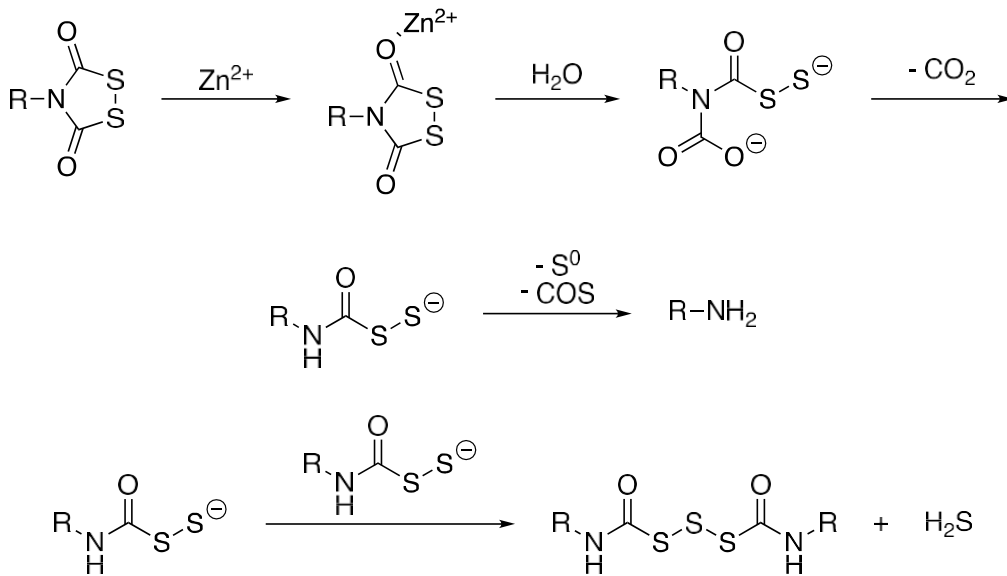


Figure F.48 Lack of H_2S release from **PhDTS** in the presence of $Zn(OAc)_2$



Scheme F.1 Proposed mechanism of Zn^{2+} -mediated COS/H_2S release from DTS-functionalized amines in the presence of carbonic anhydrase at physiological pH

Comparison of Cysteine- and Lysine-Mediated COS/H₂S Release from PhDTS

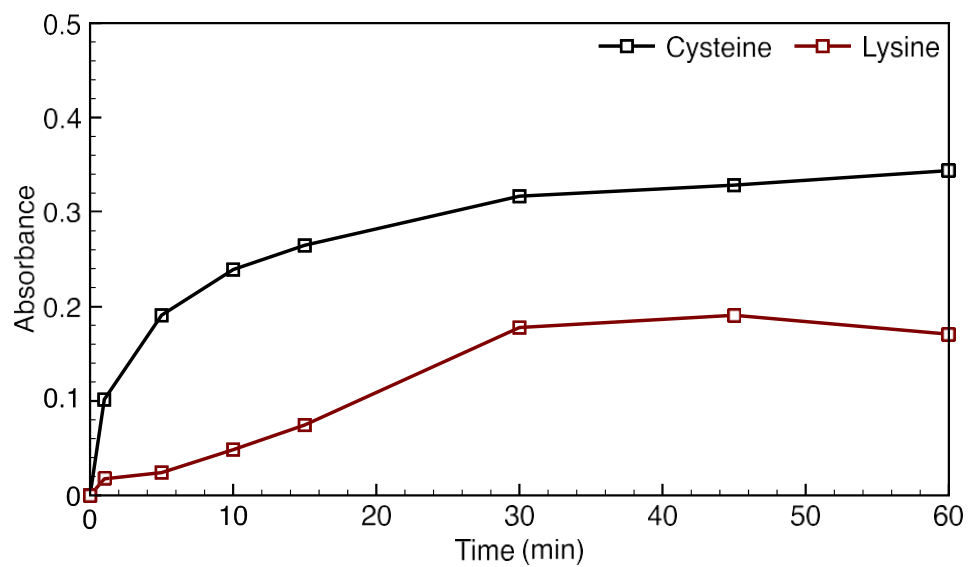


Figure F.49 Comparison of cysteine- and lysine-mediated COS/H₂S release from **PhDTS** (25 μ M) in the presence of nucleophile (500 μ M, 20 equiv.) and carbonic anhydrase (25 μ g/mL) in 20 mL 10 mM PBS (pH 7.4) at 25 $^{\circ}$ C.

APPENDIX G

SUPPLEMENTARY INFORMATION FOR CHAPTER VII

Appendix G is the supplementary information for Chapter VII of this dissertation. It includes spectra and experimental data relevant to the content in Chapter VII.

Synthesis and Purification of Carbonyl Sulfide

KSCN (25 g, 0.26 mol) was dissolved in deionized H₂O (150 mL) and added to a closed addition funnel. Concentrated H₂SO₄ (50 mL) and a stir bar were added to a three-necked round bottom flask. KOH (100 g, 1.78 mol) was dissolved in deionized H₂O (100 mL) and added to the first gas washing bottle. Aniline (25 mL, 0.27 mol) was dissolved in anhydrous ethanol (75 mL) and added to the second gas washing bottle. Ice chips were added directly to the third gas washing bottle. Concentrated H₂SO₄ (50 mL) was added directly to the fourth gas washing bottle. A sulfide-quenching solution containing Zn(OAc)₂ (24 g, 0.13 mol), sodium citrate dihydrate (2.25 g, 7.65 mmol), NaOH (1.66 g, 41.5 mmol), and bleach (300 mL) was added to a 1 L graduated cylinder. The solution was filled to 1 L with deionized H₂O. The gas washing bottles were sealed with vacuum grease and the system was assembled as shown below (Figure G.1).



Figure G.1 Assembled glassware for synthesis and purification of COS

The assembled system was charged with a stream of nitrogen and sparged for approximately 1 hour. The potassium thiocyanate and concentrated H_2SO_4 solutions were both sparged for 30 min. To begin the synthesis of COS, nitrogen sparging was stopped and aqueous potassium thiocyanate was added dropwise to concentrated H_2SO_4 .

Note: *This reaction is very exothermic.*

The purified COS was collected in a 500 mL round bottom, Schlenk storage flask with a Teflon Kontes screw valve with a 14/20 sidearm joint. After approximately two-thirds of the potassium thiocyanate solution was added, the storage flask was sealed, and the excess COS gas was bubbled directly into the sulfide-quenching solution.

The purity of the synthesized COS (g) could be assessed by ^{13}C NMR (Figure G.2). The gas was bubbled directly into an NMR tube containing 0.5 mL CD_3CN briefly.

$^{13}\text{C}\{^1\text{H}\}$ (125 MHz, CD_3CN), δ (ppm): 154.34.

NMR Spectra

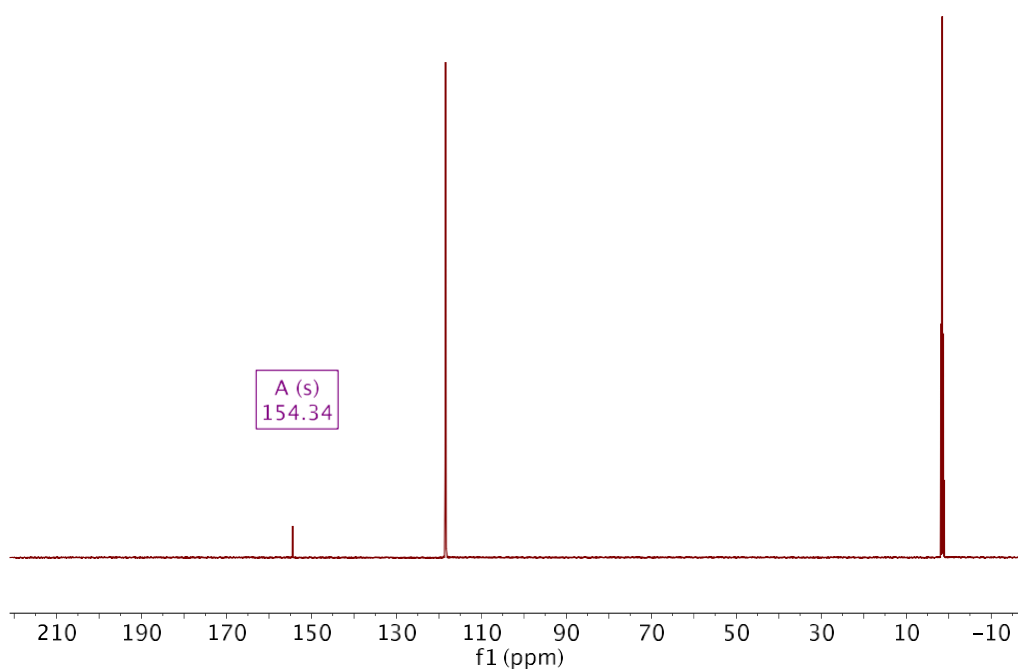


Figure G.2 $^{13}\text{C}\{^1\text{H}\}$ NMR spectrum of COS (g) in CD_3CN .

REFERENCES CITED

1. (a) Abe, K.; Kimura, H. The possible role of hydrogen sulfide as an endogenous neuromodulator. *Journal of Neuroscience* **1996**, *16* (3), 1066-1071; (b) Li, L.; Hsu, A.; Moore, P. K. Actions and interactions of nitric oxide, carbon monoxide and hydrogen sulphide in the cardiovascular system and in inflammation--a tale of three gases! *Pharmacol Ther* **2009**, *123* (3), 386-400; (c) Wang, R. Two's company, three's a crowd: can H₂S be the third endogenous gaseous transmitter? *FASEB J* **2002**, *16* (13), 1792-8.
2. (a) Cuevasanta, E.; Moller, M. N.; Alvarez, B. Biological chemistry of hydrogen sulfide and persulfides. *Arch Biochem Biophys* **2017**, *617*, 9-25; (b) Hartle, M. D.; Pluth, M. D. A practical guide to working with H₂S at the interface of chemistry and biology. *Chem Soc Rev* **2016**, *45* (22), 6108-6117; (c) Li, Q.; Lancaster, J. R., Jr. Chemical foundations of hydrogen sulfide biology. *Nitric Oxide* **2013**, *35*, 21-34; (d) Ono, K.; Akaike, T.; Sawa, T.; Kumagai, Y.; Wink, D. A.; Tantillo, D. J.; Hobbs, A. J.; Nagy, P.; Xian, M.; Lin, J.; Fukuto, J. M. Redox chemistry and chemical biology of H₂S, hydropersulfides, and derived species: implications of their possible biological activity and utility. *Free Radic Biol Med* **2014**, *77*, 82-94; (e) Szabo, C. A timeline of hydrogen sulfide (H₂S) research: From environmental toxin to biological mediator. *Biochem Pharmacol* **2018**, *149*, 5-19; (f) Zhao, Y.; Biggs, T. D.; Xian, M. Hydrogen sulfide (H₂S) releasing agents: chemistry and biological applications. *Chem Commun (Camb)* **2014**, *50* (80), 11788-805.
3. Calvert, J. W.; Coetzee, W. A.; Lefer, D. J. Novel insights into hydrogen sulfide--mediated cytoprotection. *Antioxid Redox Signal* **2010**, *12* (10), 1203-17.
4. (a) Cao, X.; Ding, L.; Xie, Z. Z.; Yang, Y.; Whiteman, M.; Moore, P. K.; Bian, J. S. A Review of Hydrogen Sulfide Synthesis, Metabolism, and Measurement: Is Modulation of Hydrogen Sulfide a Novel Therapeutic for Cancer? *Antioxid Redox Signal* **2019**, *31* (1), 1-38; (b) Durante, W. Hydrogen Sulfide Therapy in Diabetes-Accelerated Atherosclerosis: A Whiff of Success. *Diabetes* **2016**, *65* (10), 2832-4; (c) Kasinath, B. S.; Feliers, D.; Lee, H. J. Hydrogen sulfide as a regulatory factor in kidney health and disease. *Biochem Pharmacol* **2018**, *149*, 29-41; (d) Kolluru, G. K.; Shen, X.; Bir, S. C.; Kevil, C. G. Hydrogen sulfide chemical biology: pathophysiological roles and detection. *Nitric Oxide* **2013**, *35*, 5-20.
5. (a) Cao, X.; Cao, L.; Ding, L.; Bian, J. S. A New Hope for a Devastating Disease: Hydrogen Sulfide in Parkinson's Disease. *Mol Neurobiol* **2018**, *55* (5), 3789-3799; (b) Panthi, S.; Manandhar, S.; Gautam, K. Hydrogen sulfide, nitric oxide, and neurodegenerative disorders. *Transl Neurodegener* **2018**, *7*, 3; (c) Shefa, U.; Kim, M. S.; Jeong, N. Y.; Jung, J. Antioxidant and Cell-Signaling Functions of Hydrogen Sulfide in the Central Nervous System. *Oxid Med Cell Longev* **2018**, *2018*, 1873962.
6. Chen, Y.; Wang, R. The message in the air: hydrogen sulfide metabolism in chronic respiratory diseases. *Respir Physiol Neurobiol* **2012**, *184* (2), 130-8.

7. (a) Donnarumma, E.; Trivedi, R. K.; Lefer, D. J. Protective Actions of H₂S in Acute Myocardial Infarction and Heart Failure. *Compr Physiol* **2017**, *7* (2), 583-602; (b) Yu, X. H.; Cui, L. B.; Wu, K.; Zheng, X. L.; Cayabyab, F. S.; Chen, Z. W.; Tang, C. K. Hydrogen sulfide as a potent cardiovascular protective agent. *Clin Chim Acta* **2014**, *437*, 78-87; (c) Wu, D.; Wang, J.; Li, H.; Xue, M.; Ji, A.; Li, Y. Role of Hydrogen Sulfide in Ischemia-Reperfusion Injury. *Oxid Med Cell Longev* **2015**, *2015*, 186908.
8. Kondo, K.; Bhushan, S.; King, A. L.; Prabhu, S. D.; Hamid, T.; Koenig, S.; Murohara, T.; Predmore, B. L.; Gojon, G., Sr.; Gojon, G., Jr.; Wang, R.; Karusula, N.; Nicholson, C. K.; Calvert, J. W.; Lefer, D. J. H₂S protects against pressure overload-induced heart failure via upregulation of endothelial nitric oxide synthase. *Circulation* **2013**, *127* (10), 1116-27.
9. (a) Wang, G.; Li, W.; Chen, Q.; Jiang, Y.; Lu, X.; Zhao, X. Hydrogen sulfide accelerates wound healing in diabetic rats. *Int J Clin Exp Pathol* **2015**, *8* (5), 5097-104; (b) Zheng, D.; Chen, Z.; Chen, J.; Zhuang, X.; Feng, J.; Li, J. Exogenous hydrogen sulfide exerts proliferation, anti-apoptosis, migration effects and accelerates cell cycle progression in multiple myeloma cells via activating the Akt pathway. *Oncol Rep* **2016**, *36* (4), 1909-16.
10. Alshorafa, A. K.; Guo, Q.; Zeng, F.; Chen, M.; Tan, G.; Tang, Z.; Yin, R. Psoriasis is associated with low serum levels of hydrogen sulfide, a potential anti-inflammatory molecule. *Tohoku J Exp Med* **2012**, *228* (4), 325-32.
11. Yang, G.; Sun, X.; Wang, R. Hydrogen sulfide-induced apoptosis of human aorta smooth muscle cells via the activation of mitogen-activated protein kinases and caspase-3. *FASEB J* **2004**, *18* (14), 1782-4.
12. (a) Gemici, B.; Wallace, J. L. Anti-inflammatory and Cytoprotective Properties of Hydrogen Sulfide. In *Hydrogen Sulfide in Redox Biology, Pt B*, Cadenas, E.; Packer, L., Eds. 2015; Vol. 555, pp 169-193; (b) Wallace, J. L. Hydrogen sulfide-releasing anti-inflammatory drugs. *Trends Pharmacol Sci* **2007**, *28* (10), 501-5; (c) Wallace, J. L.; Blackler, R. W.; Chan, M. V.; Da Silva, G. J.; Elsheikh, W.; Flannigan, K. L.; Gamaniek, I.; Manko, A.; Wang, L.; Motta, J. P.; Buret, A. G. Anti-inflammatory and cytoprotective actions of hydrogen sulfide: translation to therapeutics. *Antioxid Redox Signal* **2015**, *22* (5), 398-410.
13. Wu, D.; Hu, Q.; Liu, X.; Pan, L.; Xiong, Q.; Zhu, Y. Z. Hydrogen sulfide protects against apoptosis under oxidative stress through SIRT1 pathway in H9c2 cardiomyocytes. *Nitric Oxide* **2015**, *46*, 204-12.
14. (a) Tamizhselvi, R.; Moore, P. K.; Bhatia, M. Inhibition of hydrogen sulfide synthesis attenuates chemokine production and protects mice against acute pancreatitis and associated lung injury. *Pancreas* **2008**, *36* (4), e24-31; (b) Zanardo, R. C.; Brancialeone, V.; Distrutti, E.; Fiorucci, S.; Cirino, G.; Wallace, J. L. Hydrogen sulfide is an endogenous modulator of leukocyte-mediated inflammation. *FASEB J* **2006**, *20* (12), 2118-20.

15. (a) Bora, P.; Chauhan, P.; Pardeshi, K. A.; Chakrapani, H. Small molecule generators of biologically reactive sulfur species. *RSC Advances* **2018**, *8* (48), 27359-27374; (b) Dillon, K. M.; Powell, C. R.; Matson, J. B. Self-Immolative Prodrugs: Effective Tools for the Controlled Release of Sulfur Signaling Species. *Synlett* **2019**, *30* (5), 525-531; (c) Papapetropoulos, A.; Whiteman, M.; Cirino, G. Pharmacological tools for hydrogen sulphide research: a brief, introductory guide for beginners. *Br J Pharmacol* **2015**, *172* (6), 1633-7; (d) Powell, C. R.; Dillon, K. M.; Matson, J. B. A review of hydrogen sulfide (H₂S) donors: Chemistry and potential therapeutic applications. *Biochem Pharmacol* **2018**, *149*, 110-123; (e) Song, Z. J.; Ng, M. Y.; Lee, Z.-W.; Dai, W.; Hagen, T.; Moore, P. K.; Huang, D.; Deng, L.-W.; Tan, C.-H. Hydrogen sulfide donors in research and drug development. *Med. Chem. Commun.* **2014**, *5* (5), 557-570; (f) Szabo, C.; Papapetropoulos, A. International Union of Basic and Clinical Pharmacology. CII: Pharmacological Modulation of H₂S Levels: H₂S Donors and H₂S Biosynthesis Inhibitors. *Pharmacol Rev* **2017**, *69* (4), 497-564; (g) Wu, D.; Hu, Q.; Zhu, Y. Therapeutic application of hydrogen sulfide donors: the potential and challenges. *Front Med* **2016**, *10* (1), 18-27.
16. Steiger, A. K.; Pardue, S.; Kevil, C. G.; Pluth, M. D. Self-Immolative Thiocarbamates Provide Access to Triggered H₂S Donors and Analyte Replacement Fluorescent Probes. *J Am Chem Soc* **2016**, *138* (23), 7256-9.
17. Zheng, Y.; Yu, B.; Ji, K.; Pan, Z.; Chittavong, V.; Wang, B. Esterase-Sensitive Prodrugs with Tunable Release Rates and Direct Generation of Hydrogen Sulfide. *Angew Chem Int Ed Engl* **2016**, *55* (14), 4514-8.
18. Fukami, T.; Yokoi, T. The emerging role of human esterases. *Drug Metab Pharmacokinet* **2012**, *27* (5), 466-77.
19. Chauhan, P.; Bora, P.; Ravikumar, G.; Jos, S.; Chakrapani, H. Esterase Activated Carbonyl Sulfide/Hydrogen Sulfide (H₂S) Donors. *Org Lett* **2017**, *19* (1), 62-65.
20. Steiger, A. K.; Marcatti, M.; Szabo, C.; Szczesny, B.; Pluth, M. D. Inhibition of Mitochondrial Bioenergetics by Esterase-Triggered COS/H₂S Donors. *ACS Chem Biol* **2017**, *12* (8), 2117-2123.
21. Levinn, C. M.; Steiger, A. K.; Pluth, M. D. Esterase-Triggered Self-Immolative Thiocarbamates Provide Insights into COS Cytotoxicity. *ACS Chem Biol* **2019**, *14* (2), 170-175.
22. Shukla, P.; Khodade, V. S.; SharathChandra, M.; Chauhan, P.; Mishra, S.; Siddaramappa, S.; Pradeep, B. E.; Singh, A.; Chakrapani, H. "On demand" redox buffering by H₂S contributes to antibiotic resistance revealed by a bacteria-specific H₂S donor. *Chem Sci* **2017**, *8* (7), 4967-4972.
23. (a) Brown, J. M.; Wilson, W. R. Exploiting tumour hypoxia in cancer treatment. *Nat Rev Cancer* **2004**, *4* (6), 437-47; (b) Wilson, W. R.; Hay, M. P. Targeting hypoxia in cancer therapy. *Nat Rev Cancer* **2011**, *11* (6), 393-410.

24. Zhao, Y.; Pluth, M. D. Hydrogen Sulfide Donors Activated by Reactive Oxygen Species. *Angew Chem Int Ed Engl* **2016**, *55* (47), 14638-14642.
25. Zhao, Y.; Henthorn, H. A.; Pluth, M. D. Kinetic Insights into Hydrogen Sulfide Delivery from Caged-Carbonyl Sulfide Isomeric Donor Platforms. *J Am Chem Soc* **2017**, *139* (45), 16365-16376.
26. Chauhan, P.; Jos, S.; Chakrapani, H. Reactive Oxygen Species-Triggered Tunable Hydrogen Sulfide Release. *Org Lett* **2018**, *20* (13), 3766-3770.
27. Hu, Y.; Li, X.; Fang, Y.; Shi, W.; Li, X.; Chen, W.; Xian, M.; Ma, H. Reactive oxygen species-triggered off-on fluorescence donor for imaging hydrogen sulfide delivery in living cells. *Chem Sci* **2019**, *10* (33), 7690-7694.
28. Lehrman, L. Thioacetamide as a source of hydrogen sulfide in qualitative analysis. *Journal of Chemical Education* **1955**, *32* (9).
29. Martelli, A.; Testai, L.; Citi, V.; Marino, A.; Pugliesi, I.; Barresi, E.; Nesi, G.; Rapposelli, S.; Taliani, S.; Da Settimo, F.; Breschi, M. C.; Calderone, V. Arylthioamides as H₂S Donors: l-Cysteine-Activated Releasing Properties and Vascular Effects in Vitro and in Vivo. *ACS Med Chem Lett* **2013**, *4* (10), 904-8.
30. Zhou, Z.; von Wantoch Rekowski, M.; Coletta, C.; Szabo, C.; Bucci, M.; Cirino, G.; Topouzis, S.; Papapetropoulos, A.; Giannis, A. Thioglycine and L-thiovaline: biologically active H(2)S-donors. *Bioorg Med Chem* **2012**, *20* (8), 2675-8.
31. Lecher, H. Z.; Greenwood, R. A.; Whitehouse, K. C.; Chao, T. H. The Phosphonation of Aromatic Compounds with Phosphorus Pentasulfide. *Journal of the American Chemical Society* **1956**, *78* (19), 5018-5022.
32. Pedersen, B. S.; Scheibye, S.; Nilsson, N. H.; Lawesson, S. O. STUDIES ON ORGANOPHOSPHORUS COMPOUNDS .10. SYNTHESSES OF THIOKETONES. *Bulletin Des Societes Chimiques Belges* **1978**, *87* (3), 223-228.
33. Li, L.; Whiteman, M.; Guan, Y. Y.; Neo, K. L.; Cheng, Y.; Lee, S. W.; Zhao, Y.; Baskar, R.; Tan, C. H.; Moore, P. K. Characterization of a novel, water-soluble hydrogen sulfide-releasing molecule (GYY4137): new insights into the biology of hydrogen sulfide. *Circulation* **2008**, *117* (18), 2351-60.
34. Nin, D. S.; Idres, S. B.; Song, Z. J.; Moore, P. K.; Deng, L. W. Biological Effects of Morpholin-4-Ium 4 Methoxyphenyl (Morpholino) Phosphinodithioate and Other Phosphorothioate-Based Hydrogen Sulfide Donors. *Antioxid Redox Signal* **2020**, *32* (2), 145-158.
35. Park, C. M.; Zhao, Y.; Zhu, Z.; Pacheco, A.; Peng, B.; Devarie-Baez, N. O.; Bagdon, P.; Zhang, H.; Xian, M. Synthesis and evaluation of phosphorodithioate-based hydrogen sulfide donors. *Mol Biosyst* **2013**, *9* (10), 2430-4.

36. Feng, W.; Teo, X. Y.; Novera, W.; Ramanujulu, P. M.; Liang, D.; Huang, D.; Moore, P. K.; Deng, L. W.; Dymock, B. W. Discovery of New H₂S Releasing Phosphordithioates and 2,3-Dihydro-2-phenyl-2-sulfanylenebenzo[d][1,3,2]oxazaphospholes with Improved Antiproliferative Activity. *J Med Chem* **2015**, *58* (16), 6456-80.
37. Kang, J.; Li, Z.; Organ, C. L.; Park, C. M.; Yang, C. T.; Pacheco, A.; Wang, D.; Lefer, D. J.; Xian, M. pH-Controlled Hydrogen Sulfide Release for Myocardial Ischemia-Reperfusion Injury. *J Am Chem Soc* **2016**, *138* (20), 6336-9.
38. Sagi, A.; Weinstain, R.; Karton, N.; Shabat, D. Self-immolative polymers. *J Am Chem Soc* **2008**, *130* (16), 5434-5.
39. Zhao, Y.; Steiger, A. K.; Pluth, M. D. Colorimetric Carbonyl Sulfide (COS)/Hydrogen Sulfide (H₂S) Donation from gamma-Ketothiocarbamate Donor Motifs. *Angew Chem Int Ed Engl* **2018**, *57* (40), 13101-13105.
40. Gilbert, A. K.; Zhao, Y.; Otteson, C. E.; Pluth, M. D. Development of Acid-Mediated H₂S/COS Donors That Respond to a Specific pH Window. *J Org Chem* **2019**, *84* (22), 14469-14475.
41. Barresi, E.; Nesi, G.; Citi, V.; Piragine, E.; Piano, I.; Taliani, S.; Da Settimo, F.; Rapposelli, S.; Testai, L.; Breschi, M. C.; Gargini, C.; Calderone, V.; Martelli, A. Iminothioethers as Hydrogen Sulfide Donors: From the Gasotransmitter Release to the Vascular Effects. *J Med Chem* **2017**, *60* (17), 7512-7523.
42. Martelli, A.; Testai, L.; Citi, V.; Marino, A.; Bellagambi, F. G.; Ghimenti, S.; Breschi, M. C.; Calderone, V. Pharmacological characterization of the vascular effects of aryl isothiocyanates: is hydrogen sulfide the real player? *Vascul Pharmacol* **2014**, *60* (1), 32-41.
43. Lin, Y.; Yang, X.; Lu, Y.; Liang, D.; Huang, D. Isothiocyanates as H₂S Donors Triggered by Cysteine: Reaction Mechanism and Structure and Activity Relationship. *Org Lett* **2019**, *21* (15), 5977-5980.
44. Dawson, P. E.; Muir, T. W.; Clark-Lewis, I.; Kent, S. B. Synthesis of proteins by native chemical ligation. *Science* **1994**, *266* (5186), 776-9.
45. Cerda, M. M.; Zhao, Y.; Pluth, M. D. Thionoesters: A Native Chemical Ligation-Inspired Approach to Cysteine-Triggered H₂S Donors. *J Am Chem Soc* **2018**, *140* (39), 12574-12579.
46. Cerda, M. M.; Newton, T. D.; Zhao, Y.; Collins, B. K.; Hendon, C. H.; Pluth, M. D. Dithioesters: simple, tunable, cysteine-selective H₂S donors. *Chem Sci* **2019**, *10* (6), 1773-1779.

47. Kim, N. H.; Moon, H.; Kim, J. H.; Huh, Y.; Kim, Y. J.; Kim, B. M.; Kim, D. A benzothioate native chemical ligation-based cysteine-selective fluorescent probe. *Dyes and Pigments* **2019**, *171*.
48. Zhao, Y.; Kang, J.; Park, C. M.; Bagdon, P. E.; Peng, B.; Xian, M. Thiol-activated gem-dithiols: a new class of controllable hydrogen sulfide donors. *Org Lett* **2014**, *16* (17), 4536-9.
49. Zhu, Y.; Romero, E. L.; Ren, X.; Sanca, A. J.; Du, C.; Liu, C.; Karim, Z. A.; Alshbool, F. Z.; Khasawneh, F. T.; Zhou, J.; Zhong, D.; Geng, B. Clopidogrel as a donor probe and thioenol derivatives as flexible promoieties for enabling H₂S biomedicine. *Nat Commun* **2018**, *9* (1), 3952.
50. Zhao, Y.; Wang, H.; Xian, M. Cysteine-activated hydrogen sulfide (H₂S) donors. *J Am Chem Soc* **2011**, *133* (1), 15-7.
51. Zhao, Y.; Yang, C.; Organ, C.; Li, Z.; Bhushan, S.; Otsuka, H.; Pacheco, A.; Kang, J.; Aguilar, H. C.; Lefer, D. J.; Xian, M. Design, Synthesis, and Cardioprotective Effects of N-Mercapto-Based Hydrogen Sulfide Donors. *J Med Chem* **2015**, *58* (18), 7501-11.
52. Zhao, Y.; Bhushan, S.; Yang, C.; Otsuka, H.; Stein, J. D.; Pacheco, A.; Peng, B.; Devarie-Baez, N. O.; Aguilar, H. C.; Lefer, D. J.; Xian, M. Controllable hydrogen sulfide donors and their activity against myocardial ischemia-reperfusion injury. *ACS Chem Biol* **2013**, *8* (6), 1283-90.
53. Foster, J. C.; Powell, C. R.; Radzinski, S. C.; Matson, J. B. S-arylothiooximes: a facile route to hydrogen sulfide releasing compounds with structure-dependent release kinetics. *Org Lett* **2014**, *16* (6), 1558-61.
54. Kang, J.; Ferrell, A. J.; Chen, W.; Wang, D.; Xian, M. Cyclic Acyl Disulfides and Acyl Selenylsulfides as the Precursors for Persulfides (RSSH), Selenylsulfides (RSeSH), and Hydrogen Sulfide (H₂S). *Org Lett* **2018**, *20* (3), 852-855.
55. Hamsath, A.; Wang, Y.; Yang, C. T.; Xu, S.; Canedo, D.; Chen, W.; Xian, M. Acyl Selenyl Sulfides as the Precursors for Reactive Sulfur Species (Hydrogen Sulfide, Polysulfide, and Selenyl Sulfide). *Org Lett* **2019**, *21* (14), 5685-5688.
56. Roger, T.; Raynaud, F.; Bouillaud, F.; Ransy, C.; Simonet, S.; Crespo, C.; Bourguignon, M. P.; Villeneuve, N.; Vilaine, J. P.; Artaud, I.; Galardon, E. New biologically active hydrogen sulfide donors. *Chembiochem* **2013**, *14* (17), 2268-71.
57. (a) Yang, C. T.; Devarie-Baez, N. O.; Hamsath, A.; Fu, X. D.; Xian, M. S-Persulfidation: Chemistry, Chemical Biology, and Significance in Health and Disease. *Antioxid Redox Signal* **2019**; (b) Park, C. M.; Weerasinghe, L.; Day, J. J.; Fukuto, J. M.; Xian, M. Persulfides: current knowledge and challenges in chemistry and chemical biology. *Mol Biosyst* **2015**, *11* (7), 1775-85.

58. Pluth, M.; Bailey, T.; Hammers, M.; Hartle, M.; Henthorn, H.; Steiger, A. Natural Products Containing Hydrogen Sulfide Releasing Moieties. *Synlett* **2015**, *26* (19), 2633-2643.
59. Benavides, G. A.; Squadrino, G. L.; Mills, R. W.; Patel, H. D.; Isbell, T. S.; Patel, R. P.; Darley-Usmar, V. M.; Doeller, J. E.; Kraus, D. W. Hydrogen sulfide mediates the vasoactivity of garlic. *Proc Natl Acad Sci U S A* **2007**, *104* (46), 17977-82.
60. Liang, D.; Wu, H.; Wong, M. W.; Huang, D. Diallyl Trisulfide Is a Fast H₂S Donor, but Diallyl Disulfide Is a Slow One: The Reaction Pathways and Intermediates of Glutathione with Polysulfides. *Org Lett* **2015**, *17* (17), 4196-9.
61. Cai, Y. R.; Hu, C. H. Computational Study of H₂S Release in Reactions of Diallyl Polysulfides with Thiols. *J Phys Chem B* **2017**, *121* (26), 6359-6366.
62. Yao, H.; Luo, S.; Liu, J.; Xie, S.; Liu, Y.; Xu, J.; Zhu, Z.; Xu, S. Controllable thioester-based hydrogen sulfide slow-releasing donors as cardioprotective agents. *Chem Commun (Camb)* **2019**, *55* (44), 6193-6196.
63. Cerda, M. M.; Hammers, M. D.; Earp, M. S.; Zakharov, L. N.; Pluth, M. D. Applications of Synthetic Organic Tetrasulfides as H₂S Donors. *Org Lett* **2017**, *19* (9), 2314-2317.
64. Bolton, S. G.; Cerda, M. M.; Gilbert, A. K.; Pluth, M. D. Effects of sulfane sulfur content in benzyl polysulfides on thiol-triggered H₂S release and cell proliferation. *Free Radic Biol Med* **2019**, *131*, 393-398.
65. Toohey, J. I. Sulfur signaling: is the agent sulfide or sulfane? *Anal Biochem* **2011**, *413* (1), 1-7.
66. Ercole, F.; Whittaker, M. R.; Halls, M. L.; Boyd, B. J.; Davis, T. P.; Quinn, J. F. Garlic-inspired trisulfide linkers for thiol-stimulated H₂S release. *Chem Commun (Camb)* **2017**, *53* (57), 8030-8033.
67. Zhao, Y.; Cerda, M. M.; Pluth, M. D. Fluorogenic hydrogen sulfide (H₂S) donors based on sulfenyl thiocarbonates enable H₂S tracking and quantification. *Chem Sci* **2019**, *10* (6), 1873-1878.
68. Zhao, Y.; Steiger, A. K.; Pluth, M. D. Cysteine-activated hydrogen sulfide (H₂S) delivery through caged carbonyl sulfide (COS) donor motifs. *Chem Commun (Camb)* **2018**, *54* (39), 4951-4954.
69. Severino, B.; Corvino, A.; Fiorino, F.; Luciano, P.; Frecentese, F.; Magli, E.; Saccone, I.; Di Vaio, P.; Citi, V.; Calderone, V.; Servillo, L.; Casale, R.; Cirino, G.; Vellecco, V.; Bucci, M.; Perissutti, E.; Santagada, V.; Caliendo, G. 1,2,4-Thiadiazolidin-3,5-diones as novel hydrogen sulfide donors. *Eur J Med Chem* **2018**, *143*, 1677-1686.

70. (a) Ai, X.; Mu, J.; Xing, B. Recent Advances of Light-Mediated Theranostics. *Theranostics* **2016**, *6* (13), 2439-2457; (b) Chen, H.; Zhao, Y. Applications of Light-Responsive Systems for Cancer Theranostics. *ACS Appl Mater Interfaces* **2018**, *10* (25), 21021-21034.
71. Devarie-Baez, N. O.; Bagdon, P. E.; Peng, B.; Zhao, Y.; Park, C. M.; Xian, M. Light-induced hydrogen sulfide release from "caged" gem-dithiols. *Org Lett* **2013**, *15* (11), 2786-9.
72. (a) Li, Z.; Li, D.; Wang, L.; Lu, C.; Shan, P.; Zou, X.; Li, Z. Photocontrollable water-soluble polymeric hydrogen sulfide (H₂S) donor. *Polymer* **2019**, *168*, 16-20; (b) Wang, L.; Ma, F.; Zou, X.; Li, Z. Block copolymer nanoparticles as light-induced hydrogen sulfide (H₂S) donors. *J Control Release* **2015**, *213*, e71-2.
73. Chen, W.; Chen, M.; Zang, Q.; Wang, L.; Tang, F.; Han, Y.; Yang, C.; Deng, L.; Liu, Y. N. NIR light controlled release of caged hydrogen sulfide based on upconversion nanoparticles. *Chem Commun (Camb)* **2015**, *51* (44), 9193-6.
74. Fukushima, N.; Ieda, N.; Sasakura, K.; Nagano, T.; Hanaoka, K.; Suzuki, T.; Miyata, N.; Nakagawa, H. Synthesis of a photocontrollable hydrogen sulfide donor using ketoprofenate photocages. *Chem Commun (Camb)* **2014**, *50* (5), 587-9.
75. Fukushima, N.; Ieda, N.; Kawaguchi, M.; Sasakura, K.; Nagano, T.; Hanaoka, K.; Miyata, N.; Nakagawa, H. Development of photo-controllable hydrogen sulfide donor applicable in live cells. *Bioorg Med Chem Lett* **2015**, *25* (2), 175-8.
76. Xiao, Z.; Bonnard, T.; Shakouri-Motlagh, A.; Wylie, R. A. L.; Collins, J.; White, J.; Heath, D. E.; Hagemeyer, C. E.; Connal, L. A. Triggered and Tunable Hydrogen Sulfide Release from Photogenerated Thiobenzaldehydes. *Chemistry* **2017**, *23* (47), 11294-11300.
77. Yi, S. Y.; Moon, Y. K.; Kim, S.; Kim, S.; Park, G.; Kim, J. J.; You, Y. Visible light-driven photogeneration of hydrogen sulfide. *Chem Commun (Camb)* **2017**, *53* (86), 11830-11833.
78. Zhao, Y.; Bolton, S. G.; Pluth, M. D. Light-Activated COS/H₂S Donation from Photocaged Thiocarbamates. *Org Lett* **2017**, *19* (9), 2278-2281.
79. Sharma, A. K.; Nair, M.; Chauhan, P.; Gupta, K.; Saini, D. K.; Chakrapani, H. Visible-Light-Triggered Uncaging of Carbonyl Sulfide for Hydrogen Sulfide (H₂S) Release. *Org Lett* **2017**, *19* (18), 4822-4825.
80. (a) Dabrowski, J. M.; Arnaut, L. G. Photodynamic therapy (PDT) of cancer: from local to systemic treatment. *Photochem Photobiol Sci* **2015**, *14* (10), 1765-80; (b) Phan, T. G.; Bullen, A. Practical intravital two-photon microscopy for immunological research: faster, brighter, deeper. *Immunol Cell Biol* **2010**, *88* (4), 438-44.
81. Stacko, P.; Muchova, L.; Vitek, L.; Klan, P. Visible to NIR Light Photoactivation of Hydrogen Sulfide for Biological Targeting. *Org Lett* **2018**, *20* (16), 4907-4911.

82. Woods, J. J.; Cao, J.; Lippert, A. R.; Wilson, J. J. Characterization and Biological Activity of a Hydrogen Sulfide-Releasing Red Light-Activated Ruthenium(II) Complex. *J Am Chem Soc* **2018**, *140* (39), 12383-12387.
83. Luo, X.; Wu, J.; Lv, T.; Lai, Y.; Zhang, H.; Lu, J.-J.; Zhang, Y.; Huang, Z. Synthesis and evaluation of novel O₂-derived diazeniumdiolates as photochemical and real-time monitoring nitric oxide delivery agents. *Organic Chemistry Frontiers* **2017**, *4* (12), 2445-2449.
84. Venkatesh, Y.; Das, J.; Chaudhuri, A.; Karmakar, A.; Maiti, T. K.; Singh, N. D. P. Light triggered uncaging of hydrogen sulfide (H₂S) with real-time monitoring. *Chem Commun (Camb)* **2018**, *54* (25), 3106-3109.
85. Steiger, A. K.; Yang, Y.; Royzen, M.; Pluth, M. D. Bio-orthogonal "click-and-release" donation of caged carbonyl sulfide (COS) and hydrogen sulfide (H₂S). *Chem Commun (Camb)* **2017**, *53* (8), 1378-1380.
86. Bruins, J. J.; Blanco-Ania, D.; van der Doef, V.; van Delft, F. L.; Albada, B. Orthogonal, dual protein labelling by tandem cycloaddition of strained alkenes and alkynes to ortho-quinones and azides. *Chem Commun (Camb)* **2018**, *54* (53), 7338-7341.
87. Powell, C. R.; Foster, J. C.; Okyere, B.; Theus, M. H.; Matson, J. B. Therapeutic Delivery of H₂S via COS: Small Molecule and Polymeric Donors with Benign Byproducts. *J Am Chem Soc* **2016**, *138* (41), 13477-13480.
88. Powell, C. R.; Kaur, K.; Dillon, K. M.; Zhou, M.; Alaboalirat, M.; Matson, J. B. Functional N-Substituted N-Thiocarboxyanhydrides as Modular Tools for Constructing H₂S Donor Conjugates. *ACS Chem Biol* **2019**, *14* (6), 1129-1134.
89. Kaur, K.; Carrazzone, R. J.; Matson, J. B. The Benefits of Macromolecular/Supramolecular Approaches in Hydrogen Sulfide Delivery: A Review of Polymeric and Self-Assembled Hydrogen Sulfide Donors. *Antioxid Redox Signal* **2020**, *32* (2), 79-95.
90. Wang, R. Physiological implications of hydrogen sulfide: a whiff exploration that blossomed. *Physiol Rev* **2012**, *92* (2), 791-896.
91. Kabil, O.; Banerjee, R. Enzymology of H₂S biogenesis, decay and signaling. *Antioxid Redox Signal* **2014**, *20* (5), 770-82.
92. Wallace, J. L.; Wang, R. Hydrogen sulfide-based therapeutics: exploiting a unique but ubiquitous gasotransmitter. *Nat Rev Drug Discov* **2015**, *14* (5), 329-45.
93. Zhao, W.; Zhang, J.; Lu, Y.; Wang, R. The vasorelaxant effect of H₂S as a novel endogenous gaseous K(ATP) channel opener. *EMBO J* **2001**, *20* (21), 6008-16.
94. Kimura, H. Hydrogen sulfide induces cyclic AMP and modulates the NMDA receptor. *Biochem Biophys Res Commun* **2000**, *267* (1), 129-33.

95. Papapetropoulos, A.; Pyriochou, A.; Altaany, Z.; Yang, G.; Marazioti, A.; Zhou, Z.; Jeschke, M. G.; Branski, L. K.; Herndon, D. N.; Wang, R.; Szabo, C. Hydrogen sulfide is an endogenous stimulator of angiogenesis. *Proc Natl Acad Sci U S A* **2009**, *106* (51), 21972-7.
96. DeLeon, E. R.; Stoy, G. F.; Olson, K. R. Passive loss of hydrogen sulfide in biological experiments. *Anal Biochem* **2012**, *421* (1), 203-7.
97. Yang, X.; Guo, Y.; Strongin, R. M. Conjugate addition/cyclization sequence enables selective and simultaneous fluorescence detection of cysteine and homocysteine. *Angew Chem Int Ed Engl* **2011**, *50* (45), 10690-3.
98. Valiyaveetil, F. I.; MacKinnon, R.; Muir, T. W. Semisynthesis and folding of the potassium channel KcsA. *J Am Chem Soc* **2002**, *124* (31), 9113-20.
99. Johnson, E. C.; Kent, S. B. Insights into the mechanism and catalysis of the native chemical ligation reaction. *J Am Chem Soc* **2006**, *128* (20), 6640-6.
100. Steiger, A. K.; Zhao, Y.; Pluth, M. D. Emerging Roles of Carbonyl Sulfide in Chemical Biology: Sulfide Transporter or Gasotransmitter? *Antioxid Redox Signal* **2018**, *28* (16), 1516-1532.
101. Hewitt, R. J.; Ong, M. J. H.; Lim, Y. W.; Burkett, B. A. Investigations of the Thermal Responsiveness of 1,4,2-Oxathiazoles. *European Journal of Organic Chemistry* **2015**, *2015* (30), 6687-6700.
102. Prangova, L.; Osternack, K.; Voss, J. ELECTROREDUCTION OF ORGANIC-COMPOUNDS .26. ONE-ELECTRON REDUCTION OF O-PHENYL ARENECARBOTHIOATES AS STUDIED BY DIFFERENTIAL-PULSE POLAROGRAPHY AND CYCLOVOLTAMMETRY. *Journal of Chemical Research-S* **1995**, (6), 234-&.
103. Legnani, L.; Toma, L.; Caramella, P.; Chiacchio, M. A.; Giofre, S.; Delso, I.; Tejero, T.; Merino, P. Computational Mechanistic Study of Thionation of Carbonyl Compounds with Lawesson's Reagent. *J Org Chem* **2016**, *81* (17), 7733-40.
104. Siegel, L. M. A Direct Microdetermination for Sulfide. *Anal Biochem* **1965**, *11* (1), 126-32.
105. Castro, E. A. Kinetics and Mechanisms of Reactions of Thiol, Thiono, and Dithio Analogues of Carboxylic Esters with Nucleophiles. *Chem Rev* **1999**, *99* (12), 3505-3524.
106. Um, I. H.; Lee, J. Y.; Kim, H. T.; Bae, S. K. Curved Hammett plot in alkaline hydrolysis of O-aryl thionobenzoates: change in rate-determining step versus ground-state stabilization. *J Org Chem* **2004**, *69* (7), 2436-41.

107. Um, I. H.; Hwang, S. J.; Yoon, S.; Jeon, S. E.; Bae, S. K. Aminolysis of O-aryl thionobenzoates: amine basicity combines with modulation of the nature of substituents in the leaving group and thionobenzoate moiety to control the reaction mechanism. *J Org Chem* **2008**, *73* (19), 7671-7.
108. Benesch, R. E.; Benesch, R. The Acid Strength of the -SH Group in Cysteine and Related Compounds. *Journal of the American Chemical Society* **1955**, *77* (22), 5877-5881.
109. Beesley, R. M.; Ingold, C. K.; Thorpe, J. F. CXIX.—The formation and stability of spiro-compounds. Part I. spiro-Compounds from cyclohexane. *J. Chem. Soc., Trans.* **1915**, *107* (0), 1080-1106.
110. Oliveira, B. L.; Guo, Z.; Bernardes, G. J. L. Inverse electron demand Diels-Alder reactions in chemical biology. *Chem Soc Rev* **2017**, *46* (16), 4895-4950.
111. Walsh, C. T.; Nolan, E. M. Morphing peptide backbones into heterocycles. *Proc Natl Acad Sci U S A* **2008**, *105* (15), 5655-6.
112. Miethke, M.; Marahiel, M. A. Siderophore-based iron acquisition and pathogen control. *Microbiol Mol Biol Rev* **2007**, *71* (3), 413-51.
113. Gehring, A. M.; Mori, I.; Perry, R. D.; Walsh, C. T. The nonribosomal peptide synthetase HMWP2 forms a thiazoline ring during biogenesis of yersiniabactin, an iron-chelating virulence factor of *Yersinia pestis*. *Biochemistry* **1998**, *37* (33), 11637-50.
114. Quadri, L. E.; Keating, T. A.; Patel, H. M.; Walsh, C. T. Assembly of the *Pseudomonas aeruginosa* nonribosomal peptide siderophore pyochelin: In vitro reconstitution of aryl-4, 2-bisthiazoline synthetase activity from PchD, PchE, and PchF. *Biochemistry* **1999**, *38* (45), 14941-54.
115. Schneider, T. L.; Shen, B.; Walsh, C. T. Oxidase domains in epothilone and bleomycin biosynthesis: thiazoline to thiazole oxidation during chain elongation. *Biochemistry* **2003**, *42* (32), 9722-30.
116. Lim, Y. W.; Hewitt, R. J.; Burkett, B. A. The Dual Reactivity of 5-S/5-O-Phenyl-1,4,2-oxathiazoles: A Fragmentation Pathway That Affords Nitriles in the Presence of Water. *European Journal of Organic Chemistry* **2015**, *2015* (22), 4840-4842.
117. Zhang, G.; Liu, C.; Yi, H.; Meng, Q.; Bian, C.; Chen, H.; Jian, J. X.; Wu, L. Z.; Lei, A. External Oxidant-Free Oxidative Cross-Coupling: A Photoredox Cobalt-Catalyzed Aromatic C-H Thiolation for Constructing C-S Bonds. *J Am Chem Soc* **2015**, *137* (29), 9273-80.
118. Kim, T. S.; Lee, Y. J.; Jeong, B. S.; Park, H. G.; Jew, S. S. Enantioselective synthesis of (R)- and (S)-alpha-alkylcysteines via phase-transfer catalytic alkylation. *J Org Chem* **2006**, *71* (21), 8276-8.

119. Chiefari, J.; Chong, Y. K.; Ercole, F.; Krstina, J.; Jeffery, J.; Le, T. P. T.; Mayadunne, R. T. A.; Meijs, G. F.; Moad, C. L.; Moad, G.; Rizzardo, E.; Thang, S. H. Living Free-Radical Polymerization by Reversible Addition-Fragmentation Chain Transfer: The RAFT Process. *Macromolecules* **1998**, *31* (16), 5559-5562.
120. (a) Chiefari, J.; Mayadunne, R. T. A.; Moad, C. L.; Moad, G.; Rizzardo, E.; Postma, A.; Thang, S. H. Thiocarbonylthio Compounds (SC(Z)S-R) in Free Radical Polymerization with Reversible Addition-Fragmentation Chain Transfer (RAFT Polymerization). Effect of the Activating Group Z. *Macromolecules* **2003**, *36* (7), 2273-2283; (b) Chong, Y. K.; Krstina, J.; Le, T. P. T.; Moad, G.; Postma, A.; Rizzardo, E.; Thang, S. H. Thiocarbonylthio Compounds [SC(Ph)S-R] in Free Radical Polymerization with Reversible Addition-Fragmentation Chain Transfer (RAFT Polymerization). Role of the Free-Radical Leaving Group (R). *Macromolecules* **2003**, *36* (7), 2256-2272.
121. Cerda, M. M.; Zhao, Y.; Pluth, M. D. Thionoesters: A Native Chemical Ligation-Inspired Approach to Cysteine-Triggered H₂S Donors. *Journal of the American Chemical Society* **2018**, *140* (39), 12574-12579.
122. Newton, J. J.; Britton, R.; Friesen, C. M. Base-Catalyzed Transesterification of Thionoesters. *J Org Chem* **2018**, *83* (20), 12784-12792.
123. Mustafa, A. K.; Gadalla, M. M.; Snyder, S. H. Signaling by gasotransmitters. *Sci Signal* **2009**, *2* (68), re2.
124. Wang, R. Two's company, three's a crowd: can H₂S be the third endogenous gaseous transmitter? *Faseb Journal* **2002**, *16* (13), 1792-1798.
125. Altaany, Z.; Yang, G.; Wang, R. Crosstalk between hydrogen sulfide and nitric oxide in endothelial cells. *J Cell Mol Med* **2013**, *17* (7), 879-88.
126. Yang, G.; Zhao, K.; Ju, Y.; Mani, S.; Cao, Q.; Puukila, S.; Khaper, N.; Wu, L.; Wang, R. Hydrogen sulfide protects against cellular senescence via S-sulphydration of Keap1 and activation of Nrf2. *Antioxid Redox Signal* **2013**, *18* (15), 1906-19.
127. (a) Wallace, J. L.; Wang, R. Hydrogen sulfide-based therapeutics: exploiting a unique but ubiquitous gasotransmitter. *Nature Reviews Drug Discovery* **2015**, *14* (5), 329-345; (b) Zheng, Y.; Yu, B.; De La Cruz, L. K.; Roy Choudhury, M.; Anifowose, A.; Wang, B. Toward Hydrogen Sulfide Based Therapeutics: Critical Drug Delivery and Developability Issues. *Med Res Rev* **2018**, *38* (1), 57-100.
128. Whiteman, M.; Li, L.; Rose, P.; Tan, C. H.; Parkinson, D. B.; Moore, P. K. The effect of hydrogen sulfide donors on lipopolysaccharide-induced formation of inflammatory mediators in macrophages. *Antioxid Redox Signal* **2010**, *12* (10), 1147-54.
129. DeLeon, E. R.; Stoy, G. F.; Olson, K. R. Passive loss of hydrogen sulfide in biological experiments. *Analytical Biochemistry* **2012**, *421* (1), 203-207.

130. (a) Powell, C. R.; Dillon, K. M.; Matson, J. B. A review of hydrogen sulfide (H₂S) donors: Chemistry and potential therapeutic applications. *Biochemical Pharmacology* **2018**, *149*, 110-123; (b) Szabo, C.; Papapetropoulos, A. International Union of Basic and Clinical Pharmacology. CII: Pharmacological Modulation of H₂S Levels: H₂S Donors and H₂S Biosynthesis Inhibitors. *Pharmacological Reviews* **2017**, *69* (4), 497-564; (c) Zhao, Y.; Biggs, T. D.; Xian, M. Hydrogen sulfide (H₂S) releasing agents: chemistry and biological applications. *Chemical Communications* **2014**, *50* (80), 11788-11805.
131. Li, L.; Rossoni, G.; Sparatore, A.; Lee, L. C.; Del Soldato, P.; Moore, P. K. Anti-inflammatory and gastrointestinal effects of a novel diclofenac derivative. *Free Radic Biol Med* **2007**, *42* (5), 706-19.
132. Zheng, Y.; Yu, B.; Ji, K.; Pan, Z.; Chittavong, V.; Wang, B. Esterase-Sensitive Prodrugs with Tunable Release Rates and Direct Generation of Hydrogen Sulfide. *Angewandte Chemie-International Edition* **2016**, *55* (14), 4514-4518.
133. (a) Xiao, Z.; Bonnard, T.; Shakouri-Motlagh, A.; Wylie, R. A. L.; Collins, J.; White, J.; Heath, D. E.; Hagemeyer, C. E.; Connal, L. A. Triggered and Tunable Hydrogen Sulfide Release from Photogenerated Thiobenzaldehydes. *Chemistry-a European Journal* **2017**, *23* (47), 11294-11300; (b) Woods, J. J.; Cao, J.; Lippert, A. R.; Wilson, J. J. Characterization and Biological Activity of a Hydrogen Sulfide-Releasing Red Light-Activated Ruthenium(II) Complex. *Journal of the American Chemical Society* **2018**, *140* (39), 12383-12387.
134. Steiger, A. K.; Pardue, S.; Kevil, C. G.; Pluth, M. D. Self-Immolative Thiocarbamates Provide Access to Triggered H₂S Donors and Analyte Replacement Fluorescent Probes. *Journal of the American Chemical Society* **2016**, *138* (23), 7256-7259.
135. (a) Zhao, Y.; Steiger, A. K.; Pluth, M. D. Colorimetric Carbonyl Sulfide (COS)/Hydrogen Sulfide (H₂S) Donation from gamma-Ketothiocarbamate Donor Motifs. *Angewandte Chemie-International Edition* **2018**, *57* (40), 13101-13105; (b) Sharma, A. K.; Nair, M.; Chauhan, P.; Gupta, K.; Saini, D. K.; Chakrapani, H. Visible-Light-Triggered Uncaging of Carbonyl Sulfide for Hydrogen Sulfide (H₂S) Release. *Organic Letters* **2017**, *19* (18), 4822-4825; (c) Powell, C. R.; Foster, J. C.; Okyere, B.; Theus, M. H.; Matson, J. B. Therapeutic Delivery of H₂S via COS: Small Molecule and Polymeric Donors with Benign Byproducts. *Journal of the American Chemical Society* **2016**, *138* (41), 13477-13480.
136. Ercole, F.; Whittaker, M. R.; Halls, M. L.; Boyd, B. J.; Davis, T. P.; Quinn, J. F. Garlic-inspired trisulfide linkers for thiol-stimulated H₂S release. *Chemical Communications* **2017**, *53* (57), 8030-8033.
137. Cerda, M. M.; Hammers, M. D.; Earp, M. S.; Zakharov, L. N.; Pluth, M. D. Applications of Synthetic Organic Tetrasulfides as H₂S Donors. *Organic Letters* **2017**, *19* (9), 2314-2317.
138. Filipovic, M. R.; Zivanovic, J.; Alvarez, B.; Banerjee, R. Chemical Biology of H₂S Signaling through Persulfidation. *Chem Rev* **2018**, *118* (3), 1253-1337.

139. (a) Zhao, Y.; Wang, H.; Xian, M. Cysteine-Activated Hydrogen Sulfide (H₂S) Donors. *Journal of the American Chemical Society* **2011**, *133* (1), 15-17; (b) Zhao, Y.; Yang, C.; Organ, C.; Li, Z.; Bhushan, S.; Otsuka, H.; Pacheco, A.; Kang, J.; Aguilar, H. C.; Lefer, D. J.; Xian, M. Design, Synthesis, and Cardioprotective Effects of N-Mercapto-Based Hydrogen Sulfide Donors. *Journal of Medicinal Chemistry* **2015**, *58* (18), 7501-7511; (c) Foster, J. C.; Powell, C. R.; Radzinski, S. C.; Matson, J. B. S-Aroylthiooximes: A Facile Route to Hydrogen Sulfide Releasing Compounds with Structure-Dependent Release Kinetics. *Organic Letters* **2014**, *16* (6), 1558-1561.
140. (a) Foster, J. C.; Radzinski, S. C.; Zou, X.; Finkielstein, C. V.; Matson, J. B. H₂S-Releasing Polymer Micelles for Studying Selective Cell Toxicity. *Mol Pharm* **2017**, *14* (4), 1300-1306; (b) Ercole, F.; Mansfeld, F. M.; Kavallaris, M.; Whittaker, M. R.; Quinn, J. F.; Halls, M. L.; Davis, T. P. Macromolecular Hydrogen Sulfide Donors Trigger Spatiotemporally Confined Changes in Cell Signaling. *Biomacromolecules* **2016**, *17* (1), 371-83.
141. Ozturk, T.; Ertas, E.; Mert, O. Use of Lawesson's reagent in organic syntheses. *Chem Rev* **2007**, *107* (11), 5210-78.
142. Siegel, L. M. A DIRECT MICRODETERMINATION FOR SULFIDE. *Analytical Biochemistry* **1965**, *11* (1), 126-&.
143. (a) Levesque, G.; Arsene, P.; Fanneau-Bellenger, V.; Pham, T. N. Protein thioacylation: 2. Reagent stability in aqueous media and thioacylation kinetics. *Biomacromolecules* **2000**, *1* (3), 400-6; (b) Thomas, D. B.; Convertine, A. J.; Hester, R. D.; Lowe, A. B.; McCormick, C. L. Hydrolytic Susceptibility of Dithioester Chain Transfer Agents and Implications in Aqueous RAFT Polymerizations†. *Macromolecules* **2004**, *37* (5), 1735-1741.
144. Austgen, J. R.; Hermann, G. E.; Dantzler, H. A.; Rogers, R. C.; Kline, D. D. Hydrogen sulfide augments synaptic neurotransmission in the nucleus of the solitary tract. *J Neurophysiol* **2011**, *106* (4), 1822-32.
145. Zhao, W. M.; Zhang, J.; Lu, Y. J.; Wang, R. The vasorelaxant effect of H₂S as a novel endogenous gaseous K-ATP channel opener. *Embo Journal* **2001**, *20* (21), 6008-6016.
146. Sen, N.; Paul, B. D.; Gadalla, M. M.; Mustafa, A. K.; Sen, T.; Xu, R.; Kim, S.; Snyder, S. H. Hydrogen sulfide-linked sulfhydration of NF-kappaB mediates its antiapoptotic actions. *Mol Cell* **2012**, *45* (1), 13-24.
147. Hartle, M. D.; Pluth, M. D. A practical guide to working with H₂S at the interface of chemistry and biology. *Chemical Society Reviews* **2016**, *45* (22), 6108-6117.
148. Martelli, A.; Testai, L.; Citi, V.; Marino, A.; Bellagambi, F. G.; Ghimenti, S.; Breschi, M. C.; Calderone, V. Pharmacological characterization of the vascular effects of aryl isothiocyanates: Is hydrogen sulfide the real player? *Vascular Pharmacology* **2014**, *60* (1), 32-41.

149. Li, L.; Whiteman, M.; Guan, Y. Y.; Neo, K. L.; Cheng, Y.; Lee, S. W.; Zhao, Y.; Baskar, R.; Tan, C.-H.; Moore, P. K. Characterization of a novel, water-soluble hydrogen sulfide - Releasing molecule (GYY4137): New insights into the biology of hydrogen sulfide. *Circulation* **2008**, *117* (18), 2351-2360.
150. Martelli, A.; Testai, L.; Citi, V.; Marino, A.; Pugliesi, I.; Barresi, E.; Nesi, G.; Rapposelli, S.; Taliani, S.; Da Settimo, F.; Breschi, M. C.; Calderone, V. Arylthioamides as H₂S Donors: L-Cysteine-Activated Releasing Properties and Vascular Effects in Vitro and in Vivo. *Acs Medicinal Chemistry Letters* **2013**, *4* (10), 904-908.
151. Beltowski, J. Hydrogen sulfide in pharmacology and medicine--An update. *Pharmacol Rep* **2015**, *67* (3), 647-58.
152. Benavides, G. A.; Squadrito, G. L.; Mills, R. W.; Patel, H. D.; Isbell, T. S.; Patel, R. P.; Darley-Usmar, V. M.; Doeller, J. E.; Kraus, D. W. Hydrogen sulfide mediates the vasoactivity of garlic. *Proceedings of the National Academy of Sciences of the United States of America* **2007**, *104* (46), 17977-17982.
153. Zhao, Y.; Bhushan, S.; Yang, C.; Otsuka, H.; Stein, J. D.; Pacheco, A.; Peng, B.; Devarie-Baez, N. O.; Aguilar, H. C.; Lefer, D. J.; Xian, M. Controllable Hydrogen Sulfide Donors and Their Activity against Myocardial Ischemia-Reperfusion Injury. *Acs Chemical Biology* **2013**, *8* (6), 1283-1290.
154. Liang, D.; Wu, H.; Wong, M. W.; Huang, D. Diallyl Trisulfide Is a Fast H₂S Donor, but Diallyl Disulfide Is a Slow One: The Reaction Pathways and Intermediates of Glutathione with Polysulfides. *Organic Letters* **2015**, *17* (17), 4196-4199.
155. Yeh, Y. Y.; Liu, L. Cholesterol-lowering effect of garlic extracts and organosulfur compounds: human and animal studies. *J Nutr* **2001**, *131* (3s), 989S-93S.
156. Pluth, M. D.; Bailey, T. S.; Hammers, M. D.; Hartle, M. D.; Henthorn, H. A.; Steiger, A. K. Natural Products Containing Hydrogen Sulfide Releasing Moieties. *Synlett* **2015**, *26* (19), 2633-2643.
157. Iciek, M.; Kwiecien, I.; Wlodek, L. Biological properties of garlic and garlic-derived organosulfur compounds. *Environ Mol Mutagen* **2009**, *50* (3), 247-65.
158. Derbesy, G.; Harpp, D. N. A simple method to prepare unsymmetrical di- tri- and tetrasulfides. *Tetrahedron Letters* **1994**, *35* (30), 5381-5384.
159. Zysman-Colman, E.; Harpp, D. N. Optimization of the synthesis of symmetric aromatic tri- and tetrasulfides. *J Org Chem* **2003**, *68* (6), 2487-9.
160. Smilkstein, M. J.; Knapp, G. L.; Kulig, K. W.; Rumack, B. H. Efficacy of oral N-acetylcysteine in the treatment of acetaminophen overdose. Analysis of the national multicenter study (1976 to 1985). *N Engl J Med* **1988**, *319* (24), 1557-62.

161. Flanagan, R. J.; Meredith, T. J. Use of N-acetylcysteine in clinical toxicology. *The American Journal of Medicine* **1991**, *91* (3), S131-S139.
162. Pickering, T. L.; Saunders, K. J.; Tobolsky, A. V. Disproportionation of organic polysulfides. *Journal of the American Chemical Society* **1967**, *89* (10), 2364-2367.
163. Hartle, M. D.; Hansen, R. J.; Tresca, B. W.; Praker, S. S.; Zakharov, L. N.; Haley, M. M.; Pluth, M. D.; Johnson, D. W. A Synthetic Supramolecular Receptor for the Hydrosulfide Anion. *Angew Chem Int Ed Engl* **2016**, *55* (38), 11480-4.
164. Peng, B.; Liu, C.; Li, Z.; Day, J. J.; Lu, Y.; Lefer, D. J.; Xian, M. Slow generation of hydrogen sulfide from sulfane sulfurs and NADH models. *Bioorg Med Chem Lett* **2017**, *27* (3), 542-545.
165. Toohey, J. I. Sulfur signaling: Is the agent sulfide or sulfane? *Analytical Biochemistry* **2011**, *413* (1), 1-7.
166. Toohey, J. I. Sulphane sulphur in biological systems: a possible regulatory role. *Biochem J* **1989**, *264* (3), 625-32.
167. Wang, R. PHYSIOLOGICAL IMPLICATIONS OF HYDROGEN SULFIDE: A WHIFF EXPLORATION THAT BLOSSOMED. *Physiological Reviews* **2012**, *92* (2), 791-896.
168. Kimura, H.; Nagai, Y.; Umemura, K.; Kimura, Y. Physiological roles of hydrogen sulfide: synaptic modulation, neuroprotection, and smooth muscle relaxation. *Antioxid Redox Signal* **2005**, *7* (5-6), 795-803.
169. Yang, G.; Wu, L.; Jiang, B.; Yang, W.; Qi, J.; Cao, K.; Meng, Q.; Mustafa, A. K.; Mu, W.; Zhang, S.; Snyder, S. H.; Wang, R. H₂S as a physiologic vasorelaxant: hypertension in mice with deletion of cystathionine gamma-lyase. *Science* **2008**, *322* (5901), 587-90.
170. Whiteman, M.; Li, L.; Rose, P.; Tan, C.-H.; Parkinson, D. B.; Moore, P. K. The Effect of Hydrogen Sulfide Donors on Lipopolysaccharide-Induced Formation of Inflammatory Mediators in Macrophages. *Antioxidants & Redox Signaling* **2010**, *12* (10), 1147-1154.
171. Filipovic, M. R.; Zivanovic, J.; Alvarez, B.; Banerjee, R. Chemical Biology of H₂S Signaling through Persulfidation. *Chemical Reviews* **2018**, *118* (3), 377-461.
172. Lau, N.; Pluth, M. D. Reactive sulfur species (RSS): persulfides, polysulfides, potential, and problems. *Curr Opin Chem Biol* **2019**, *49*, 1-8.
173. Kimura, H. Hydrogen sulfide and polysulfides as biological mediators. *Molecules* **2014**, *19* (10), 16146-57.

174. Iciek, M.; Wlodek, L. Biosynthesis and biological properties of compounds containing highly reactive, reduced sulfane sulfur. *Pol J Pharmacol* **2001**, *53* (3), 215-25.
175. Mishanina, T. V.; Libiad, M.; Banerjee, R. Biogenesis of reactive sulfur species for signaling by hydrogen sulfide oxidation pathways. *Nat Chem Biol* **2015**, *11* (7), 457-64.
176. Ida, T.; Sawa, T.; Ihara, H.; Tsuchiya, Y.; Watanabe, Y.; Kumagai, Y.; Suematsu, M.; Motohashi, H.; Fujii, S.; Matsunaga, T.; Yamamoto, M.; Ono, K.; Devarie-Baez, N. O.; Xian, M.; Fukuto, J. M.; Akaike, T. Reactive cysteine persulfides and S-polythiolation regulate oxidative stress and redox signaling. *Proc Natl Acad Sci U S A* **2014**, *111* (21), 7606-11.
177. Mikami, Y.; Shibuya, N.; Kimura, Y.; Nagahara, N.; Ogasawara, Y.; Kimura, H. Thioredoxin and dihydrolipoic acid are required for 3-mercaptopyruvate sulfurtransferase to produce hydrogen sulfide. *Biochem J* **2011**, *439* (3), 479-85.
178. Artaud, I.; Galardon, E. A persulfide analogue of the nitrosothiol SNAP: formation, characterization and reactivity. *ChemBiochem* **2014**, *15* (16), 2361-4.
179. Yu, B.; Zheng, Y.; Yuan, Z.; Li, S.; Zhu, H.; De La Cruz, L. K.; Zhang, J.; Ji, K.; Wang, S.; Wang, B. Toward Direct Protein S-Persulfidation: A Prodrug Approach That Directly Delivers Hydrogen Persulfide. *J Am Chem Soc* **2018**, *140* (1), 30-33.
180. Powell, C. R.; Dillon, K. M.; Wang, Y.; Carrazzone, R. J.; Matson, J. B. A Persulfide Donor Responsive to Reactive Oxygen Species: Insights into Reactivity and Therapeutic Potential. *Angew Chem Int Ed Engl* **2018**, *57* (21), 6324-6328.
181. Chauvin, J. R.; Griesser, M.; Pratt, D. A. Hydropersulfides: H-Atom Transfer Agents Par Excellence. *J Am Chem Soc* **2017**, *139* (18), 6484-6493.
182. Bailey, T. S.; Pluth, M. D. Reactions of isolated persulfides provide insights into the interplay between H₂S and persulfide reactivity. *Free Radic Biol Med* **2015**, *89*, 662-7.
183. Bailey, T. S.; Zakharov, L. N.; Pluth, M. D. Understanding hydrogen sulfide storage: probing conditions for sulfide release from hydrodisulfides. *J Am Chem Soc* **2014**, *136* (30), 10573-6.
184. Jiang, C. S.; Muller, W. E.; Schroder, H. C.; Guo, Y. W. Disulfide- and polysulfide-containing metabolites from marine organisms. *Chem Rev* **2012**, *112* (4), 2179-207.
185. Steudel, R. The chemistry of organic polysulfanes R-S(n)-R (n > 2). *Chem Rev* **2002**, *102* (11), 3905-45.
186. Block, E. The Organosulfur Chemistry of the Genus *Allium* - Implications for the Organic Chemistry of Sulfur. *Angewandte Chemie International Edition in English* **1992**, *31* (9), 1135-1178.

187. (a) Powolny, A. A.; Singh, S. V. Multitargeted prevention and therapy of cancer by diallyl trisulfide and related Allium vegetable-derived organosulfur compounds. *Cancer Lett* **2008**, *269* (2), 305-14; (b) Li, Y.; Zhang, J.; Zhang, L.; Si, M.; Yin, H.; Li, J. Diallyl trisulfide inhibits proliferation, invasion and angiogenesis of osteosarcoma cells by switching on suppressor microRNAs and inactivating of Notch-1 signaling. *Carcinogenesis* **2013**, *34* (7), 1601-10; (c) Xiao, D.; Lew, K. L.; Kim, Y. A.; Zeng, Y.; Hahm, E. R.; Dhir, R.; Singh, S. V. Diallyl trisulfide suppresses growth of PC-3 human prostate cancer xenograft in vivo in association with Bax and Bak induction. *Clin Cancer Res* **2006**, *12* (22), 6836-43; (d) Li, W.; Tian, H.; Li, L.; Li, S.; Yue, W.; Chen, Z.; Qi, L.; Hu, W.; Zhu, Y.; Hao, B.; Gao, C.; Si, L.; Gao, F. Diallyl trisulfide induces apoptosis and inhibits proliferation of A549 cells in vitro and in vivo. *Acta Biochim Biophys Sin (Shanghai)* **2012**, *44* (7), 577-83; (e) Wang, Y. B.; Qin, J.; Zheng, X. Y.; Bai, Y.; Yang, K.; Xie, L. P. Diallyl trisulfide induces Bcl-2 and caspase-3-dependent apoptosis via downregulation of Akt phosphorylation in human T24 bladder cancer cells. *Phytomedicine* **2010**, *17* (5), 363-8.
188. Antosiewicz, J.; Herman-Antosiewicz, A.; Marynowski, S. W.; Singh, S. V. c-Jun NH(2)-terminal kinase signaling axis regulates diallyl trisulfide-induced generation of reactive oxygen species and cell cycle arrest in human prostate cancer cells. *Cancer Res* **2006**, *66* (10), 5379-86.
189. Hosono, T.; Fukao, T.; Ogihara, J.; Ito, Y.; Shiba, H.; Seki, T.; Ariga, T. Diallyl trisulfide suppresses the proliferation and induces apoptosis of human colon cancer cells through oxidative modification of beta-tubulin. *J Biol Chem* **2005**, *280* (50), 41487-93.
190. Liu, H.; Radford, M. N.; Yang, C. T.; Chen, W.; Xian, M. Inorganic hydrogen polysulfides: chemistry, chemical biology and detection. *Br J Pharmacol* **2019**, *176* (4), 616-627.
191. Licht, S.; Davis, J. Disproportionation of Aqueous Sulfur and Sulfide: Kinetics of Polysulfide Decomposition. *The Journal of Physical Chemistry B* **1997**, *101* (14), 2540-2545.
192. Xu, S.; Wang, Y.; Radford, M. N.; Ferrell, A. J.; Xian, M. Synthesis of Unsymmetric Trisulfides from 9-Fluorenylmethyl Disulfides. *Org Lett* **2018**, *20* (2), 465-468.
193. Zysman-Colman, E.; Harpp, D. N. Optimization of the synthesis of symmetric aromatic tri- and tetrasulfides. *Journal of Organic Chemistry* **2003**, *68* (6), 2487-2489.
194. Harpp, D. N.; Granata, A. ORGANIC SULFUR CHEMISTRY .21. TRISULFIDE FORMATION BY ALKOXIDE DECOMPOSITION OF SULFENYLTHIOCARBONATES. *Tetrahedron Letters* **1976**, (35), 3001-3004.
195. Bailey, T. S.; Pluth, M. D. Reactions of isolated persulfides provide insights into the interplay between H₂S and persulfide reactivity. *Free Radical Biology and Medicine* **2015**, *89*, 662-667.

196. Ahrika, A.; Robert, J.; Anouti, M.; Paris, J.; Jiang, Z.-H.; Yan, S.-P.; Wang, G.-L.; Yao, X.-K.; Wang, H.-G.; Tuchagues, J. P.; Ögren, M. Nucleophilic Substitution of Alkyl Halides by Electrogenerated Polysulfide Ions in N,N-dimethylacetamide. *Acta Chemica Scandinavica* **1999**, *53* (7), 513-520.
197. Coletta, C.; Papapetropoulos, A.; Erdelyi, K.; Olah, G.; Modis, K.; Panopoulos, P.; Asimakopoulou, A.; Gero, D.; Sharina, I.; Martin, E.; Szabo, C. Hydrogen sulfide and nitric oxide are mutually dependent in the regulation of angiogenesis and endothelium-dependent vasorelaxation. *Proc Natl Acad Sci U S A* **2012**, *109* (23), 9161-6.
198. Szczesny, B.; Modis, K.; Yanagi, K.; Coletta, C.; Le Trionnaire, S.; Perry, A.; Wood, M. E.; Whiteman, M.; Szabo, C. AP39, a novel mitochondria-targeted hydrogen sulfide donor, stimulates cellular bioenergetics, exerts cytoprotective effects and protects against the loss of mitochondrial DNA integrity in oxidatively stressed endothelial cells in vitro. *Nitric Oxide* **2014**, *41*, 120-30.
199. Yuan, S.; Shen, X.; Kevil, C. G. Beyond a Gasotransmitter: Hydrogen Sulfide and Polysulfide in Cardiovascular Health and Immune Response. *Antioxid Redox Signal* **2017**, *27* (10), 634-653.
200. Malone Rubright, S. L.; Pearce, L. L.; Peterson, J. Environmental toxicology of hydrogen sulfide. *Nitric Oxide* **2017**, *71*, 1-13.
201. Zhao, W.; Zhang, J.; Lu, Y.; Wang, R. The vasorelaxant effect of H₂S as a novel endogenous gaseous K_{ATP} channel opener. *EMBO J* **2001**, *20* (21), 6008-16.
202. Abe, K.; Kimura, H. The possible role of hydrogen sulfide as an endogenous neuromodulator. *The Journal of Neuroscience* **1996**, *16* (3), 1066-1071.
203. Levinn, C. M.; Cerda, M. M.; Pluth, M. D. Activatable Small-Molecule Hydrogen Sulfide Donors. *Antioxid Redox Signal* **2020**, *32* (2), 96-109.
204. Levinn, C. M.; Cerda, M. M.; Pluth, M. D. Development and Application of Carbonyl Sulfide-Based Donors for H₂S Delivery. *Acc Chem Res* **2019**, *52* (9), 2723-2731.
205. Haritos, V. S.; Dojchinov, G. Carbonic anhydrase metabolism is a key factor in the toxicity of CO₂ and COS but not CS₂ toward the flour beetle *Tribolium castaneum* [Coleoptera: Tenebrionidae]. *Comp Biochem Physiol C Toxicol Pharmacol* **2005**, *140* (1), 139-47.
206. Roth, M. E.; Green, O.; Gnaim, S.; Shabat, D. Dendritic, Oligomeric, and Polymeric Self-Immolative Molecular Amplification. *Chem Rev* **2016**, *116* (3), 1309-52.
207. Chauhan, P.; Bora, P.; Ravikumar, G.; Jos, S.; Chakrapani, H. Esterase Activated Carbonyl Sulfide/Hydrogen Sulfide (H₂S) Donors. *Organic Letters* **2017**, *19* (1), 62-65.

208. (a) Zhao, Y.; Henthorn, H. A.; Pluth, M. D. Kinetic Insights into Hydrogen Sulfide Delivery from Caged-Carbonyl Sulfide Isomeric Donor Platforms. *Journal of the American Chemical Society* **2017**, *139* (45), 16365-16376; (b) Chauhan, P.; Jos, S.; Chakrapani, H. Reactive Oxygen Species-Triggered Tunable Hydrogen Sulfide Release. *Organic Letters* **2018**, *20* (13), 3766-3770.
209. Powell, C. R.; Foster, J. C.; Swilley, S. N.; Kaur, K.; Scannelli, S. J.; Troya, D.; Matson, J. B. Self-Amplified Depolymerization of Oligo(thiourethanes) for the Release of COS/H₂S. *Polym Chem* **2019**, *10* (23), 2991-2995.
210. Monks, T. J.; Jones, D. C. The metabolism and toxicity of quinones, quinonimines, quinone methides, and quinone-thioethers. *Curr Drug Metab* **2002**, *3* (4), 425-38.
211. Bolton, J. L.; Turnipseed, S. B.; Thompson, J. A. Influence of quinone methide reactivity on the alkylation of thiol and amino groups in proteins: studies utilizing amino acid and peptide models. *Chem Biol Interact* **1997**, *107* (3), 185-200.
212. Barany, G.; Merrifield, R. B. A new amino protecting group removable by reduction. Chemistry of the dithiasuccinoyl (Dts) function. *J Am Chem Soc* **1977**, *99* (22), 7363-5.
213. Barany, G.; Merrifield, R. B. Kinetics and mechanism of the thiolytic removal of the dithiasuccinoyl (Dts) amino protecting group. *Journal of the American Chemical Society* **1980**, *102* (9), 3084-3095.
214. Siegel, L. M. A direct microdetermination for sulfide. *Analytical Biochemistry* **1965**, *11* (1), 126-132.
215. Elliott, S.; Lu, E.; Rowland, F. S. Rates and mechanisms for the hydrolysis of carbonyl sulfide in natural waters. *Environmental Science & Technology* **1989**, *23* (4), 458-461.
216. Poole, L. B. The basics of thiols and cysteines in redox biology and chemistry. *Free Radic Biol Med* **2015**, *80*, 148-57.
217. Saito, R.; Sato, T.; Ikai, A.; Tanaka, N. Structure of bovine carbonic anhydrase II at 1.95 Å resolution. *Acta Crystallogr D Biol Crystallogr* **2004**, *60* (Pt 4), 792-5.
218. Ponomarov, O.; Padělková, Z.; Hanusek, J. Mechanism of sulfur transfer from 1,2,4-dithiazolidine-3,5-diones to triphenylphosphines. *Journal of Physical Organic Chemistry* **2013**, *26* (7), 560-564.
219. Hill, S. V.; Thea, S.; Williams, A. Degradation in aqueous solution of O-aryl N-arylthioncarbamates to aryloxide ions and isothiocyanates. A study of Leffler's assumption. *Journal of the Chemical Society, Perkin Transactions 2* **1983**, (4), 437-446.
220. Lavis, L. D.; Raines, R. T. Bright ideas for chemical biology. *ACS Chem Biol* **2008**, *3* (3), 142-55.

221. Fiorucci, S.; Orlandi, S.; Mencarelli, A.; Caliendo, G.; Santagada, V.; Distrutti, E.; Santucci, L.; Cirino, G.; Wallace, J. L. Enhanced activity of a hydrogen sulphide-releasing derivative of mesalamine (ATB-429) in a mouse model of colitis. *Br J Pharmacol* **2007**, *150* (8), 996-1002.
222. Hanwell, M. D.; Curtis, D. E.; Lonie, D. C.; Vandermeersch, T.; Zurek, E.; Hutchison, G. R. Avogadro: an advanced semantic chemical editor, visualization, and analysis platform. *J Cheminform* **2012**, *4* (1), 17.
223. Frisch, M. J. T., G. W.; Schlegel, H. B.; Scuseria, G. E.; Robb, M. A.; Cheeseman, J. R.; Scalmani, G.; Barone, V.; Mennucci, B.; Petersson, G. A.; Nakatsuji, H.; Caricato, M.; Li, X.; Hratchian, H. P.; Izmaylov, A. F.; Bloino, J.; Zheng, G.; Sonnenberg, J. L.; Hada, M.; Ehara, M.; Toyota, K.; Fukuda, R.; Hasegawa, J.; Ishida, M.; Nakajima, T.; Honda, Y.; Kitao, O.; Nakai, H.; Vreven, T.; Montgomery, J. A., Jr.; Peralta, J. E.; Ogliaro, F.; Bearpark, M.; Heyd, J. J.; Brothers, E.; Kudin, K. N.; Staroverov, V. N.; Kobayashi, R.; Normand, J.; Raghavachari, K.; Rendell, A.; Burant, J. C.; Iyengar, S. S.; Tomasi, J.; Cossi, M.; Rega, N.; Millam, J. M.; Klene, M.; Knox, J. E.; Cross, J. B.; Bakken, V.; Adamo, C.; Jaramillo, J.; Gomperts, R.; Stratmann, R. E.; Yazyev, O.; Austin, A. J.; Cammi, R.; Pomelli, C.; Ochterski, J. W.; Martin, R. L.; Morokuma, K.; Zakrzewski, V. G.; Voth, G. A.; Salvador, P.; Dannenberg, J. J.; Dapprich, S.; Daniels, A. D.; Farkas, Ö.; Foresman, J. B.; Ortiz, J. V.; Cioslowski, J.; Fox, D. J. . *Gaussian 09 Rev. D.02*, Wallingford, CT, 2009.
224. Lee, C.-L.; Brimblecombe, P. Anthropogenic contributions to global carbonyl sulfide, carbon disulfide and organosulfides fluxes. *Earth-Science Reviews* **2016**, *160*, 1-18.
225. (a) Andreae, M. O.; Merlet, P. Emission of trace gases and aerosols from biomass burning. *Global Biogeochemical Cycles* **2001**, *15* (4), 955-966; (b) Andreae, M. O. Emission of trace gases and aerosols from biomass burning – an updated assessment. *Atmospheric Chemistry and Physics* **2019**, *19* (13), 8523-8546.
226. Campbell, J. E.; Whelan, M. E.; Seibt, U.; Smith, S. J.; Berry, J. A.; Hilton, T. W. Atmospheric carbonyl sulfide sources from anthropogenic activity: Implications for carbon cycle constraints. *Geophysical Research Letters* **2015**, *42* (8), 3004-3010.
227. Vainio, E.; Brink, A.; Demartini, N.; Hupa, M.; Vesala, H.; Tormonen, K.; Kajolinn, T. In-Furnace Measurement of Sulphur and Nitrogen Species in a Recovery Boiler. *J. Pulp Pap. Sci.* **2010**, *36* (3-4), 135-142.
228. Watts, S. F. The mass budgets of carbonyl sulfide, dimethyl sulfide, carbon disulfide and hydrogen sulfide. *Atmospheric Environment* **2000**, *34* (5), 761-779.
229. Ferm, R. J. The Chemistry Of Carbonyl Sulfide. *Chemical Reviews* **1957**, *57* (4), 621-640.
230. Leman, L.; Orgel, L.; Ghadiri, M. R. Carbonyl sulfide-mediated prebiotic formation of peptides. *Science* **2004**, *306* (5694), 283-6.

231. Balazy, M.; Abu-Yousef, I. A.; Harpp, D. N.; Park, J. Identification of carbonyl sulfide and sulfur dioxide in porcine coronary artery by gas chromatography/mass spectrometry, possible relevance to EDHF. *Biochem Biophys Res Commun* **2003**, *311* (3), 728-34.
232. Kamboures, M. A.; Blake, D. R.; Cooper, D. M.; Newcomb, R. L.; Barker, M.; Larson, J. K.; Meinardi, S.; Nussbaum, E.; Rowland, F. S. Breath sulfides and pulmonary function in cystic fibrosis. *Proc Natl Acad Sci U S A* **2005**, *102* (44), 15762-7.
233. (a) Zhou, J.; Ma, H. Design principles of spectroscopic probes for biological applications. *Chem Sci* **2016**, *7* (10), 6309-6315; (b) Jiao, X.; Li, Y.; Niu, J.; Xie, X.; Wang, X.; Tang, B. Small-Molecule Fluorescent Probes for Imaging and Detection of Reactive Oxygen, Nitrogen, and Sulfur Species in Biological Systems. *Anal Chem* **2018**, *90* (1), 533-555.
234. Tudose, A.; Demonceau, A.; Delaude, L. Imidazol(in)ium-2-carboxylates as N-heterocyclic carbene precursors in ruthenium–arene catalysts for olefin metathesis and cyclopropanation. *Journal of Organometallic Chemistry* **2006**, *691* (24-25), 5356-5365.
235. Delaude, L.; Demonceau, A.; Wouters, J. Assessing the Potential of Zwitterionic NHC·CS₂Adducts for Probing the Stereoelectronic Parameters of N-Heterocyclic Carbenes. *European Journal of Inorganic Chemistry* **2009**, *2009* (13), 1882-1891.
236. Hans, M.; Wouters, J.; Demonceau, A.; Delaude, L. Synthesis and Organocatalytic Applications of Imidazol(in)ium-2-thiocarboxylates. *European Journal of Organic Chemistry* **2011**, *2011* (35), 7083-7091.
237. Zhou, X.; Lee, S.; Xu, Z.; Yoon, J. Recent Progress on the Development of Chemosensors for Gases. *Chem Rev* **2015**, *115* (15), 7944-8000.
238. Neethirajan, S.; Jayas, D. S.; Sadistap, S. Carbon Dioxide (CO₂) Sensors for the Agri-food Industry—A Review. *Food and Bioprocess Technology* **2008**, *2* (2), 115-121.
239. Guo, Z.; Song, N. R.; Moon, J. H.; Kim, M.; Jun, E. J.; Choi, J.; Lee, J. Y.; Bielawski, C. W.; Sessler, J. L.; Yoon, J. A benzobisimidazolium-based fluorescent and colorimetric chemosensor for CO₂. *J Am Chem Soc* **2012**, *134* (43), 17846-9.
240. Hopkinson, M. N.; Richter, C.; Schedler, M.; Glorius, F. An overview of N-heterocyclic carbenes. *Nature* **2014**, *510* (7506), 485-96.
241. Svoronos, P. D. N.; Bruno, T. J. Carbonyl Sulfide: A Review of Its Chemistry and Properties. *Industrial & Engineering Chemistry Research* **2002**, *41* (22), 5321-5336.
242. Zhang, C.-J.; Zhang, X.-H. Chemoselective Coupling of CS₂ and Epoxides for Producing Poly(thioether)s and COS via Oxygen/Sulfur Atom Exchange. *Macromolecules* **2019**, *53* (1), 233-239.